

Late Transition Metal Complexes of Pentafluorophenylphosphino- Pincer Ligands

by

Bradley George Anderson



A thesis
submitted to Victoria University of Wellington
in fulfilment of the
requirements for the degree of
Doctor of Philosophy
in Chemistry

Victoria University of Wellington

2012

Abstract

This thesis details the synthesis of new examples of electron-poor pincer ligands, featuring bis(pentafluorophenyl)phosphine donors attached to 1,3-substituted phenylene or 2,6-substituted pyridine backbones, to create tridentate PCP and PNP ligands. The effect of the ligands' electronic nature on the coordination chemistry and ease of pincer complex synthesis with late transition metals is discussed, as is the catalytic activity of the resultant palladium pincer complexes in the Heck and Suzuki reactions.

Symmetric PCP and PNP ligands possessing bis(pentafluorophenyl)phosphinite and bis(pentafluorophenyl)phosphoraminate functionalities were synthesised by reaction of bis(pentafluorophenyl)phosphine bromide with resorcinol, 3-hydroxybenzyl-di-*tert*-butylphosphine, 2,6-diaminopyridine, or 2,6-dihydropyridine, affording 1,3-[(C₆F₅)₂PO]₂C₆H₄ (POCOPH, **1**), 1-[(C₆F₅)₂PO]-3-(^tBu₂PCH₂)₂C₆H₄ (POCCPH, **3**), 2,6-[(C₆F₅)₂PNH]₂C₆H₃N (PNNNP, **10**), and 2,6-[(C₆F₅)₂PO]₂C₆H₃N (PONOP, **11**) respectively. The previously reported 1,3-[(C₆F₅)₂PCH₂]₂C₆H₄ (PCCCCPH, **2**) was also synthesised, with the literature yield improved upon by the use of magnesium-anthracene to generate the required Grignard reagent.

The coordination chemistry of the POCOPH ligand **1** with platinum(0) alkene and platinum(II) dimethyl precursors revealed an affinity for the formation of *cis*-bridged oligomeric structures. The dimer [(POCOPH)Pt(nb)]₂ (**14**, nb = norbornene) was isolated and crystallographically characterised from the reaction between **1** and [Pt(nb)₃]. The solid state structure revealed the presence of stabilising π - π interactions between the aromatic ligand backbones, which were also observed in solution by ¹H NMR spectroscopy. Reactions of ligand **1** with platinum and palladium dichloride or chloromethyl starting materials led to rare examples of *cis,trans*-dimers of the type *cis,trans*-[(POCOPH)MClX]₂ (M = Pd, Pt; X = Cl, Me). In part due to facile dimer formation with **1**, metallation of the ligand backbone to form the tridentate pincer complex [(POCOP)PtCl] (**25**) required long reaction times and high temperatures. It was observed that platinum dichloride starting materials with

more strongly binding ancillary ligands were less prone to oligomer formation, and could facilitate more rapid metallation to form **25**. More facile pincer complex formation was also observed for more electron-rich ligands with both PCP and PNP pincer ligands.

The electron poor platinum and palladium POCOP, PCCCP, and POCCP pincer complexes (where the free ligand had been deprotonated upon metallation) were synthesised and subsequently converted into the metal carbonyl species $[(PCP)M(CO)]^+$. Analysis of C–O stretching frequencies by infrared spectroscopy confirmed complexes of POCOP ligand **1** were the most electron poor, while those of POCCP ligand **3** were the most electron rich. Decarbonylation of the palladium pincer complexes was observed in solution and in the solid state, and was more facile for complexes with a higher wavenumber C–O stretch.

Reaction of the $[(PCP)PtCl]$ pincer complexes with methyl nucleophiles revealed that treatment with methylmagnesium iodide resulted in halide exchange, while methyllithium promoted nucleophilic attack at phosphorus. Spectroscopic data indicated that in one instance this led to pentafluorophenyl migration to the metal centre to form a $[(PCP)Pt(C_6F_5)]$ complex. Dimethylzinc was successful in methylating the platinum PCP complexes; however, it was observed to degrade the palladium PCP pincer complexes. Treatment of the rhodium PNP pincer complex $[(PNNP)RhCl]$ (**49**) with dimethylzinc also resulted in degradation, which spectroscopic evidence indicated proceeded *via* ligand deprotonation and the formation of a zinc adduct of **49**. Low temperature protonolysis of the $[(PCP)PtMe]$ species did not reveal any information about possible interactions between the metal and liberated methane.

The catalytic activity of the electron-poor $[(PCP)PdCl]$ complexes were assessed in the Heck and Suzuki cross-coupling reactions. The complexes of **1**, **2**, and **3** were all found to possess only modest activity in the Heck reaction, functioning as precatalysts which decomposed to give catalytically-active Pd(0) colloids. Under milder Suzuki reaction conditions, the most electron-poor complex, $[(POCOP)PdCl]$ (**28**) proved to be one of the most active pincer catalysts known for this reaction, able to achieve a turnover number of 176,000 for the coupling of electronically-deactivated aryl bromides and phenylboronic acid. Mercury poisoning tests revealed that Suzuki reactions catalysed by **28** proceeded *via* a homogeneous active species.

Acknowledgments

Thanks to the boss, Prof. John L. Spencer. Your support, guidance, and experience has been much appreciated during this interesting, challenging, tough and testing time. Thanks to Mum, Dad, and Gran; your enthusiastic support for me in my scholastic endeavours has always been a source of motivation. Cheers to all of the Spencer group members, past and present; Almas, Chris, David, Jacqui, Kathryn, Melanie, Sarah, Teresa. I am especially grateful to Almas and Kathryn for their assistance in developing some half-decent lab skills during my formative years in chemical research.

Thanks to Dr. John Ryan, Ian Vorster, Dr. Robert Keyzers, and Dr. Jono Singh for their assistance with NMR spectroscopy and mass spectrometry. Cheers to Emma for being a better rhodium chemist than me. Thanks to the SPCS administrative and technical staff; you guys keep the School running smoothly and have made all the little surprises that come with doing research a bit easier to deal with.

Thanks to the CMFC for an increased appreciation of appropriately aged distillates (especially their rheological properties). Thanks those to whom I've talked to about work, your advice and feedback was appreciated. Finally, cheers to the jokers who I've called mates, you've helped keep me sane. It can't have been easy.

Table of Contents

Abstract	ii
Acknowledgments	iv
Table of Contents	v
List of Figures	viii
List of Schemes	x
List of Tables	xii
Glossary	xiii
1 Introduction	1
1.1 Metal-Ligand Coordination Complexes	1
1.2 Pincer Complexes	2
1.2.1 Uses of Pincer Complexes With Phosphorus Donors	5
1.3 Electron-Poor Ligands	7
1.3.1 Electron-Poor Pincer Complexes	9
1.4 Synthesis of PCP and PNP Pincer Complexes	10
1.5 Palladium-Catalysed Cross-Coupling	14
1.6 Research Objectives	15
1.7 Concluding Remarks	15
2 Ligand Synthesis	17
2.1 Synthesis of Pentafluorophenyl-Substituted PCP Pincer Ligands . . .	19
2.2 Synthesis of Pentafluorophenyl-Substituted PNP Pincer Ligands . . .	25
2.3 Attempted Synthesis of Trifluoromethylaryl-Substituted Ligands . . .	26
2.4 Concluding Remarks	27
3 Coordination Chemistry of PCP Pincer Ligands	29
3.1 Historical Overview	29
3.2 Coordination to Pt(0)	31
3.3 Coordination to Pt(II)	38

3.3.1	Reactions with [PtMe ₂ (1,5-hexadiene)]	38
3.3.2	Reactions with [PtCl ₂ (1,5-hexadiene)]	42
3.3.3	Reactions with [PtClMe(1,5-hexadiene)]	49
3.3.4	Reactions with [PdCl ₂ (NCMe) ₂]	53
3.3.5	Literature Precedent for <i>cis,trans</i> -Dimers	57
3.4	Concluding Remarks	58
4	Synthesis and Reactivity of PCP Pincer Complexes	61
4.1	Synthesis of PCP Pincer Complexes	61
4.1.1	Effect of Metal Precursor on PCP Pincer Synthesis	62
4.1.2	Effect of the Ligand on PCP Pincer Synthesis	66
4.2	Reactions of Pt/Pd Pincer Compounds	68
4.2.1	Synthesis of Pincer Metal-Carbonyl Compounds	68
4.2.2	Methylation of Pincer Chloride Complexes	80
4.2.3	Protonation of Platinum Methyl Complexes	87
4.3	Concluding Remarks	88
5	Synthesis and Reactivity of PNP Pincer Complexes	90
5.1	Synthesis of Platinum PNP Complexes	91
5.2	Synthesis of Rhodium PNP Species	94
5.3	Concluding Remarks	104
6	Catalytic Activity of Palladium Pincer Complexes	106
6.1	Palladium Pincer Complexes in Catalysis	106
6.2	Mechanistic Implications of Catalysis with PCP Pincer Complexes . .	107
6.3	Performance of [(PCP)PdCl] Species in the Heck Reaction	110
6.3.1	Results of Heck Reactions	111
6.3.2	Active Species Generation and Reaction Mechanism	115
6.4	Performance of [(PCP)PdCl] Species in the Suzuki Reaction	120
6.4.1	Results of Suzuki Reactions	121
6.4.2	Active Species Generation and Reaction Mechanism	129
6.5	Concluding remarks	140
7	Conclusions	143
8	Experimental	147
8.1	General Procedures	147
8.2	Transition Metal Precursors	148
8.3	Ligands	150
8.4	Platinum Complexes	153
8.5	Palladium Complexes	165
8.6	Rhodium Complexes	171

8.7 Catalytic Testing	174
References	177

List of Figures

1.1	Examples of pincer ligand structures.	3
1.2	Outline of the alkane metathesis reaction.	6
1.3	Outline of water splitting by pincer complexes.	7
1.4	Electronic effects of phosphorus substituents.	8
1.5	Electronic influence on transfer-dehydrogenation catalysis.	9
1.6	Facially-coordinated, electron-poor PCP pincer complexes	10
3.1	ORTEP diagram of [(POCOPH)Pt(nb)] ₂ · 2 CH ₂ Cl ₂ (14).	33
3.2	ORTEP diagram of [(POCOPH)Pt(nb)] ₂ · 2 CH ₂ Cl ₂ (14).	36
3.3	Effect of π - π stacking on the ¹ H NMR data of compounds 14–16	40
3.4	Two possible structural isomers of [(POCCPH)PtMe ₂] _x	42
3.5	Formation of [(POCOP)PtCl] from [PtCl ₂ (hex)].	47
3.6	Potential structures for the metallation intermediate 20	48
3.7	Stacked plot showing <i>cis,trans</i> dimers 19 and 21	52
3.8	Formation of [(POCOP)PtCl] from [PtClMe(hex)].	54
3.9	Previously reported <i>cis,trans</i> -dimers.	57
4.1	Effect of ancillary ligand binding strength on dimer formation.	64
4.2	Molecular orbital diagram of carbon monoxide.	71
4.3	ORTEP diagram of [(POCOP)Pt(CO)][SbF ₆] (31).	73
4.4	Anion packing of [(POCOP)Pt(CO)][SbF ₆] (31).	75
4.5	IR spectra showing carbonylation of 29 and decarbonylation of 35	77
4.6	Decarbonylation of compounds 34 , 35 , and 36	79
4.7	Spectroscopic data for byproduct 46	85
4.8	Protonation of 43 and 45 at low temperature.	87
5.1	Synthesis of the PNNNP rhodium complex 49	96
5.2	NMR spectra for the rhodium-methylzinc adduct 51	99
6.1	Outline of the classic “textbook” Heck catalytic cycle.	108
6.2	Representative examples of cyclometallated P–C chelates.	109
6.3	Heck reactions of 28 and 29	114
6.4	Suzuki reactions of 28 , 29 , 30 and (DPPF)PdCl ₂	124
6.5	Raw data for Suzuki reactions at 100 °C.	125

6.6	Suzuki reactions of 28 and 30 at 80 and 60 °C.	127
6.7	Suzuki reactions of 28 with and without the addition of mercury. . .	128
6.8	Outline of the classic “textbook” Suzuki catalytic cycle.	130
6.9	Effect of sterics on aryl coordination.	131
6.10	Redox-free mechanism for the Suzuki reaction.	132
6.11	Resonance stabilisation in the Suzuki reaction.	134
6.12	Plots of decomposition products from palladium pincer complexes. . .	138

List of Schemes

1.1	Synthetic methodology for PCP and PNP pincers.	11
1.2	Synthesis of “click” PCP pincer ligands.	12
1.3	Synthesis of pincer ligands <i>via</i> “ligand introduction”.	13
1.4	Outline of the Heck and Suzuki cross-coupling reactions.	14
2.1	Synthesis of the phosphinite pincer ligand 1	19
2.2	Synthesis of the phosphine pincer ligand 2	20
2.3	Conventional phosphine syntheses unable to produce 2	21
2.4	Synthesis of the phosphine-phosphinite pincer ligand 3	23
2.5	Synthesis of the PNP pincer ligands 10 and 11	25
2.6	Attempted synthesis of PCP pincer ligand 13	27
3.1	Formation of a pincer complex and oligomeric byproduct.	29
3.2	Oligomer formation from the reaction of 1 with [Pt(COD) ₂].	31
3.3	Formation of [(POCOPH)Pt(nb)] ₂ (14).	32
3.4	Formation of [(POCOPH)PtMe ₂] _x species 15 and 16	39
3.5	Formation of [(POCOPH)PtCl ₂] _x species.	44
3.6	Formation of <i>cis,trans</i> -[(POCOPH)PtClMe] ₂ species (21).	51
3.7	Formation of <i>cis,trans</i> -[(POCOPH)PdCl ₂] ₂ species (23).	56
4.1	Effect of starting material on the metallation reaction of ligand 1 . . .	62
4.2	Synthesis of the pincer complex 1 from different starting materials. .	66
4.3	Metallation of the pincer backbone to form 25	67
4.4	Attempted methylations of 25	82
4.5	Synthesis of 44 and conversion back to 26 by ambient H ₂ O.	82
5.1	Synthesis of the PNNNP pincer complex 47	92
5.2	Formation of the oligomer 48	93
5.3	Non-innocent behaviour of PCNCP complexes.	95
5.4	N-Methylation of the PNNNP ligand.	101
5.5	Rhodium iodide chemistry	103
6.1	Pd(IV) intermediates in the Heck reaction.	109
6.2	Chelate-assisted oxidative addition to form a Pd(IV) complex. . . .	110
6.3	Amine-promoted decomposition path for PCP pincer complexes. . . .	115

6.4	Alternate decomposition path for PCP pincer complexes.	116
6.5	P–O bond hydrolysis in a PCP pincer complex.	118
6.6	NMR-scale Suzuki reaction of 28	135
6.7	Pathway for Pd(0) active catalyst formation in P–C chelates.	136

List of Tables

1.1	Variable parameters of pincer ligands.	4
2.1	Effect of phosphine substituents on the TEP.	18
2.2	NMR data of degradation product 9	24
3.1	Bond distances and angles of $[(\text{POCOPH})\text{Pt}(\text{nb})]_2 \cdot 2 \text{CH}_2\text{Cl}_2$ (14). . .	34
3.2	Crystallographic data of $[(\text{POCOP})\text{Pt}(\text{nb})]_2 \cdot 2 \text{CH}_2\text{Cl}_2$ (14).	34
3.3	^{31}P NMR data of dimeric compounds containing ligand 1	59
4.1	Infrared C–O stretches of pincer carbonyl complexes.	70
4.2	Bond distances and angles for $[(\text{POCOP})\text{Pt}(\text{CO})][\text{SbF}_6]$ (31).	74
4.3	Crystallographic data for complex $[(\text{POCOP})\text{Pt}(\text{CO})][\text{SbF}_6]$ (31). . .	74
6.1	Results of the Heck reaction with 28 , 29 , and 30	112
6.2	Results of the Suzuki reaction with 28 , 29 , and 30	122

Glossary

COD	1,5-cyclooctadiene
dba	<i>trans,trans</i> -dibenzylideneacetone
FWHM	full width at half maximum
GCMS	gas chromatography mass spectrometry
hex	1,5-hexadiene
HMBC	heteronuclear multiple-bond correlation
HOMO	highest occupied molecular orbital
HRMS	high resolution mass spectrometry
LUMO	lowest unoccupied molecular orbital
m/z	mass to charge ratio
nb	norbornene
TEP	Tolman Electronic Parameter
TOF	turnover frequency, moles of product produced per mole of catalyst per hour
TON	turnover number, moles of product produced per mole of catalyst

Notes on terminology

PCP, PNP, ECE, etc. — specifies generic tridentate pincer ligands that coordinate through the donor atoms specified (where E represents any donor atom).

POCOP, POCCP, PNNNP, etc. — represents pincer ligands possessing substituted 1,3-phenylene or 2,6-pyridyl backbones. The first, third, and fifth letters denote the ligating atoms, while the second and fourth letters indicate the linkages between donor groups and the aromatic backbone.

POCOPH, PCCCPH, POCCPH, etc. — denotes that the aromatic backbone of the particular PCP pincer ligand is unmetallated and therefore possesses a proton on the potentially ligating carbon atom.

[(pincer)ML_n] — it has become a literature convention to present pincer complexes with the pincer ligand appearing in brackets before the metal atom.

Chapter 1

Introduction

This thesis provides an account of research into the synthesis and coordination chemistry of pincer ligands possessing electron-withdrawing substituents. Particular attention was paid to the nature of intermediate species formed during the synthesis of pincer complexes, as well as the effect of ligand electronics on the ease of pincer complex formation and reactivity. The performance of the palladium complexes of these electron-poor pincer ligands was also evaluated in the Heck and Suzuki cross-coupling reactions.

1.1 Metal-Ligand Coordination Complexes

The realm of metal-ligand coordination chemistry is invariably a vast and diverse one. With the abundance of metals, donor atoms, and ligand architectures at the chemists' disposal, there are a multitude of potential complexes that can be formed. Each ligand bound to the metal centre will affect both the physical space around the metal centre, and the electron density on the metal itself. While each metal atom possesses its own intrinsic electronic character, it is the manipulation of the metal's steric and electronic environment by the ligand that goes a long way to determining the reactivity of metal complexes.

One of the foundations of coordination chemistry, and in particular organometallic chemistry, is the principle that with the appropriate choice of ligand the electronic and steric parameters of a metal centre can be manipulated. This allows the rational design of coordination complexes with specific objectives in mind. For example,

cisplatin, *cis*-[PtCl₂(NH₃)₂], is effective at binding to DNA and killing cancer cells *via* apoptosis. With accrued knowledge about how the modification of the amine and chloride ligands affect the structure and reactivity of these platinum complexes, more effective anti-cancer agents have been and continue to be developed.¹ This parable demonstrates the foundation that underpins coordination chemistry: the more that is known about *how* the electronic and steric modification of ligands affect the reactivity of their metal complexes, the greater the degree to which the reactivity of the complexes can be optimised.

Multidentate ligands further expand upon this foundation. By incorporating more than one donor group into a single ligand, the distance between groups can be manipulated and constrained, impacting the geometries available to coordination complexes, as well as introducing the ability of ligands to bridge and connect multiple metal centres. These properties can be exploited to allow a high degree of fine-tuning; in catalysis the chelate effect is particularly useful, as it helps to increase the stability of metal complexes with multidentate ligands.² The presence of different types of donor group can also direct reactions to occur preferentially at specific sites, while hemilabile binding of donor groups can afford additional coordination sites if required, while still stabilising the metal in the absence of competition for the coordination site.³ The ability of these multidentate ligands to adopt bridging coordination modes also allows for the formation of large, highly-ordered structures. These multinuclear structures can then expand upon the existing properties of a complex, potentially transforming homogeneous catalysts into heterogeneous catalysts,⁴ and also giving rise to new properties that depend on long-range order, such as luminescence.⁵

As multidentate ligands can offer considerable advantages over monodentate ligands, the importance of understanding the effects of ligand modification becomes increasingly important. To be able to design metal complexes with specific objectives or properties in mind, it is crucial to understand how the steric and electronic character of the ligand affects the structure and chemistry of the resultant metal complexes.

1.2 Pincer Complexes

One particular type of coordination complex that has demonstrated considerable versatility, applicability, and durability in the scientific literature is that of the pincer ligand. These are defined as being tridentate chelating ligands which co-

ordinate to metal centres predominantly in a meridional fashion. While this definition of what comprises a pincer ligand is very broad, one trait that is often present in pincer ligands is a rigid backbone, to constrain the degrees of freedom and favour planar coordination geometries. Common motifs that have been employed in pincer ligands are: bisoxazoliny-phenyls,⁶ diphenylamine-derivatives,⁷ diazaborolidines,⁸ 1,8-substituted anthracyls,⁹ N-heterocyclic carbene-derivatives,¹⁰ 1,3-substituted ferrocenyls,¹¹ and 1,3,5-substituted aromatics containing pendant chains,¹² as shown in Figure 1.1. Pincer ligands are typically named according to the ligating atoms present, and where the deprotonation of a donor group is required to achieve tridentate pincer coordination, the presence of the proton on the free ligand is usually denoted with an ‘H’. Figure 1.1 describes, from top left to bottom right, NCNH, PNPH, PBPH, PCPH, CNC, PCPH, and SCSH pincer ligands.

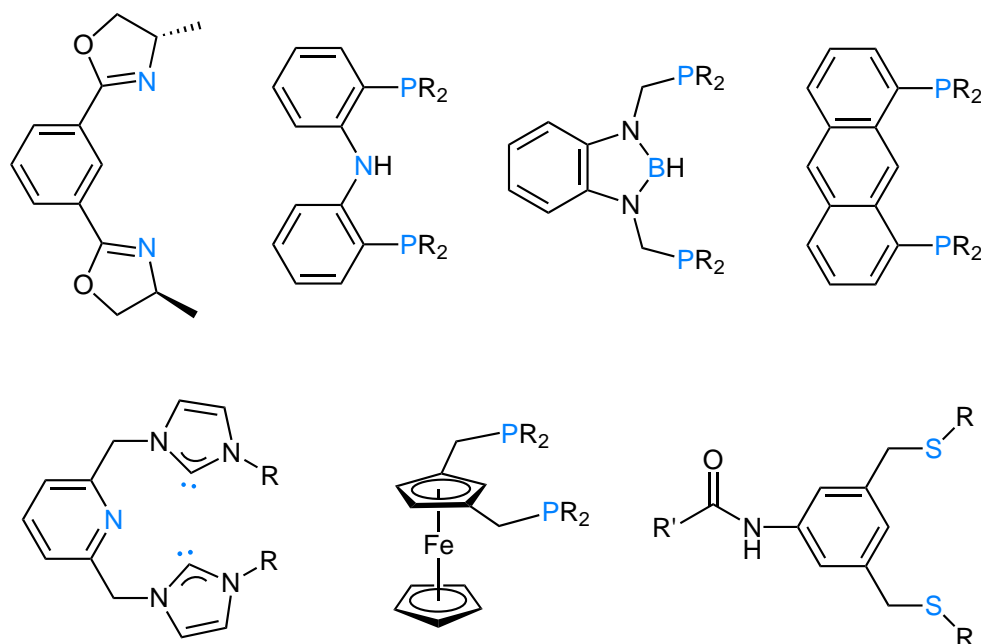


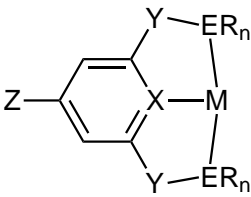
Figure 1.1 Representative examples demonstrating a range of pincer ligand structures.

This range of structural motifs used as pincer ligands serves to highlight their versatility. While maintaining a tridentate, meridional coordination mode, the ligand can possess a range of donor atoms, both anionic and neutral, as light as boron or as heavy as arsenic. While the ligands highlighted in Figure 1.1 generally have C_2 symmetry, asymmetric pincer ligands can be readily generated by varying either the spacer groups between the donor atom and ligand backbone (often referred to as the “arms” of the pincer ligand),¹³ or by variation of these donor groups themselves (with PNN pincers being a typical example).¹⁴

The rigid, planar framework provided by pincer ligands is desirable from a chemical point of view as it inhibits cyclometallation of the substituents on donor groups,

which engenders a high thermal stability to pincer complexes. This makes pincer compounds particularly suited for catalytic processes that operate at high temperatures. Another feature of pincer ligands is the fact that upon coordination to a metal centre the donor groups on the “arms” of the pincer ligand adopt a mutually *trans* configuration, while the backbone is coordinated *trans* to an ancillary ligand on the metal. This provides an optimal configuration for catalysis, in which the *trans*-influence (the labilisation of ligands *trans* to a specific ligand) is utilised to good effect. Ligands with a low or moderate *trans*-influence (such as phosphines) can be placed on the arms, where they will be coordinated *trans* to each other, and therefore undergo minimal mutual destabilisation. With the placement of a donor group with a high *trans*-influence on the ligand backbone, ligand coordination *trans* to pincer backbone will be labilised. This helps to prevent inhibition of pincer catalysts by solvent or ancillary ligand coordination.

Table 1.1 Variable parameters of pincer ligands and their control over the steric and electronic properties of complexes. Table adapted from the review by Choi, MacArthur, Brookhart, and Goldman.¹⁵

	Group	Major Effect(s) of Variation
	ER _n	Steric control by varying substituents; control of electron density; lability.
	Y	Control over electron density; indirect control on steric properties.
	X	Electronic effects, particularly <i>trans</i> -influence.
	Z	Remote control of electron density; solubility control.

Most common elements
 E: P, N, S, O, As
 X: C, N, B
 Y: CH₂, O, NH

Despite the range of complicated ligand backbones that can adopt a pincer coordination mode, the most common structural motifs for pincers are those bearing 1,3-substituted phenyl or 2,6-substituted pyridyl groups. However, the simplicity of these aromatic backbones belies the intricacies that can be introduced into the ligands due to their modular nature. Table 1.1 summarises the modification of these backbones and the effect of each component on the ligand as a whole. The ability of pincer ligands to be highly amenable to structural diversity, while still maintaining a reliable and predictable coordination mode, makes them ideal substrates for the investigation of how ligand modifications affect the reactivity of the resultant metal complexes.

1.2.1 Uses of Pincer Complexes With Phosphorus Donors

Of the multitude of pincer complexes that have been reported, arguably, those that have demonstrated the greatest utility are ligands with at least one phosphorus donor atom. The advantage of incorporating phosphorus donors within the pincer coordination motif is that the soft electronic nature and π -acceptor character of phosphines are ideal for stabilising late transition metals, especially those in low oxidation states. Late transition metal complexes are renowned for their performance in homogeneous catalysis and small molecule activation, with pincer complexes of late transition metals being particularly effective. They have been shown to facilitate organic transformations such as the Heck, Suzuki, Sonogashira, Stille, and Negishi cross-coupling reactions, as well as asymmetric allylic alkylations, hydroaminations, transfer hydrogenations, and aldol-type reactions. Summaries of this work have been detailed in a number of review papers.^{16–20}

While pincer complexes are able to assist the chemist with transformations in organic synthesis, they are also at the forefront of research into some of the major developments in organometallic chemistry. One of the most intriguing reactions facilitated by phosphine-based pincer complexes is that of alkane dehydrogenation. In 1996, Jensen, Kaska, and co-workers discovered an iridium PCP pincer species capable of promoting catalytic dehydrogenation of cyclooctane in the presence of a hydrogen acceptor species.²¹ This pincer catalyst offered an advantage over other homogeneous dehydrogenation catalysts as it was stable in solution for prolonged periods under the reaction conditions, and outperformed heterogeneous dehydrogenation catalysts by dehydrogenating a much larger range of substrates and operating at a considerably lower temperature (150 °C as opposed to 500–900 °C for heterogeneous species).¹⁵ This transfer-dehydrogenation has been shown to be selective for the formation of terminal alkenes, with the catalyst undergoing minimal inhibition or degradation.

This facile dehydrogenation of alkanes catalysed by iridium PCP pincer complexes has led to the development of a system for alkane metathesis, which may in the future aid the production of synthetic fuels from low-cost feedstocks. In this tandem catalytic system (Figure 1.2), an alkane undergoes pincer-catalysed transfer-dehydrogenation, with the resultant alkene subjected to metathesis using Schrock-type molybdenum or tungsten carbene catalysts.²² These alkene metathesis products then act as the hydrogen acceptor species for the alkene transfer-dehydrogenation step, generating new alkane products from the original alkane starting materials.²³ Currently, problems exist with alkene isomerisation leading to a distribution of products being obtained,²² nonetheless this proof of concept is surely an exciting one.

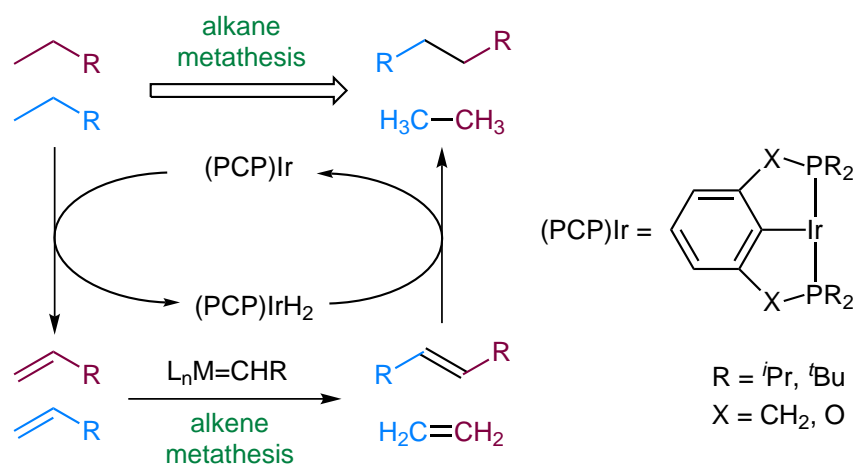


Figure 1.2 Outline of the alkane metathesis reaction. Figure adapted from Haibach *et al.*²²

Catalytic alkane dehydrogenation is an example of the selective cleavage and subsequent reaction of carbon-hydrogen bonds, otherwise known as C–H activation. This has been a topic of major intrigue and focus, with the March 1995 issue of *Accounts of Chemical Research* denoting it one of the “Holy Grails” of chemistry.²⁴ A further breakthrough in this field has been achieved by the Brookhart research group, with the first full characterisation in solution of a methane σ -complex, $[(\text{PNP})\text{Rh}(\text{CH}_4)]$.^{25*} This complex, in which a methane molecule is bound to a PNP pincer-ligated rhodium centre through the interaction between a C–H bond and the metal, provides a basis for research into how the strength of this metal-methane interaction can be manipulated and ultimately exploited to achieve C–H bond functionalisation.

Phosphorus-containing pincer complexes have also shown promise in water splitting — the separation of water into molecular hydrogen and oxygen. Cheap and ready access to this technology is heralded as reducing dependence on fossil fuels and bringing about a hydrogen economy, and hence is a major drawcard for chemical research.²⁷ Investigations undertaken with PCN platinum²⁸ and PNN ruthenium²⁹ pincer complexes have confirmed key underlying principles that water splitting technology will need to exploit (Figure 1.3).²⁷ While these reactions have not been incorporated into a complete catalytic cycle, they indicate that such complexes can offer viable inroads into achieving organometallic water splitting.

*The first evidence for σ -coordination of methane to metal centres was provided by Perutz and Turner, by photolysis of metal carbonyl complexes in a methane matrix at 20 K.²⁶ Due to the low temperatures required for reactions carried out in liquid methane, reaction mixtures were analysed by infrared and visible spectroscopy. The generation of a σ -methane ligand in the inner coordination sphere of the metal complex by the Brookhart group allowed the reaction to be carried out in a suitable solvent for NMR spectroscopy (CDCl_2F), which provided a greater amount of data on the structure of the methane complex than either infrared or visible spectroscopy could.

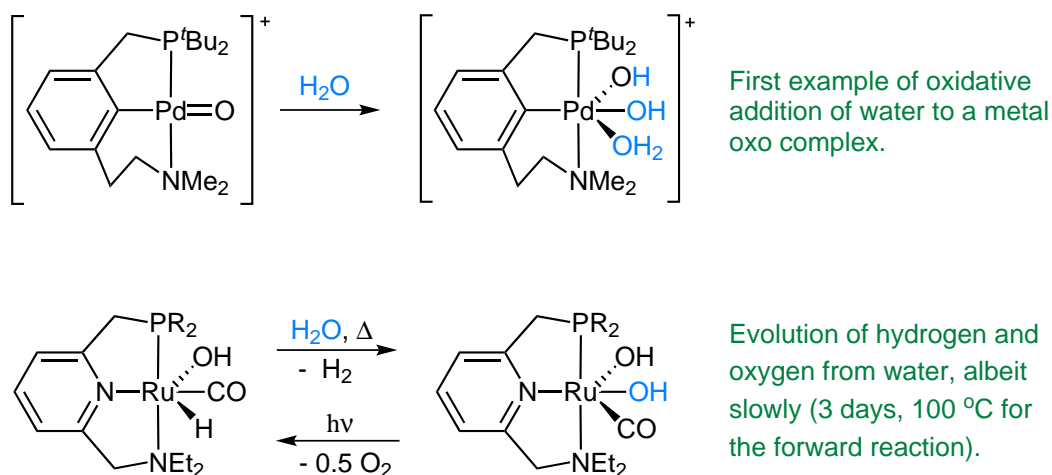


Figure 1.3 Outline of water splitting by pincer complexes.

1.3 Electron-Poor Ligands

Whilst PCP and PNP pincer ligands have been well studied and successfully employed in a number of intriguing catalytic processes, previous work has predominantly focussed on complexes possessing electron-rich phosphorus donors, such as di-*tert*-butyl or diisopropyl phosphines. Substantially less work has been undertaken to investigate the effect of incorporating electron-poor donor groups into the pincer framework.

There have been a number of reports in which electron-withdrawing groups have been integrated into established ligand motifs and resulted in a significant increase in catalytic performance of the resultant complexes.^{30–32} This effect may appear counterintuitive, as many of the mechanisms prevalent in organometallic transformations are dependent on reactions proceeding through the conventional oxidative addition and reductive elimination pathways. Since oxidative addition is predominantly reliant on electron donation from the metal centre into the σ^* -antibonding orbital of the bond being cleaved, reducing the electron density on the metal should disfavour oxidative addition and reduce the activity of the catalyst. However, electron-deficient metal centres will be poorer at stabilising high oxidation states than electron-rich metals, and consequently reductive elimination steps will be enhanced. Moreover, for important reactions such as C–H activation, calculations have shown a number of reaction pathways may be possible (electrophilic, ambiphilic, and nucleophilic),³³ and that the introduction of electron-withdrawing ligands should generate favourable charge transfer interactions in some instances.³⁴

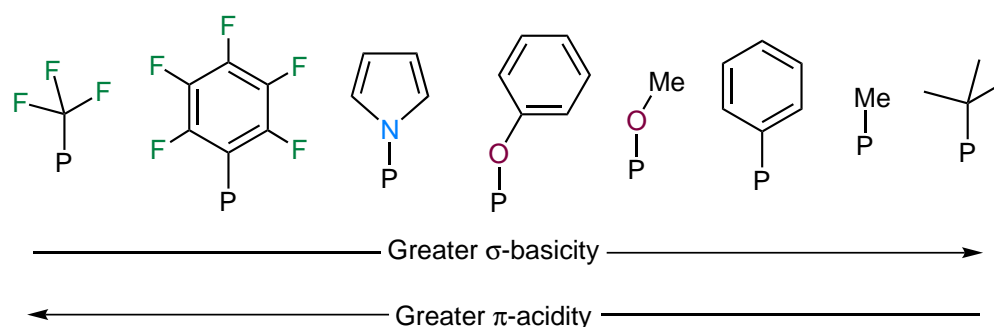


Figure 1.4 Electronic effects of phosphorus substituents.

Numerous studies, both computational and experimental, have been undertaken to develop a comprehensive hierarchy of the degree to which substituents affect the electron density on the phosphorus centre.^{35–37} As phosphorus-metal bonding has both a σ -donor and a π -acceptor component, in principle, as the substituents on the phosphorus become more electronegative, the σ -donor ability of the phosphorus is reduced, while its π -acceptor ability is increased (Figure 1.4). In practice, the two components are difficult to distinguish; a case in point being the pentafluorophenyl substituent, which had previously been regarded as increasing the π -acceptor ability of the phosphorus donor, but may now be regarded as predominantly decreasing the σ -donor ability phosphorus ligands.³⁸ Regardless of the exact nature of this electronic effect, fluoroalkyl and fluoroaryl substituents will typically produce very electron-poor metal centres upon coordination; together with phosphites they represent a widely used means of generating electron-withdrawing phosphorus-donor ligands. Fluoroarylphosphine ligands in particular have demonstrated unique reactivities and enhanced catalytic activity over their perprotio analogues,³⁹ making them ideal candidates for incorporation into the pincer ligand motif.

The effect imparted by electron-withdrawing groups on the metal centre can also be quantified *via* the synthesis of metal-carbonyl derivatives of pincer complexes. The frequency of the C–O stretch in the infrared spectrum will reflect the amount of electron density on the metal centre; a more electron-rich metal complex will be able to contribute a greater amount of electron density to the carbonyl through π -backbonding, so will display a C–O stretching frequency at a lower wavenumber than for a more electron-poor metal complex.

1.3.1 Electron-Poor Pincer Complexes

Complexes of electron-poor PCP and PNP pincer ligands, while relatively rare, have shown a number of interesting traits worthy of further investigation. The Brookhart group has examined the effect that substitution of the PCP pincer backbone *para* to the coordinated metal centre (carbon C-5 of the ligand) has on the reactivity of these complexes in iridium-catalysed transfer-dehydrogenation.⁴⁰ It was found that the turnover numbers obtained showed a rough correlation with the electron-withdrawing ability of the substituent: the more withdrawing the substituent, the more active the catalyst (Figure 1.5).[†] Similarly, replacement of methylene groups on the arms of the ligand with oxygen atoms was observed to increase the activity by one order of magnitude, due to lower σ -donor ability and greater π -acceptor ability of phosphinites compared to phosphine ligands. The higher activity of the more electron-poor catalysts was thought to be due to their propensity for π -coordination of alkenes over C–H oxidative addition, reducing catalyst inhibition by the *tert*-butylethylene starting material.⁴²

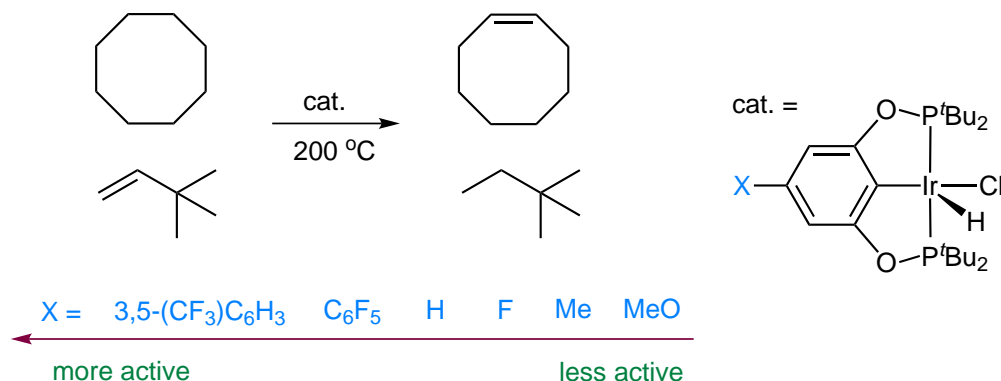


Figure 1.5 Effect of electronic modification of iridium pincer catalysts for the transfer dehydrogenation reaction.

To try to enhance this electron-withdrawing effect, a small number of pincer complexes have been reported whereby the electron-withdrawing substituents are located on the phosphorus donors, putting them in close proximity to the metal centre. An interesting consequence of increasing the electron-withdrawing nature of the ligands is that the mutually *trans* coordination of phosphorus donors becomes unfavourable. This forces some five- and six-coordinate pincer complexes to adopt a facial (rather than meridional) coordination geometry of the pincer ligand (Figure 1.6).^{43–45} As

[†]It is important to note that the introduction of the same substituent at C-5 of the aromatic backbone may cause a different effect to substitution at the phosphorus. A good example of this occurs for alkoxy groups. Compared to alkyl substituents, alkoxy substituents produce more electron-poor phosphorus donors, as they lower the energy of the LUMO on the phosphorus,⁴¹ increasing π -acidity. However, when attached directly to the ligand backbone, they produce more electron-rich aromatic rings due to resonance effects.

well as indicating that electron-deficient pincer ligands may provide access to unusual coordination geometries, the five-coordinate complexes possess ancillary ligands separated by 90° instead of the usual 120° for meridionally coordinated pincer ligands, a property that may favour reductive elimination steps in catalysis.

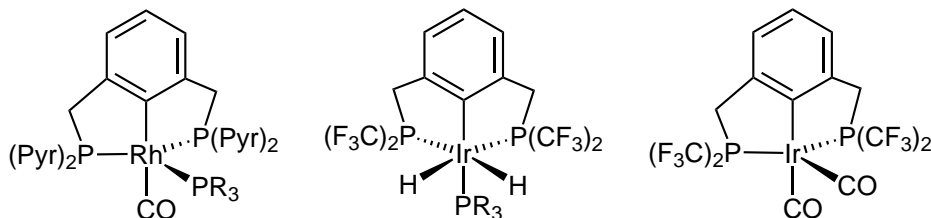


Figure 1.6 Pincer complexes with electron-poor PCP ligands, displaying unusual facial coordination geometry.

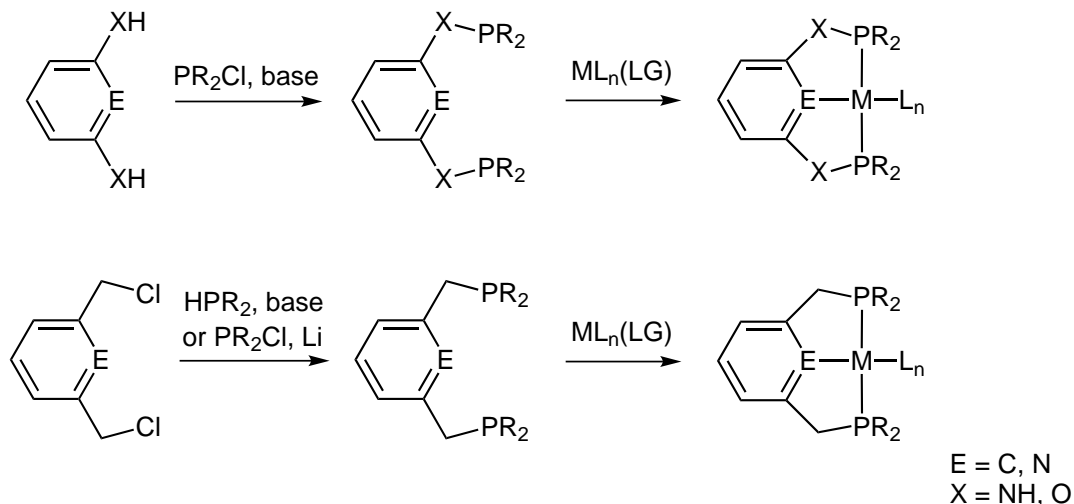
A further electron-deficient PCP pincer complex that has demonstrated an unusual reactivity is the 2,4,6-(CF_3) $_3\text{C}_6\text{H}_2$ -substituted [(POCOP)Ir(N_2)] pincer complex synthesised by the Brookhart group.⁴⁶ In the crystalline form, this complex has demonstrated the ability to undergo exchange of the nitrogen ligand for oxygen, hydrogen, carbon monoxide, ammonia, and ethene, while maintaining its crystallinity. Furthermore, single crystals of this iridium pincer complex were shown to catalyse the selective hydrogenation of ethene in the presence of propene, indicating that catalysis occurred to some extent within the confines of the crystal lattice. As such, this electron-deficient pincer complex appears to be a step towards bringing the selectivity and fine tuning demonstrated by homogeneous catalysts into the realm of heterogeneous catalysis.

1.4 Synthesis of PCP and PNP Pincer Complexes

Owing to the interesting possibilities presented by pincer ligands possessing phosphorus donors, this research focusses on PCPH and PNP pincer ligands. The synthesis of such ligands and their complexes have been accomplished utilising a number of different methodologies.

The most common synthetic method for the formation of pincer complexes involves two general steps: first the installation of the donor arms of the ligand on to the backbone, then reaction of the ligand with an appropriate metal precursor to yield the tridentate pincer complex (Scheme 1.1). The methods used to attach the phosphorus donor groups to the ligand backbone generally rely on established organophosphorus

chemistry, with separate donor groups able to be installed sequentially on the backbone to generate asymmetric PCP'H or PNP' ligands.¹³ From the outset there is the opportunity to introduce diversity into the structure; as the reaction conditions required to attach the phosphorus donor groups are relatively general and occur under mild conditions (with the exception of the lithiation step in Scheme 1.1) they are tolerant to other functionalities present on the ligand backbone.

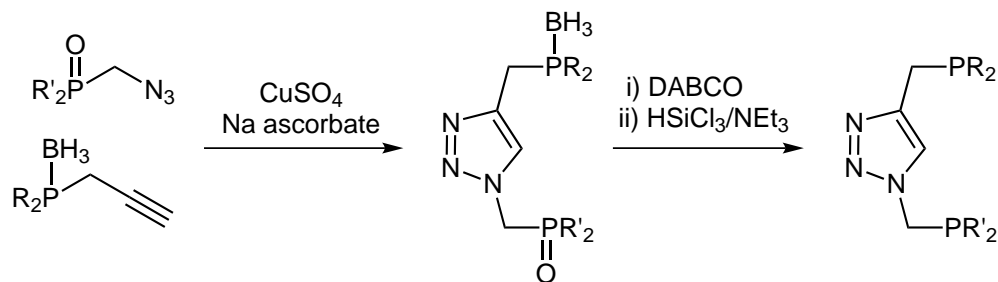


Scheme 1.1 Common synthetic methodology employed for PCP and PNP pincer complexes. Lithiation is only required where the secondary phosphine is not sufficiently nucleophilic to react directly with the benzylic chloride. Typically triethylamine is used as a base. LG represents a neutral leaving group.

The complexation of the ligand to the metal is rather more simple for PNP pincers than for PCP pincers. In both cases the metal precursor is usually in the oxidation state desired for the resultant pincer complex, is stabilised by readily displaced neutral ancillary ligands (commonly acetonitrile or cyclooctadiene), and often contains an anionic leaving group (LG). Coordination of phosphorus donors in place of the ancillary ligands occurs first, followed by displacement of the leaving group by the donor group on the ligand backbone to achieve the tridentate pincer coordination mode. This backbone coordination is significantly more facile for PNP ligands than for PCPH ligands, as the former only requires ligand displacement from the metal, while the latter also requires the cleavage of the strong C–H bond at the carbon on the backbone between the ligand arms (carbon C-2, denoted E in Scheme 1.1). This increased energy requirement for tridentate coordination of PCPH pincer ligands can lead to their adopting diphosphine-like bridging coordination modes when reactions are carried out under conditions where C–H cleavage is not facile.⁴⁷

To overcome the difficulty involved in breaking this strong C–H bond to achieve

ligand metallation, the pincer ligands can alternatively be prepared with bromide or iodide substituents on C-2. This approach is typically combined with a starting material in the zero oxidation state (such as $[\text{Pd}_2(\text{dba})_3]$), as oxidative addition of the carbon-halide bond will yield the pincer halide complex $[(\text{PCP})\text{MX}]$. In reactions with palladium precursors, the presence of the reactive C–Br or C–I bonds results in oxidative addition at temperatures of around 75 °C for bromides⁴⁸ and as low as 20 °C for iodides,⁴⁹ whereas temperatures in excess of 100 °C are often required for metallation *via* C–H cleavage.

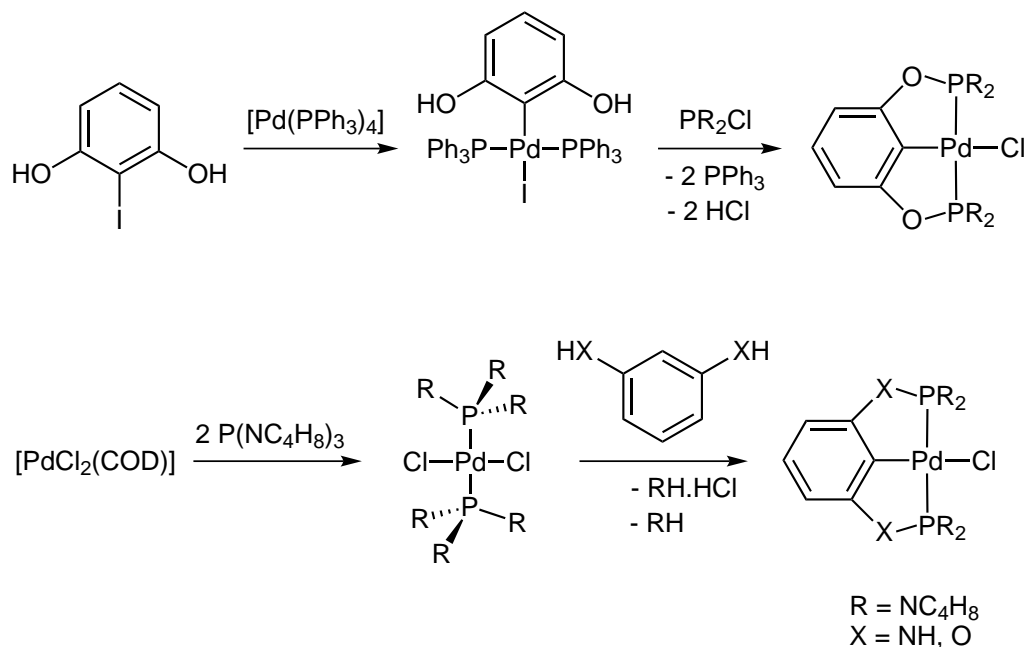


Scheme 1.2 Synthesis of PCP pincer ligands using the azide-alkyne Huisgen cycloaddition.

An alternative approach to the synthesis of PCPH pincer ligands has been reported using click chemistry (copper-catalysed azide-alkyne Huisgen cycloaddition). Rather than begin with an intact ligand backbone and install functionality upon this, the click methodology focusses on the synthesis of various donor groups attached to alkyne and azide moieties (Scheme 1.2). These donor groups can then be “clicked” together, with the triazole unit formed in the cycloaddition reaction becoming the ligand backbone.⁵⁰ This elegant scheme allows different combinations of donor groups to be readily incorporated into PCPH pincer ligands. However, the triazole ligand backbone is not as inert as phenyl or pyridyl backbones, potentially detracting from the traditionally robust nature of pincer complexes.

A further synthetic method that has been used for the synthesis of palladium PCP complexes is the “ligand introduction route”.⁵¹ In this method (Scheme 1.3, top scheme), Kimura and associates first attach the 1,3-dihydroxy-substituted aromatic backbone to the tetrakis-triphenylphosphine palladium metal precursor through oxidative addition of a C–I bond. The phosphorus donors of the pincer ligand are then installed in a condensation reaction between the hydroxyls of the metallated species and a disubstituted phosphine chloride. Finally, tridentate pincer coordination is achieved by displacement of the remaining triphenylphosphine ligands from the metal by the phosphorus donor groups, utilising the chelate effect. In what can be seen as a “reverse ligand introduction route”, Bolliger and colleagues first introduce the phosphorus donor groups on to the metal centre through simple coor-

dination chemistry (Scheme 1.3, bottom scheme), then install the ligand backbone *via* P–N cleavage of a piperidyl substituent on the phosphorus and subsequent elimination of piperidinium hydrochloride.⁵² Heating to 100 °C is then required to promote metallation of the aromatic backbone. However, reaction times are remarkably short, with reactions reaching completion after 45 minutes at the most.



Scheme 1.3 Synthesis of PCP pincer ligands *via* “ligand introduction” methods.

While these “ligand introduction” methodologies are elegant routes to PCP pincer complexes, they can only be used in certain circumstances. The method of Kimura and associates (Scheme 1.3, top scheme) becomes less effective with increasing ligand bulk; reactions with PPh_2Cl are complete after one hour, whereas reactions with $\text{P}(o\text{-tolyl})_2\text{Cl}$ require 24 hours.⁵¹ The method of Bolliger and colleagues (Scheme 1.3, bottom scheme) is reliant on the tertiary phosphine groups possessing substituents that can be readily displaced;⁵² reactions with alkyl or aryl phosphines would not be expected to proceed due to the strength of the P–C bond. Moreover, both of these methods can only be used to produce ligands with O or NH linkages between the donor groups and ligand backbone.

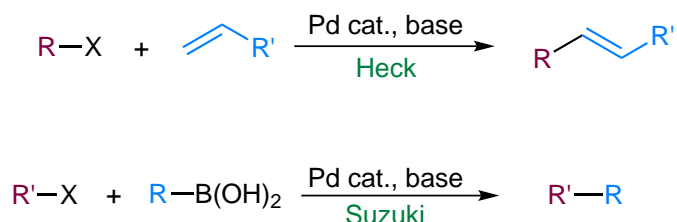
In the work reported herein, PCPH ligands possessing a proton (rather than a halide) at the C-2 position were used. As they are more commonly used than their halide-substituted analogues they offer a greater comparability to the scientific literature, and are synthesised from a readily available starting material (dichloro-*m*-xylene). The requirement for C–H activation of the ligand to achieve pincer coordination also offers an insight into how manipulation of the ligand’s electronic character affects the prevalence of bridging coordination modes, as well as the ease of backbone

metallation.

1.5 Palladium-Catalysed Cross-Coupling

As mentioned previously, phosphine-based palladium pincer complexes have been successfully utilised in the Heck and Suzuki cross-coupling reactions. The Heck reaction was first reported in 1972,⁵³ and the Suzuki reaction in 1979;⁵⁴ these palladium-catalysed reactions immediately proved useful, and are now vital tools for carbon-carbon bond formation in synthetic organic chemistry. Richard Heck, Akira Suzuki, and Ei-ichi Negishi were awarded the 2010 Nobel Prize in Chemistry for their discovery of these cross-coupling reactions.

The basis of both the Heck and Suzuki reactions is the reaction between a carbon electrophile (usually an organohalide) and a carbon nucleophile (an alkene or boronic acid/ester), mediated by a palladium catalyst and an external base (Scheme 1.4). The Heck reaction is often performed in basic or highly polar solvents at temperatures above 100 °C, while Suzuki reactions can be carried out at temperatures below 100 °C in non-polar solvents. This allows the performance and durability of potential catalyst species to be assessed under a wide range of conditions.



where R must be unsaturated

Scheme 1.4 Outline of the Heck and Suzuki cross-coupling reactions. The red highlights electrophilic groups, while the blue highlights nucleophilic groups, in order to demonstrate the similarity between the reactions.

The Heck and Suzuki reactions provide a means to quantify how the incorporation of electron-withdrawing groups into PCP pincer ligands affects the catalytic performance of their palladium complexes. The use of palladium pincer species in cross-coupling reactions dates back to 1997;⁵⁵ this 15 year history, together with the ubiquity of the Heck and Suzuki reactions in the scientific literature ensures an abundance of data for comparison, and makes these reactions suitable yardsticks for

measuring the catalytic performance of new electron-poor palladium pincer complexes.

1.6 Research Objectives

The aims of this project are to synthesise new, electron-poor PCPH and PNP pincer ligands using fluoroaryl electron-withdrawing substituents on the phosphorus donors, and to evaluate their coordination chemistry with platinum, palladium, and rhodium precursors. It is also to investigate how the electronic character of the pincer ligand affects the ease of ligand metallation and pincer complex formation.

To quantify the electronic effects of the electron-withdrawing groups on the metal centre, carbonyl derivatives of these electron-poor pincer complexes will be synthesised and analysed by infrared spectroscopy. The performance of the new palladium compounds will also be assessed in Heck and Suzuki cross-coupling reactions, to determine if any relationship can be established between catalytic activity for these reactions and the electronic nature of the metal centre.

1.7 Concluding Remarks

The description “pincer ligand” encompasses a large range of structures, all tridentate, with a preference for forming rigid, well-defined, thermally stable coordination complexes with transition metals. The most renowned of these species possess simple aromatic backbones with one or more phosphorus donor groups. Not only do these phosphorus-containing pincer complexes perform well in reactions that aid organic synthesis, but are also prominent in cutting edge areas of research, such as alkane metathesis and water splitting.

However, to be able to improve on current technologies, an understanding of how the steric and electronic properties of the ligands are manifested in the properties of the metal complexes themselves is desirable. Complexes of electron-poor pincer ligands are not well represented in the scientific literature, yet these complexes have demonstrated unusual coordination geometries and increased catalytic activity over their more electron-rich analogues. Thus, the incorporation of electron-withdrawing

groups into PCP and PNP coordination motifs should allow the synthesis of a new range of electron-poor phosphorus-containing pincer complexes.

The electronic character of each metal complex will be established by performing infrared spectroscopy on metal carbonyl derivatives of these new pincer complexes, allowing the relative electron density on each metal centre to be established. To assess the impact of the electron-withdrawing groups on the formation of pincer complexes, the coordination chemistry and metallation of the pincer ligands will be studied. Finally, Heck and Suzuki reactions will be carried out with the electron-poor palladium compounds, to determine the extent that the electronic nature of the metal centre affects catalytic activity in cross-coupling reactions.

Chapter 2

Ligand Synthesis

In order to synthesise electron-poor pincer ligands, the appropriate choice of functional groups is required to inductively withdraw electron density away from the donor atoms and any metal bound to them. As mentioned in the previous chapter, electron-poor pincer ligands can be created by modifying the substituents either on the ligand backbone, the “arms” of the pincer that connect the donor groups to the backbone, or the substituents on the donor groups themselves. Modification of the donor groups was deemed to be the most promising route to the formation of electron-deficient pincer complexes; the donor groups bind directly to the metal centre and so have a large influence on the electronic character of the resultant metal complex.

Bis(pentafluorophenyl)phosphine was regarded as the best choice for the phosphorus donor group of the ligand; pentafluorophenylphosphines have been shown to be similar to aryl phosphinites in their ability to produce electron-poor metal centres, although they are not as effective as halophosphines or trifluoromethyl-substituted phosphines in this regard.³⁷ The electronic effect of a substituent on a phosphorus donor atom can be approximated with the Tolman Electronic Parameter (TEP), a measure of how each group affects the CO stretching frequency of a nickel carbonyl complex. Larger TEP values indicate lower electron density on the nickel centre, and a less electron-donating or more electron-withdrawing substituent. Values for C₆F₅ are compared to other common substituents in Table 2.1, confirming the electron-poor nature of pentafluorophenylphosphine complexes.

Whereas the phosphinite, trifluoromethyl, and halide substituents all increase the π -acceptor ability (π -acidity) of the phosphorus donor, it is thought that pentafluorophenyl substituents instead drastically reduce the σ -donor ability of the phosphorus

Table 2.1 Effect of phosphine substituents on the Tolman Electronic Parameter.³⁷ A larger value indicates a more electron-poor metal centre.

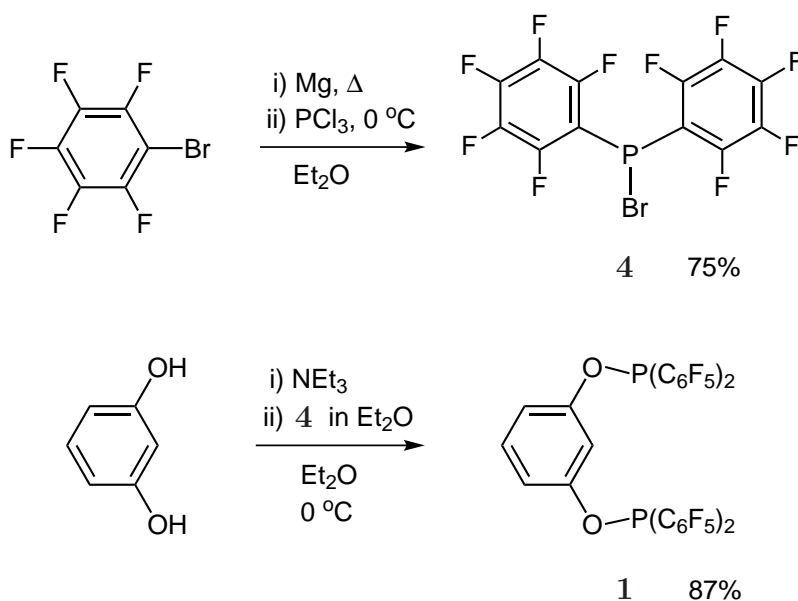
Substituent	^t Bu	Me	Ph	OPh	C ₆ F ₅	Cl	CF ₃
Effect on TEP (cm ⁻¹)	0.0	2.6	4.3	9.7	11.2	14.8	19.6

atom,³⁸ offering a point of contrast to these groups. Regardless of the exact nature of the electronic influence of pentafluorophosphines, they represent a class of compounds that are effective in producing electron-poor metal centres, and have been sparsely utilised in pincer ligands (with only complexes of ruthenium⁵⁶ and palladium⁵⁷ of one such ligand reported to date). Moreover, work has been reported on the synthesis and coordination chemistry of a bis(trifluoromethyl)phosphine PCP pincer ligand,⁵⁸ which enables direct comparisons to be made between the effect of the perfluorinated ligand substituents C₆F₅ and CF₃ on the chemistry of the resultant complexes.

As PCP pincer ligands with 1,3-substituted phenylene backbones are the most ubiquitous of pincer ligands,¹⁷ these provide an ideal starting point for the incorporation of the bis(pentafluorophenyl)phosphine moieties, as they allow for a high degree of comparability with the scientific literature. Three PCP pincer ligands were established as synthetic targets, with each possessing a different electronic character. The phosphinite ligand 1,3-[(C₆F₅)₂PO]₂C₆H₄ (referred to as POCOPH, **1**) was desirable as it should be the most electron-withdrawing of all the ligands, combining the low σ -donor ability of the bis(pentafluorophenyl)phosphine with the high π -acceptor ability of the phosphinite functionality. The phosphine ligand 1,3-[(C₆F₅)₂PCH₂]₂C₆H₄ (PCCCPH, **2**) was targeted as it was already known⁵⁷ but had scarcely been investigated in terms of coordination chemistry, and also possessed the more robust and widely used methylene bridges between the backbone and phosphine donors. The final PCP pincer ligand targeted was the asymmetric phosphine-phosphinite 1-[(C₆F₅)₂PO]-3-(^tBu₂PCH₂)₂C₆H₄ (POCCPH, **3**). This was desirable as it combined the electron-poor bis(pentafluorophenyl)phosphinite group with the electron-rich di-*tert*-butylphosphine donor group, allowing the mutually *trans* arrangement of donor and acceptor phosphines in resultant metal complexes to be studied. It was also desirable to investigate whether the introduction of an electron-rich donor would simply reduce the influence of the electron-poor donor, or give rise to new synergic effects.

2.1 Synthesis of Pentafluorophenyl-Substituted PCP Pincer Ligands

The synthesis of bis(pentafluorophenyl)phosphine-substituted pincer ligands first required the synthesis of the appropriate phosphine halide, Ar_2PX , as this comprises the basic building block of the ligand and the means for incorporation of the electron-poor phosphorus donor into the pincer framework. Bis(pentafluorophenyl)phosphine bromide (**4**), was synthesised according to literature protocols.⁵⁹ This involved a Grignard-type reaction used to attach the pentafluorophenyl substituents to the phosphorus centre; purification by vacuum distillation afforded the product **4** in good yield (Scheme 2.1). The large steric bulk of the pentafluorophenyl group is advantageous in this instance, as it prevents trisubstitution to form the tertiary phosphine. Interestingly, while the reaction proceeds from a phosphine chloride starting material, halide exchange results in the product being a phosphine bromide.



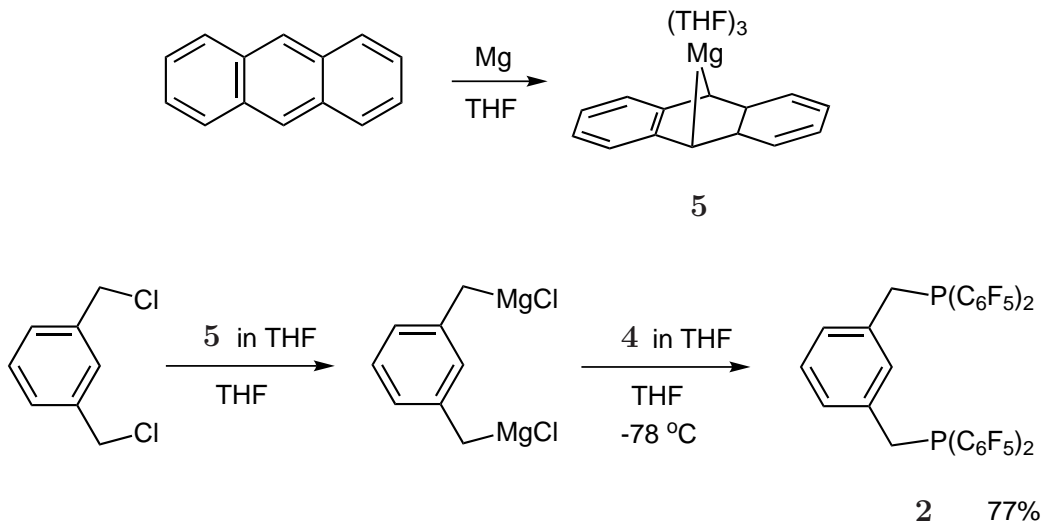
Scheme 2.1 Synthesis of the phosphinite pincer ligand **1**.

The synthesis of the POCOPH ligand **1** was then carried out *via* the reaction of the phosphine halide **4** with resorcinol (benzene-1,3-diol), as is typical for the formation of phosphinite compounds (Scheme 2.1).¹⁸ The reaction to form ligand **1** was performed according to a published procedure for the synthesis of a pentafluorophenylphosphinite ligand containing a BINOL backbone (where BINOL is 1,1'-bi-2-naphthol).⁶⁰ Dropwise addition of a solution of **4** in diethyl ether to a cooled mixture of resorcinol and triethylamine in diethyl ether resulted in the formation of a thick white suspension. Isolation of the supernatant liquid by filtration followed by removal of the volatiles *in vacuo* and recrystallisation from hexane/toluene afforded

ligand **1** in good yield.

Spectroscopic data for **1** was consistent with its formulation as the pentafluorophenyl-substituted POCOPH pincer ligand. The ^{31}P NMR spectrum of **1** displayed a quintet resonance (with $^3J_{\text{P-F}} = 35.0$ Hz, due to the phosphorus coupling to the four *ortho* fluorines of the pentafluorophenyl substituents) at $\delta_{\text{P}} = 87.1$ ppm, significantly downfield of the starting material **4** ($\delta_{\text{P}} = 12.1$ ppm). This downfield shift is typically observed upon the formation of phosphinite compounds, with representative examples reported by Morales-Morales⁶¹ and Motoyama.⁶² The ^1H and ^{19}F NMR spectra also displayed the expected number of environments for ligand **1** (three proton and three fluorine environments). To date, bis(pentafluorophenyl)phosphinite ligands have not been a significant synthetic target, with only a small number of compounds known, mostly comprising two phosphinite donors linked by a chiral, aliphatic backbone.^{63,64} The POCOPH compound **1** is the first example of the incorporation of the $\text{OP}(\text{C}_6\text{F}_5)_2$ functionality into a pincer ligand.

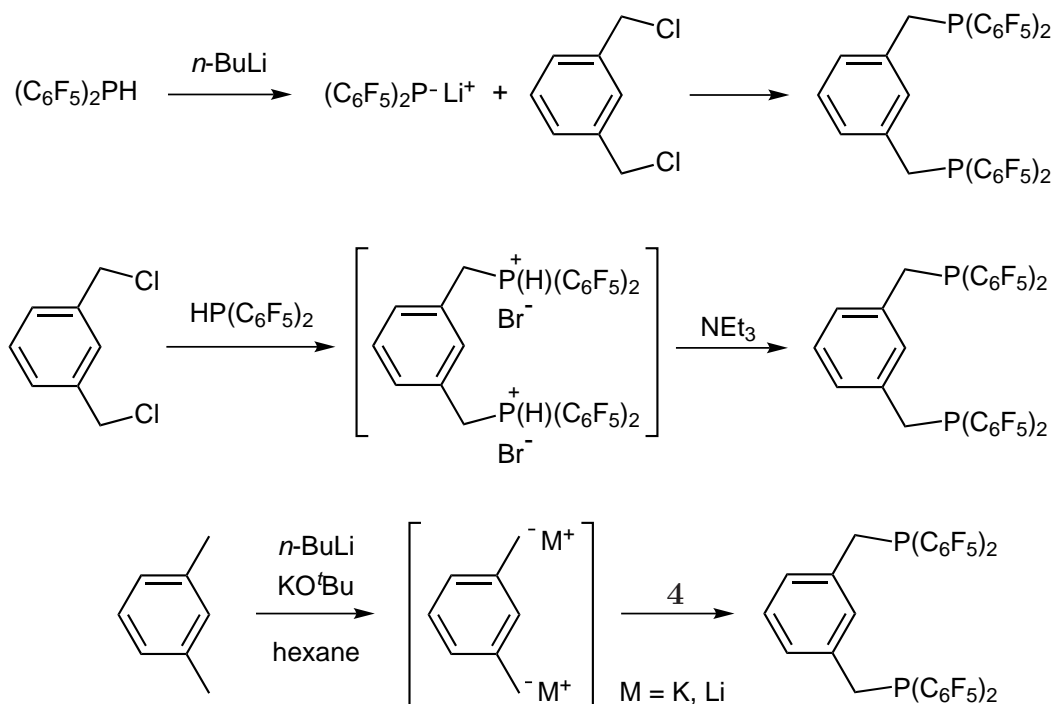
The synthesis of the PCCCPH ligand **2** has previously been reported by Chase and colleagues,⁵⁷ preparing the ligand *via* the reaction of **4** with the bis-Grignard reagent 1,3-(ClMgCH_2) $_2\text{C}_6\text{H}_4$. However, in replicating this procedure, the preparation of the Grignard reagent was found to be difficult and unreliable, typically resulting in low yields of the desired phosphine product (the greatest yield obtained in five attempts being 39%, only slightly lower than the 51% stated in the literature⁵⁷). An improved synthesis of **2** was employed, generating the bis-Grignard reagent with the more potent magnesiator, $[\text{Mg}(\text{anthracene})(\text{THF})_3]$ (**5**).



Scheme 2.2 Synthesis of the phosphine pincer ligand **2**.

The magnesium anthracene complex **5** was synthesised by the prolonged reaction of magnesium powder with anthracene in THF,⁶⁵ and isolated as an orange solid after stirring for four days (Scheme 2.2). This magnesium complex **5** was then used to generate the desired bis-Grignard reagent by reaction with α,α' -dichloro-*m*-xylene in THF. Subsequent reaction of the bis-Grignard reagent with the pentafluorophenylphosphine bromide **4** afforded the desired PCCCPH ligand **2**. The NMR data were consistent with the synthesis of **2**, displaying the expected four environments in the ^1H NMR spectrum, of which the methylene signal appeared as a doublet, due to coupling to the phosphorus atom. The phosphine signal itself appeared as a quintet in the ^{31}P NMR spectrum at -46.3 ppm, consistent with literature data for this compound.⁵⁷

Purification of **2** was achieved *via* column chromatography in air, as per the method of Chase,⁵⁷ giving **2** as a white solid in a yield of 67%, substantially greater than those obtained without the magnesium anthracene complex **5**. Due to the high air sensitivity and susceptibility to oxidation of most phosphine ligands, column chromatography is not usually employed during their purification. However, the pentafluorophenyl substituents of **2** serve to reduce the availability of the lone-pair of electrons on the phosphorus for bonding, making **2** sufficiently air-stable as to allow purification by column chromatography in air. Nonetheless, small amounts of the phosphine oxide were detected in samples of **2** left standing under ambient conditions overnight, and thus samples of the ligand (as well as all ligands reported herein) were stored under an inert atmosphere.



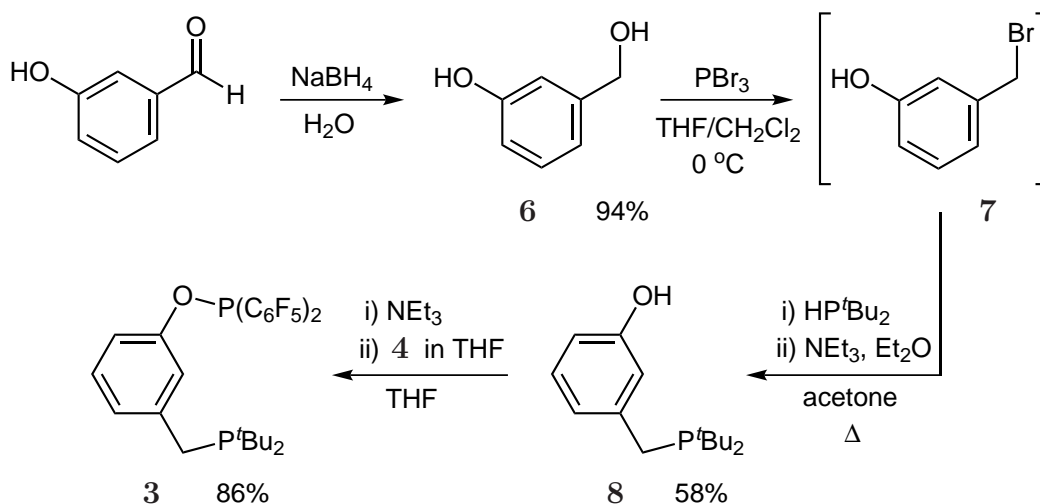
Scheme 2.3 Conventional phosphine syntheses unable to produce **2**.

The synthesis of the PCCCPH ligand **2** *via* a Grignard-type reaction scheme was required as reports indicated that **2** was unable to be synthesised using the two most common synthetic methodologies: by reaction of the benzylic halide either with the lithiated phosphine $\text{LiP}(\text{C}_6\text{F}_5)_2$, or with the secondary phosphine $\text{HP}(\text{C}_6\text{F}_5)_2$ followed by deprotonation of the intermediate halide salts using an amine base (Scheme 2.3).⁵⁷ This was attributed primarily to the bis(pentafluorophenyl)phosphine being too poor a nucleophile to displace the halides from the benzylic starting material, and also the poor stability of the $(\text{C}_6\text{F}_5)_2\text{P}^-$ anion, decomposing in solution even at $-78\text{ }^\circ\text{C}$.^{66*} Similar problems have been encountered in the synthesis of other fluoroarylphosphine phosphine ligands, as described in the review by Pollock and colleagues.³⁹ An alternate synthesis of **2** *via* reaction of the phosphine bromide **4** with the dimetallated intermediate $1,3-(\text{MCH}_2)_2\text{C}_6\text{H}_4$ (where M is potassium or lithium) was also attempted and found to be unsuccessful, with **2** comprising only a minor part of the reaction mixture. This is likely due to the low selectivity of metallation at the benzylic positions.⁶⁸

The unsymmetrical POCCPH pincer ligand **3** was prepared in a similar manner to that of the two previously published examples of phosphine-phosphinite pincer ligands.^{13,69} The synthesis (Scheme 2.4) followed literature procedures for the reduction of 3-hydroxybenzaldehyde to 3-hydroxybenzyl alcohol (**6**),⁷⁰ and then bromination of the benzylic hydroxyl with phosphorus tribromide to give 3-hydroxybenzyl bromide (**7**).⁷¹ Intermediate **7** was reported to degrade over time, so was used in the crude form for the subsequent reaction. The P^tBu_2 moiety was then installed by nucleophilic attack of di-*tert*-butylphosphine at the benzylic carbon of **7**, followed by deprotonation of the phosphorus with triethylamine. While such a reaction does not proceed with electron-poor phosphines (and hence could not be used in the synthesis of **2**), the higher nucleophilicity of the *tert*-butyl-substituted phosphine allowed the reaction to proceed smoothly, giving the benzylic phosphine **8** in a 58% yield across the two steps from **6**. The synthesis was completed by formation of the phosphinite P–O linkage by reaction of the phenol functionality of **8** with the bis(pentafluorophenyl)phosphine bromide **4**, in an almost identical manner to the synthesis of the POCOPH ligand **1**. The new phosphine-phosphinite ligand **3** was isolated as a pale yellow oil, which solidified into a cream-coloured solid on cooling to $-15\text{ }^\circ\text{C}$, in an 86% yield. This corresponded to an overall yield of 46% for the four steps from 3-hydroxybenzaldehyde.

The NMR data of ligand **3** showed that the replacement of one of the $\text{OP}(\text{C}_6\text{F}_5)_2$ groups of **1** with a $\text{CH}_2\text{P}^t\text{Bu}_2$ group had only a small effect on the chemical shift of

*The use of $(\text{C}_6\text{F}_5)_2\text{P}^-$ as a nucleophile has previously been reported in the literature,⁶⁷ but the phosphide itself was unable to be isolated, or trapped by coordination to transition metal ions. Subsequent work has been unable to isolate or reliably use bis(pentafluorophenyl)phosphide.



Scheme 2.4 Synthesis of the phosphine-phosphinite pincer ligand **3**.

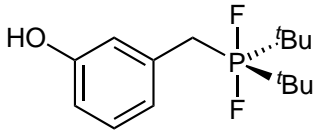
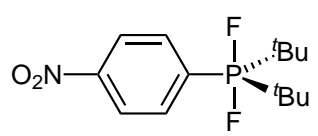
the remaining phosphinite, which appeared as a quintet resonance in the ^{31}P NMR spectrum at 82.9 ppm, close to the phosphinite chemical shift of **1** ($\delta_{\text{P}} = 87.1$ ppm). As expected, the phosphorus atom of the $\text{CH}_2\text{P}^t\text{Bu}_2$ group is significantly more shielded, appearing as a singlet in the ^{31}P NMR spectrum at 34.3 ppm. The proton spectrum is unremarkable, with four aromatic proton environments observed due to the asymmetry of the ligand backbone, and small P-H couplings displayed by the *tert*-butyl methyl groups ($^3J_{\text{P-H}} = 10.8$ Hz) as well as the benzylic methylene ($^2J_{\text{P-H}} = 2.6$ Hz).

The POCCPH ligand **3** is the first pincer ligand reported to possess both strongly electron-rich and electron-poor donor groups; the previous two reports of POCCPH ligands both possess the comparatively less electron-poor OP^iPr_2 group. Moreover, both the $\text{P}(\text{C}_6\text{F}_5)_2$ and P^tBu_2 moieties have been calculated to possess similar cone angles of 171° for $\text{PPh}(\text{C}_6\text{F}_5)_2$, and 170° for PPh^tBu_2 .^{37,38} Whilst cone angles only provide a rough guide as to the steric influence exerted by the ligands (not taking into account for example, the ability of the planar pentafluorophenyl substituents to interleave or stack, whereas *tert*-butyl groups cannot), these values indicate that bis(pentafluorophenyl)phosphines and di-*tert*-butylphosphines are at least comparable in terms of size. Therefore, there should be minimal steric differences between ligands **1**, **2**, and **3**, allowing any differences in reactivity between resultant complexes to be attributed primarily to electronic effects.

Ligand **3** was found to have undergone significant decomposition over the course of eight months stored at -15°C . Analysis of samples of **3** by NMR spectroscopy revealed the presence of a new product **9**, as well as several unidentified minor products. Spectroscopic data of **9** was highly indicative of addition of two fluorine atoms to the phosphorus atoms of the P^tBu_2 group, to form a new phosphorus(V)

PF₂^{*t*}Bu₂ group. The ¹H NMR spectrum of **9** revealed both the methyl protons of the *tert*-butyl groups and the methylene protons of the benzylic ligand backbone were coupling to two fluorine atoms, with each resonance appearing as a doublet of triplets instead of the doublets observed for ligand **3**. The ³¹P and ¹⁹F spectra of **9** were also consistent with the formation of a PF₂^{*t*}Bu₂ degradation product; the phosphorus signal appeared as a triplet, and a doublet resonance was observed for the fluorine signal, with each displaying a mutual phosphorus-fluorine coupling constant of 723 Hz.

Table 2.2 Comparison of NMR data of degradation product **9** in CDCl₃ with that of (4-NO₂-C₆H₄)PF₂^{*t*}Bu₂. Data is for the PF₂^{*t*}Bu₂ moiety of each compound.

	 Compound 9	 (4-NO ₂ -C ₆ H ₄)PF ₂ ^{<i>t</i>} Bu ₂ ^{<i>a</i>}
¹ H, δ _H	1.16 (dt, <i>J</i> = 18.1, 2.8 Hz)	1.17 (dt, <i>J</i> = 19.2, 2.8 Hz)
³¹ P, δ _P	−20.5 (t, ¹ <i>J</i> _{P-F} = 723 Hz)	−29.0 (t, ¹ <i>J</i> _{P-F} = 754 Hz)
¹⁹ F, δ _F	−49.1 (d, ¹ <i>J</i> _{P-F} = 723 Hz)	−56.1 (d, ¹ <i>J</i> _{P-F} = 754 Hz)

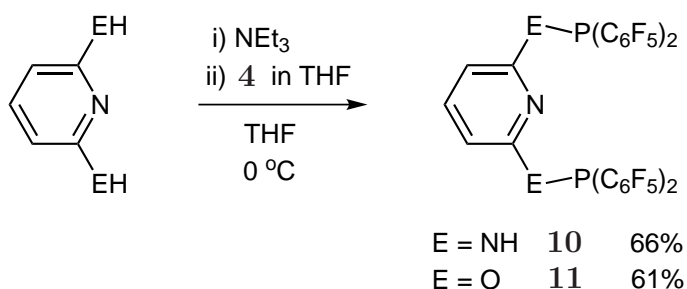
^{*a*}Data from Yandulov and Tran.⁷²

The spectroscopic data of **9** were very similar to the spectroscopic data reported for (4-NO₂-C₆H₄)PF₂^{*t*}Bu₂ (Table 2.2). As no resonance in the ³¹P NMR spectrum was observed for a OP(C₆F₅)₂ moiety associated with the degradation product **9**, the P–O bond was presumed to have been cleaved, giving **9** the formula (3-OH-C₆H₄)PF₂^{*t*}Bu₂. The fluorine atoms directly bound to the phosphorus are likely to have originated from the *ortho* or *para* positions of the pentafluorophenyl substituents on the phosphinite group, as these aromatic fluorines have been reported to be particularly susceptible to nucleophilic attack,^{73–75} even from phosphorus nucleophiles.⁷⁶ However, the mechanism for the fluorination of the di-*tert*-butyl phosphine group is not known. Attempts to purify the mixture by column chromatography were unsuccessful, with neither the POCCPH ligand **3** or the degradation product **9** able to be isolated. As such, the exact nature of **9** could not be unambiguously confirmed.

2.2 Synthesis of Pentafluorophenyl-Substituted PNP Pincer Ligands

With the synthesis of the pentafluorophenyl-substituted PCPH pincer ligands **1**, **2**, and **3** achieved, the synthesis of similar PNP pincer ligands was explored. The PNP pincer ligands made attractive synthetic targets as they could be prepared with a similar synthetic methodology to that of the previously synthesised PCP pincer ligands, starting from 2,6-substituted pyridine derivatives instead of 1,3-substituted phenylenes. An advantage of the PNP coordination motif is that the ligands contain only neutral donor atoms with available lone pairs of electrons, meaning that no ligand activation step is required to achieve tridentate “pincer” coordination to a metal centre (contrasting with the C-2 deprotonation required for PCP pincer coordination).

From the comparatively straightforward synthesis of the POCOPH ligand **1**, it was clear that the easiest way to incorporate bis(pentafluorophenyl)phosphine groups into the pincer motif was by direct reaction of the phosphine bromide **4** with an aromatic hydroxyl, to form a new P–O bond. As P–N bonds could be formed by the analogous reaction with aromatic amines, the new electron-poor PNNNP (**10**) and PONOP (**11**) ligands were synthesised *via* the reaction of **4** with 2,6-diaminopyridine and 2,6-dihydroxypyridine respectively (Scheme 2.5). The NMR data were as expected for the new compounds **10** and **11**, with each displaying two aromatic proton environments in their ^1H NMR spectra, and the expected quintet resonances in the ^{31}P NMR spectra (at $\delta_{\text{P}} = -10.8$ and 70.2 ppm respectively). It was interesting to note that in moving from a phenyl backbone in the POCOPH ligand **1** to a pyridyl backbone in the PONOP ligand **11**, the extra electron density furnished to the aromatic ring by the nitrogen served to increase the shielding of the phosphorus donor atoms, shifting the ^{31}P NMR resonance from 87.1 ppm in **1** to 70.2 ppm in **11**.



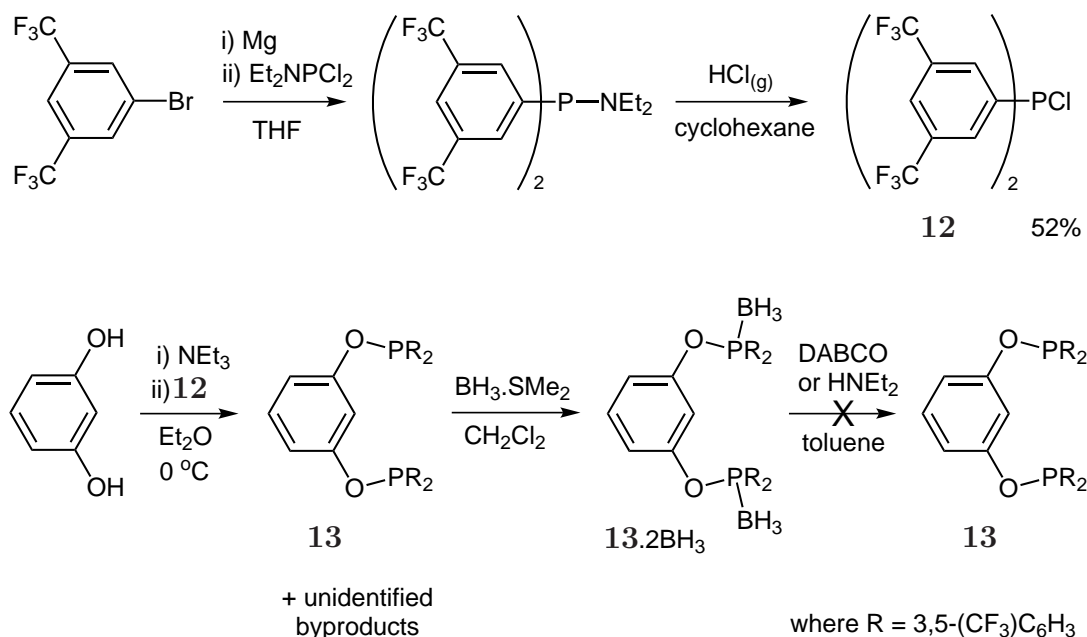
Scheme 2.5 Synthesis of the PNP pincer ligands **10** and **11**.

These reactions were performed under similar conditions to the synthesis of the POCOPH ligand **1** (using triethylamine as a base, stirring the reaction mixture at 0 °C for one hour then warming to room temperature overnight), affording the PNP pincer complexes **10** and **11** in modest yields of 66% and 61% respectively. Notably, the previously reported syntheses of PONOP and PNNNP ligands required much harsher conditions, with elevated temperatures of 65–80 °C and either prolonged reaction times (about one week)⁷⁷ or the addition of the strong base *n*-butyllithium.^{78,79} As these reported syntheses were for ligands that possessed *tert*-butyl and isopropyl substituents, they were substantially more electron-rich than ligands **10** and **11**. It appears that the significant electron-withdrawing character of the pentafluorophenyl substituents serves to enhance the reactivity of the phosphine bromide **4** with aryl amines and alcohols, facilitating the synthesis of the PNP ligands **10** and **11**.

2.3 Attempted Synthesis of Trifluoromethylaryl-Substituted Ligands

To offer a point of comparison with the pentafluorophenyl-containing ligands, the synthesis of PCP pincer ligands containing 3,5-bis(trifluoromethyl)phenyl substituents was pursued. Phosphine ligands possessing these trifluoromethylaryl substituents have been shown to possess a slightly more electron-donating character and a slightly smaller steric influence than the analogous pentafluorophenyl phosphines.⁸⁰ However, the smaller size of the 3,5-(CF₃)₂C₆H₃ group introduces the possibility of trisubstitution to form the tertiary phosphine P[3,5-C₆H₃(CF₃)₂]₃ during the synthesis of the halophosphine ligand precursor [3,5-(CF₃)₂C₆H₃]₂PCl (**12**) when trichlorophosphine is used as a starting material (as in the synthesis of the pentafluorophenylphosphine bromide **4**). To avoid this, the halophosphine **12** was prepared from the diethylamine-protected phosphine chloride Et₂NPCl₂, as the diethylamine group is not displaced by the aryl Grignard reagent, preventing tertiary phosphine formation (Scheme 2.6).⁸¹ Removal of the diethylamine protecting group by reaction with hydrogen chloride gas gave the desired phosphine chloride species **12**.

With **12** in hand, synthesis of the desired 3,5-bis(trifluoromethyl)phenyl-substituted phosphinite pincer ligand (**13**) was then attempted from resorcinol (Scheme 2.6), as for the synthesis of the pentafluorophenyl-substituted POCOPH ligand **1**. However, reaction between **12** and resorcinol did not proceed selectively at room temperature, affording the desired ligand **13** (in about 65% yield, identified by NMR spectroscopy,



Scheme 2.6 Attempted synthesis of PCP pincer ligand **13**.

$\delta_{\text{P}} = 102.0$ ppm) along with four unidentified minor products. Ligand **13** was not able to be purified by recrystallisation, and proved to be too sensitive to purify by column chromatography in air. To overcome this, **13** was borane-protected by stirring with a stoichiometric amount of $\text{BH}_3 \cdot \text{SMe}_2$, affording the air-stable adduct **13.2BH₃**. The reaction mixture was successfully purified by column chromatography on silica. However, attempts at deprotecting the pure **13.2BH₃** with either DABCO (1,4-diazabicyclo[2.2.2]octane)⁸² or the less basic diethylamine⁸³ were unsuccessful. In both instances deprotection led to the formation of decomposition products which NMR spectroscopy indicated were likely to be $\text{HP}[\text{C}_6\text{H}_3(\text{CF}_3)_2]_2$ and $\text{HP(O)}[\text{C}_6\text{H}_3(\text{CF}_3)_2]_2$ or similar species (at $\delta_{\text{P}} = -42.6$ and 10.6 ppm respectively). This is likely to be promoted through P–O cleavage by nucleophilic attack of the amine base on the electron-poor, electrophilic phosphorus centre. Thus ligand **13** could not be isolated and the synthesis of further 3,5-bis(trifluoromethyl)phenyl-substituted ligands was not pursued, owing to the sufficient diversity of the POCOP (**1**), PCCCP (**2**), POCCP (**3**), PNPNP (**10**), and PONOP (**11**) ligands already in hand.

2.4 Concluding Remarks

A range of bis(pentafluorophenyl)phosphine-substituted PCPH and PNP pincer ligands were prepared using bis(pentafluorophenyl)phosphine bromide (**4**). Reactions

between **4** and aromatic alcohols or amines proceeded selectively at room temperature, giving the desired phosphinite or phosphoramine ligand in yields of typically 60–70%. This method provided a simple yet effective strategy for the synthesis of electron-poor pincer ligands **1**, **10**, and **11**, as well as for the mixed phosphine-phosphinite ligand **3**.

The synthesis of the PCCCPH pincer ligand **2** proved to be more difficult than for the aforementioned ligands, as common literature protocols for the synthesis of phosphine pincer ligands could not be employed due to the low nucleophilicity of **4**, along with the low stability of its anionic form, $(\text{C}_6\text{F}_5)_2\text{P}^-$. Ligand **2** was generated *via* the reaction of **4** with the bis-Grignard reagent derived from α,α' -dichloro-*m*-xylene. Formation of the bis-Grignard reagent from the magnesium anthracene complex **5** afforded a substantial increase in the isolated yield of **2** when compared to the formation of the Grignard reagent directly from magnesium turnings.

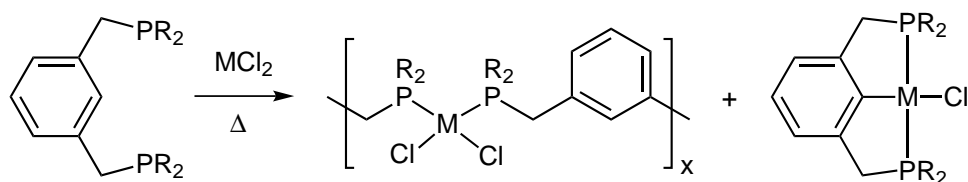
The formation of further electron-poor PCPH pincer ligands with trifluoromethylated aromatic substituents was attempted, but the resultant phosphinite ligand **13** was unable to be purified by recrystallisation or column chromatography in air. Formation of the borane-protected adduct **13**.2BH₃ followed by column chromatography resulted in sufficient purification of the protected ligand. However, deprotection could not be achieved by using established literature protocols, and the synthesis of pincer ligands containing 3,5-bis(trifluoromethyl)phenyl substituents was not pursued further.

Chapter 3

Coordination Chemistry of PCP Pincer Ligands

3.1 Historical Overview

The first κ^3 -PCP complexes were reported by Moulton and Shaw in 1976.⁸⁴ Having noted that cyclometallation reactions were prevalent in complexes with bulky phosphine ligands, they designed a ligand in which an aromatic carbon flanked by two $\text{CH}_2\text{P}^t\text{Bu}_2$ groups would readily undergo *ortho*-metallation to give a tridentate PCP coordination motif. While the nickel and palladium pincer complexes $[(\text{PCP})\text{MCl}]$ were readily synthesised from the appropriate metal chlorides, it was noted that the analogous platinum pincer complex was formed in poor yields, with insoluble polymers of the type $[(\text{PCPH})\text{PtCl}_2]_x$ being formed (Scheme 3.1).



Scheme 3.1 Formation of a cyclometallated κ^3 -PCP pincer complex, along with a bridged κ^2 -PP oligomer (where M is typically Pt or Pd). The oligomer may contain metal centres in either *cis* or *trans* coordination geometries.

By replacing the aromatic ligand backbone with an alkyl chain, the energy requirement for metallation can be increased, allowing these unmetallated, multimetallic compounds to be isolated and characterised. Reactions between the aliphatic

phosphines $^t\text{Bu}_2\text{P}(\text{CH}_2)_n\text{P}^t\text{Bu}_2$ (where $n = 5-8$) and platinum and palladium salts showed that the formation of κ^2 -PP bridged dimeric and oligomeric species of the type $[\text{MCl}_2\{^t\text{Bu}_2\text{P}(\text{CH}_2)_n\text{P}^t\text{Bu}_2\}]_x$ was very facile.⁸⁵ Upon heating these compounds, the pentane-bridged diphosphine ($n = 5$) underwent cyclometallation to produce the tridentate pincer species $[\text{PtCl}(^t\text{Bu}_2\text{P}(\text{CH}_2)_2\text{CH}(\text{CH}_2)_2\text{P}^t\text{Bu}_2)]$. The metallation of these dimers and oligomers revealed that they were not unwanted byproducts produced during pincer synthesis, but rather were intermediates that in many cases could be further reacted to form the metallated pincer compounds.

Further insight into the importance of these bridged κ^2 -PP coordination compounds in the formation of pincer complexes was provided by Rimml and Venanzi in 1983. Reactions using the phenyl-substituted pincer ligand 1,3-bis(diphenylphosphino)-*m*-xylene was seen to produce oligomeric species of the type *cis*- $[(\text{PCPH})\text{PtX}_2]_n$ along with the desired PCP pincer species.⁸⁶ None of the corresponding *trans*-oligomer was observed, leading the authors to speculate that *trans*-oligomer formation was conducive to pincer complex formation, as it brought the C-H bond which is to be activated closer to the metal centre. This was able to explain why *tert*-butyl phosphine groups assisted the cyclometallation, as their large steric bulk favoured the formation of *trans*-bridged coordination complexes.

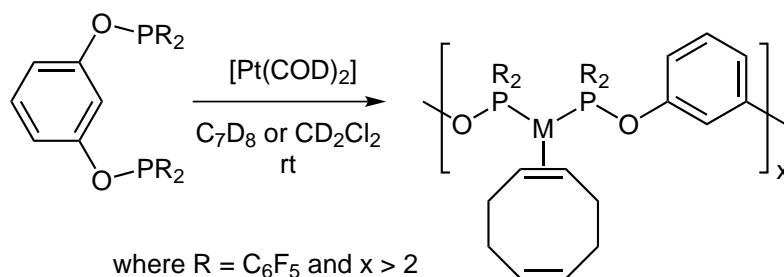
Because bis-phosphines have a known predilection for κ^2 -coordination modes, and in many instances ligand cyclometallation is not facile, bridged dimeric and oligomeric structures represent important precursors in the synthesis of κ^3 -PCP pincer complexes. However, despite the prevalence of these bridged structures in pincer synthesis, comparatively little work has been reported on their formation during the metallation reaction, and how their presence affects the ease of pincer formation.

Therefore, the coordination chemistry of the electron-deficient PCPH pincer ligands **1**, **2**, and **3** with platinum and palladium was investigated. An advantage of utilising electron-poor phosphine ligands in these metallation reactions is that they have the potential to favour coordination modes and geometries that differ from those of their more electron-rich counterparts, an effect that has been previously observed in 5- and 6-coordinate iridium and rhodium complexes.^{43,45} This preference for less conventional coordination geometries was anticipated to stabilise coordination complexes and metallation reaction intermediates not often observed in the literature, in the hope that examination of these species would reveal more about the nature of pincer complex formation.

3.2 Coordination to Pt(0)

Coordination chemistry of the most electron-poor ligand, POCOPH, **1**, was initially explored with platinum(0). While the coordination chemistry of *ortho*-xylyl-type diphosphines with Group 10 metals in the zero oxidation state has long been established,⁸⁷ minimal work has been reported with the analogous *meta*-substituted ligands. It was hoped that the highly electron-poor nature of **1** would facilitate electrophilic metallation of the backbone to produce the tridentate oxidative addition product, [(POCOP)PtR], where R is an alkyl group arising from a neutral alkene ligand on the platinum precursor accepting the metallated proton.

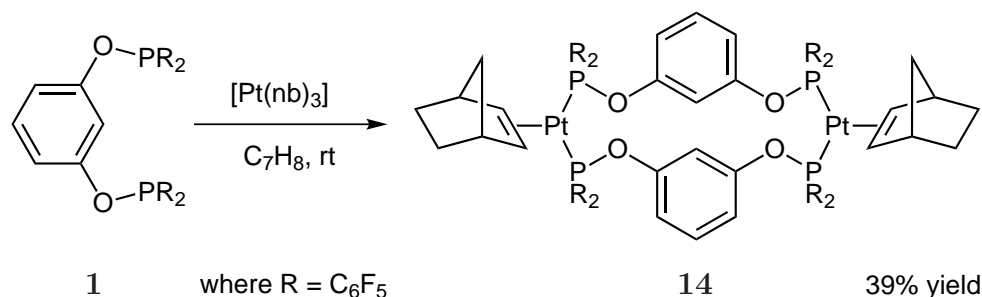
Initial reactions with [Pt(nb)₃] and [Pt(COD)₂] (where nb = norbornene and COD = 1,5-cyclooctadiene) were carried out in NMR tubes, allowing the reaction progress to be continually monitored by ¹H, ¹⁹F, and ³¹P NMR spectroscopy. Reactions involving [Pt(COD)₂] were seen to produce a single product; however, in both toluene-*d*₈ and dichloromethane-*d*₂ large amounts of poorly-soluble material were present, and spectra possessed broad resonances with a poor signal-to-noise ratio. The product displayed a ³¹P NMR shift of 108.9 ppm and a ¹J_{Pt-P} coupling of 5448 Hz; the downfield shift of the phosphorus signal and very large platinum-phosphorus coupling indicated coordination of a phosphorus donor *trans* to the weakly-coordinated η²-1,5-cyclooctadiene ligand.* Unfortunately, the ¹H NMR data could not unambiguously confirm the presence of coordinated 1,5-cyclooctadiene due to the very broad, weak nature of the signals. This data, together with the poorly soluble nature of the product and its similarity to the analogous norbornene species discussed below, allowed the product to be tentatively assigned as an oligomer of the type [(POCOPH)Pt(η²-COD)]_x, where x may be > 2, (due to the very low solubility of the observed product, Scheme 3.2).



Scheme 3.2 Oligomer formation from the reaction of **1** with [Pt(COD)₂].

*In all coordination chemistry with **1** reported herein, ¹J_{Pt-P} values of > 4200 Hz were diagnostic for coordination of the phosphorus atoms *trans* to a ligand of low *trans*-influence, typically a chloride or an η²-alkene.

Compared to reactions with the COD starting material, NMR-scale reactions between $[\text{Pt}(\text{nb})_3]$ and **1** produced substantially smaller quantities of insoluble material and much sharper signals in the NMR spectra. The phosphorus NMR data of the major product ($\delta_{\text{P}} = 100.5$ ppm, $^1J_{\text{Pt-P}} = 4623$ Hz), with a single phosphorus environment and large platinum-phosphorus coupling, along with the observation of coordinated norbornene in the ^1H NMR spectrum ($\delta_{\text{H}} = 2.75$ ppm, $^2J_{\text{Pt-H}} = 70.8$ Hz, $\text{HC}=\text{CH}$) was again indicative of the formation of a $[(\text{POCOPH})\text{Pt}(\text{nb})]_x$ species. The product was isolated by repeating the reaction on a larger scale in toluene, separating the desired product from less soluble polymers and higher oligomers by extraction into dichloromethane (Scheme 3.3). High Resolution Mass Spectrometry (HRMS) confirmed that the product of this reaction was the dimeric species $[(\text{POCOPH})\text{Pt}(\text{nb})]_2$ (**14**), observed as the sodium ion adduct without coordinated norbornene at $m/z = 2087$ amu.



Scheme 3.3 Formation of $[(\text{POCOPH})\text{Pt}(\text{nb})]_2$ (**14**) from the reaction of **1** with $[\text{Pt}(\text{nb})_3]$.

An additional $[(\text{POCOPH})\text{Pt}(\text{nb})]_x$ species with similar spectroscopic data to **14** was observed as a minor product in many of these reactions. The ^{31}P NMR data ($\delta_{\text{P}} = 102.1$ ppm, $^1J_{\text{Pt-P}} = 4700$ Hz) again suggested the coordination of the phosphorus *trans* to a norbornene ligand, which was observed in the ^1H NMR overlapping with the norbornene resonances of **14**. Over time the NMR signals of this oligomeric species disappeared as it was either converted to **14** or precipitated out of solution as polymeric material. The disappearance of this minor product was observed to occur faster in toluene and benzene than in dichloromethane. Where small quantities of this byproduct were found to still be present in reactions of **1** and $[\text{Pt}(\text{nb})_3]$ in dichloromethane even after 48 hours at reflux, resuspension of the material in toluene followed by heating to 50 °C for 12 hours resulted in complete disappearance of this minor product. The reason for these reactions proceeding faster in toluene than dichloromethane may be due to the aromatic solvent providing the ligand with stabilising π - π interactions during the rearrangement process from oligomer to dimer, thereby minimising the energetic barrier to this transformation.

Crystals of **14** suitable for single crystal X-ray diffraction were grown from a dichloromethane solution layered with methanol. The X-ray crystal structure (Figure 3.1) supports the NMR and HRMS assignment of **14** as a dimer, crystallising as the dichloromethane solvate $[(\text{POCOPH})\text{Pt}(\text{nb})]_2 \cdot 2\text{CH}_2\text{Cl}_2$ in the monoclinic space group $P2_1/n$. As this is a centrosymmetric space group, the asymmetric unit can be proscribed about one half of the molecule, with the other half generated through the centre of inversion. Important bond lengths and angles are summarised in Table 3.1, and crystallographic data collection and refinement parameters are stated in Table 3.2.

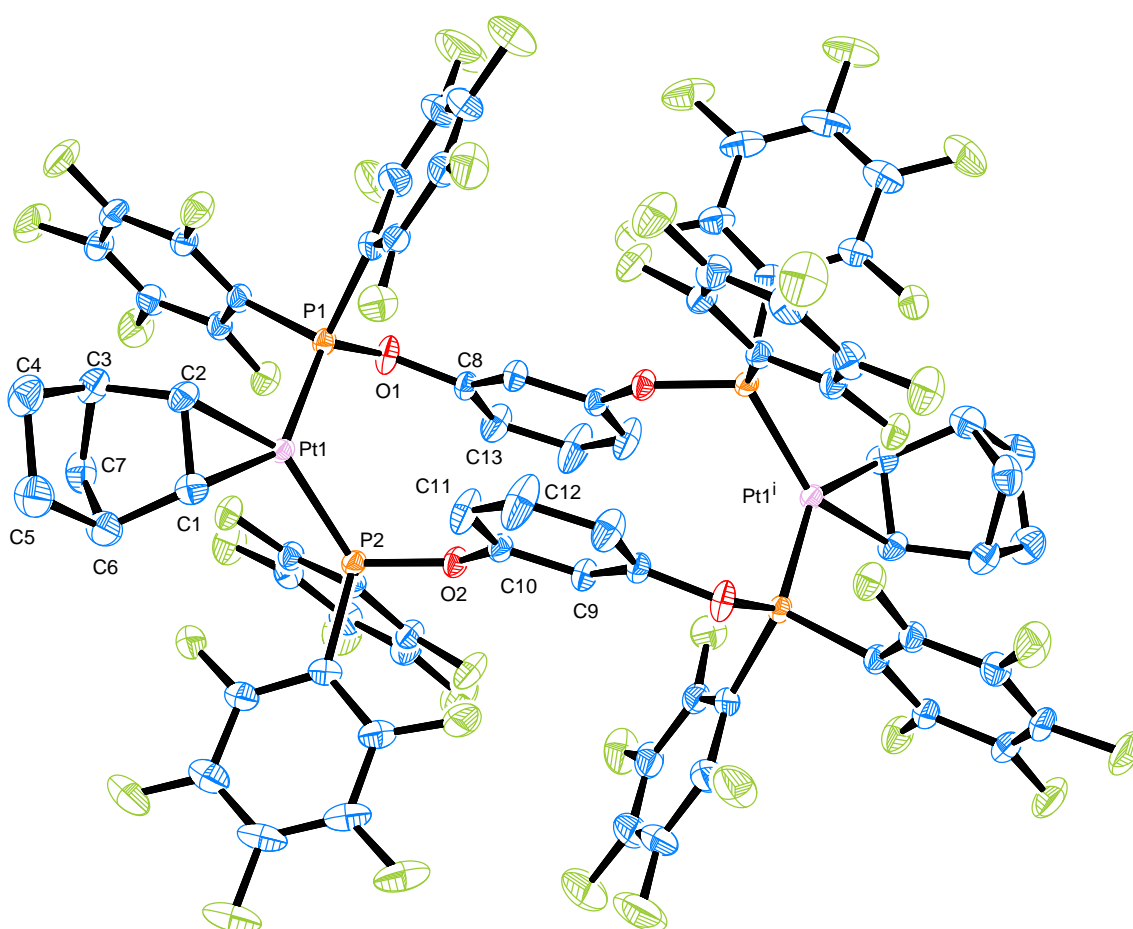


Figure 3.1 ORTEP diagram of $[(\text{POCOPH})\text{Pt}(\text{nb})]_2 \cdot 2\text{CH}_2\text{Cl}_2$ (**14**) (50% probability thermal ellipsoids). Dichloromethane solvate and hydrogen atoms omitted for clarity. Atoms denoted by ⁱ are generated from the asymmetric unit by inversion.

Table 3.1 Selected bond distances (Å) and angles (°) of $[(\text{POCOP})\text{Pt}(\text{nb})]_2 \cdot 2 \text{CH}_2\text{Cl}_2$ (**14**).

Bond distances (Å)		Bond angles (°)	
Pt1–C1	2.153(2)	P1–Pt1–P2	108.04(2)
Pt1–C2	2.139(2)	P1–Pt1–C2	103.80(7)
Pt1–P1	2.2110(6)	P2–Pt1–C1	109.12(6)
Pt1–P2	2.2224(5)	Pt1–P1–O1	121.37 (7)
C1–C2	1.434(3)	Pt1–P2–O2	117.14(6)
Pt1 \cdots Pt1 ⁱ	8.4535(2)	P1–P2 \cdots C1–C2	179.6(2)

Table 3.2 Crystallographic data of $[(\text{POCOP})\text{Pt}(\text{nb})]_2 \cdot 2 \text{CH}_2\text{Cl}_2$ (**14**).

Empirical formula	$\text{C}_{74}\text{H}_{28}\text{F}_{40}\text{O}_4\text{P}_4\text{Pt}_2 \cdot 2 \text{CH}_2\text{Cl}_2$
Formula weight	2424.88
Crystal system	Monoclinic
Space group	$P2_1/n$
a/Å	14.0338(4)
b/Å	18.4499(5)
c/Å	15.2852(4)
$\alpha/^\circ$	90.00
$\beta/^\circ$	91.299(2)
$\gamma/^\circ$	90.00
V/Å ³	3956.66(19)
Z	2
Cell determination reflections	9272
Cell determination range, $\theta_{\min} \longrightarrow \theta_{\max}/^\circ$	2.24 \longrightarrow 32.53
Temperature/K	113(2)
Radiation type	Mo K α
Radiation (λ)/Å	0.71073
Crystal size/ mm	0.37 \times 0.36 \times 0.31
$D_{\text{calc}}/\text{g m}^{-3}$	2.035
F(000)	2328
μ/mm^{-1}	3.89
Experimental absorption correction type	None
Reflections collected	117634, $R_{\text{equiv}} = 0.0467$
Index range h	–21 \longrightarrow 21
Index range k	–26 \longrightarrow 28
Index range l	–23 \longrightarrow 22
θ range/°	2.58 \longrightarrow 33.23
Independent reflections	14920
Reflections [$I > 2\sigma(I)$]	12169
Restraints/parameters	0/586
GOF	1.032
R_1 [$I > 2\sigma(I)$]	0.0279
w R_2 [$I > 2\sigma(I)$]	0.0629
R_1 [all data]	0.0415
w R_2 [all data]	0.0678
Residual density/e Å ^{–3}	–1.221 $<$ 2.599

The structure revealed two trigonal planar platinum cores, bridged by two molecules of **1** in a *cis*- κ^2 -PP fashion, with the norbornene bound “in-plane” in a conventional η^2 manner (P1–P2 \cdots C1–C2 torsion angle of 179.6°). While NMR data demonstrated that the norbornene is in a symmetrical coordination environment in solution, crystal packing constraints cause it to be pushed 2.7° from the normal, closer to P1. Compound **14** is only the third reported crystal structure[†] containing the [P₂M⁰(nb)] coordination environment (where M is metal in the zero oxidation state). In comparison to the previously reported structures,^{88,89} **14** contains a relatively short norbornene C=C bond (1.434(3) Å compared to 1.460(11) and 1.469(8) Å for reported structures) and a longer Pt–C bond (average of 2.146(4) Å compared to 2.109(15) and 2.113(10) Å for reported structures), possibly indicating a weakly bound norbornene. It may be anticipated that the electrophilic platinum centre of **14** generated by the electron-poor phosphinite **1** should foster a strong metal-alkene interaction by acting as a better electron acceptor. However, the reduced electron density on the platinum clearly limits the extent to which π -backbonding occurs in this system, explaining the short norbornene C=C bond (through less donation into the π^* orbital) and the long Pt–C distance.

Complex **14** displayed a platinum-carbon coupling of 259 Hz between the platinum and the coordinated alkene, significantly lower than the corresponding value of 344 Hz reported for the *tert*-butyl-substituted compound [(dtbpe)Pt(nb)] (where dtbpe is 1,2-bis(di-*tert*-butylphosphino)ethane).⁸⁹ This data also suggests a weaker metal-norbornene interaction is present in **14** than in its more electron-rich analogue, consistent with decreased π -backbonding to the alkene for the electron-poor complex **14**. Comparison of NMR data with similar pentafluorophenyl-substituted compounds was not possible, as compound **14** represents only the second reported instance of a platinum-alkene complex containing a pentafluorophenyl moiety, and the first such compound to be crystallographically characterised. The compound [{(C₆F₅)₃P]₂Pt(nb)] has been reported by the Pringle research group,⁸⁰ but no ¹H or ¹³C NMR data were provided to indicate the strength of the Pt-alkene interaction.

The P–Pt–P angle in **14** of 108.04(2)° is smaller than the idealised trigonal planar bond angles of 120°, but larger than the significantly constrained P–Pt–P bite angles of approximately 89° seen in norbornene complexes with chelating rather than bridged phosphines.^{88,89} The observed geometry is in good agreement with that expected for a platinum-alkene complex containing bulky phosphorus-donor ligands, with complexes of the type [Pt(nb){P(OAr)₃}]₂ displaying P–Pt–P bond angles of around 105°. ⁹⁰ A similar coordination geometry is also adopted by *cis*-bridged platinum(II) dimers when a group with a small steric bulk (such as a methyl)

[†]According to a search of the Cambridge Structural Database, v5.33, February 2012 update.

is *trans* to the phosphorus, giving P–Pt–P angles of around 103°. ^{58,91}

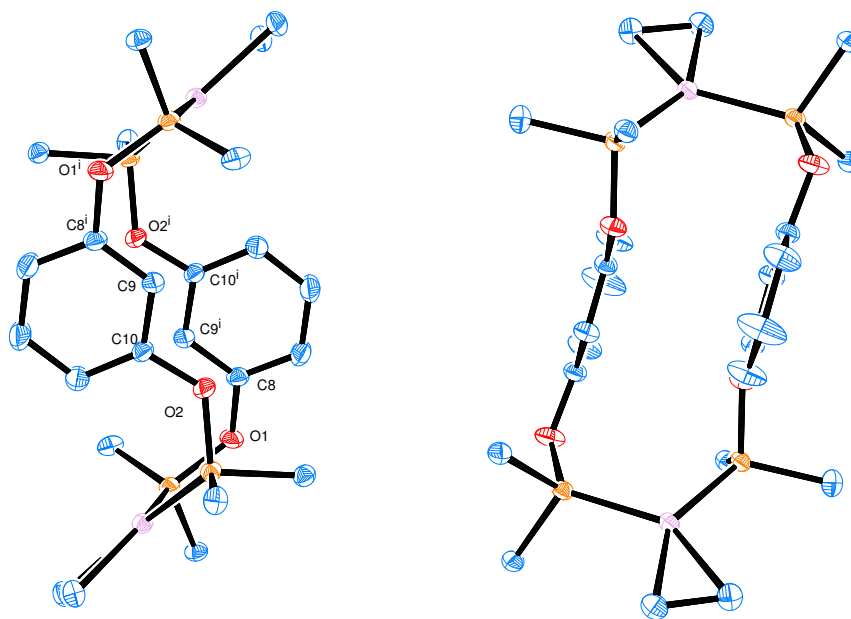


Figure 3.2 ORTEP diagram of $[(\text{POCOPH})\text{Pt}(\text{nb})]_2 \cdot 2 \text{CH}_2\text{Cl}_2$ (**14**) (50% probability thermal ellipsoids). Dichloromethane solvate, hydrogen atoms, norbornene and pentafluorophenyl substituents (except for carbons bound directly to platinum or phosphorus) omitted for clarity. Atoms denoted by ⁱ are generated from the asymmetric unit by inversion.

Another distinctive feature of the structure of **14** is the folding of the aryl backbones to lie parallel to each other (Figure 3.2). This is somewhat unusual, as all previously reported *cis*-dimers have rings canted towards each other by at least 10°; ^{58,91,92} in **14** they lie within 2° of parallel. This favourable “parallel displaced” configuration of the aromatic backbones, as well as the short interatomic distances ($\text{O2} \cdots \text{C9}^i = 3.201(3) \text{ \AA}$, $\text{C10} \cdots \text{C9}^i = 3.321(3) \text{ \AA}$, $\text{C10} \cdots \text{C10}^i = 3.387(3) \text{ \AA}$) indicate that π - π interactions should occur between the aromatic rings, ⁹³ conferring additional stability to the dimeric structure. As these favourable intramolecular interactions would not be available to an oligomeric species, this may explain why the oligomeric product initially observed appears to further rearrange to form the dimeric species **14** over time.

With **14** in hand and unambiguously characterised as the platinum-norbornene *cis*-dimer $[(\text{POCOPH})\text{Pt}(\text{nb})]_2$, attempts were made to promote metallation of the aromatic backbone at the 2-C position. Initially, thermolysis of toluene-*d*₈ solutions of **14** at 75 °C over a period of days was seen to have no significant effect; the only notable change in these solutions being the gradual appearance of decomposition products between 6.2–5.8 ppm in the ¹H NMR spectra, accompanied by a slight decrease in signal-to-noise ratio. Increasing the temperature to 100 °C did not produce

any observable metallation, instead serving to hasten decomposition.

The strong bases DMAP and DBU were employed in an attempt to promote the metallation under milder conditions, as they have been seen to facilitate metallation of pincer ligands in Ni(II) complexes.⁹⁴ The addition of DMAP to chloroform-*d* solutions of **14** at room temperature resulted in quantitative formation of a new complex, tentatively formulated as *trans*-[(POCOPH)Pt(L)]₂ (where L is a neutral ligand, either norbornene or the amine base) on the basis of NMR data. Instead of the downfield shift of the signal in the ³¹P NMR spectrum that usually accompanies pincer metallation, this compound displayed an upfield shift and decrease in platinum-phosphorus coupling constant consistent with a *trans*-dimer ($\delta_P = 49.5$ ppm, $^1J_{Pt-P} = 3250$ Hz), as well as diagnostic signals for the unmetallated ligand **1** in the ¹H NMR spectrum. Attempts to isolate this compound were unsuccessful, and attempts to promote metallation of the new *trans* species led to degradation and a loss of signals in the ³¹P NMR spectrum. Performing one-pot reactions with [Pt(nb)₃], ligand **1**, and DMAP or DBU were seen to solely produce degradation products, resulting in intractable mixtures that displayed no soluble, phosphorus-containing species.

In an attempt to avoid this decomposition, metallations were attempted using the strong non-nucleophilic base sodium hydride. Reactions were performed on an NMR scale, with an excess of sodium hydride (approximately ten equivalents) added to a dichloromethane-*d*₂ solution of **14**. No reaction was observed after heating for 18 hours at 40 °C, indicating that even in the presence of a strong base such as sodium hydride present the metallation reaction was not facile.

Acid was also employed to assist metallation of the ligand backbone to form a κ^3 -PCP pincer complex. The addition of acid to Pt(0) η^2 -norbornene complexes has been seen in some cases to result in the formation of the Pt(II) norbornyl species.⁸⁹ In employing the acid as an oxidant it was hoped that this would allow the norbornyl group generated to act as a proton acceptor, leaving as norbornane and forming the cationic, 14-electron pincer complex [(PCP)Pt]⁺. Treatment of dichloromethane-*d*₂ solutions of **14** with HBF₄ · Et₂O at -78 °C was seen to immediately produce a large number of broad, unidentified signals in the ¹H, ¹⁹F and ³¹P NMR spectra, with an intractable brown precipitate gradually forming in solution, accompanied by a decrease in signal-to-noise ratio in the NMR spectra of all nuclei studied. Protonation under milder conditions was also attempted using the carbacid HPhC(SO₂CF₃)₂. Solutions of **14** were treated with 1.4 equivalents of HPhC(SO₂CF₃)₂ and subjected to thermolysis in a range of solvents. No reaction was observed after prolonged heating at 40 °C in dichloromethane-*d*₂, 60 °C in benzene-*d*₆, and 50 °C in acetone-*d*₆.

Therefore, while the strong acid $\text{HBF}_4 \cdot \text{Et}_2\text{O}$ led to degradation of the platinum complex, the milder carbacid was not a strong enough oxidant to facilitate metallation to produce a platinum(II) complex, indicating that acid-promoted oxidation is not likely to provide viable route to pincer complexes from these platinum(0) dimers.

3.3 Coordination to Pt(II)

3.3.1 Reactions with $[\text{PtMe}_2(\text{1,5-hexadiene})]$

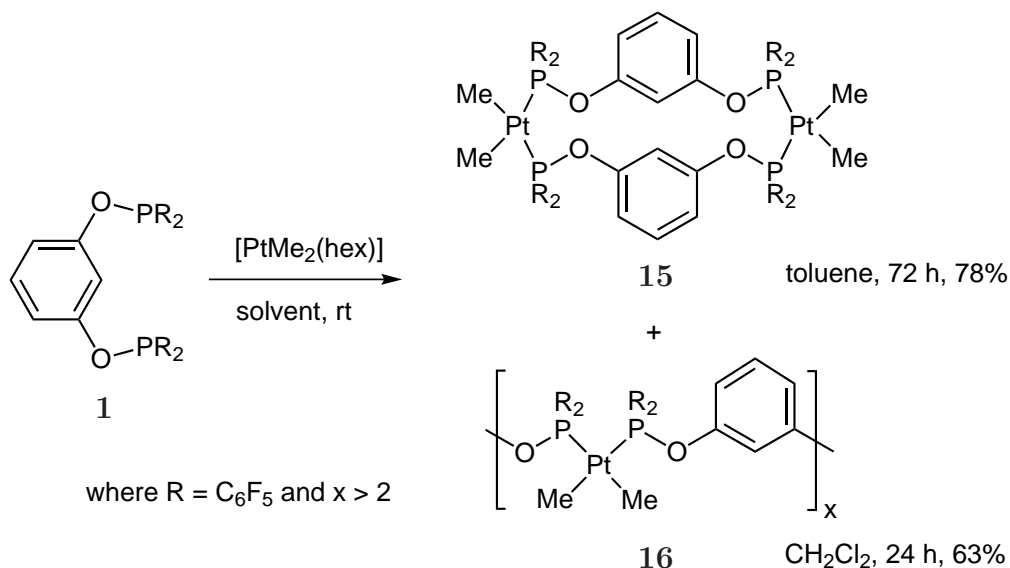
As attempts at generating a platinum-alkyl pincer complex $[(\text{PCP})\text{PtR}]$ from the Pt(0) norbornene dimer **14** were unsuccessful, the Pt(II) compound $[\text{PtMe}_2(\text{hex})]$ (where hex = 1,5-hexadiene) was investigated for its utility as a precursor toward the synthesis of a platinum-methyl pincer complex $[(\text{PCP})\text{PtMe}]$. It has been demonstrated in the literature that $[(\text{PCP})\text{PtMe}]$ complexes can be obtained in moderate yields directly from platinum dimethyl precursors.⁵⁸

As for the corresponding platinum(0) reactions, the coordination chemistry of **1** to $[\text{PtMe}_2(\text{hex})]$ was initially performed on a small scale in NMR tubes, allowing real-time monitoring of reaction progress by NMR spectroscopy. Reactions in both toluene- d_8 and dichloromethane- d_2 showed the formation of two major species **15** and **16** at room temperature. Each compound displayed ^1H NMR signals consistent with symmetrical, unmetallated aryl ligand backbones, and relatively small platinum-phosphorus couplings (≈ 2200 Hz) in the ^{31}P NMR spectrum, indicative of phosphorus coordination *trans* to a methyl group (which possess a large *trans* influence). This allowed for the formulation of both **15** and **16** as *cis*- $[(\text{POCOPH})\text{PtMe}_2]_x$ species. Compounds **15** and **16** displayed markedly different solubilities, and as such they were able to be separated and isolated by precipitation of the less soluble **16** by the addition of hexane to reaction mixtures in toluene.

Analysis by HRMS indicated that the more soluble species **15** was the dimeric compound *cis*- $[(\text{POCOPH})\text{PtMe}_2]_2$, with the $[\text{M}+\text{Na}]^+$ ion detected at $m/z = 2147$ amu. No adequate mass spectrometry results were obtained for **16**; in some cases traces of **15** were observed and in others no peaks attributable to a $[(\text{POCOPH})\text{PtMe}_2]_x$ species were observed. Liquid Chromatography Mass Spectrometry (LCMS) was performed in order to overcome contamination of each species by minor amounts of the other; however, LCMS was unsuccessful in this respect, as both compounds either degraded or were retained on the column. As such, while the HRMS

data were consistent with the formulation of **15** as the dimeric compound *cis*-[(POCOPH)PtMe₂]₂, it was not able to be definitively established.

Compound **16** is likely to be a cyclic [(POCOPH)PtMe₂]_x oligomer of relatively low molecular weight ($x = 3$ or 4); it is significantly less soluble than the dimeric **15** in common organic solvents, yet soluble enough that sufficient NMR data could be acquired for characterisation. It is highly unlikely to be a *cis*-monomer. Such species are well established for complexes of PCPH ligands with alkyl backbones (as the backbone can readily contort out of the coordination plane of the metal to minimise steric strain),^{95–97} but are seldom formed at room temperature in complexes with aromatic ligand backbones, due to the demands of forming a rigid, eight-membered chelate ring.⁹¹



Scheme 3.4 Formation of [(POCOPH)PtMe₂]_x species (**15** and **16**) from the reaction of **1** with [PtMe₂(hex)].

In the synthesis of **15** (Scheme 3.4), it was observed that longer reaction times and the use of toluene instead of dichloromethane increased the yield of the dimeric complex. This parallels observations in the synthesis of the analogous platinum(0) dimer **14**. While the corresponding platinum(0) oligomer was not soluble enough to characterise, it was noted that the dimer synthesis proceeded more rapidly and with the formation of less insoluble white material in benzene and toluene than in dichloromethane. As mentioned above, this may be due to stabilising interactions from the aromatic solvent increasing the rate of reaction.

The platinum [(POCOPH)PtMe₂]_x compounds **15** and **16** possessed very similar NMR spectroscopic data. However, in ¹H NMR spectra of the two species, there was a distinct chemical shift difference between protons on C-2 of each aromatic

backbone. For the oligomer **16** this proton was observed between the other two aromatic proton environments of the backbone at $\delta_{\text{H}} = 6.94$ ppm, whereas for the dimer **15** this proton was the most upfield of all the aromatic proton signals, appearing at $\delta_{\text{H}} = 6.42$ ppm. This observation of an upfield shift in H-2 again displayed parallels to the norbornene dimer **14**, where the H-2 signal was observed at $\delta_{\text{H}} = 6.35$ ppm. As the solid state structure of **14** displayed a distinct π - π interaction between the two ligand backbones, centred about H-2 (Figure 3.2), it is likely that this proton environment is shielded by the shared π -electrons, accounting for the observation of a upfield shift of H-2 in the two dimeric structures (Figure 3.3). Similar shielding of aromatic protons by π -stacking has been established in ^1H NMR spectroscopy of organic molecules.⁹⁸ It would be very difficult for the oligomeric structure **16** to adopt a conformation in solution possessing these intramolecular π - π interactions, and consequently **16** displayed an H-2 resonance at a similar chemical shift to the other aromatic protons of the backbone.

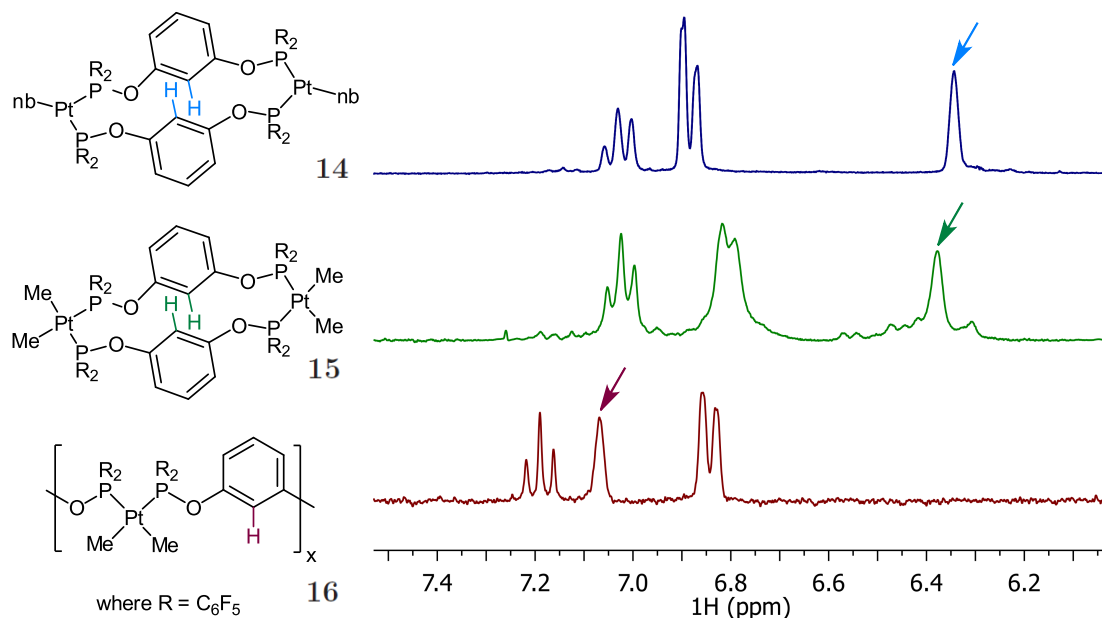


Figure 3.3 Effect of π - π stacking on the ^1H NMR spectra of compounds **14**, **15**, and **16** in acetone- d_6 .

Reaction mixtures containing the $[(\text{POCOPH})\text{PtMe}_2]_x$ species **15** and **16** were then heated to promote metallation and formation of the pincer $[(\text{POCOP})\text{PtMe}]$ species. Thermolysis of toluene solutions at 90 °C was seen to produce predominantly one new species, **17**. NMR signals of the species were extremely broad, rendering ^1H NMR data of little use in structural assignment. However, the ^{31}P NMR spectrum displayed two broad singlets in a 1:1 ratio at 113.1 and 96.3 ppm, with platinum-phosphorus coupling constants of 2032 and 2722 Hz respectively. This indicated the presence of phosphorus donors both *cis* and *trans* to a methyl group; the high solubility of the species in toluene and the propensity of ligand **1** to form bridged

κ^2 -PP dimers (see below) suggested that the complex was likely to be dimeric. This allowed for the tentative assignment of **17** as *cis,trans*-[(POCOP)PtMe₂]₂. Similar *cis,trans*-dimers were isolated from the reaction of ligand **1** with platinum dichloride and platinum chloromethyl precursors, and are subsequently discussed in detail.

Metallation of **17** was not observed to any appreciable extent after 20 hours at 90 °C. Upon increasing the temperature to 100 °C, the formation of the desired pincer species [(POCOP)PtMe] was detected ($\delta_P = 108.5$ ppm, $^1J_{Pt-P} = 3760$ Hz; verified by comparison with an independently synthesised sample, as is described in the Chapter 4). However, the appearance of this species was also accompanied by the formation of other unknown metallated pincer species, as well as the formation of perfluorinated biphenyl (C₁₂F₁₀), indicating the degradation of the ligand at these elevated temperatures.

In an attempt to reduce the temperatures required for this metallation, identical reactions were carried out in acetone. It was hoped that a more polar solvent would assist with the proton transfer during metallation and stabilise any charged transition states, minimising the energetic barrier to pincer complex formation. Reactions performed in acetone-*d*₆ in sealed NMR tubes heated to 75 °C were observed again to produce the broad resonances of **17**, without the observation of any products resulting from metallation. The addition of the amine bases DMAP and DBU to toluene solutions of [(POCOP)PtMe₂]_x was also attempted; however, as in the analogous reactions with the platinum-norbornene dimer **14**, only decomposition and a loss of signal in ³¹P NMR spectra was observed.

To investigate whether the difficulty in synthesising the metallated platinum methyl complex [(POCOP)PtMe] was due to the highly electron-deficient nature of the metal centre, or due to the inherent instability of **1** possessing highly polarised P–O bonds, reactions with the more electron-donating *tert*-butyl-substituted ligand **3** were performed. The reaction between **3** and [PtMe₂(hex)] was carried out in benzene-*d*₆ on an NMR scale. On standing at room temperature a number of products were initially observed by NMR spectroscopy. The major (and only identified) species in solution possessed two broad phosphorus signals in a 1:1 ratio at 88.7 and 48.3 ppm, with platinum-phosphorus coupling constants of 2268 and 1825 Hz respectively. The small downfield shift of the ³¹P NMR signal of each of the phosphorus donors from those of the free ligand (where $\delta_P = 82.9$ and 34.3 ppm), combined with relatively small one bond platinum-phosphorus couplings (around 2000 Hz) was consistent with the formation of a κ^2 -PP bridged species *cis*-[(POCCPH)PtMe₂]_x.

It is interesting to note that the di-*tert*-butyl phosphine moiety experienced a greater

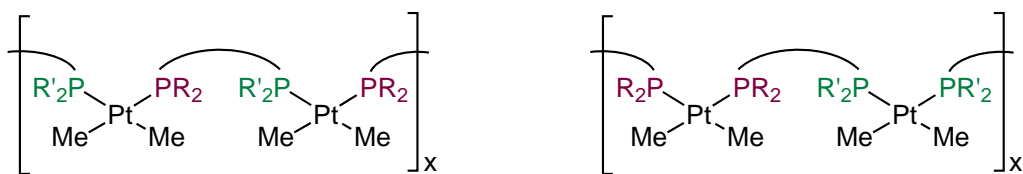


Figure 3.4 The two possible structural isomers that $[(\text{POCCPH})\text{PtMe}_2]_x$ may adopt in solution.

degree of deshielding than the bis(pentafluorophenyl)phosphinite on coordination to the platinum (with the δ_{P} moving downfield by 14.0 for the phosphine and 5.8 ppm for the phosphinite), as the more electron-donating $\text{CH}_2\text{P}^t\text{Bu}_2$ group contributed more electron density to the platinum than the more electron-withdrawing $\text{OP}(\text{C}_6\text{F}_5)_2$ group did. Due to this difference in σ -basicity, it may be expected that initial coordination of the *tert*-butyl phosphine would be favoured over coordination of the pentafluorophenyl phosphinite, yielding a complex containing two distinct platinum centres (Figure 3.4, right). However, due to the broad nature of the phosphorus resonances (full width at half height maximum of 75 and 98 Hz respectively) it is difficult to determine the exact coordination environment of the metal; the *cis* phosphorus-phosphorus coupling expected where different P-donors are coordinated to the same metal centre is on the order of tens of Hertz in similar platinum dimethyl complexes,⁹⁹ meaning that such a coupling may be present but not resolved in this instance.

On standing at room temperature, the NMR resonances of the $[(\text{POCCPH})\text{PtMe}_2]_x$ species were observed to broaden even further, producing a large number of unidentified signals in the ^{31}P NMR spectrum between 90 and 60 ppm. Thermolysis of the reaction mixture at 60 °C for 48 hours produced only small amounts of the desired $[(\text{POCCP})\text{PtMe}]$ pincer species (assigned on the agreement of ^{31}P NMR data with independently synthesised $[(\text{POCCP})\text{PtMe}]$, described in the Chapter 4). However, upon increasing the temperature to 85 °C for 24 hours, degradation of the platinum methyl complex along with formation of perfluorinated biphenyl was observed. As such, the thermolysis of platinum dimethyl dimers did not proceed with sufficient selectivity to provide a viable route to metallated pincer complexes.

3.3.2 Reactions with $[\text{PtCl}_2(1,5\text{-hexadiene})]$

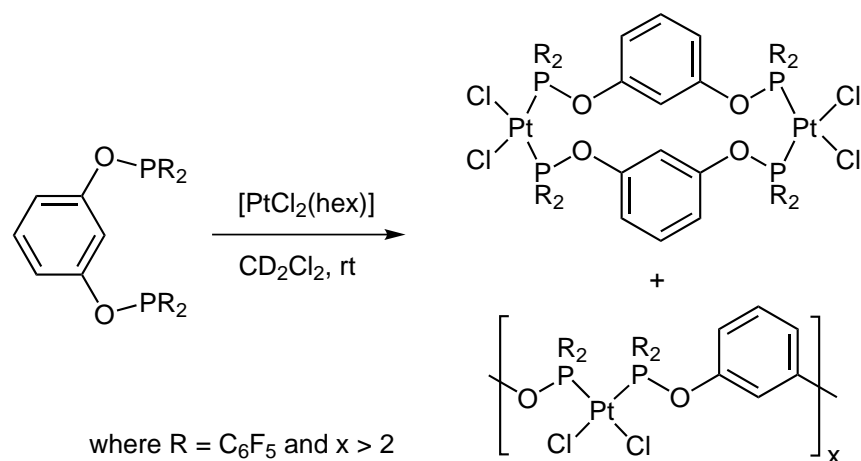
Due to the difficulty in obtaining the metallated PCP pincer complexes of **1** from platinum(0) and platinum(II) dimethyl starting materials, reactions of ligand **1** with

platinum(II) dichloride starting materials were investigated. Platinum chlorides represent the traditional precursors for the synthesis of pincer complexes. However, the readily available platinum chloride (itself polymeric) and $[\text{PtCl}_2(\text{NCR})_2]$ complexes are not ideal for pincer formation, due to a high propensity to form insoluble $[(\text{PCPH})\text{PtCl}_2]_x$ polymers.^{84,86} The use of alkene-stabilised transition metal starting materials has been observed to minimise this polymer formation.¹⁰⁰ Platinum dichloro(1,5-hexadiene) was chosen as a starting material, as it is similar to the frequently used $[\text{PtCl}_2(\text{COD})]$, and enabled a direct comparison with the chemistry of the corresponding platinum dimethyl starting material already investigated.

Despite the previous observations that reactions between **1** and platinum precursors proceeded fastest in benzene and toluene, initial investigations into the coordination chemistry of **1** with $[\text{PtCl}_2(\text{hex})]$ were undertaken in dichloromethane, as $[\text{PtCl}_2(\text{hex})]$ is only sparingly soluble in non-polar solvents. Monitoring of these reactions *in situ* by NMR spectroscopy revealed the immediate formation of two very similar products with resonances in the ^{31}P NMR spectrum at 53.0 and 51.8 ppm, and platinum-phosphorus coupling constants of 4614 and 4503 Hz respectively. The observation of large $^1J_{\text{Pt-P}}$ values and a ^{31}P chemical shift upfield from that of the free ligand ($\delta_{\text{P}} = 87.1$ ppm) indicated that the phosphorus donors were coordinated *trans* to the chloride (which possesses a low *trans*-influence). This indicated the formation of *cis*- $[(\text{POCOPH})\text{PtCl}_2]_x$ species (likely a dimer and a higher oligomer, as in reactions with norbornene and dimethyl precursors, Scheme 3.5). Due to the presence of broad signals in the ^1H NMR spectrum, further spectroscopic characterisation of these compounds was not able to be performed.

Solutions of the *cis*- $[(\text{POCOPH})\text{PtCl}_2]_x$ species in dichloromethane were heated at reflux (in a 60 °C oil bath) for 96 hours to investigate the formation of other stable coordination compounds in solution, and to determine whether metallation was facile at this temperature. Phosphorus-31 NMR spectroscopy revealed the very slow formation of the metallated product $[(\text{POCOP})\text{PtCl}]$ ($\delta_{\text{P}} = 107.6$ ppm) over this time, albeit in only trace amounts, with *cis*- $[(\text{POCOPH})\text{PtCl}_2]_x$ species still comprising the major part of the reaction mixtures.

The formation of solely *cis*- $[(\text{POCOPH})\text{PtCl}_2]_x$ compounds was notable, as platinum dimers with bridging phosphorus donor ligands have been reported with both *cis* and *trans* coordination modes.¹⁰¹ This is due to a balance between antisymbiotic effects and electrostatic effects during the formation of these compounds. Antisymbiotic effects concern the *trans*-influence of the donor atoms, with high *trans*-influence donor ligands preferentially bonding *trans* to low *trans*-influence ligands, to prevent mutual destabilisation.¹⁰² While this is usually applied to σ -donors, a similar principle



Scheme 3.5 Formation of [(POCOPH)PtCl₂]_x species from the reaction of **1** with [PtCl₂(hex)] in dichloromethane.

applies to π -acceptors — mutually *trans*-coordinated π -acceptors will compete for back-donation from the same d orbital on the metal, leading to destabilisation compared to a mutually *cis* arrangement. Conversely, electrostatic effects dictate that an alternating arrangement of the negatively charged halide ligands and neutral phosphorus donors around the metal centre will minimise through-space electrostatic repulsion.¹⁰³ Thus, a strong contribution from antisymbiotic effects usually leads to compounds with a *cis* geometry, whereas electrostatic effects favour the formation of *trans* complexes. Moreover, it is likely that the polar nature of the dichloromethane solvent favours the formation of the *cis* complex over the *trans*, as *cis*-PtR₂X₂ compounds will possess a net dipole, which is cancelled out in a *trans* arrangement of substituents. While solvent effects may play a part in determining which dimer is favoured, in other reported dimers of the type [(PCPH)PtCl₂]₂, compounds containing phosphine ligands adopted *trans* coordination geometries,^{91,97} whilst compounds containing phosphinite or phosphite ligands adopted *cis* coordination geometries.^{92,104} This indicated that the π -acceptor nature of the ligand in these complexes plays a large part in determining the stereochemistry at the platinum centre, with the π -acid nature of **1** likely to account for the *cis* geometry of the species observed in solution.

Owing to the failure of reactions in dichloromethane to generate the metallated pincer complex in substantial quantities, the coordination chemistry of **1** with [PtCl₂(hex)] in benzene and toluene was also investigated. The platinum starting material was only very slightly soluble in benzene-*d*₆, yet monitoring of reaction mixtures by NMR spectroscopy revealed quantitative formation of a new platinum complex **18** at room temperature.

The NMR spectra of compound **18** showed ³¹P resonances at $\delta_P = 85.4$ and 51.4 ppm

in an approximately 1:1 ratio. The downfield signal appeared as a quintet ($^3J_{\text{P-F}} = 36.8$ Hz), while the upfield signal appeared as a singlet, displaying platinum-phosphorus coupling of 4531 Hz. The observation of fluorine-phosphorus coupling in the upfield signal was indicative of **18** possessing an uncoordinated $\text{P}(\text{C}_6\text{F}_5)_2$ moiety: phosphorus-fluorine coupling was observed in the ^{31}P NMR spectra of all the free ligands, but was not observed upon coordination to a metal centre. The chemical shift and platinum-phosphorus coupling constant observed for the upfield ^{31}P NMR signal was very similar to that of the *cis*-[(POCOPH)PtCl₂]_x species previously observed, indicating that **18** contained both an uncoordinated phosphorus and a phosphorus coordinated *trans* to a chloride. Examination of the ^1H NMR spectrum of **18** revealed that it was the 2:1 ligand to metal complex *cis*-[(κ^1 -POCOPH)₂PtCl₂], as no coordinated 1,5-hexadiene was observed, excluding the possibility of the 1:1 complex [(κ^1 -POCOPH)PtCl₂(η^2 -C₆H₁₀)]. The ^1H NMR signals of the aromatic backbone of **18** were consistent with its formulation as the 2:1 complex, with the four proton environments all having discrete signals in a 1:1:1:1 ratio, as a result of the asymmetry present in the ligand. Unlike for the *cis*-dimers **14** and **15**, the signal of H-2 for this *cis*-2:1 complex was not shifted upfield due to π - π interactions between the ligand backbones, with the H-2 environment observed downfield of the other proton environments of the ligand. This indicated that the π -stacking of ligand backbones in the *cis*-dimers is only favourable when the backbones are already held in close proximity to each other, as the interactions between backbones were not maintained in absence of a second metal centre.

Upon heating reaction mixtures containing the 2:1 complex **18** and [PtCl₂(hex)] to 80 °C, further reaction to produce a new coordination complex, **19**, was observed. This new species again possessed two ^{31}P NMR signals in a 1:1 ratio, with both signals displaying platinum-phosphorus coupling. The chemical shift and coupling constants of these signals ($\delta_{\text{P}} = 80.6$ and 55.5 ppm, $^1J_{\text{Pt-P}} = 3357$ and 4582 Hz respectively) showed that **19** possessed phosphorus donors coordinated both *cis* and *trans* to the chloride ligands, indicating that the free phosphinite groups of **18** had coordinated in a mutually *trans* fashion to a PtCl₂ moiety, to form *cis,trans*-[(POCOPH)PtCl₂]₂ (**19**). Again the ^1H NMR spectrum of **19** displayed four distinct aromatic proton environments in a 1:1:1:1 ratio, consistent with the formulation of **19** as a *cis,trans*-dimer. Notably, the ^1H NMR chemical shift of the H-2 proton environment in the *cis,trans*-dimer was downfield of the other aromatic proton environments. Similar to the 2:1 complex **18**, this revealed that the π - π interactions present in the *cis*-dimers were not present in this *cis,trans*-dimer **19**. This demonstrated that the π -stacking of ligand backbones was dependent on *both* metal centres possessing a *cis* coordination environment; the presence of just one metal centre with *trans* geometry is prohibitive to the generation of π - π interactions, likely due to the

extra physical separation between ligand backbones provided by the *trans* metal centre.

The *cis,trans*-dimer **19** was more effectively synthesised by heating the reaction mixture to 80 °C for approximately two minutes shortly after suspending the reactants in solution, to ensure dissolution of the platinum starting material. Complete formation of **19** was observed by NMR spectroscopy upon standing for 12 hours at room temperature. Removal of the solvent from the NMR sample *in vacuo* and washing with hexane furnished a sample of **19** for analysis by HRMS, which confirmed the dimeric nature of **19**. It was interesting to observe that during the formation of **19** — and even during subsequent heating of solutions of **19** — in no instances was the isomerisation of the *cis,trans*-dimer to the *cis*-dimer observed. This is somewhat unexpected, as the *cis*-dimer was observed to be the thermodynamic product in reactions performed in dichloromethane. Isomerisation from *trans*-[(PP)PtCl₂]₂ to *cis*-[(PP)PtCl₂]₂ complexes has previously been observed at temperatures as low as –50 °C;¹⁰⁵ the absence of a similar isomerisation from **19** to *cis*-[(POCOPH)PtCl₂]₂ indicated that the *cis,trans* configuration must be conferred a particular stability in benzene and toluene.

Solutions of **19** were subjected to thermolysis to promote metallation and the formation of the pincer complex [(POCOP)PtCl]. Heating at temperatures of 60 °C and above resulted in the very slow reaction of **19** to form a new platinum compound **20**, which subsequently reacted to produce the desired pincer species with very good selectivity (Figure 3.5). Intermediate **20** displayed a single, extremely shielded resonance in the ³¹P NMR spectrum at $\delta_P = 14.0$ ppm, with a large platinum-phosphorus coupling constant of 4408 Hz. The ³¹P NMR data indicated the symmetric coordination of the phosphorus donors, each coordinated *trans* to a chloride. However, while the observed coupling was similar to the earlier reported *cis*-[(POCOPH)PtCl₂]_x species ($\delta_P \approx 52$ ppm, $^1J_{Pt-P} \approx 4500$ Hz), the ³¹P NMR resonance of **20** appeared almost 40 ppm upfield, confirming that **20** could not be a previously observed *cis*-dimer or oligomer. Unfortunately, as **20** was observed as a labile species during the course of a reaction (and was formed and subsequently reacted at elevated temperatures), no ¹H NMR signals could be definitively assigned to it.

Potential intermediates in the metallation reaction to form [(POCOP)PtCl] included an A-frame dimer,¹⁰⁶ a dimer distorted by intramolecular H-Cl interactions,¹⁰⁷ an arenium complex,¹⁰⁸ a *cis*-monomer complex,⁹¹ and a platinum(IV) complex with a facially-coordinated pincer ligand (Figure 3.6).⁴³ However, due to the fact that **20** possessed a large phosphorus-platinum coupling of 4408 Hz, diagnostic of a *P-trans*-Cl configuration, all but the *cis*-monomer and *fac*-platinum(IV) complexes

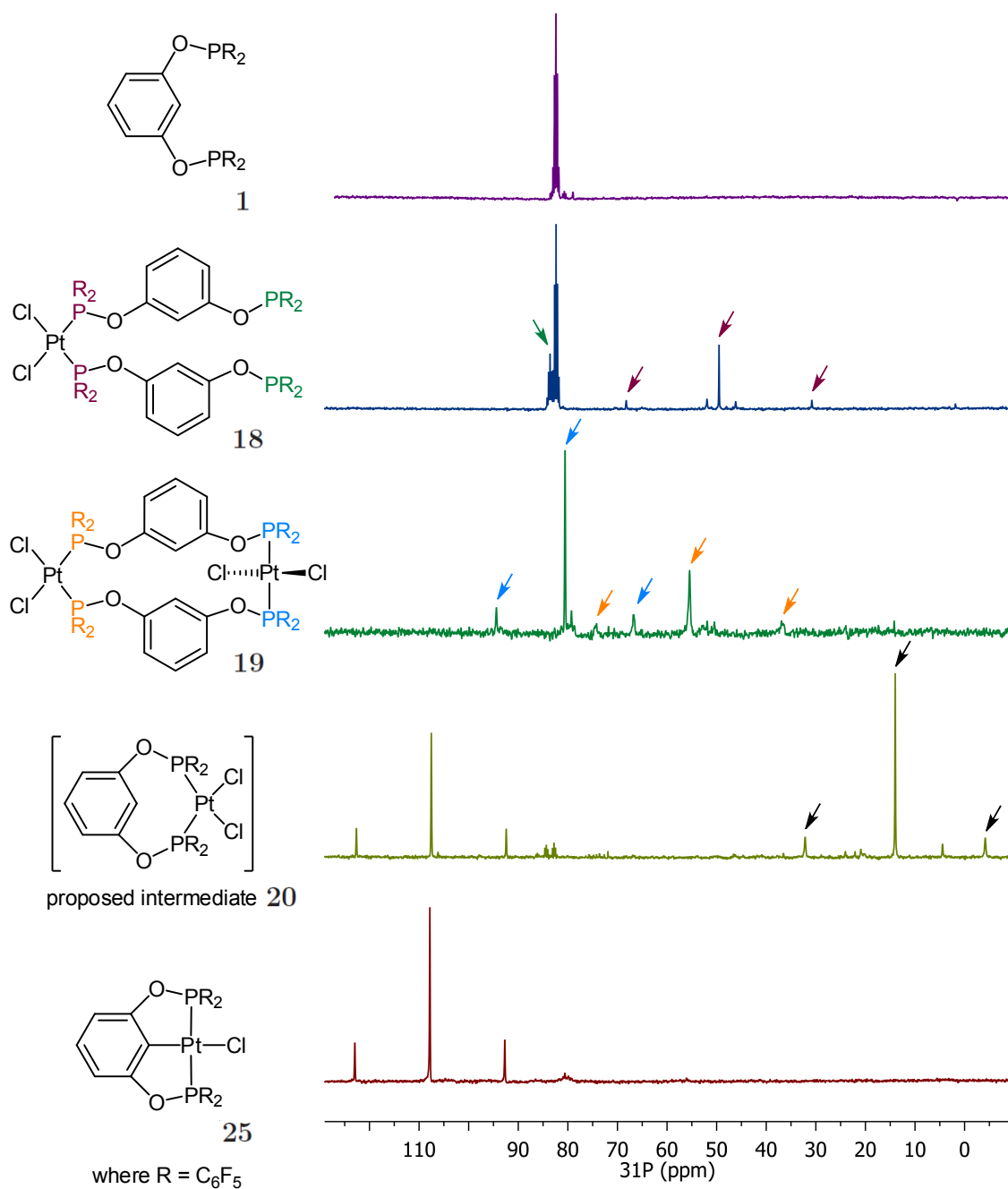


Figure 3.5 Stacked plot of ^{31}P NMR spectra showing the course of the metallation reaction to form $[(\text{POCOP})\text{PtCl}]$ from $[\text{PtCl}_2(\text{hex})]$ in toluene- d_8 .

had to be discounted as potential intermediates, as each required a mutually *trans* coordination of phosphorus donors. The *fac*-platinum(IV) species was the least likely candidate of the two remaining possibilities; no hydride signals were detected in the ^1H NMR spectrum of these reaction mixtures, oxidative addition of the aromatic C-H bond should produce an intermediate with the metallated ring and hydride occupying mutually *cis* coordination sites (producing two inequivalent phosphorus environments), and a platinum(IV) species would not be expected to be stable over the course of hours at 60 °C. This left the *cis*-monomer as the most likely structure for intermediate **20**. This structure was consistent with the spectroscopic data. The upfield shift in the ^{31}P NMR resonance (from 80.6 and 55.5 ppm in the *cis,trans*-dimer **19**, to 14.0 ppm in **20**) was attributed to ring strain associated with the formation of a rigid, 8-membered chelate. Analogous shielding of phosphorus atoms due to ring strain has been observed for 4-membered chelate rings with *cis*-bidentate phosphines.¹⁰⁹

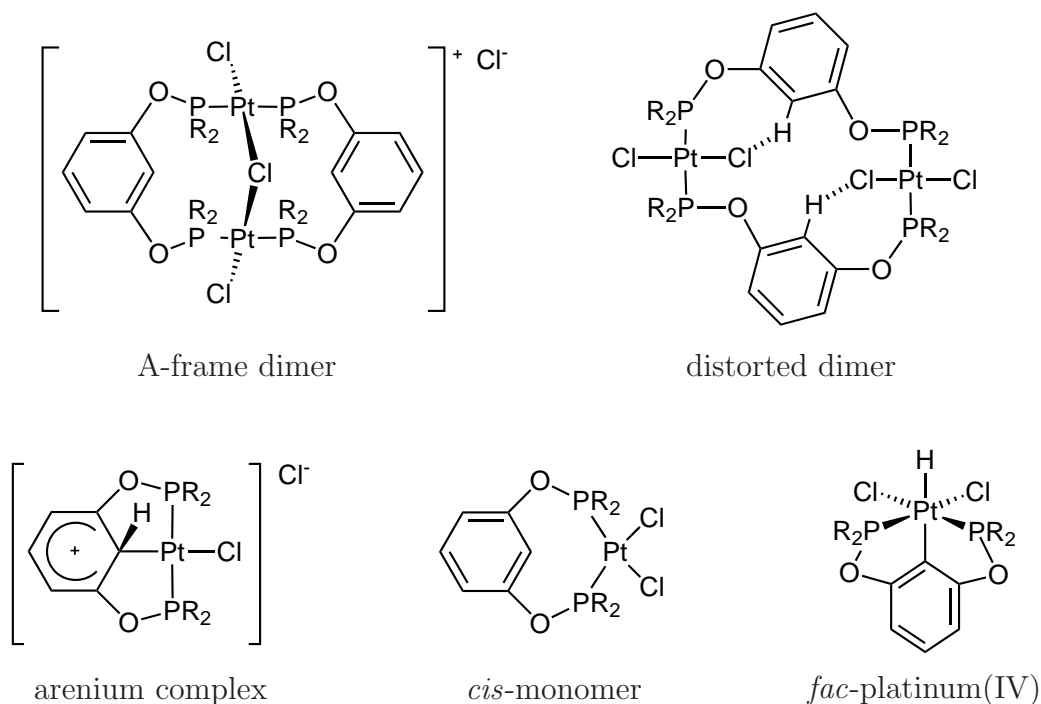


Figure 3.6 Potential structures for the metallation intermediate **20**.

Tentative assignment of a *cis*-monomeric structure for the metallation intermediate **20** fit with observations of pincer cyclometallation in the literature. *Cis*-monomeric structures have been proposed as unisolated intermediates for reactions with other PCPH ligands,^{97,110,111} and have been isolated in reactions of metal precursors with PCCCPMe ligands (where cyclometallation is hindered by the presence of a methyl group on C-2).⁹¹ The formulation of **20** as a *cis*-monomer was also in accordance with the behaviour of **20** in reaction mixtures. A *cis*-monomeric structure is expected to be high in energy, requiring the redistribution of the bridging ligands onto

a single metal centre, as well as the formation of a rigid, eight-membered *cis*-chelate ring. Accordingly, **20** was formed slowly, and only at elevated temperatures. A *cis*-monomeric structure is also predisposed to metallation, with H-2 in close proximity to the metal centre, which can account for the observation that **20** reacted directly to produce the metallated pincer complex [(POCOP)PtCl], and was only observed in trace amounts at temperatures above which metallation is facile (>110 °C). As such, the most likely structure for **20** is that of a *cis*-monomer, making **20** an important intermediate observed in the formation of the [(POCOP)PtCl] pincer species.

3.3.3 Reactions with [PtClMe(1,5-hexadiene)]

The coordination chemistry of **1** was also explored with [PtClMe(hex)], to examine how the presence of both a strong *trans*-influence (methyl) and weak *trans*-influence (chloride) ligand would affect the nature of the complexes formed. The replacement of a chloride ligand with a methyl group renders the [PtClMe(hex)] complex much more soluble in non-polar solvents than the corresponding dichloride complex. This increased solubility was advantageous as, for most starting materials studied, reactions in benzene occurred faster and with less oligomer formation than the corresponding reactions in dichloromethane.

The synthesis of [PtClMe(hex)] has not previously been reported, with the compound observed as a byproduct in the synthesis of [PtMe₂(hex)], and obtained during the purification of [PtMe₂(hex)] by sublimation, in yields of typically $< 1\%$. The synthesis of [PtClMe(hex)] was attempted by the addition of one equivalent of dimethylzinc to [PtCl₂(hex)]; however, this was seen to produce the dimethyl complex [PtMe₂(hex)] as the major product, along with unreacted starting material. The synthesis of [PtClMe(hex)] was achieved by methylation of the dichloride precursor with an excess of dimethylzinc, then chlorination of the resultant dimethyl complex with one equivalent of acetyl chloride (in a manner similar to the synthesis of the related [PtClMe(COD)] species),¹¹² affording the new platinum chloromethyl starting material in a modest overall yield of 46% for the two-step reaction.

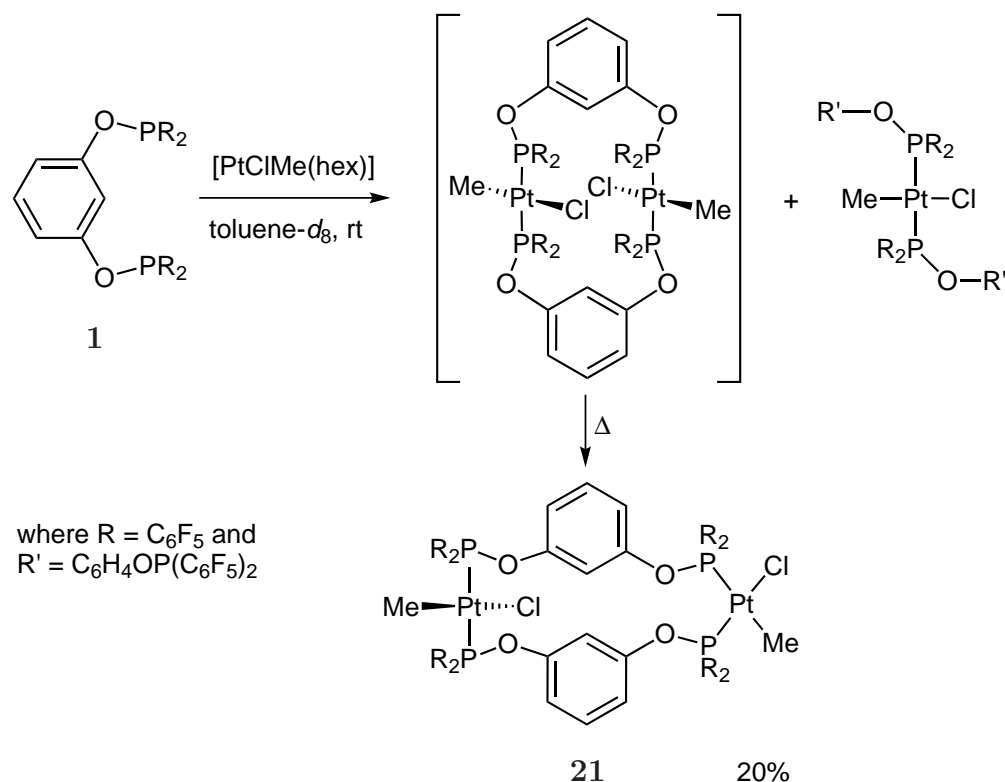
Reactions between the phosphinite ligand **1** and [PtClMe(hex)] in toluene-*d*₈ at room temperature were seen to immediately produce a number of spectroscopically similar coordination compounds. The major species in solution displayed a resonance in the ³¹P NMR spectrum at $\delta_P = 89.2$ ppm and displayed platinum-phosphorus coupling of 4071 Hz. As there were no other phosphorus signals of significant intensity to be related to this signal, the observation of a single ³¹P NMR signal shifted down-

field from that of the free ligand **1** was indicative of the formation of a symmetric species containing mutually *trans* phosphorus donors; *trans*-[(POCOPH)PtClMe]₂. Also present in some reaction mixtures of **1** and [PtClMe(hex)] was the analogous 2:1 complex, *trans*-[(POCOPH)₂PtClMe], displaying ³¹P NMR resonances for the uncoordinated phosphorus atom at $\delta_P = 87.9$ ppm, possessing the characteristic quintet coupling pattern of the uncoordinated phosphinite. The ligated phosphorus atom appeared at $\delta_P = 84.8$ ppm with $^1J_{Pt-P}$ of 4032 Hz; again the ³¹P NMR data were diagnostic of mutually *trans*-coordinated phosphorus donors.[‡] Sufficient proton NMR data for these complexes were not obtained, due to the complex nature of the reaction mixtures.

This initial coordination chemistry of ligand **1** with [PtClMe(hex)] offered some distinct contrasts to that of the same ligand with the analogous [PtCl₂(hex)] starting material; the 2:1 dichloride complex possessed a *cis* geometry, while the 2:1 chloromethyl complex adopted a *trans* geometry. This difference in coordination geometry can be attributed to antisymbiotic effects; the strong *trans*-influence of the methyl group dictates that it preferentially sits *trans* to the ligand with the lowest *trans*-influence, chloride. The stabilisation imparted by this Me-*trans*-Cl coordination must be sufficient that it can overcome the unfavourable interactions generated upon P-*trans*-P coordination (which was not observed for the platinum dichloride complexes), whereby the phosphinite ligands compete for backdonation of electron density from the same metal d-orbital.

The energetics of this system must be very finely balanced; on standing at room temperature *trans*-[(POCOPH)₂PtClMe] was seen to slowly isomerise to form the new *cis,trans*-dimer, *cis,trans*-[(POCOPH)PtClMe]₂ (**21**) (Scheme 3.6). This isomerisation could be facilitated by gentle heating, with compound **21** constituting greater than 80% of the reaction mixture (by ³¹P NMR spectroscopy) after heating solutions of **1** and [PtClMe(hex)] at 40 °C overnight. This *cis,trans*-isomer could then be isolated in spectroscopically pure state by passage of the reaction mixture through a short column of neutral alumina in air (allowing any of the *trans*-2:1 compound to be oxidised and removed from solution), followed by removal of the solvent *in vacuo* and washing with cold pentane. High Resolution Mass Spectrometry confirmed the dimeric nature of **21**, with species from the loss of a chloride ligand with and without coordinated acetonitrile (at $m/z = 2171$ and 2130 amu respectively) being the only ions detected.

[‡]For comparison, the *trans*-coordinated phosphorus donor in the platinum dichloride *cis,trans*-dimer **19** appeared at $\delta_P = 80.6$ ppm, with a $^1J_{Pt-P} = 3357$ Hz. It was observed throughout this work that platinum chloromethyl complexes displayed platinum-phosphorus coupling constants about 20% larger than the analogous platinum dichloride complexes.



Scheme 3.6 Formation of *cis,trans*-[(POCOPH)PtClMe]₂ species (**21**) with the *trans*-[(POCOPH)₂PtClMe] minor product.

Characterisation of **21** by ³¹P NMR spectroscopy revealed three phosphorus environments in a 1:2:1 ratio. The most upfield and most downfield of signals corresponded to one phosphorus donor group each, and displayed chemical shifts and platinum-phosphorus coupling constants consistent with phosphorus coordinated *trans* to a methyl ($\delta_{\text{P}} = 94.4$ ppm, $^1J_{\text{Pt-P}} = 2066$ Hz) and phosphorus coordinated *trans* to a chloride ($\delta_{\text{P}} = 62.1$ ppm, $^1J_{\text{Pt-P}} = 5494$ Hz). Each of these peaks was observed to be split slightly, due to the weak *cis* coupling between the two phosphorus nuclei ($^2J_{\text{P-P}} = 15.4$ Hz). The most intense phosphorus resonance corresponded to two phosphorus donors, and possessed resonances in the ³¹P NMR spectrum very similar to that of the *trans* 2:1 complex ($\delta_{\text{P}} = 90.3$ ppm, $^1J_{\text{Pt-P}} = 4028$ Hz), marking this signal as having arisen from the mutually *trans*-coordinated phosphines. A notable feature of the ³¹P NMR data of **21** is that the platinum-phosphorus coupling constants for both the P-*trans*-P and P-*trans*-Cl environments were exactly 20% larger than the analogous coupling constants for the dichloride *cis,trans*-dimer, indicating that the replacement of a chloride for a methyl at each platinum centre produced a stronger platinum-phosphorus interaction. Proton and phosphorus-31 NMR spectra were also obtained at 50 °C to confirm that the observed signals were arising from a single, asymmetric dimer rather than a number of dimers in equilibrium. The ratio of ¹H and ³¹P NMR signals did not change (or even broaden substantially) from 20 °C to 50 °C, confirming that **21** is a *cis,trans*-dimer.

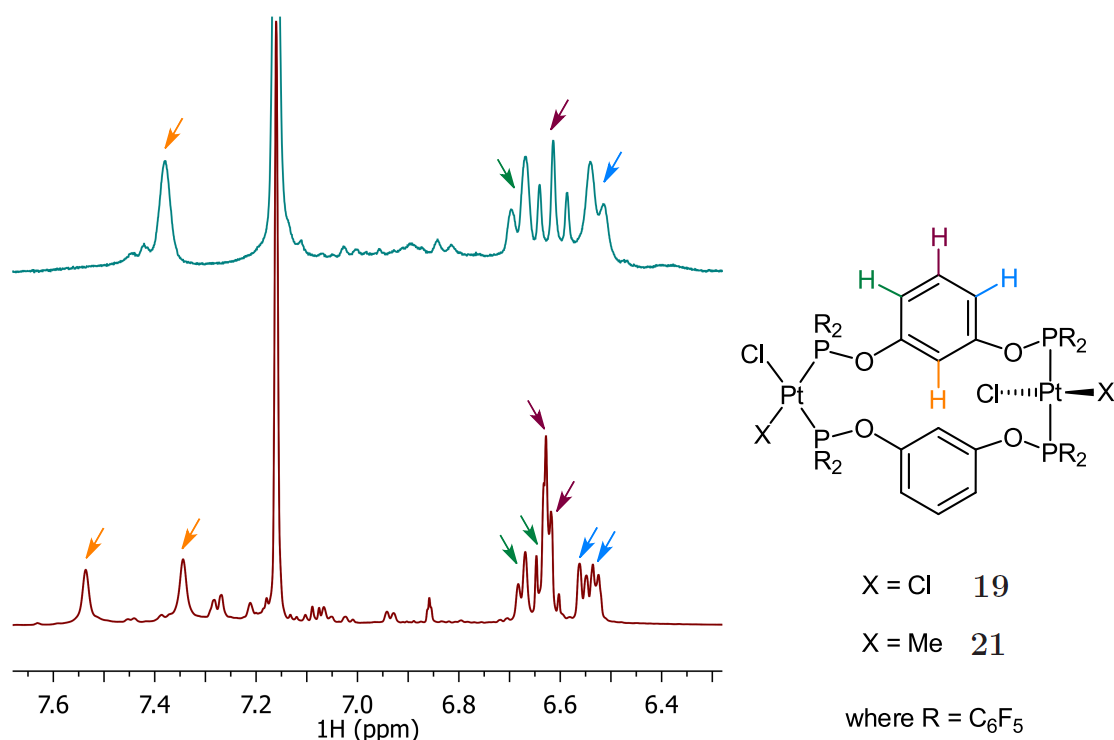


Figure 3.7 Stacked plot of ^1H NMR spectra of *cis,trans*-[(POCOPH)PtCl $_2$] $_2$ (**19**, top) and *cis,trans*-[(POCOPH)PtClMe] $_2$ (**21**, bottom) in benzene- d_6 , demonstrating the spectroscopic similarities between the dimers.

Despite the large chemical shift difference between the two *cis*-phosphorus atoms in the ^{31}P NMR spectrum of **21** (approximately 32 ppm), the aromatic ligand backbones only experienced very small changes in ^{13}C NMR chemical shift (on average, equivalent carbon environments on each ring differed by 0.3 ppm), which indicated that this asymmetric coordination mode did not result in the polarisation of one ring over the other. The ^1H NMR spectrum of **21** bore a striking similarity to the characteristic ^1H NMR spectrum of the corresponding *cis,trans*-dichloride complex **19**, in which the broader H-4,6 signals flanked a sharp H-5 signal, with H-2 shifted slightly downfield (Figure 3.7). This served to demonstrate the spectroscopic similarities between **19** and **21**. The use of ^1H - ^{31}P Heteronuclear Multiple Bond Correlation (HMBC) NMR experiments proved to be a very useful tool for the full assignment of the spectroscopic data for **21**. As the bis(pentafluorophenyl)phosphine donor groups did not possess any protons and did not display large chemical shift variations of the pentafluorophenyl carbon environments, conventional ^1H - ^{13}C HMBC experiments were of little use in establishing the connectivity of both the aromatic ligand backbones and the methyl groups to either the *cis*- or the *trans*-coordinated metal centre. Moreover, no ^1H - ^{13}C HMBC correlations between the ligand backbone and methyl groups were observed, due to the prohibitively long distance over which the coupling was to occur. However, through the use of ^1H - ^1H and ^1H - ^{13}C 2D NMR experiments to fully assign each aromatic ligand backbone, the connectivity between each backbone and the four phosphorus donors was established with ^1H - ^{31}P HMBC

spectroscopy. Similarly, the observation of strong coupling between the protons of each platinum-methyl group and either the mutually *cis* or the mutually *trans* phosphorus atoms *via* ^1H – ^{31}P HMBC spectroscopy readily enabled the spectroscopic assignment of each methyl group to a metal centre. Although ^1H – ^{31}P HMBC spectroscopy is not a widely used tool in organometallic chemistry, it proved invaluable in the assignment of spectroscopic data for the asymmetric *cis,trans*-dimer **21**.

As for the previous dimeric complexes investigated, **21** was subjected to thermolysis in toluene- d_8 to examine how facile the metallation reaction was, and also to probe the nature of any intermediates observed. The reaction to form the metallated [(POCOP)PtCl] pincer species proceeded faster from the chloromethyl dimer **21** than from the platinum dichloride dimer **19**, and without detectable amounts of any intermediate species (Figure 3.8).

The absence of an intermediate observed in the metallation of dimer **21** is consistent with the metallation reaction requiring rearrangement to a *cis*-monomeric species before C–H activation and pincer complex formation can occur, as was previously indicated during the thermolysis of **19**. Due to the platinum-phosphorus interactions being stronger in **21** than in **19** (as evidenced by the magnitude of platinum-phosphorus coupling constants), it may be expected that the energy barrier for the rearrangement from the dimer to the monomer will be greater for the chloromethyl dimer **21** than for the dichloride dimer **19**. However, C–H activation of a chloromethyl *cis*-monomer will be more facile than for a dichloride *cis*-monomer, as the elimination of methane is more favourable than the elimination of HCl (discussed in more detail in Chapter 4). Compared to **19**, this combination of a higher energy barrier for intermediate formation and a lower energy barrier for metallation of **21** predictably results in a much shorter-lived intermediate for the metallation of the chloromethyl dimer **21**, and a *cis*-monomeric intermediate is not detected by NMR spectroscopy.

3.3.4 Reactions with $[\text{PdCl}_2(\text{NCMe})_2]$

The investigation of reactions between the POCOPH ligand **1** and platinum starting materials revealed the propensity of this phosphinite ligand to form a large number of dimeric and oligomeric structures, which possessed both *cis* and *trans* coordination geometries. The advantage of investigating this chemistry with platinum complexes was that the magnitude of the platinum-phosphorus coupling revealed information about the nature of the ligand coordinated *trans* to the phosphorus-donor, and so

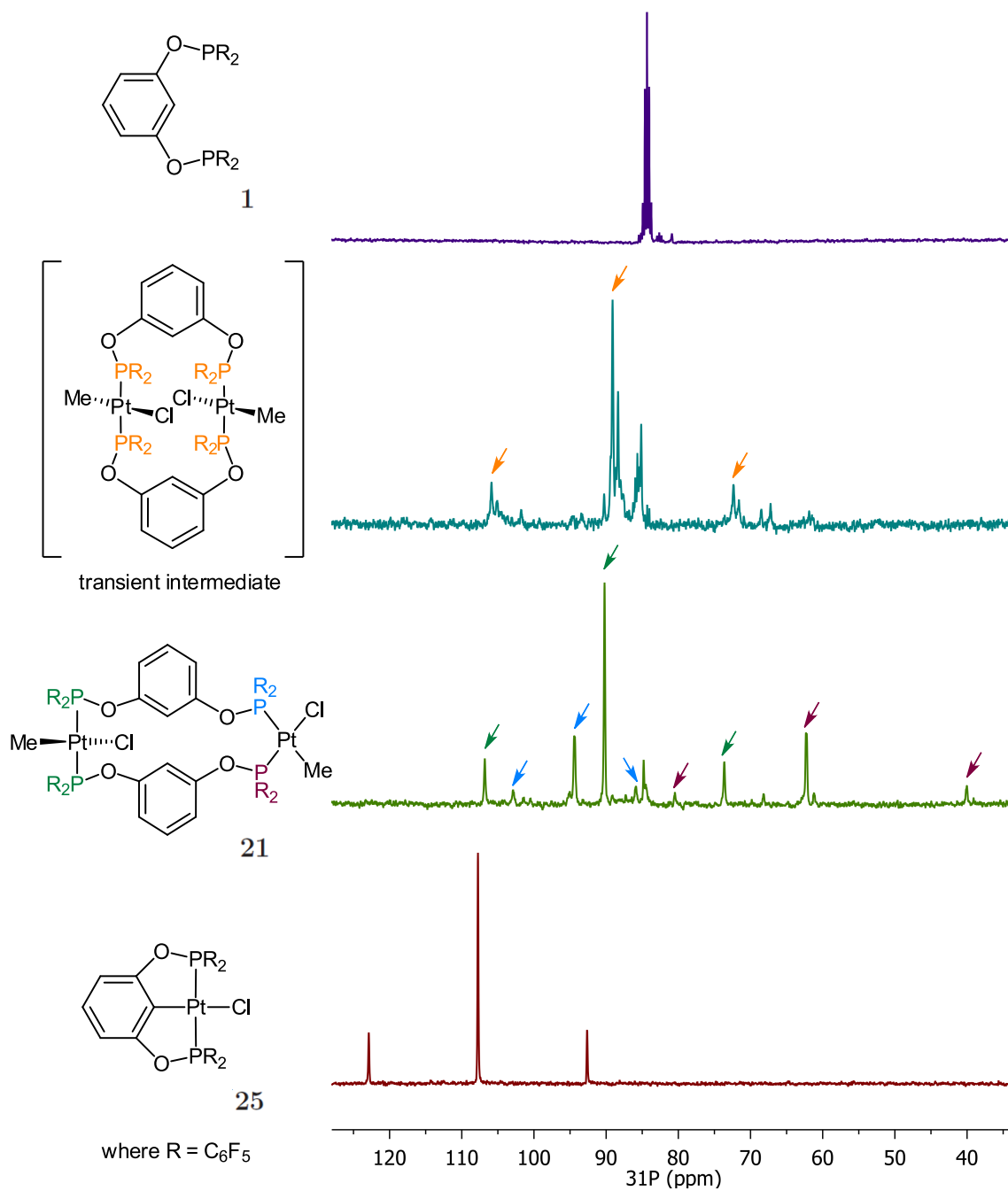


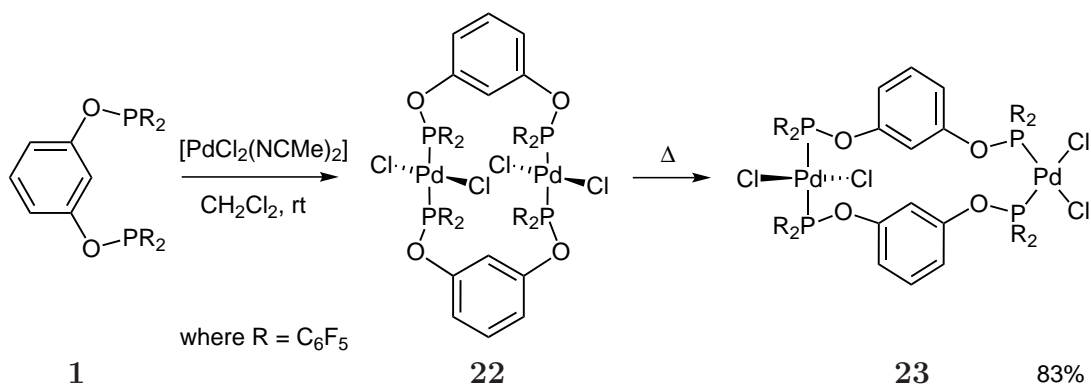
Figure 3.8 Stacked plot of ^{31}P NMR spectra showing the course of the metallation reaction to form $[(\text{POCOP})\text{PtCl}]$ from $[\text{PtClMe}(\text{hex})]$ in toluene- d_8 .

provided a crucial tool in distinguishing between *cis* and *trans* configurations. With the spectroscopic data for the *cis*-, *trans*-, and *cis,trans*-dimers established using platinum chemistry, this spectroscopic data could be employed to help elucidate the structure of products formed in analogous reactions with palladium.

Reactions between **1** and $[\text{PdCl}_2(\text{NCMe})_2]$ were initially performed in benzene- d_6 , as this solvent had produced the most interesting results with platinum precursors. Analysis of the reaction mixtures by ^{31}P NMR spectroscopy indicated the initial formation of the symmetric complex **22**, which possessed one phosphorus environment in the ^{31}P NMR spectrum, at $\delta_{\text{P}} = 88.3$ ppm. This was likely to be *trans*- $[(\text{POCOPH})\text{PdCl}_2]_2$ owing to the phosphorus chemical shift slightly downfield of the free ligand (mutually *trans* phosphorus coordination was observed to appear at chemical shifts close to that of the free ligand in the ^{31}P NMR spectra of platinum complexes, whereas phosphorus coordination *trans* to a chloride produced a significant upfield shift of this phosphorus resonance). However, this complex possessed broad signals in the ^1H NMR spectrum and was seen to react further to give a poorly soluble yellow precipitate, hindering the characterisation of species in these reaction mixtures.

The reactions were repeated in dichloromethane- d_2 to increase the solubility of the products in solution. NMR spectroscopy revealed the immediate formation of the previously observed *trans*-dimer **22**, which was observed to isomerise into the corresponding *cis,trans*-dimer (**23**) over the course of about an hour at room temperature (Scheme 3.7). This product displayed signals in the ^{31}P NMR spectrum in a 1:1 ratio at 88.7 and 78.5 ppm (for the P-*trans*-P and P-*trans*-Cl environments respectively), shifted downfield from similar environments in the platinum analogue **19**, as the less electron-rich palladium did not shield the phosphinite ligands to the extent that platinum did. The ^{31}P NMR resonance of the phosphorus nuclei attached to the *cis*-coordinated palladium centre also appeared slightly broader than those on the *trans*-coordinated palladium, an effect also seen in the spectra of the analogous platinum complex **19**. The proton NMR spectrum of **23** also resembles that of the platinum *cis,trans*-dimer **19**: the chemical shifts and lineshapes for the resonances of protons H-2, H-4, and H-6 are similar, but the H-5 signal for the palladium complex appears approximately 0.5 ppm upfield of that in the platinum complex. It is not immediately clear why this may be; however, it may indicate that these similar species adopt slightly different conformations in solution.

It was found that **23** could be readily obtained from dichloromethane solutions of **1** and $[\text{PdCl}_2(\text{NCMe})_2]$ heated at reflux overnight. The dimeric nature of this *cis,trans* species was confirmed by HRMS analysis, detected as the $[\text{M}-\text{Cl}]^+$ ion, as $m/z =$



Scheme 3.7 Formation of *cis,trans*-[(POCOPH)PdCl₂]₂ species (**23**) via the *trans*-[(POCOPH)PdCl₂]₂ intermediate (**22**).

1995 amu. This also confirmed that the initial reaction product **22** was likely to be a dimer (rather than a higher oligomer), due to its ready isomerisation to **23** and its solubility in benzene. On continued reflux in dichloromethane, **23** was not seen to react any further; however, upon heating above 100 °C in toluene quantitative conversion to the metallated [(POCOP)PdCl] pincer species was observed. During this metallation reaction a transient intermediate was observed by ³¹P NMR spectroscopy as a single resonance at $\delta_P = 45.6$ ppm; while this chemical shift was suitably downfield of the signals corresponding to **23**, insufficient data were gathered on this species to speculate as to whether this may indicate the presence of a *cis*-monomeric complex as a metallation intermediate.

The initial formation of the palladium *trans*-dimer **22** in dichloromethane, whereby under identical conditions for platinum a *cis*-dimer is favoured, is likely to be due to electrostatic effects. The greater ionic character of metal-ligand bonding on palladium serves to enhance the electrostatic repulsion between mutually *cis* chloride ligands, destabilising the *cis* geometry favoured by antisymbiotic and solvent effects. This also serves to account for the formation of a *trans*-dimer in the absence of strongly *trans* directing ligands. The preference of platinum and palladium dimers of the type [(POCOPH)MCl₂]₂ to adopt a stable *cis,trans* configuration is interesting, especially considering that the three examples of *cis,trans* dimers (**19**, **21**, and **23**) represent complexes both with and without strongly *trans* directing ligands, and rearrange to form these asymmetric dimers from the initial formation of both *cis* and *trans* complexes. For coordination complexes of the phosphinite ligand **1**, the *cis,trans*-dimeric structure must offer a balance between antisymbiotic and electrostatic effects that is energetically favourable for all compounds, despite their differences.

3.3.5 Literature Precedent for *cis,trans*-Dimers

Dimeric compounds containing two metal centres with identical donor groups but different coordination geometry are extremely rare in the literature. To date, only six examples of such compounds have been published,^{113–116} falling into three different classes (Figure 3.9). The most remarkable feature of these structures is that they do not bear any striking similarities to one another. Nitrogen, phosphorus, arsenic, and antimony donor ligands are all represented, linked by backbones of one, three, or eleven atoms in length.

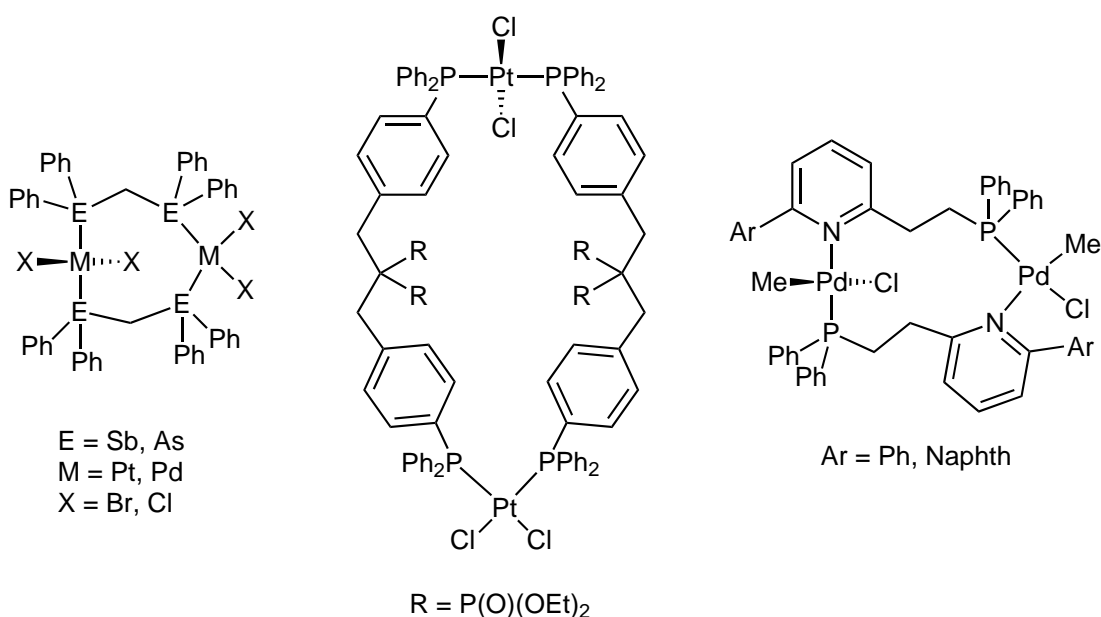


Figure 3.9 Previously reported *cis,trans*-dimers.

All of the reported *cis,trans*-dimers contain aromatic substituents on donor atoms, and all contain at least one halide on each metal centre. As aryl substitution is seen to decrease the σ -donor ability of pnictogens,³⁸ this may indicate that the formation of *cis,trans*-dimers is favoured by, or at least accessible to, poorly σ -donating ligands. This is likely due to the rearrangement processes required for the formation of these complexes; while the *in situ* formation of previously reported *cis,trans*-dimers has not been investigated, this work indicates that they are formed through the rearrangement of symmetric isomers in solution (as observed in the formation of the platinum chloromethyl *cis,trans*-dimer **21** and the palladium dichloro *cis,trans*-dimer **23**). During such a rearrangement a pnictogen ligand will have to migrate between orbitals on the platinum, with the energy barrier to this migration being smaller for poorer σ -donor ligands, due to their weaker interactions with the metal centre.

The steric influence exerted by the ligands will also play a role in enabling the formation of *cis,trans*-dimers. The effect of sterics was observed in the formation of dimeric species with bridging pyridine-phosphine ligands: a *cis,trans* coordination geometry was favoured for phenyl and 1-naphthyl substituents on the pyridyl ring, while a *trans,trans* coordination geometry was favoured for ligands with the bulkier 9-anthracyl substituent.¹¹⁵ Therefore it is plausible that for a *cis,trans* dimeric structure to be favoured, there needs to be a fine balance of steric and electronic factors at work, that serve to destabilise the *cis*-dimer to the point where isomerisation to the *trans*-dimer is almost favoured, with *cis,trans* coordination providing a thermodynamically stable trade-off between the two conventional dimeric forms. It is possible that such an effect is observed in this work; the compound $[(\text{POCOPH})\text{PtCl}_2]_2$ adopted a thermodynamically stable *cis*-dimeric structure in dichloromethane, but formed an equally stable *cis,trans*-dimer in toluene, due to the absence of the polar solvent’s stabilisation of *cis* coordination modes. While *cis,trans*-dimer formation appears to require a fine balance between steric and electronic effects, along with the ability to readily isomerise between coordination geometries, it is not clear how this unusual coordination geometry lowers the total energy of the system to an extent where the *cis,trans*-dimer is favoured as the thermodynamic product.

3.4 Concluding Remarks

The coordination chemistry of group 10 metals with the phosphinite donor ligand **1** was typified by the formation of a range of dimeric species, displaying *cis*, *trans*, and the unusual *cis,trans* coordination geometries (Table 3.3). This was primarily due to the electron-poor nature of **1** hindering metallation (discussed further in the Chapter 4), and allowing for coordination compounds and metallation intermediates to be more readily studied than with similar electron-rich ligands.

The coordination chemistry of Pt(0)-alkene species with **1** was typified by the formation of oligomeric compounds of the type *cis*- $[(\text{POCOPH})\text{Pt}(\eta^2\text{-alkene})]_x$, with poor solubilities and unknown molecular weights. However, reaction between $[\text{Pt}(\text{nb})_3]$ and **1** afforded the dimeric species **14**, the first crystallographically characterised example of a platinum-alkene complex containing a pentafluorophenyl phosphine group. The solid state structure of **14** revealed a weakly bound norbornene group — due to the electron-poor metal centre being unable to participate adequately in π -backbonding — and also a stabilising “parallel displaced” π - π interaction between the aromatic ligand backbones. Attempts at generating platinum(II) pincer species

Table 3.3 ^{31}P NMR data of dimeric compounds containing ligand **1**.

Formula	Compound	Coordination	δ_{P} (ppm)	$^1J_{\text{Pt-P}}$ (Hz)
<i>cis</i> -[(POCOPH)Pt(nb) ₂] ₂	14	<i>cis</i>	100.5	4623
<i>cis</i> -[(POCOPH)PtMe ₂] ₂	15	<i>cis</i>	89.9	2202
<i>cis</i> -[(κ^1 -POCOPH) ₂ PtCl ₂]	18	uncoordinated	85.4	—
		<i>cis</i>	51.4	4531
<i>cis,trans</i> -[(POCOPH)PtCl ₂] ₂	19	<i>trans</i>	80.6	3357
		<i>cis</i>	55.5	4582
<i>cis,trans</i> -[(POCOPH)PtClMe] ₂	21	<i>cis</i> (<i>trans</i> -Me)	94.4	2066
		<i>trans</i>	90.3	4028
		<i>cis</i> (<i>trans</i> -Cl)	62.1	5494
<i>trans</i> -[(POCOPH)PdCl ₂] ₂	22	<i>trans</i>	88.3	—
<i>cis,trans</i> -[(POCOPH)PdCl ₂] ₂	23	<i>trans</i>	88.7	—
		<i>cis</i>	78.5	—

through metallation of the ligand backbone were unsuccessful, regardless of whether the metallation was attempted under acidic, basic, or thermal conditions.

The coordination chemistry of **1** with [PtMe₂(hex)] was found to be similar to the coordination chemistry of **1** with platinum(0), forming the κ^2 -PP bridged dimer *cis*-[(POCOPH)PtMe₂]₂ at room temperature, along with small amounts of a higher oligomer, *cis*-[(POCOPH)PtMe₂]_x. Traces of the metallated pincer species [(POCOP)PtMe] were detected during thermolysis of solutions of **15** and **16**, but these reactions lacked selectivity and were prone to decomposition. Monitoring of the reactions by NMR spectroscopy suggested that a new dimer, *cis,trans*-[(POCOPH)PtMe₂]₂ (**17**) may be formed as an intermediate in the metallation reaction. Analogous reactions with the more electron-donating POCCPH ligand **3** allowed the metallated pincer complex to be formed at a lower reaction temperature, although decomposition and a lack of selectivity was still observed. Therefore, for pincer ligands containing the electron-withdrawing bis(pentafluorophenyl)phosphinite functionality, [PtMe₂(hex)] did not represent a viable starting material for the formation of the metallated [(PCP)PtMe] pincer complex.

Reactions between **1** and platinum chloride starting materials proved to be better suited for the synthesis of pincer complexes, with the metallated products formed selectively upon prolonged heating of reaction mixtures. The coordination chemistry between platinum chloride starting materials and ligand **1** at room temperature proved to be especially interesting, with the unexpected formation of *cis,trans*-dimers **19** and **21** for both the dichloride and chloromethyl platinum complexes. Spectroscopic investigation into the formation of these compounds revealed that each had an initial preference for opposing coordination geometries before rearrangement into the *cis,trans*-dimer; the dichloride starting material formed the *cis*-monomeric

compound **18**, while the chloromethyl starting material produced a *trans*-dimer.

Spectroscopic data obtained from the coordination of **1** to platinum was used to assist in identification of coordination compounds formed in reactions with the palladium precursor $[\text{PdCl}_2(\text{NCMe})_2]$. Data indicated an initial preference for *trans*-dimer formation, even in polar solvents, followed by a rapid rearrangement to form another *cis,trans*-dimeric species, **23**. All three *cis,trans*-dimers (**19**, **21**, and **24**) were found to be stable in aromatic solvents at temperatures up to 60 °C, with extended thermolysis of these solutions promoting C–H activation to form metallated pincer complexes.

These *cis,trans*-dimers represent a very rare coordination geometry, with only six other compounds reported to date. Comparison of previously published species with the compounds described in this work show that a surprisingly diverse range of donor atoms and backbone lengths are present in *cis,trans*-dimers. However, all compounds appear to have pnictogen donor atoms capable of ready migration between metal orbitals, allowing for facile isomerisation from any kinetic products formed to the thermodynamically favoured *cis,trans*-dimer. It also appears that the balance between steric and electronic effects play a crucial role in disfavouring the *cis*- and *trans*-dimers, producing the *cis,trans* configuration. As such, these unusual dimers present an unanticipated class of compounds formed during the synthesis of PCP pincer complexes.

Chapter 4

Synthesis and Reactivity of PCP Pincer Complexes

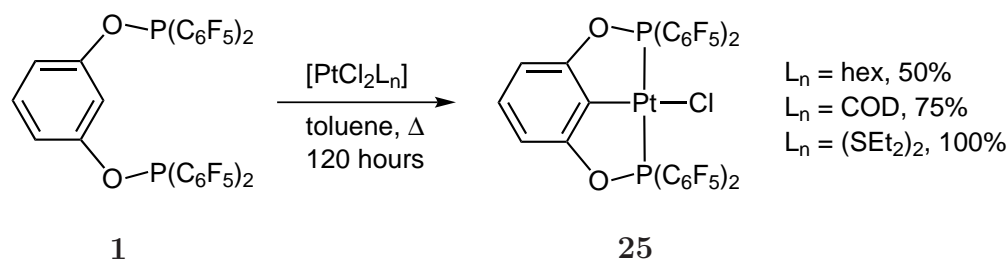
The initial coordination chemistry of the electron-poor POCOPH pincer ligand **1** with platinum and palladium precursors (outlined in Chapter 3) revealed that incorporation of electron-withdrawing groups onto the ligand backbone served to make ligand metallation less facile, instead favouring the formation of bridged, oligomeric structures. To probe the barrier to ligand metallation and pincer complex formation, the effect of the transition metal starting material was investigated.

4.1 Synthesis of PCP Pincer Complexes

From the exploration of the coordination chemistry of the phosphinite ligand **1** with platinum and palladium starting materials, it was clear that metal chloride starting materials offered the most successful route to the metallated pincer complex. However, the elevated reaction temperatures and long reaction times required to facilitate metallation in some instances were observed to lead to the partial decomposition of the desired species in solution. As it became clear that there was a reasonable degree of difficulty in the convenient synthesis and isolation of these compounds, a range of starting materials were assessed for their ability to readily produce the metallated pincer complexes. There have been no direct comparisons of starting materials for the synthesis of PCP pincer compounds reported in the literature to date.

4.1.1 Effect of Metal Precursor on PCP Pincer Synthesis

Owing to the difficulty in generating the pincer complex $[(\text{POCOP})\text{PtCl}]$ (**25**) from the $[\text{PtCl}_2(\text{hex})]$ starting material, reactions with the more commonly used $[\text{PtCl}_2(\text{COD})]$ starting material were performed. By undertaking reactions with the hexadiene and cyclooctadiene starting materials simultaneously under identical conditions, it was observed that reactions with $[\text{PtCl}_2(\text{COD})]$ produced **25** at a faster rate than those with $[\text{PtCl}_2(\text{hex})]$. However, both reactions were observed to proceed very slowly; after 120 hours at reflux in toluene reactions performed with the cyclooctadiene starting material had reached approximately 75% completion, while the hexadiene starting material had only achieved about a 50% conversion (as assessed by integrations of signals in the ^1H and ^{19}F NMR spectra). As for reactions with $[\text{PtCl}_2(\text{hex})]$, reactions with $[\text{PtCl}_2(\text{COD})]$ were also observed to proceed *via* the *cis,trans*-dimer **19**. However while reactions between ligand **1** and $[\text{PtCl}_2(\text{hex})]$ were observed to produce dimeric species such as **19** at room temperature, no reaction occurred between **1** and $[\text{PtCl}_2(\text{COD})]$ at room temperature, even after 72 hours.



Scheme 4.1 Effect of starting material on the progress of the metallation of ligand **1** to form **25**. Percentage values represent the approximate conversion of ligand to the metallated product, as observed by ^{31}P NMR spectroscopy.

Another starting material that has been used successfully in the synthesis of platinum pincer compounds is $[\text{PtCl}_2(\text{SEt}_2)_2]$.¹¹⁷ Reactions between $[\text{PtCl}_2(\text{SEt}_2)_2]$ and **1** were observed to proceed much faster than those performed with the platinum-diene precursors; formation of the pincer complex **25** was observed to be about 75% complete after 64 hours, reaching completion after 120 hours at reflux in toluene (Scheme 4.1). Compared to the reactions performed with $[\text{PtCl}_2(\text{diene})]$ precursors, considerably smaller amounts of the *cis,trans*-dimer intermediate were observed throughout the course of the reaction. In reactions between $[\text{PtCl}_2(\text{SEt}_2)_2]$ and **1** at room temperature, the free ligand **1**, along with a species that has tentatively been assigned as the 1:1 complex $[(\kappa^1\text{-POCOPH})\text{PtCl}_2(\text{SEt}_2)]$ are the major components of the reaction mixture. This new platinum complex possessed the characteristic quintet signal of the uncoordinated phosphinite at 85.4 ppm in the

^{31}P NMR spectrum, with a corresponding singlet at 68.9 ppm that displayed a platinum-phosphorus coupling constant of 4240 Hz, likely to represent phosphorus coordination *trans* to a chloride. The alternate isomer with the diethyl sulfide coordinated *trans* to the phosphorus could not be ruled out, but was unlikely, as phosphorus coordination *trans* to sulfur should result in platinum-phosphorus coupling constants about 500–1000 Hz smaller than for phosphorus coordination *trans* to chloride,^{118,119} which typically had values between 4600–4200 Hz for platinum dichloride complexes of **1**.

The spectroscopic data of this 1:1 complex was very similar to that of the 2:1 complex **18**, the major difference being the appearance of the coordinated phosphorus atom downfield from that in **18** ($\delta_{\text{P}} = 51.4$ ppm). The broad signals of coordinated diethyl sulfide were observed in the ^1H NMR spectrum, but due to overlap with free diethyl sulfide and resonances of the starting material, the presence of diethyl sulfide in the new platinum complex could not be definitively established. However, on the basis that this species contains a κ^1 -bound phosphinite ligand and is not the 2:1 complex previously observed, a 1:1 complex with bound diethyl sulfide is the most likely structure. Despite some uncertainty as to the nature of this species, it is clear that at room temperature, the reaction between ligand **1** and $[\text{PtCl}_2(\text{SEt}_2)_2]$ produced none of the previously observed dimeric or oligomeric $[(\text{POCOPH})\text{PtCl}_2]_x$ species.

From these results, it is clear that for $[\text{PtCl}_2\text{L}_n]$ starting materials, the ease of formation of the pincer complex **25** depends on the ancillary ligand L_n , with diethyl sulfide > cyclooctadiene > hexadiene. This order of reactivity correlated roughly with the ability of these neutral ligands to bind to platinum: cyclooctadiene has been reported to displace hexadiene from platinum,¹²⁰ but dimethyl sulfide and cyclooctadiene have been reported to displace each other from platinum, indicating that they bind with a similar strength to the metal centre.^{121,122} However, upon κ^1 -coordination of ligand **1** to the platinum, diethyl sulfide would be expected to be a significantly better ligand than the η^2 -COD; the COD is no longer stabilised by the chelate effect, and the electron-withdrawing nature of the phosphinite does not provide the metal centre with significant electron density to stabilise the COD by π -backbonding.

This stability series (diethyl sulfide > cyclooctadiene > hexadiene) also correlated well with qualitative observations of the amount of *cis,trans*-dimer **19** present in reaction mixtures; the more readily displaced the ancillary ligand, the more facile the formation of dimer **19**, the longer **19** persisted in solution, and the slower the formation of the metallated pincer species. It can be surmised that platinum precursors with more difficult to displace neutral ligands are less prone to dimer formation;

once a $\kappa^1\text{-}[(\text{PCPH})\text{PtCl}_2\text{L}]$ intermediate is formed, not only will the pendant phosphorus donor have to displace a strongly-bound ligand from the metal to form a dimer, it will also be in competition with the already displaced, strongly binding ancillary ligand to do so. Therefore, neutral ligands that bind more strongly to this $\kappa^1\text{-}[(\text{PCPH})\text{PtCl}_2\text{L}]$ intermediate will be displaced from the platinum centre by phosphorus at temperatures closer to those required for metallation, minimising the build up of dimer species in solution (Figure 4.1). The observation of increased levels of dimer in the less facile metallation reactions is in agreement with the earlier postulation that the presence of **19** results in an increased barrier to metallation, due to the energy costs of rearrangement from this stable configuration into one from which metallation can readily occur (such as a *cis*-monomeric configuration). Empirically, palladium starting materials with PPh_3 and COD ligands have been observed to reduce the formation of $[(\text{PCP})\text{PdCl}_2]_x$ species and increase yields of the metallated product when compared to starting materials with the more readily displaced nitrile ancillary ligands.¹²³

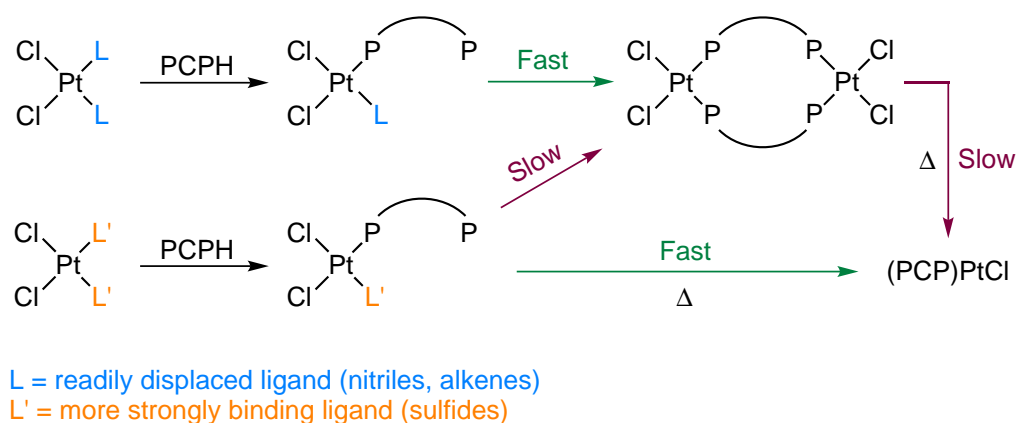


Figure 4.1 Effect of ancillary ligand binding strength on dimer formation. Ligands that are more readily displaced from the $\kappa^1\text{-}[(\text{PCPH})\text{PtCl}_2\text{L}]$ intermediate will favour dimer formation (top), while less readily displaced ligands will favour monomer formation (bottom). Ligand metallation to form the pincer complex is more facile from the monomer than the dimer.

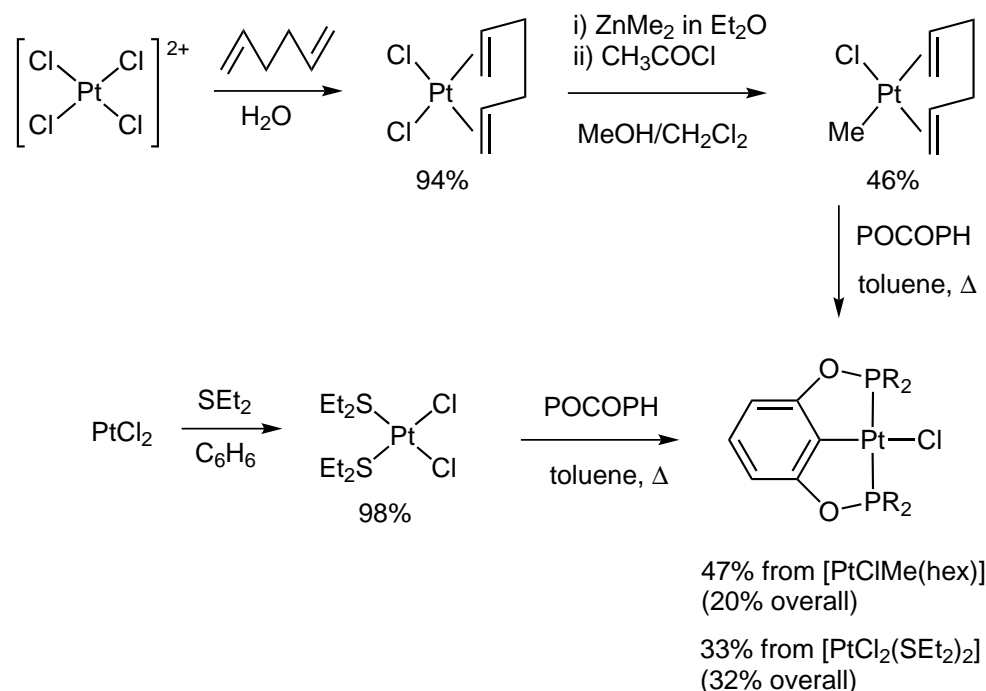
As altering the ancillary ligand(s) on the metal precursor was observed to have a small but significant effect on the ease of formation of **25**, the effect of altering the anionic ligand on the metal centre was examined. Replacement of a chloride ligand on $[\text{PtCl}_2(\text{COD})]$ with a hexamethyldisilazide group provides the resulting platinum complex with an internal base functionality, which has been observed to assist in the synthesis of cyclometallated pincer species at lower temperatures than can be achieved using platinum dichloride starting materials.¹²⁴ Reactions performed in benzene at reflux were reported to achieve metallation of even the difficult cyclohexyl backbones within six hours. However, no significant reaction

between $[\text{PtCl}\{\text{N}(\text{SiMe}_3)_2\}(\text{COD})]$ and ligand **1** was observed in benzene- d_6 after 33 hours at 80 °C; only after a further 20 hours at reflux in toluene were significant amounts of **25** detected. While the internal base functionality served to reduce the time required for metallation to occur, it did not significantly reduce the temperature at which metallation was facile. Attempts to promote more facile metallation from the dichloride starting materials $[\text{PtCl}_2(\text{hex})]$ and $[\text{PtCl}_2(\text{SEt}_2)_2]$ *via* the addition of triethylamine as external base were unsuccessful, as the formation of **25** was observed to proceed at approximately the same rate regardless of whether the external base was present or absent.

The effect of the anionic ligand on the metallation reaction was also investigated through the use of the platinum chloromethyl starting material $[\text{PtClMe}(\text{hex})]$, as the similar $[\text{PtClMe}(\text{COD})]$ starting material has been used to good effect in the synthesis of pincer complexes in the literature.^{58,100} Reactions between ligand **1** and $[\text{PtClMe}(\text{hex})]$ showed that complete formation of $[(\text{POCOP})\text{PtCl}]$ had occurred after 48 hours at reflux in toluene, substantially quicker than reactions performed with the dichloride starting material $[\text{PtCl}_2(\text{hex})]$. This result is interesting when considering that reactions between the platinum dimethyl derivative $[\text{PtMe}_2(\text{hex})]$ and ligand **1** produced only small amounts of the pincer complex $[(\text{POCOP})\text{PtMe}]$.

The observation that the platinum chloro(methyl) starting material offers a more efficient route to metallated pincer complexes than the analogous platinum dichloride starting material is likely due to the methyl group acting as a better proton acceptor than the chloride, with the methane generated also likely to be a better leaving group than hydrogen chloride. No traces of $[(\text{POCOP})\text{PtMe}]$ are detected in reactions starting from $[\text{PtClMe}(\text{hex})]$, demonstrating methyl group has a much larger affinity for the metallated proton than the chloride group. However, as only small amounts of the metallated product were observed in reactions between **1** and the dimethyl starting material $[\text{PtMe}_2(\text{hex})]$, the chloride ligand must also assist the reaction. One such way this may occur is for the chloride to generate favourable $\text{H} \cdots \text{Cl}$ interactions with the C–H bond being broken, weakening the bond and lowering the energy required for C–H activation. In such a $\text{H} \cdots \text{Cl}$ interaction, the chloride may also act as a shuttle, assisting the proton transfer to the methyl leaving group. Theoretical calculations have shown that this chloride-assisted proton transfer is favoured during the oxidative addition of methane in the Shilov reaction.¹²⁵ In the synthesis of pincer compounds, a dimeric intermediate of the type $[(\text{PCPH})\text{PtClX}]_2$ has been isolated and crystallographically characterised, in which the chloride ligands interact strongly with the proton on C-2 of the ligand backbone, resulting in a weakened C–H bond (as seen in the distorted dimer structure mentioned in Chapter 3, Figure 3.6).¹⁰⁷ It is thought that the chloride ligand helps

to facilitate metallation through this interaction .



Scheme 4.2 Synthesis of the pincer complex **1** *via* platinum dichloride and chloromethyl starting materials.

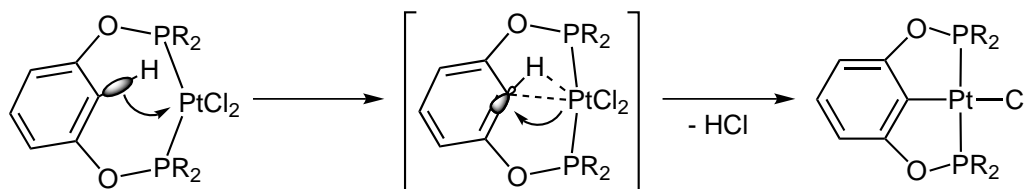
While the experimental data indicated that for the synthesis of **25**, the reactivity of starting materials was in the order of $[\text{PtCl}\{\text{N}(\text{SiMe}_3)_2\}(\text{COD})] > [\text{PtClMe}(\text{hex})] > [\text{PtCl}_2(\text{SEt}_2)_2] > [\text{PtCl}_2(\text{COD})] > [\text{PtCl}_2(\text{hex})]$, the ease of starting material synthesis should also be considered. The syntheses of the most reactive compounds $[\text{PtCl}\{\text{N}(\text{SiMe}_3)_2\}(\text{COD})]$ ¹²⁴ and $[\text{PtClMe}(\text{hex})]$ (see experimental section) both required organometallic starting materials of the type $[\text{PtCl}_2(\text{diene})]$, which were then treated with pyrophoric reagents and gave only modest yields of the desired species (approximately 45 - 70%). However, the less reactive $[\text{PtCl}_2(\text{SEt}_2)_2]$ could be synthesised from the treatment of platinum(II) chloride with diethyl sulfide, and obtained in yields of typically > 95%. So while the monochloride starting materials were observed to require shorter reaction times and gave greater yields of the metallated product **25**, it must be taken into account whether this value represents a greater overall yield from the original platinum starting material (Scheme 4.2).

4.1.2 Effect of the Ligand on PCP Pincer Synthesis

The cyclometallation reaction to form pincer complexes has been known to be dependent upon the steric bulk on the donor atoms of the ligand, with bulky groups such as *tert*-butyls favouring pincer formation. However, the electronic aspects of the cyclometallation reaction have been reported to vary depending on the nature of

the metal and ligand;¹²⁶ while numerous studies have been devoted to cyclometallation reactions in the literature, the electronic aspects of metallation to form PCP pincer complexes have scarcely been reported, save for reports that ligands containing π -accepting phosphite functionalities are unusually difficult to metallate.^{92,104} From the reactions between the POCOPH ligand **1** and platinum starting materials, it was clear that metallation in this instance was substantially less facile than reported reactions with other PCP pincer ligands. While this proved to be valuable in investigating the coordination chemistry of **1**, it was clearly detrimental to the convenient synthesis of the pincer complex **25**. To provide an indication of how the electronic nature of the ligand affected the ease of metallation, the pincer ligands POCOPH (**1**), PCCCPH (**2**), and POCCPH (**3**) were reacted with $[\text{PtCl}_2(\text{SEt}_2)_2]$ in NMR tubes. This allowed frequent *in situ* monitoring of the reaction progress by NMR spectroscopy, enabling the time each reaction required to reach completion to be evaluated.

For these small-scale reactions, it was observed that the reaction with the most electron-donating POCCPH ligand **3** reached completion first, after 17 hours at reflux in toluene- d_8 . The reaction with the PCCCPH ligand **2** reached completion after 33 hours, almost double the time of ligand **3**, while the reaction with electron-poor POCOPH ligand **1** occurred very slowly and had only reached about 50% completion after 33 hours at reflux in toluene. As ligands **1**, **2**, and **3** all have a similar steric bulk this is a clear indication that more electron-donating ligands increase the ease of the metallation reaction.



Scheme 4.3 Metallation of the pincer backbone to form **25**. Donation of electron density from the C–H σ -orbital to the metal forms an agostic transition state. Backdonation from the metal into the C–H σ^* -orbital completes the bond scission.

As these cyclometallation reactions have been observed to proceed *via* agostic intermediates/transition states,¹²⁷ it may seem intuitive for an electron deficient metal centre to enhance this C–H activation step by withdrawing electron density from the C–H σ -bonding orbital in an electrophilic manner. However once the C–H agostic interaction with the metal is established, backdonation from the metal into the C–H σ^* -antibonding orbital is required to complete the scission of this bond (Scheme 4.3).¹²⁸ This backdonation is difficult for electron-poor metal complexes

to achieve, and hence cyclometallation reactions with **1**, **2**, and **3** are seen to be less facile than for reported reactions with more basic phosphine ligands.¹²⁹ Furthermore, pincer ligands with electron-withdrawing groups may generate less stable agostic intermediates. As the aromatic backbone is attached at C-1 and C-3 to the electron-poor phosphorus donors, any inductive withdrawal of electron density from the π -system of the ligand backbone should cause a contraction of the orbitals on C-2, destabilising any agostic metal-ligand interactions. This effect has been observed for reactions with palladium, whereby the incorporation of electron-withdrawing groups *ortho* to aromatic C–H bonds decreases the rate of the metallation reaction.^{130,131} This difficulty in promoting metallation with electron-poor ligands was also observed in the initial reports of the coordination chemistry of the PCCCPH ligand **2** with ruthenium, whereby attempts to produce the pincer complex by direct cyclometallation were unsuccessful, and a transcyclometallation reaction scheme had to be employed.⁵⁶

Upon scaling up these reactions to synthesise the [(PCP)PtCl] pincer complexes of ligands **1**, **2**, and **3**, the yields obtained did not directly correlate to the speed of the metallation reaction; a more facile metallation reaction did not necessarily result in an increased yield. Compound [(POCOP)PtCl] (**25**) was isolated in a 33% yield, [(PCCCP)PtCl] (**26**) in a 68% yield, and [(POCCP)PtCl] (**27**) in a 50% yield. It therefore appeared that as the number of P–O bonds in the ligand increased, so the yield of the metallated pincer complex decreased. This was supported by the observation of traces of resorcinol in ¹H NMR spectra of reactions between **1** and platinum precursors that had been subjected to prolonged thermolysis (greater than 100 hours at reflux in toluene), highlighting the lower stability of P–O bonds when compared to P–C bonds.

4.2 Reactions of Pt/Pd Pincer Compounds

4.2.1 Synthesis of Pincer Metal-Carbonyl Compounds

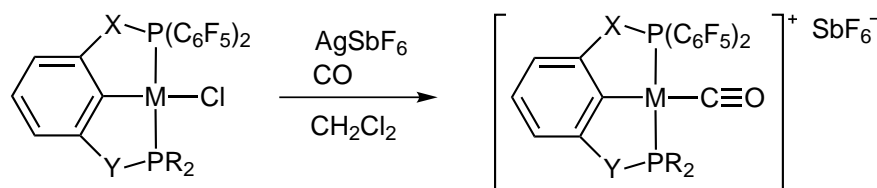
With platinum PCP pincer complexes **25**, **26**, and **27** in hand, the corresponding palladium pincer complexes were synthesised from [PdCl₂(NCMe)₂]. Palladium has demonstrated a higher reactivity than platinum for ligand cyclometallation reactions, which has been attributed to its greater electrophilicity assisting with the initial agostic interaction between the metal centre and the C–H bond being cleaved (the first step in Scheme 4.3).^{132,133} Therefore, shorter reaction times were required

to achieve ligand metallation on palladium, generally affording slightly higher yields of complexes [(POCOP)PdCl] (**28**), [(PCCCP)PdCl] (**29**), and [(POCCP)PdCl] (**30**) than for the analogous platinum complexes.

The NMR spectra of the platinum and palladium complexes were all consistent with the formation of tridentate pincer complexes. The ^{31}P NMR spectra all displayed signals downfield from those of the free ligand and unmetallated intermediates, consistent with deshielding of the phosphorus atoms upon coordination to the metal centre, followed by the loss of an electron-rich chloride ligand upon metallation. The platinum-phosphorus coupling constants of **25**, **26**, and **27** ranged from 3088 Hz to 3663 Hz, indicative of mutual *trans*-coordination of the phosphorus donors. Complexes of the asymmetric POCCP ligand **3** also displayed large *trans* phosphorus coupling of 460–470 Hz, significantly larger than that observed for the only other Group 10 metal phosphine-phosphinite pincer complex reported (388 Hz).¹³ This unusual coordination of mutually *trans* donating and accepting phosphine ligands may provide a synergy that strengthens this phosphorus-phosphorus coupling interaction.

The loss of a signal for the H-2 proton environment was evident in the ^1H NMR spectra of all compounds, with the remaining proton resonances shifted slightly upon metallation. The methylene proton signals of the PCCCP complexes [(PCCCP)PtCl] (**26**) and [(PCCCP)PdCl] (**29**) had changed in appearance, from a doublet in the free ligand **2** to virtual triplets in the metal complexes due to strong coupling through the metal atom to the second phosphorus donor. All spectroscopic data for the previously synthesised complex **29** were in agreement with that previously reported;⁵⁷ however, the isolated yield of 64% was significantly lower than the literature yield of 82%. As the previously reported synthesis proceeded *via* a two step reaction from the less readily synthesised $[\text{Pd}(\text{NCMe})_4][\text{BF}_4]_2$ starting material, the synthesis reported herein can be seen as an alternate preparation that offers a more convenient but slightly lower yielding route to **29**. In all [(PCP)MCl] complexes synthesised the ^{19}F NMR spectra are unremarkable, each showing three signals in a 2:1:2 (*ortho:para:meta*) ratio, consistent with free rotation of the pentafluorophenyl groups.

To assess the electronic characteristics of each metal centre, the metal-carbonyl derivatives [(PCP)M(CO)]⁺ were prepared by chloride abstraction with silver hexafluoroantimonate followed by exposure to carbon monoxide gas. The C–O stretches were measured by infrared (IR) spectroscopy, and are listed in Table 4.1. The C–O stretching frequency of metal carbonyls is very sensitive to the electron density on the metal centre, with more electron-rich metal centres displaying a greater de-

Table 4.1 Infrared C–O stretches of pincer carbonyl complexes.

Formula	Compound	X	Y	R	$\nu_{\text{C-O}}$ (cm^{-1})	$\Delta_{\delta_{\text{m,p}}}$ ^a (ppm)
$[(\text{POCOP})\text{Pt}(\text{CO})][\text{SbF}_6]$	31	O	O	C_6F_5	2145	15.8
$[(\text{PCCCP})\text{Pt}(\text{CO})][\text{SbF}_6]$	32	CH_2	CH_2	C_6F_5	2127	13.3
$[(\text{POCCP})\text{Pt}(\text{CO})][\text{SbF}_6]$	33	O	CH_2	<i>t</i> Bu	2111	13.8
$[(\text{POCOP})\text{Pd}(\text{CO})][\text{SbF}_6]$	34	O	O	C_6F_5	2170	15.1
$[(\text{PCCCP})\text{Pd}(\text{CO})][\text{SbF}_6]$	35	CH_2	CH_2	C_6F_5	2148	13.4
$[(\text{POCCP})\text{Pd}(\text{CO})][\text{SbF}_6]$	36	O	CH_2	<i>t</i> Bu	2140	13.9

^aValue of $\Delta_{\delta_{\text{m,p}}}$ is for the $[(\text{PCP})\text{MCl}]$ species, to reflect that this parameter may be used as an alternate evaluation of electron density within the pincer complex.

gree of π -backbonding to the carbonyl ligand, meaning that the carbonyl stretch is shifted to lower wavenumbers with increasing electron density on the metal. The observed magnitude of the C–O stretching frequency followed the pattern $\text{POCOP} > \text{PCCCP} > \text{POCCP}$; the enhanced π -acceptor ability of the phosphinite POCOP generated the most electron-poor metal centres, while the strong σ -donor ability of the *tert*-butyl phosphine in POCCP resulted in the most electron-rich metal centres.

Of note is the observation that the C–O stretches of compounds **31**, **34**, and **35** appeared at wavenumbers greater than that of free carbon monoxide (2143 cm^{-1}). While it appears counterintuitive that bonding to a metal centre may *increase* the strength of this carbon-oxygen bond, examination of the molecular orbital diagram of carbon monoxide (Figure 4.2) reveals that the HOMO is a σ^* antibonding orbital. Therefore, loss of electron density from this orbital upon coordination to the metal centre will increase the C–O bond order, resulting in a shorter, stronger bond. Similarly, the LUMO is a π^* antibonding orbital; during π -backbonding the metal centre donates electron density into this antibonding orbital, reducing the C–O bond order and weakening of the C–O bond as the amount of backdonation increases. Additionally, electrostatic factors may further serve to increase the C–O stretching frequency of metal-carbonyl complexes in complexes where minimal π -backbonding occurs.¹³⁴

Based on reported C–O stretching frequencies, the palladium complexes **34**, **35**, **36**, and the platinum complex **31** represent some of the most electron-poor PCP pincer compounds reported to date. The highest C–O stretching frequency reported for a palladium PCP pincer compound is 2141 cm^{-1} ,¹³⁵ significantly lower than the 2170 cm^{-1} displayed by the POCOP complex **34**. A platinum

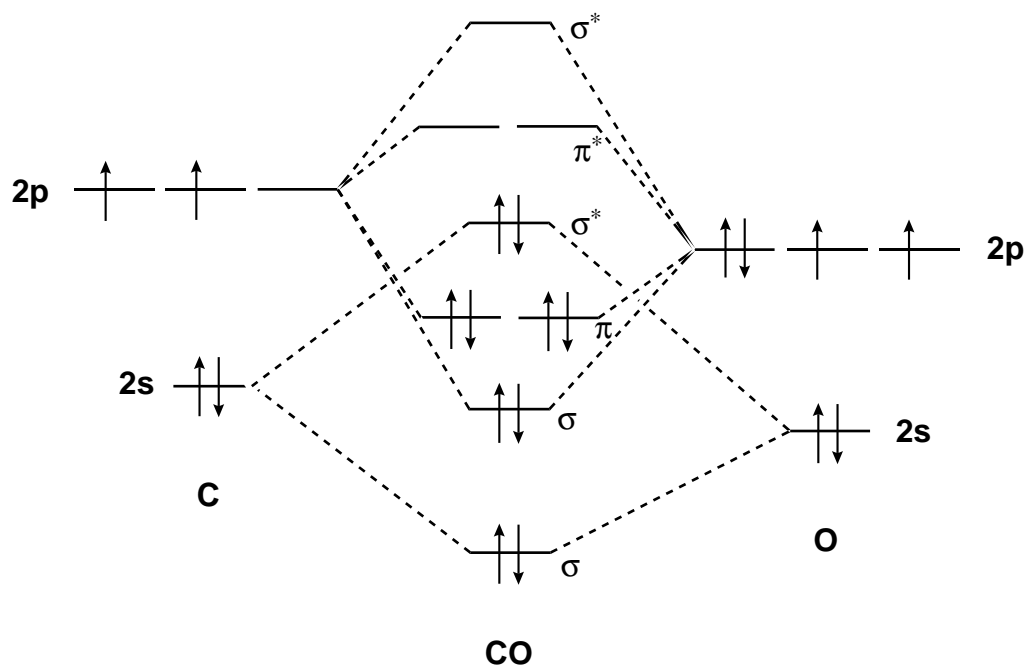


Figure 4.2 Molecular orbital diagram of carbon monoxide.

bis(trifluoromethyl)phosphine pincer complex has been reported to display a C–O stretch at 2143 cm^{-1} ,⁵⁸ higher than the analogous bis(pentafluorophenyl)phosphine **32**, but slightly lower than the phosphinite **31**, demonstrating the enhanced π -acceptor capability of trifluoromethyl phosphines over pentafluorophenyl phosphines. Most reported alkyl phosphine PCP pincer complexes have displayed C–O stretches in the range $2070\text{--}2080\text{ cm}^{-1}$,^{136,137} as the complexes reported herein possess values from $2111\text{--}2170\text{ cm}^{-1}$ they represent unusual examples of pincer complexes with very electron-poor metal centres.

Another parameter that provides information on the electronic character of these complexes is $\Delta_{\delta_{\text{m,p}}}$, the difference in chemical shift between the *meta* and *para* fluorines of the $\text{P}(\text{C}_6\text{F}_5)_2$ group. This has commonly been used to determine the degree of coordination of pentafluorophenyl borate anions,¹³⁸ but can also provide an indication of the electron density on the phosphorus atom in pentafluorophenyl phosphine ligands.⁵⁷ Values for the ligands POCOPH (**1**), PCCCPH (**2**), and POC-CPH (**3**) are 12.0, 11.1, and 11.8 ppm respectively, and reflected the slightly more electron poor nature of the pentafluorophenyl phosphinite group compared to the pentafluorophenyl phosphine group. The $\Delta_{\delta_{\text{m,p}}}$ values for the metallated complexes (Table 4.1) are predictably higher than for the free ligands, representing the loss of electron density from the phosphorus donors upon metal coordination. Of note is that for **3**, the $\Delta_{\delta_{\text{m,p}}}$ value is very similar to **1** for the free ligand (0.2 ppm lower), indicating that the electron rich *tert*-butyl phosphine is too far removed from the pentafluorophenyl phosphinite to affect it electronically. However, upon metal coordination, there is a 2.0 ppm difference (on platinum) in $\Delta_{\delta_{\text{m,p}}}$ values, indicating the

increased donor ability of the *tert*-butyl phosphine has reduced the demand of the metal for electron density from the phosphinite. While these values are an interesting measure of the electronics of the pentafluorophenyl ring (and the phosphorus donor by association), as seen in Table 4.1 they do not correlate well with the C–O stretching frequencies between complexes of different metals, or between complexes with different numbers of pentafluorophenyl-substituted donors.

The NMR data obtained for the carbonyl compounds **31**, **32**, **33**, **34**, **35**, and **36** was consistent with the synthesis of a $[(\text{PCP})\text{M}(\text{CO})]^+$ complex in each instance. Spectroscopically there were minor differences between each carbonyl complex and its parent chloride. The ^{31}P NMR signal of the $\text{P}(\text{C}_6\text{F}_5)_2$ groups experienced small chemical shift differences of 2–6 ppm, while the P^tBu_2 groups experienced substantial deshielding of between 19–26 ppm, a consequence of the cationic metal centre being able to extract further electron density from the more donating *tert*-butyl phosphines, but less so from the pentafluorophenyl phosphines or phosphinites. The pentafluorophenyl groups do experience this increased electron demand to some extent, as each carbonyl complex possessed $\Delta_{\delta_{\text{m,p}}}$ values about 1–3 ppm higher than for the analogous chloride complex. Similarly, ^1H NMR spectra showed that the proton environments of each ligand backbone were shifted downfield by an average of about 0.4 ppm, reflecting the loss of electron density from the metal centre upon the formation of these cationic carbonyl complexes.

The presence of the carbonyl ligand was confirmed in each instance by ^{13}C NMR spectroscopy, with all of the CO ligands appearing between $\delta_{\text{C}} = 177$ and 181 ppm. Platinum-phosphorus coupling was able to be resolved for the PCCCP and POCCP complexes **32** and **33**, having values of 1068 and 1064 Hz respectively, consistent with the presence of a platinum-bound carbonyl.

Single crystals of the platinum carbonyl $[(\text{POCOP})\text{Pt}(\text{CO})][\text{SbF}_6]$ (**31**) suitable for single crystal X-ray diffraction were grown by slow evaporation from a dichloromethane solution of **37** under a nitrogen atmosphere at room temperature. While there are many reported crystal structures of the phosphine PCCCP pincer complexes, there are significantly fewer examples of the corresponding phosphinite POCOP species. Compound **31** represents the first example of a crystallographically characterised Group 10 $[(\text{POCOP})\text{M}(\text{CO})]^+$ complex, and only the third X-ray crystal structure of a POCOP platinum pincer species.

The X-ray crystal structure (Figure 4.3) showed the expected tridentate κ^3 -PCP coordination of the pincer ligand, with the carbon monoxide ligand coordinated to the platinum *trans* to the metallated carbon of the pincer backbone. Impor-

tant structural data are given in Table 4.2. The solid state structure revealed a considerable distortion about the platinum centre in **31**; while the C–Pt–CO angle is close to the expected 180° ($178.72(9)^\circ$), the P–Pt–P angle of $157.73(2)^\circ$ is substantially smaller than for idealised square planar geometry. This distortion is common for similar pincer complexes, with platinum PCCCP pincer complexes typically possessing small P–Pt–P angles in the range 161 – 168° ,⁵⁸ while the only other example of a [(POCOP)PtX] species demonstrated a relatively small P–Pt–P angle of $161.20(4)^\circ$.¹²⁹ The small P–Pt–P angle in **31** was likely to be due to the electron-poor phosphorus atoms inducing polarisation and shortening of the P–O bonds (average bond length of $1.607(4)$ Å, compared to $1.644(10)$ Å in a more electron-rich platinum phosphinite¹²⁹), resulting in more strained five-membered chelate rings. This influence of short P–O bonds in decreasing the P–Pt–P angle is also observed in an isoelectronic iridium carbonyl complex possessing similarly electron-poor tris(trifluoromethyl)phenyl phosphinite donors.⁴⁶

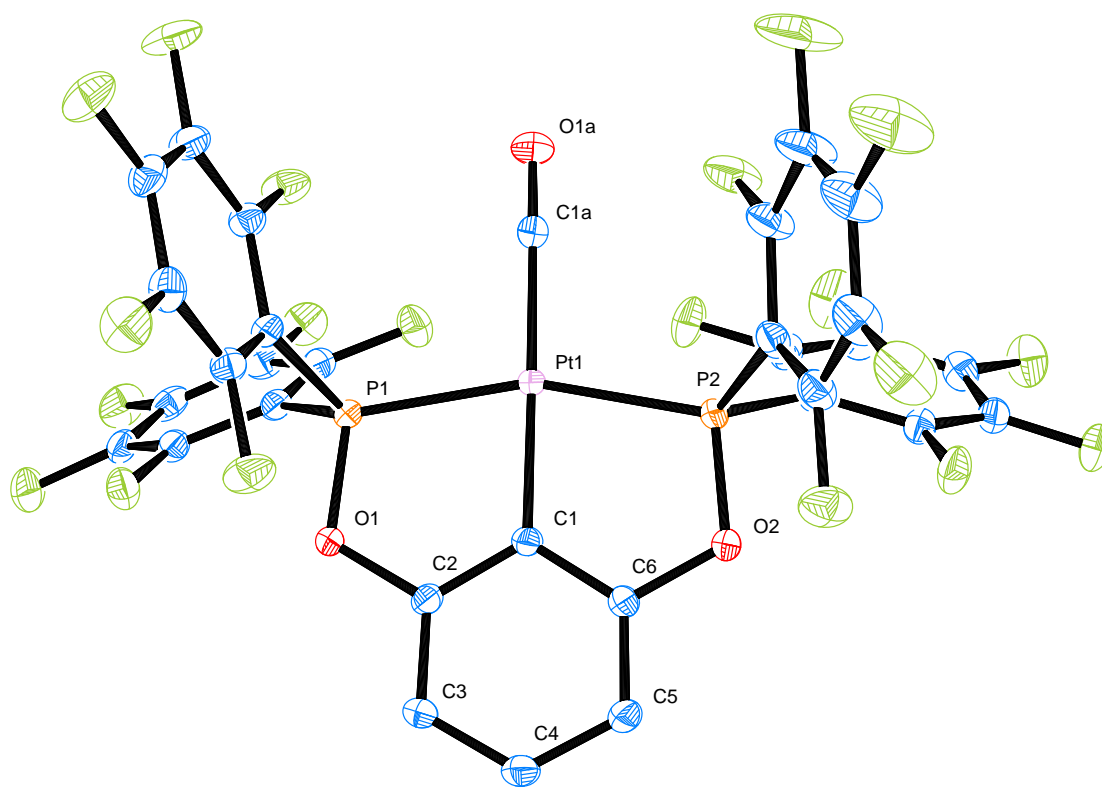


Figure 4.3 ORTEP diagram of [(POCOP)Pt(CO)][SbF₆] (**31**) (50% probability thermal ellipsoids). Hexafluoroantimonate counterion and hydrogen atoms omitted for clarity.

The C–O and Pd–C bond lengths for the carbonyl ligand of $1.117(3)$ Å and $1.962(2)$ Å were broadly consistent with the IR data ($\nu(\text{C–O}) = 2145 \text{ cm}^{-1}$), and

Table 4.2 Selected bond distances (Å) and angles (°) for complex [(POCOP)Pt(CO)][SbF₆] (**31**).

Bond distances (Å)		Bond angles (°)	
Pt1–P1	2.2748(6)	P1–Pt1–C1a	99.59(7)
Pt1–P2	2.2829(6)	P2–Pt1–C1a	102.33(7)
Pt1–C1	2.008(2)	P1–Pt1–C1	79.35(6)
Pt1–C1a	1.962(2)	P2–Pt1–C1	78.78(6)
C1a–O1a	1.117(3)	C1–Pt1–C1a	178.72(9)
Pt1...F–SbF ₅	3.529(6)	Pt1–C1a–O1a	179.2(2)

Table 4.3 Crystallographic data for complex [(POCOP)Pt(CO)][SbF₆] (**31**).

Empirical formula	C ₃₁ H ₃ F ₂₀ O ₃ P ₂ Pt · SbF ₆
Formula weight	1296.11
Crystal system	Monoclinic
Space group	<i>P</i> 2 ₁ / <i>n</i>
<i>a</i> /Å	10.0907(3)
<i>b</i> /Å	19.0384(5)
<i>c</i> /Å	18.9040(5)
α /°	90.00
β /°	103.6740(10)
γ /°	90.00
<i>V</i> /Å ³	3528.73(17)
<i>Z</i>	4
Cell determination reflections	9004
Cell determination range, $\theta_{\min} \longrightarrow \theta_{\max}$ /°	2.111 \longrightarrow 31.921
Temperature/K	113(2)
Radiation type	Mo K α
Radiation (λ)/Å	0.71073
Crystal size/ mm	0.5 \times 0.14 \times 0.14
<i>D</i> _{calc} /g m ^{−3}	2.440
<i>F</i> (000)	2424
μ /mm ^{−1}	4.99
Experimental absorption correction type	Multi-scan (SADABS)
<i>T</i> _{max} , <i>T</i> _{min}	0.7463, 0.5142
Reflections collected	101603, <i>R</i> _{equiv} = 0.0390
Index range <i>h</i>	−14 \longrightarrow 15
Index range <i>k</i>	−28 \longrightarrow 28
Index range <i>l</i>	−28 \longrightarrow 28
θ range/°	2.37 \longrightarrow 32.07
Independent reflections	11960
Reflections [<i>I</i> > 2 σ (<i>I</i>)]	10251
Restraints/parameters	0/653
GOF	1.053
<i>R</i> ₁ [<i>I</i> > 2 σ (<i>I</i>)]	0.0233
w <i>R</i> 2 [<i>I</i> > 2 σ (<i>I</i>)]	0.0558
<i>R</i> ₁ [all data]	0.0415
w <i>R</i> 2 [all data]	0.0595
Residual density/e Å ^{−3}	−0.613 < 3.016

indicated carbon monoxide coordination to an electron-poor metal centre. These values were very similar to the corresponding values reported for an electron-poor trifluoromethyl phosphine pincer compound (1.114(6) Å, 1.964(4) Å, and 2143 cm⁻¹ respectively),⁵⁸ with a sufficiently shorter C–O bond and longer Pd–C bond than in the more strongly π -backbonding isopropyl phosphine pincer complex (1.131(4) Å, 1.919(3) Å, and 2080 cm⁻¹).¹³⁷ In this case, these results confirmed the strong C–O bond suggested by IR spectroscopy. However, care must be taken when comparing small changes in X-ray crystal data, as the solid state measurement reflects the average distribution of electron density within the crystal lattice, and hence is susceptible to disorder and defects.

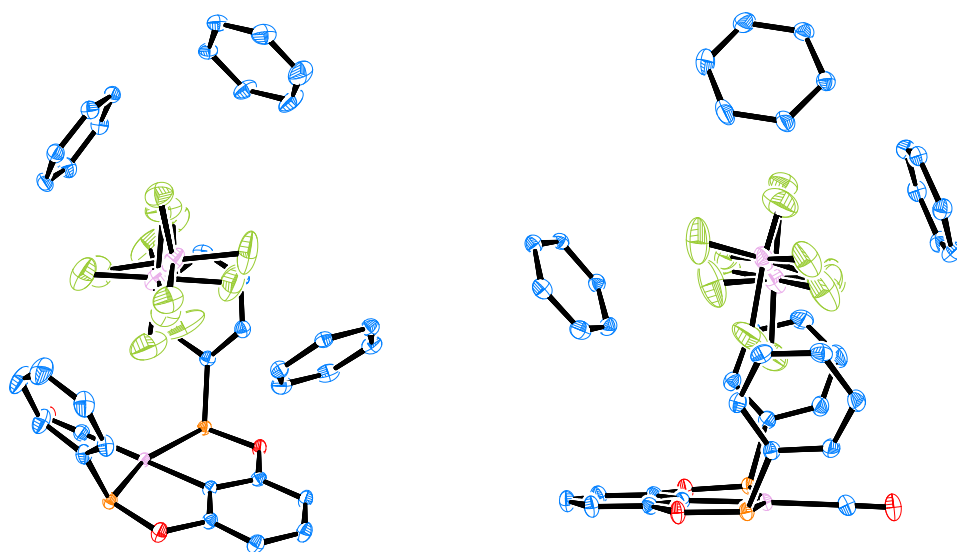


Figure 4.4 ORTEP diagram of [(POCOP)Pt(CO)][SbF₆] (**31**) showing two view of the packing of the hexafluoroantimonate anion (50% probability thermal ellipsoids). Hydrogen atoms, aromatic fluorines, and downward-facing pentafluorophenyl substituents on the phosphorus atoms omitted for clarity. Aromatic rings surrounding the anion represent pentafluorophenyl substituents of adjacent molecules of **31**.

The hexafluoroantimonate counterion in **31** displayed some disorder, which could be modelled with two superimposed and slightly offset SbF₆ octahedra, that refined to adopt an approximately 40:60 occupancy ratio. In the solid state structure the anion occupies a void in which it sits almost directly above the coordination plane of the platinum, enclosed by two pentafluorophenyl rings of the same molecule, as well as three pentafluorophenyl rings from adjacent molecules of **31** (Figure 4.4). The Pt \cdots F distance is 3.529(6) Å, slightly larger than the sum of the van der Waals radii for platinum and fluorine (3.32 Å), indicating that there is not likely to be any significant interaction between the electron-poor platinum centre and electron rich counterion. A similar, slightly shorter Pt \cdots F distance of 3.333(7) Å was observed in the crystal structure of a similar, trifluoromethyl-substituted platinum pincer

complex,⁵⁸ which suggested that such a packing arrangement may be favoured in the solid state for such structures.

All of the palladium carbonyl compounds underwent gradual loss of bound carbon monoxide, as has been noted in the literature for similar palladium species.^{52,135,136} The completely decarbonylated adduct of **35**, [(PCCCP)Pd][SbF₆] (**39**) was isolated in a spectroscopically pure state, having gradually formed over the course of months under ambient conditions. Infrared spectroscopy of **39** revealed a spectrum almost identical to that of the carbonyl complex **35**, with the absence of the C–O stretch at 2148 cm⁻¹. The Sb–F stretch of the counterion was observed at 665 cm⁻¹, which confirmed that the product remained ionic (Figure 4.5).

Solid samples of **34** and **36** had also undergone loss of carbon monoxide under ambient conditions, with the decarbonylated species **38** and **40** comprising significant amounts of the material. Characterisation of the new species **38**, **39**, and **40** by NMR spectroscopy revealed that all species displayed ¹H, ³¹P and ¹⁹F NMR signals shifted upfield from those of the parent palladium carbonyl species. The ¹H and ¹⁹F signals of both species, along with the P^{*t*}Bu₂ ³¹P NMR signal of **40**, also appeared downfield of the corresponding palladium chloride species, giving the impression that these compounds represented almost a spectroscopic ‘average’ between the [(PCP)PdCl] and [(PCP)Pd(CO)]⁺ species. This effect has previously been observed in the spectroscopic data of PCP pincer chlorides subjected to halide abstraction.¹³⁹

Carbon-13 NMR data of **39** indicated that no carbon-containing species were bound in the coordination site vacated by the carbon monoxide, while the ¹⁹F NMR spectrum displayed only the three sharp peaks in a 2:1:2 ratio expected for the freely rotating C₆F₅ groups, ruling out stabilisation of the decarbonylated species by long-lived C–F...Pd interactions. The similarity in chemical shift of the *ortho*-fluorine environments between **35** and the decarbonylated complex **39** ($\delta_F = -128.7$ ppm and -129.7 ppm respectively) also indicated that there was no rapid, fluxional interaction between the metal and the *ortho*-fluorine atoms. No signals attributed to the hexafluoroantimonate counterion were observed in the ¹⁹F NMR spectrum; however, as antimony possesses two quadrupolar NMR active isotopes (¹²¹Sb and ¹²³Sb), hexafluoroantimonate anions often appear as extremely broad signals and may be hard to detect by ¹⁹F NMR spectroscopy. Thus it is difficult to rule out stabilisation of these decarbonylated species by hexafluoroantimonate coordination. Infrared spectroscopy did not provide evidence either for or against anion coordination — while the single band for the Sb–F stretch observed at 665 cm⁻¹ may indicate anion coordination is unlikely (Figure 4.5), a single “broad asymmetric ab-

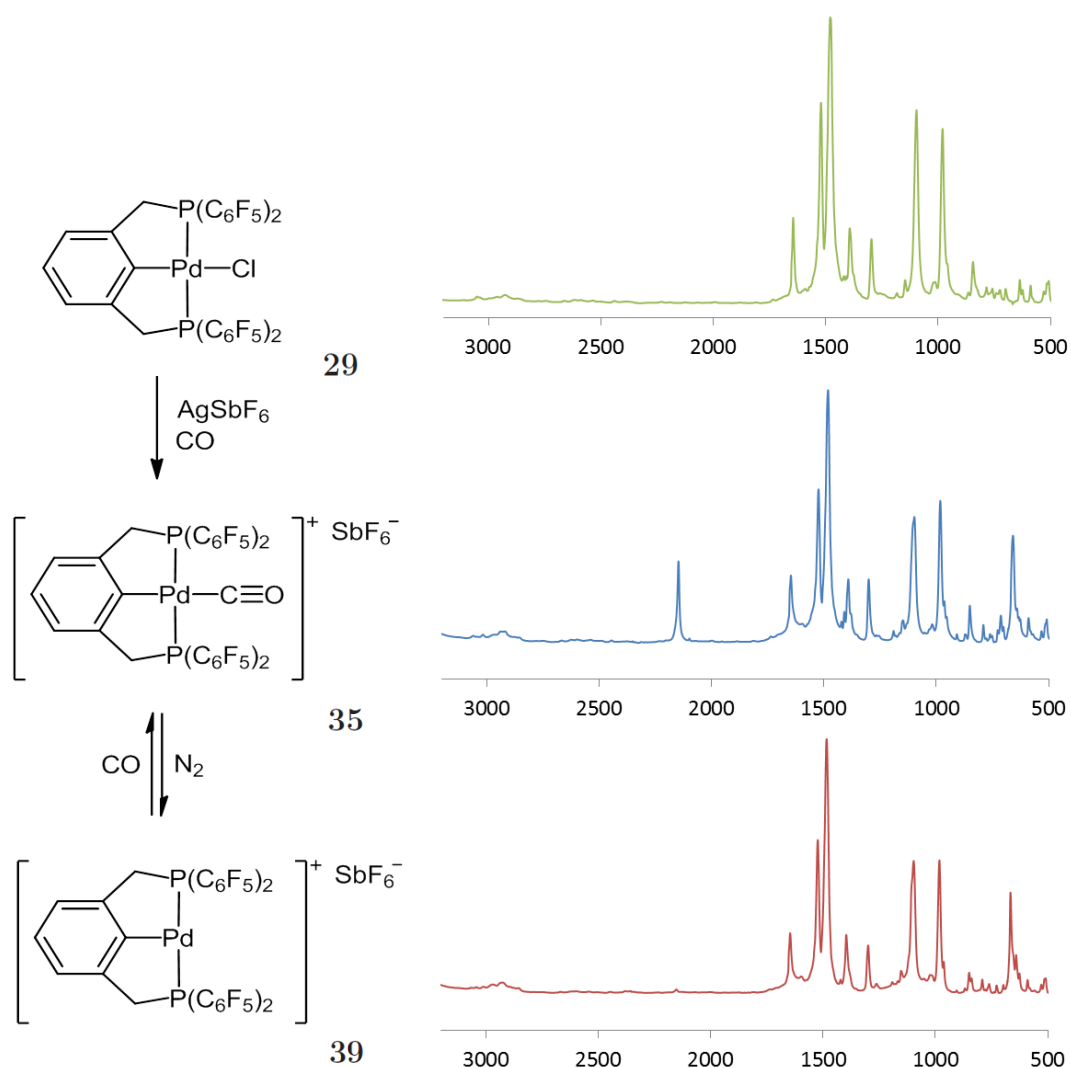


Figure 4.5 IR spectra showing carbonylation of **29** and subsequent decarbonylation of **35**. The $\text{C}\equiv\text{O}$ stretch of the carbonyl complex appears at 2148 cm^{-1} , and the SbF_6^- stretch of the hexafluoroantimonate counterion is observed around 650 cm^{-1} for both of the cationic species, but not the starting material.

sorption” at 660 cm^{-1} has been observed in an instance where hexafluoroantimonate coordination has been proven by X-ray crystallography.¹⁴⁰

To further investigate the possibility of anion coordination to the decarbonylated palladium centre, the tetrafluoroborate salt of the carbonyl $[(\text{PCCCP})\text{Pd}(\text{CO})][\text{BF}_4]$ and decarbonylated species $[(\text{PCCCP})\text{Pd}][\text{BF}_4]$ were synthesised, to enable the ^{19}F NMR chemical shifts of the anion to be established. Fluorine NMR spectroscopy did not reveal any significant differences between the anion in the carbonyl complex **35** and the decarbonylated complex **39**, as the anion appeared as either a broad singlet or two sharp singlets in a 1:4 ratio (due to ^{10}B and ^{11}B) around $\delta_{\text{F}} = -153\text{ ppm}$ for both species. Free BF_4^- has been observed at $\delta_{\text{F}} = -151\text{ ppm}$ and coordinated BF_4^- at -163 ppm ,¹⁴¹ therefore this data indicated that the decarbonylated species may possess a slight degree of metal-anion interaction in solution at room temperature, but the tetrafluoroborate anion in both **35** and **39** can be regarded as non-coordinating.

In order to determine whether small amounts of water were coordinating to the palladium centre, a solution of the decarbonylated species **39** in dichloromethane- d_2 was treated with $2\text{ }\mu\text{L}$ D_2O (approximately ten equivalents) and warmed gently to promote $\text{H}_2\text{O}/\text{D}_2\text{O}$ exchange. Analysis of the sample by NMR spectroscopy did not reveal any discernible changes resulting from treatment with D_2O , and IR spectroscopy did not show the expected O–D stretch around $2400\text{--}2700\text{ cm}^{-1}$.^{*} Thus it is unlikely that H_2O occupies the vacant coordination site generated upon loss of carbon monoxide in solution. However, IR spectroscopy performed on solid samples of **35** that had stood for weeks under ambient conditions revealed a drastic decrease in the intensity of the C–O stretch, along with the appearance of a sharp peak at 3672 cm^{-1} . This was attributed to the presence of coordinated H_2O , indicating that adventitious water took the place of carbon monoxide when this decarbonylation occurred in the solid state. As there was evidence for the decarbonylated species **39** binding water in the solid state but not in solution, it is likely that in solution the “vacant” coordination site is occupied by solvent molecules. However, this was unable to be conclusively established by NMR or infrared spectroscopy.

Quantitative regeneration of each of the palladium carbonyl complexes **34**, **35**, and **36** was achieved by passage of carbon monoxide through dichloromethane- d_2 solutions of the decarbonylated species for 15 minutes at room temperature. The carbonylation was found to be reversible, with displacement of carbon monoxide from the metal centre observed upon passage of inert gas (argon, nitrogen, or methane)

^{*}As the O–H stretch for H_2O would be expected around $3500\text{--}3700\text{ cm}^{-1}$, Hooke’s Law predicts that on doubling the mass of the hydrogen atom (upon deuterium substitution) the stretching frequency will decrease by a factor of $\sqrt{2}$, therefore appearing in the vicinity of $2400\text{--}2700\text{ cm}^{-1}$.

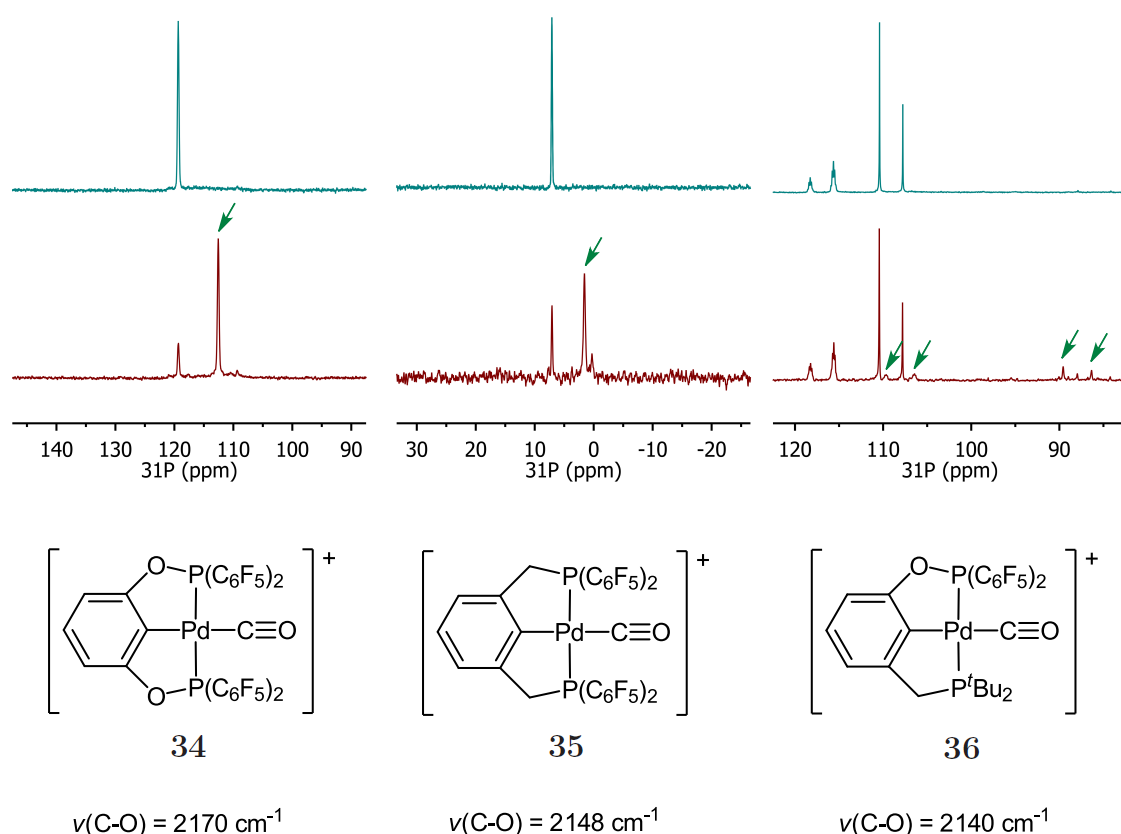


Figure 4.6 Phosphorus-31 NMR spectra showing the decarbonylation of compounds **34**, **35**, and **36** in dichloromethane- d_2 . Nitrogen was passed through solution for 30 minutes between obtaining top and bottom spectra. Resonances attributed to decarbonylated products are indicated by an arrow.

through these same solutions. The decarbonylated species were seen to slowly decompose over time in solution even under an inert atmosphere, as broad resonances appeared in the ^1H NMR spectra, accompanied by a decrease in the signal to noise ratio and the appearance of dark precipitate in solution. As previously mentioned, palladium pincer carbonyl complexes have been observed to undergo decarbonylation, however this is the first report of reversible carbon monoxide uptake for these species. The Brookhart research group has reported an electron-poor iridium PCP pincer complex capable of undergoing exchangeable binding of small gaseous molecules in the solid state,⁴⁶ but in this species the carbon monoxide is unable to be displaced.

The ease of decarbonylation of each of the carbonyl complexes **34**, **35**, and **36** was investigated by bubbling nitrogen through a dichloromethane- d_2 solution of the carbonyl compound for 30 minutes, then assessing the proportion of decarbonylated species present by NMR spectroscopy. The ease of carbonyl displacement for each species was in broad agreement with the IR stretching frequency of the C–O bond; the larger the C–O stretching frequency, the more readily the decarbonyla-

tion occurred (Figure 4.6). While there existed a moderate difference between C–O stretching frequencies of the POCOP (**34**) and PCCCP (**35**) carbonyl complexes ($\nu(\text{C–O}) = 2170$ and 2148 cm^{-1} respectively), both decarbonylation reactions were observed to proceed swiftly (progressing approximately 90% and 75% respectively after 30 minutes at room temperature). However, while the more electron-rich POCCP complex **36** possessed a C–O stretching frequency close to that of **35** ($\nu(\text{C–O}) = 2140\text{ cm}^{-1}$), its decarbonylation was much less facile, having progressed only about 10% under identical conditions to those above. Thus it appears that Pd–CO π -backbonding effects play a large part in the stabilisation of these carbonyl complexes; decarbonylation was facile for compounds expected to possess negligible backbonding (**34** and **35**), but occurred significantly more slowly for the most electron-rich compound, which is most capable of π -backbonding **36**.

4.2.2 Methylation of Pincer Chloride Complexes

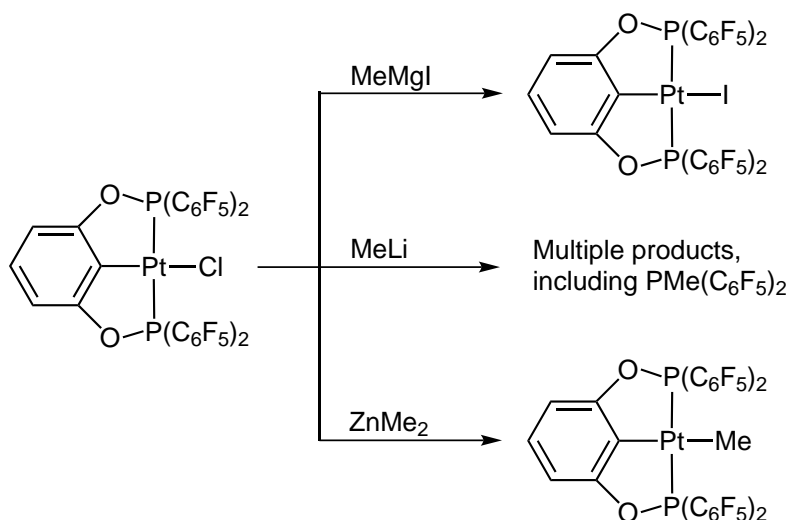
As the platinum methyl complexes $[(\text{PCP})\text{PtMe}]$ could not be synthesised directly from $[\text{PtMe}_2(\text{hex})]$, methylation of the pincer chloride complexes was examined. Methylation of $[(\text{PCCCP})\text{PtCl}]$ pincer complexes has previously been reported using methyllithium for electron-rich complexes,¹⁴² and methylmagnesium bromide for electron-poor complexes.⁵⁸

Methylation reactions were first trialled on a small scale with the most electron-poor compound $[(\text{POCOP})\text{PtCl}]$ (**25**). Reaction of **25** with methylmagnesium iodide (0.5 M solution in ether) was seen to produce a new species **41**, which had spectroscopic data similar to the starting material and the anticipated methyl complex ($\delta_{\text{P}} = 109.2\text{ ppm}$, $^1J_{\text{Pt-P}} = 3541\text{ Hz}$), but lacked the expected platinum-methyl resonance in the ^1H NMR spectrum. Analysis of **41** by HRMS was unsuccessful, as only peaks due to degradation of the ligand were observed, making it difficult to confirm whether a methyl or an iodide was coordinated to the metal centre. However, the analogous POCCP complex $[(\text{POCCP})\text{PtI}]$ (**42**) was synthesised with methylmagnesium iodide in an identical manner, and confirmed as the platinum iodide species by HRMS, with the $[\text{M}+\text{Na}]^+$ ion detected at 959 amu. Comparison of spectroscopic data between **41** and **42** indicated that the POCOP complex **41** was also the platinum iodide complex $[(\text{POCOP})\text{PtI}]$. As no traces of the desired methyl complex were detected in either of the reaction mixtures with methylmagnesium iodide, this indicated that the Grignard reagent was not a strong enough methylating agent to facilitate the formation of these platinum-methyl complexes.

Reactions between **25** and the stronger methylating agent methyllithium (1.2 M in ether) were observed to produce the desired methyl compound [(POCOP)PtMe] (**43**; $\delta_{\text{P}} = 108.5$ ppm, $^1J_{\text{Pt-P}} = 3752$ Hz) in only small amounts, along with considerable quantities of byproduct. One byproduct that could be identified was $\text{PMe}(\text{C}_6\text{F}_5)_2$. This displayed a quintet resonance in the ^{31}P NMR spectrum, which marked it as an uncoordinated ligand containing the $\text{P}(\text{C}_6\text{F}_5)_2$ functionality. The ^{31}P NMR chemical shift at $\delta_{\text{P}} = -53.1$ ppm, significantly downfield of the phosphinite ligand **1** (87.1 ppm), and close to that of the phosphine ligand **2** (-46.3 ppm), indicated that this product was a phosphine rather than phosphinite. Unfortunately the reaction mixture could not be purified to an extent where the nature of $\text{PMe}(\text{C}_6\text{F}_5)_2$ could be unambiguously confirmed by ^1H NMR spectroscopy. However, the ^{31}P NMR data is in good agreement with that previously reported for $\text{PMe}(\text{C}_6\text{F}_5)_2$,¹⁴³ indicating that this phosphine had likely been formed by nucleophilic attack by the methyl anion on the phosphorus atom of the phosphinite ligand, cleaving the P–O bond. The nucleophilic substitution of -OR groups on phosphorus by organolithium reagents has been established in the literature, being employed in the synthesis of phosphine ligands from phosphite, phosphonite, or phosphinite precursors.^{144,145} In this instance, despite coordination of the phosphinite to platinum, the pentafluorophenyl substituents render the phosphorus donor sufficiently nucleophilic that methylation at the phosphorus is competitive with methylation at the metal centre.

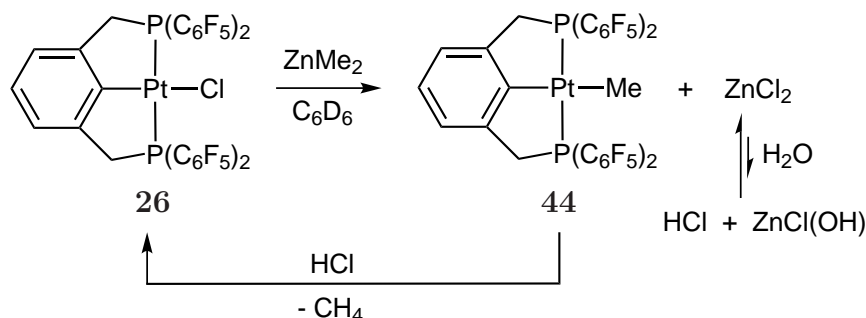
As methylmagnesium iodide had proven too weak and methyllithium had proven too strong to effectively methylate **25**, dimethyl zinc was investigated as an alternate methylating agent. A solution of dimethyl zinc in ether was synthesised by the addition of methyl iodide to a suspension of magnesium and zinc powders in diethyl ether, isolating the dimethyl zinc solution by co-distillation with the diethyl ether solvent. Reactions between **25** and dimethyl zinc were observed to produce exclusively the desired platinum methyl complex **43**. It appears that for this very electron-poor platinum compound, dimethyl zinc possesses an effective combination of high activity without sufficient nucleophilicity to facilitate P–O cleavage, making it an effective methylating agent (Scheme 4.4).

The remaining platinum chloride compounds **26** and **27** were subsequently treated with dimethylzinc solutions, in order to establish whether methylation occurred as selectively for these more electron-rich compounds as for **25**. In the case of the PC-CCP complex **26**, methylation with dimethyl zinc was observed to proceed smoothly, giving quantitative formation of the desired product [(PCCCP)PtMe] (**44**) after just three hours at room temperature. On standing for two months at room temperature in a stoppered NMR tube, significant conversion (>90%) from the methyl complex **44** back to the chloride starting material **26** was observed. This unexpected result



Scheme 4.4 The effect of different methylating agents on compound **25**.

was likely due to diffusion of water through the rubber septum; the action of this water on the zinc chloride would have produced small amounts of HCl in solution, which protonated the methyl complex, irreversibly eliminating methane and reforming the parent platinum chloride (Scheme 4.5).



Scheme 4.5 Synthesis of **44** and conversion back to **26** by action of ambient H_2O .

Methylation of the POCCP complex **27** proceeded slowly, attaining only a 50% conversion to the methylated product $[(\text{POCCP})\text{PtMe}]$ (**45**) after 44 hours at room temperature. Moderate amounts of a byproduct were also formed (present in about a 1:4 ratio with **45**), which was revealed to be the platinum iodide complex $[(\text{POCCP})\text{PtI}]$ (**42**) on comparison with an authentic sample of **42**. It transpired that the source of iodide in the reaction mixture was methyl iodide, which was present as unreacted starting material from the synthesis of the dimethyl zinc solution, as the methyl iodide possesses a similar boiling point to dimethylzinc (44 °C and 46 °C respectively). The iodide complex **42** was observed to be stable in the presence of large (greater than 10-fold) excesses of dimethyl zinc, and did not un-

dergo methylation even upon heating to 70 °C for 40 hours.

As reaction of **27** with methylmagnesium iodide had been observed to result in halide exchange, further methylation of **27** was attempted with methyllithium. Reaction between **27** and methyllithium was observed to produce predominantly the methylated product (>95% by NMR spectroscopy) **45** within 30 minutes at room temperature. This was in contrast to reactions between methyllithium and the POCOP complex **25**, which yielded a large number of degradation products.

In order to eliminate the possibility of halide exchange in these methylation reactions, a methyl iodide-free dimethyl zinc solution was prepared by repeating the aforementioned synthesis, using dibutyl ether rather than diethyl ether as the solvent. The high boiling point of dibutyl ether (142 °C) enabled neat dimethyl zinc to be isolated by fractional distillation of the reaction mixture, whereby it was diluted with toluene to concentration of approximately 1.5 M.

Upscaling the test methylations using the methyl iodide-free dimethyl zinc solution in toluene afforded the POCOP and PCCCP platinum methyl compounds **43** and **44** in yields of 76% and 87% respectively. However, when the reaction of [(POCCP)PtCl] **27** with methyllithium was repeated on a preparative scale (rather than on an NMR scale), NMR spectroscopy indicated that the reaction had produced a complex mixture containing a new product, **46**, as well as smaller amounts of the desired POCCP platinum methyl complex **45**, other unidentified minor products, and unreacted starting material **27**. It is not clear why this discrepancy in reaction selectivity should occur. Even when carried out with substoichiometric amounts of methyllithium, reaction mixtures contained predominantly the byproduct **46** and starting material. Subsequent treatment of these reaction mixtures with methyllithium did not promote further formation of the byproduct **46**, but led to the formation of a number of unidentified species. Further attempts to isolate **46** from these mixtures were ultimately unsuccessful.

While the byproduct **46** was not isolated, NMR data obtained of the reaction mixtures indicated it was likely to be a [(P^{Me}OCCP)Pt(C₆F₅)] complex, in which the methyl nucleophile had attacked the phosphinite group, causing a pentafluorophenyl group to migrate from the phosphorus to the platinum (Figure 4.7). Phosphorus-31 NMR spectroscopy revealed **46** possessed the distinctive two doublet signals of metallated complexes of the POCCP ligand **3**; however, while the P^tBu₂ group appeared close to that of the starting material (δ_P = 73.8 ppm, compared to 70.2 ppm for starting material), the signal for the phosphinite group had been shifted significantly downfield (132.0 ppm, compared to 108.7 ppm for the starting material).

This large downfield shift was consistent with the P–O bond of the phosphinite remaining unbroken, and substitution of the methyl group onto the phosphorus, as alkylphosphinites appear downfield of arylphosphinites.[†]

Incorporation of the methyl nucleophile onto the phosphinite was also indicated by a ^1H – ^{31}P HMBC experiment, with a signal at $\delta_{\text{H}} = 1.68$ observed to couple solely to the phosphinite group at $\delta_{\text{P}} = 132.0$ ppm. This signal also displayed the expected phosphorus and platinum coupling ($^2J_{\text{P-H}} = 9.5$ Hz, $^3J_{\text{Pt-H}} = 26.6$ Hz) in the ^1H NMR spectrum.

The fate of the displaced pentafluorophenyl group was revealed by ^{19}F NMR spectroscopy, with the appearance of distinctive signals with platinum coupling at $\delta_{\text{F}} = -114.3$ and -115.5 ppm ($^3J_{\text{Pt-F}} = 267$ and 230 Hz respectively). This was consistent with data for a previously reported $[(\text{PCP})\text{Pt}(\text{C}_6\text{F}_5)]$ species ($\delta_{\text{F}} = -107.2$ ppm, $^3J_{\text{Pt-P}} = 235$ Hz).¹⁴⁶ Integration of platinum-pentafluorophenyl and phosphorus-pentafluorophenyl ^{19}F NMR resonances confirmed that the two pentafluorophenyl groups were present in a 1:1 ratio. As the new methyl pentafluorophenyl phosphinite was chiral, the *tert*-butyl groups appeared diastereotopic in the ^1H NMR spectrum, as did the *ortho* and *meta* fluorines of the $\text{Pt-C}_6\text{F}_5$ group (which experienced restricted rotation). So while the byproduct **46** could not be unambiguously identified, there was sufficient evidence to indicate that reaction of **27** with methyllithium results in methylation at the phosphinite, along with pentafluorophenyl migration from the phosphinite to the platinum centre.

A similar reaction, involving methylation at phosphorus followed the migration of an aryl substituent onto a metal centre has been observed by Nakajima and colleagues upon treatment of an iron PNP pincer complex with dimethylmagnesium.¹⁴⁷ Furthermore, pentafluorophenyl migration from a bis(pentafluorophenyl)phosphine group to a metal centre has been reported to occur on rhodium carbonyl clusters containing $\text{P}(\text{C}_6\text{F}_5)_2$ groups.¹⁴⁸ Mass spectrometry data for the POCCP compounds reported herein also indicated that the P–C bond of the bis(pentafluorophenyl)phosphinite group was prone to cleavage. Data obtained for the POCCP methyl complex **45** subsequently synthesised (*vide infra*) revealed large peaks corresponding to $[\text{M-C}_6\text{F}_5+\text{MeOH}]^+$ (690 amu) and $[\text{M-C}_6\text{F}_5+\text{NCMe}]^+$ (699 amu), as well as the expected peaks due to loss of a methyl group. Mass spectroscopy also indicated that the POCCP chloride complexes $[(\text{POCCP})\text{PtCl}]$, **27**, and $[(\text{POCCP})\text{PdCl}]$, **30**, also underwent facile loss of a pentafluorophenyl substituent. For both **27** and **30**, significant peaks were observed in the mass spectra

[†]An example of this can be observed in the ^{31}P NMR data for $[(\text{POCOP})\text{PdI}]$ complexes of Kimura,⁵¹ where the diphenylphosphinite complex has a $\delta_{\text{P}} = 144.0$ ppm, whereas the diethylphosphinite complex appears downfield at $\delta_{\text{P}} = 176.9$ ppm.

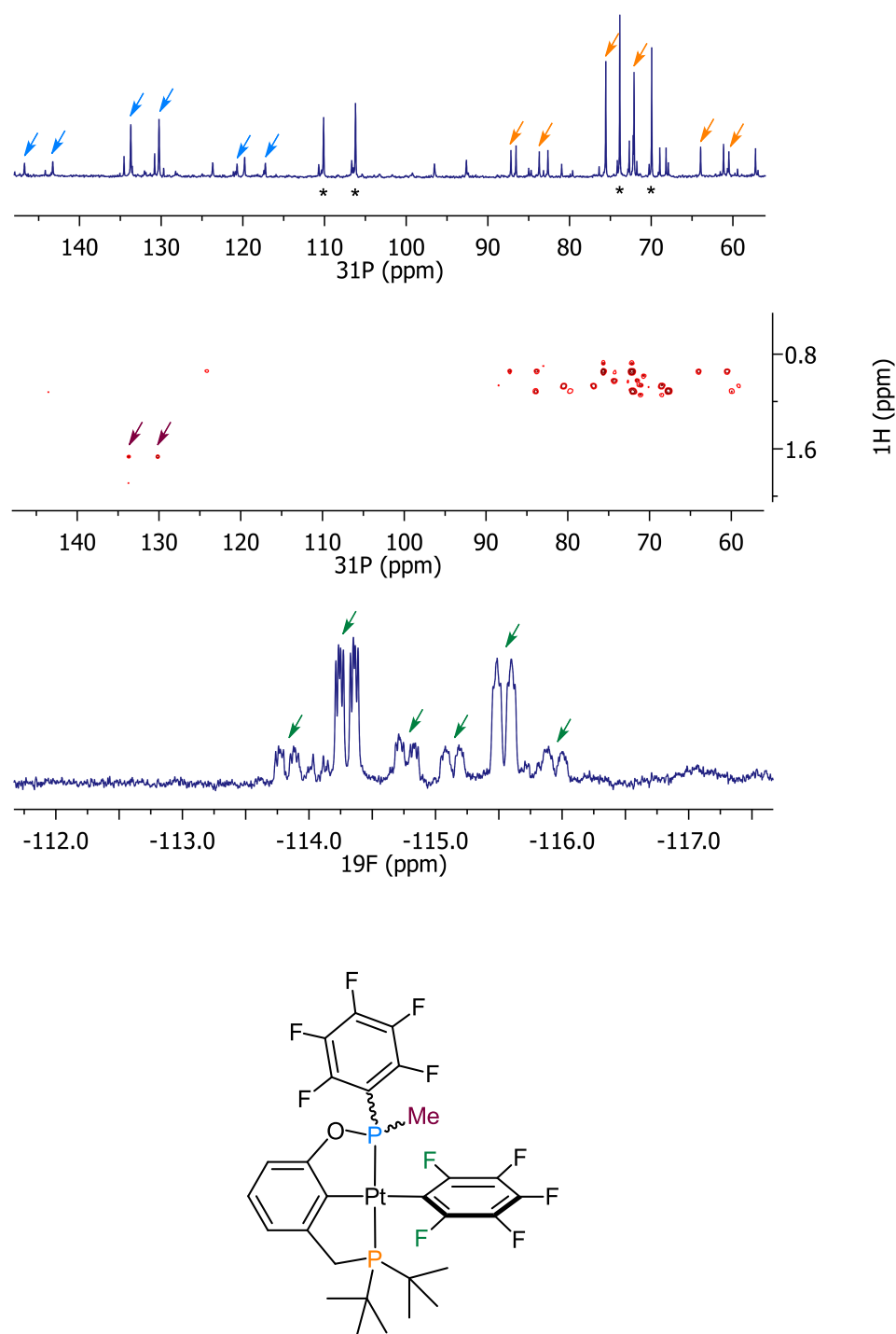


Figure 4.7 Spectroscopic data for byproduct **46**, showing, from top to bottom, the ^{31}P NMR spectrum, the ^1H - ^{31}P HMBC spectrum, and the ^{19}F NMR spectrum. The highlighted correlation in the ^1H - ^{31}P HMBC spectrum revealed the presence of a methyl group (red) attached to the phosphorus atom of the phosphinite group (blue). Distinctive ^{195}Pt coupling on the *ortho*-fluorine resonances (green) of a C_6F_5 group in the ^{19}F NMR indicated it was directly bound to the metal centre. Signals marked with an asterisk denote starting material **27** (peaks due to ^{195}Pt coupling in **27** not indicated).

at $M-144$ amu, corresponding to $[M-C_6F_5-Cl+OH+NCMe]^+$. Whilst the formation of these ions occurred under high energy conditions, the HRMS data revealed a predilection for the metallated POCCP ligand **3** to undergo the P–C cleavage observed in the formation of the pentafluorophenyl-migration product **46**.

The synthesis of the desired POCCP platinum methyl complex **45** was subsequently achieved by treatment of the parent platinum chloride **27** with the methyl iodide-free dimethyl zinc solution, as for the syntheses of the other platinum methyl compounds **43** and **44**. However, due to the more electron-rich nature of the starting material **27**, the methylation required a large excess of dimethyl zinc and prolonged reaction times (54 hours, compared to five hours for the formation of **43** and **44**), and afforded the desired compound **45** in a 63% yield.

Characterisation of platinum methyl complexes **43**, **44**, and **45** by ^{13}C NMR spectroscopy revealed the presence of platinum-methyl groups between -12 and -17 ppm, with platinum-carbon coupling constants of around 500 Hz. For the PCCCP and POCCP compounds **44** and **45**, carbon C-2 displayed a massive downfield shift of about 25 ppm on methylation. This was consistent with the replacement of an electron-rich chloride for the more poorly donating methyl group. The chemical shift of the C-2 environment of the POCOP complex **43** could not be conclusively determined due to overlap with other signals.

Analogous methylation of the POCOP and PCCCP palladium compounds **28** and **29** was attempted. Reactions performed with solutions of dimethylzinc in ether in both cases led to the formation of black solutions, while ^{31}P and ^{19}F NMR spectroscopy indicated the formation of a multitude of unidentified products in each reaction. Reaction between **29** and methylmagnesium iodide was also attempted, in the hope that the milder Grignard reagent would promote selective methylation without degradation. However, *in situ* monitoring of methylation reactions attempted with methylmagnesium iodide did not reveal the presence of any palladium-methyl resonances in the 1H NMR; only the appearance of broad, unidentified signals attributed to decomposition products were observed in the NMR spectra. Methylation of these palladium chlorides was not achieved with organometallic reagents; milder routes to methylation may be required for these electron-poor palladium compounds, as they are less robust than their platinum analogues.

4.2.3 Protonation of Platinum Methyl Complexes

As mentioned in Chapter 1, the low temperature protonation of a rhodium PNP pincer complex by the Brookhart research group yielded the first stable metal-methane σ -complex able to be fully characterised by NMR spectroscopy.²⁵ As the [(PCP)PtMe] complexes synthesised were isoelectronic with [(PNP)RhMe] complexes, the protonation reactions of these platinum methyl pincer complexes were examined in an attempt to determine the extent to which the electronic character of the ligand affected the reactivity of the Pt–Me group.

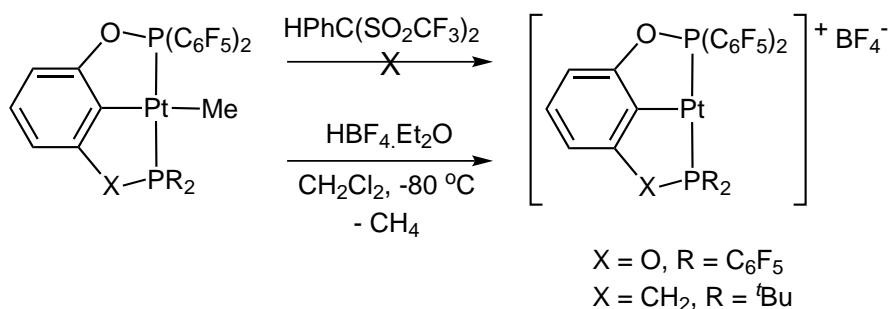


Figure 4.8 Protonation of **43** and **45** at low temperature.

The most electron-poor and least electron-poor of the platinum methyl complexes, [(POCOP)PtMe] (**43**) and [(POCCP)PtMe] (**45**) respectively, were dissolved in dichloromethane- d_2 , cooled to $-196\text{ }^\circ\text{C}$, and treated with a slight excess of the carbacid $\text{HPhC}(\text{SO}_2\text{CF}_3)_2$ (Figure 4.8). Each sample was placed in the NMR instrument and allowed to warm to $-80\text{ }^\circ\text{C}$, with the sample monitored continuously by ^1H and ^{19}F NMR spectroscopy. After twenty minutes in the instrument, neither reaction had progressed at all, and samples were withdrawn and maintained at $-78\text{ }^\circ\text{C}$. Each sample in turn was treated with an equimolar amount of tetrafluoroboric acid and immediately placed in the instrument at $-80\text{ }^\circ\text{C}$ for further analysis. NMR spectroscopy of these reaction mixtures showed that both samples had reacted immediately and completely with the acid, with only methane and the cationic [(PCP)Pt] $^+$ detected in each instance. Non-coordinated BF_4^- was detected in the ^{19}F NMR spectrum at $\delta_{\text{F}} = -152\text{ ppm}$ for each sample (coordinated BF_4^- has been observed at $\delta_{\text{F}} = -169\text{ ppm}$ for a similar cationic PCP pincer species¹³⁹), ruling out CH_4 displacement from the coordination sphere of the metal by BF_4^- , and indicating that the parent methyl complexes **43** and **45** do not interact with any liberated methane at this temperature. Similar to the decarbonylated palladium complexes **38**, **39**, and **40**, the “vacant” coordination site on the metal centre is likely to be occupied by solvent in solution, owing to the instability and high reactivity of 14-electron species.

4.3 Concluding Remarks

A major drawback to the synthesis of electron-deficient PCP pincer complexes is the increased energy barrier to ligand metallation for electron-poor ligands. The choice of starting material has a pronounced effect on the ease of synthesis of metallated pincer complexes. Altering the ancillary ligands on $[\text{PtCl}_2\text{L}_n]$ species was observed to increase the rate of metallation with increasing binding strength of donor ligand. Although this result appeared somewhat counterintuitive, readily displaced ancillary ligands favoured the formation of dimeric intermediates, which increased the barrier to metallation, as they underwent an energy-consuming rearrangement process to allow metallation to occur. With the use of more strongly donating diethyl sulfide ligands in place of 1,5-hexadiene, dimer formation was noticeably diminished and metallation of ligand **1** proceeded approximately twice as fast.

A significant increase in the reactivity of the starting material could be achieved by the substitution of an anionic chloride ligand for either a hexamethyldisilazane group or a methyl group. These substituents provided good proton-accepting leaving groups, reducing the reaction times and temperatures required for metallation. However, as these starting materials required more complicated syntheses than the simple platinum dichlorides, the increase in reactivity they provided may not offer a practical advantage in terms of time saved or overall atom economy.

The electronic nature of the ligand also played a large part in the ease of forming PCP pincer complexes. Metallation was seen to be significantly more facile for less electron-poor ligands, due to their increased ability to donate electron density into the σ^* -antibonding orbital of the C–H bond being cleaved. However, the rate of metallation was not proportional to the yields of each complex obtained; it was observed that P–O bonds were unstable for prolonged periods under metallation conditions, and the fewer P–O bonds a ligand possessed the greater the yield of the metallated complex.

With the successful synthesis of the platinum and palladium $[(\text{PCP})\text{MCl}]$ pincer compounds, these were subjected to halide abstraction and treatment with carbon monoxide to produce the metal carbonyl species $[(\text{PCP})\text{M}(\text{CO})]^+$. Examination of the carbonyl stretching frequency by infrared spectroscopy confirmed that POCOP complexes were the most electron-poor, and POCCP complexes the least electron-poor. It also revealed that a number of these compounds possessed C–O stretching frequencies greater than that of free carbon monoxide, and were among the most electron-deficient pincer compounds known to date. Crystallographic characterisation of $[(\text{POCOP})\text{Pt}(\text{CO})][\text{SbF}_6]$ revealed the expected tridentate, planar coordi-

nation of the ligand, as well as a short carbonyl C–O distance arising from the electron-deficient metal centre.

Whilst the platinum carbonyl complexes proved to be indefinitely stable, the palladium carbonyl species underwent gradual loss of carbon monoxide over time in the solid state. This CO loss could be encouraged by the passage of inert gas through solutions of the palladium carbonyl, with the carbonyl complex regenerated upon the introduction of carbon monoxide into solution. This reversible carbonyl binding was observed to be more facile with decreasing electron density on the metal centre.

Methylation of the [(PCP)PtCl] species was achieved *via* the use of dimethyl zinc; reactions with methyl magnesium iodide led to halide exchange and the formation of platinum iodide species, while methyllithium led to decomposition of the electron-poor complexes. The methylation of [(POCCP)PtCl] with methyllithium was observed to be facile and selective on an NMR scale, but upon scaling up led to nucleophilic attack on the phosphinite donor, displacing a pentafluorophenyl group which migrated to the metal to form the unusual byproduct [(P^{Me}OCCP)Pt(C₆F₅)]. In all cases treatment of the corresponding palladium pincer complexes with methylating agents led to decomposition.

Ligand electronic effects play a large part in dictating the synthesis and reactivity of platinum and palladium PCP pincer complexes. Species with highly electron-withdrawing ligands are significantly harder to synthesise than their more electron-rich analogues, and are more susceptible to decomposition or unwanted side reactions during reactions with nucleophiles. However, possessing a highly electron-deficient metal centre was seen to be a boon for the palladium pincer carbonyl species, as it favoured the reversible binding of carbon monoxide, and also allowed the electron-deficient platinum chlorides to react rapidly and selectively with dimethyl zinc.

Chapter 5

Synthesis and Reactivity of PNP Pincer Complexes

In Chapters 3 and 4, it was observed that the incorporation of electron-withdrawing bis(pentafluorophenyl)phosphine substituents into the PCP pincer framework resulted in significant energetic barriers to ligand metallation and pincer complex formation. Metallation reactions typically required prolonged thermolysis, and proceeded through a number of stable oligomeric intermediates. To circumvent the need for ligand C–H activation, the synthesis of PNP pincer complexes was investigated. The pyridyl backbone of PNP pincer ligands possesses a nitrogen donor with a lone pair of electrons, meaning the only bond broken in the metallation reaction is between the metal centre and the ligand being displaced by the pyridyl group. Without the requirement for scission of a strong C–H bond, tridentate pincer coordination should be achieved under significantly milder conditions with electron-poor PNP ligands than for the analogous PCPH ligands.

While it may assist in pincer complex formation, moving from a phenyl to a pyridyl ligand backbone will have a pronounced effect on the character of the metal complex produced. When metallated, PCP pincer ligands are nominally monoanionic, due to the deprotonated aromatic carbon, while PNP ligands carry no formal charge. This means that when identical metal complexes are prepared with PCP and PNP ligands, the complex with the PNP ligand will carry an extra +1 charge. Moreover, because the pincer coordination motif places the donor atom of the ligand backbone *trans* to an available coordination site on the metal centre, PCP and PNP complexes will possess different *trans* effects. Computational studies on platinum complexes have shown that the donor atom *trans* to the active site has a large influence on the energy barrier for C–H activation reactions, with more electronegative donor atoms

producing a lower energy barrier.^{149,150} Therefore, PNP pincer complexes may be better suited for small molecule activation reactions than PCP pincer complexes.

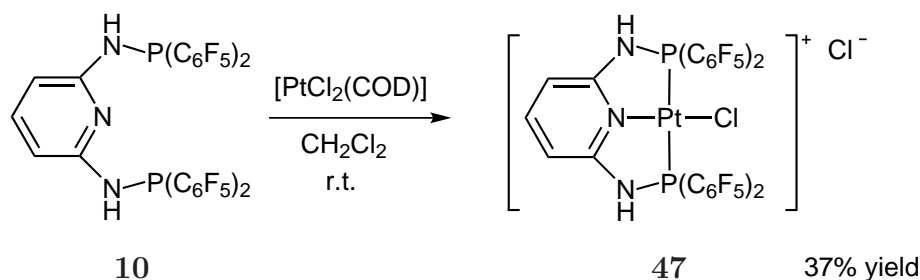
5.1 Synthesis of Platinum PNP Complexes

As the ease of PCP pincer complex formation was rigorously investigated with a number of platinum chloride starting materials, the coordination chemistry of the PNNNP and PONOP pincer ligands **10** and **11** was initially investigated with the same platinum precursors. This would enable a direct comparison of the ease of pincer complex formation between the electron-poor PCPH and PNP pincer ligands, which would also help to explore whether significant barriers to electron-poor pincer complex formation existed, other than C–H activation.

Previous reports indicated that the formation of electron-rich [(PNP)PtX]⁺ species occurred in a matter of hours from [PtX₂(diene)] precursors at room temperature in dichloromethane.⁷⁸ Ligands **10** and **11** were reacted with [PtCl₂(COD)] at room temperature in dichloromethane-*d*₂, with reaction mixtures monitored *in situ* by NMR spectroscopy. Results showed that reactions with the PNNNP pincer ligand **10** proceeded smoothly but slowly, with the quantitative formation of the pincer complex [(PNNNP)PtCl]⁺ (**47**) observed after 22 hours at room temperature. Reactions with the PONOP ligand **11** proceeded extremely slowly — after 48 hours at room temperature, starting materials still comprised the greater part of the reaction mixture.

The [(PNNNP)PtCl]⁺ complex **47** was isolated as the chloride salt upon upscaling of the initial exploratory reaction (Scheme 5.1). Mass spectrometry data confirmed the formulation of **47** as the cationic PNP pincer complex [(PNNNP)PtCl]⁺, with the [M]⁺ ion detected at 1066 amu. The NMR spectra of this compound displayed the expected three environments in the ¹H and ¹⁹F NMR spectra. The ³¹P NMR spectrum displayed a singlet resonance at $\delta_P = 30.6$ ppm (free ligand **10** appeared at $\delta_P = -10.8$ ppm), with platinum-phosphorus coupling consistent with a mutually *trans* arrangement of phosphorus donors (¹*J*_{Pt-P} = 3153 Hz), as expected upon pincer coordination.

The unexpectedly low reactivity of the PONOP ligand **11** could be attributed in part to it being significantly more electron-poor than the PNNNP ligand **10**. This differ-



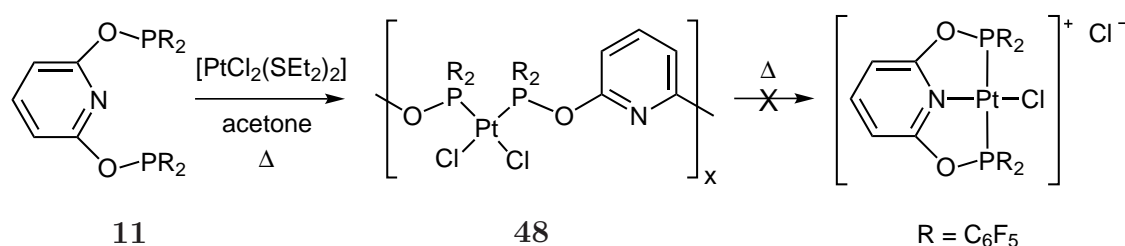
Scheme 5.1 Synthesis of the platinum PNNNP pincer compound **47**.

ence in electronic character has previously been observed for PCP pincer complexes — carbonyl stretching frequencies reported for POCOP and PNCNP complexes with identical substituents have indicated that complexes of phosphoramines are significantly more electron-rich than those of analogous phosphinites.⁵² This observation was also supported by the ^{19}F NMR $\Delta_{\text{m,p}}$ values for these PNP ligands (10.6 ppm for **10**, 12.2 ppm for **11**), which demonstrated that the phosphorus donors of the PNNNP ligand **10** were more electron-rich than those of the PONOP ligand **11**.

In order to promote the pincer coordination of the more electron-poor ligand **11**, the synthesis of $[(\text{PONOP})\text{PtCl}]^+$ was subsequently attempted in acetone, as the more polar solvent should better stabilise the charge developed during the formation of the desired cationic PNP pincer complex (according to the Hughes-Ingold Rules).¹⁵¹ Reactions were performed on an NMR scale between ligand **11** and platinum dichlorides $[\text{PtCl}_2(\text{hex})]$ and $[\text{PtCl}_2(\text{SEt}_2)_2]$ in acetone- d_6 . Analysis of the reaction mixtures by NMR spectroscopy revealed that both reactions produced the same product (**48**). However, reactions performed with $[\text{PtCl}_2(\text{SEt}_2)_2]$ proceeded more selectively than reactions with $[\text{PtCl}_2(\text{hex})]$, resulting in quantitative formation of the new species, **48**, in solution after 15 hours at room temperature.

Unfortunately, the NMR data obtained for compound **48** indicated that it was not the desired PNP pincer complex. For *all* of the pincer complexes reported herein, the ^{31}P NMR chemical shift of the phosphorus donors was observed downfield from that of the free ligand, due to the displacement of an electronegative chloride ligand upon backbone coordination. In **48**, the ^{31}P resonance was shifted significantly upfield from that of the free ligand (at $\delta_{\text{P}} = 29.0$ ppm, compared to 70.2 ppm for ligand **11**). Together with the observation of a large platinum-phosphorus coupling constant ($^1J_{\text{Pt-P}} = 4149$ Hz), this was consistent with compound **48** being the *cis*-bridged oligomeric species *cis*- $[(\text{PONOP})\text{PtCl}_2]_x$ (Scheme 5.2). For the analogous platinum POCOPH coordination chemistry discussed in Chapter 3, the ^{31}P NMR resonances of phosphorus donors of unmetallated ligands coordinated *trans* to a chloride ligand (in *cis*- $[(\text{POCOPH})_2\text{PtCl}_2]$, **18**, and *cis,trans*- $[(\text{POCOPH})\text{PtCl}_2]_2$, **19**) were shifted upfield from the free ligand by about 34 ppm, and displayed platinum-phosphorus

coupling of about 4500 Hz. This was consistent with the upfield shift from starting material of 41.2 ppm and platinum-phosphorus coupling of 4149 Hz observed for **48**, especially as PNP complexes have been observed to display platinum-phosphorus couplings around 400–500 Hz less than their PCP analogues.* Analogy with the coordination chemistry of the POCOPH ligand also suggested that the oligomer **48** is a dimer. Analysis of this oligomer by mass spectrometry gave only signals attributed to degradation of **48** inside the instrument, and so the nuclearity of **48** was not established. Reaction mixtures containing the oligomer **48** in acetone were heated to reflux for 48 hours in an attempt to promote the formation of the tridentate PONOP pincer complex. However, compound **48** appeared stable in acetone solutions up to 60 °C, and no further reaction was observed.



Scheme 5.2 Formation of the oligomeric platinum PONOP compound **48**. Synthesis of the corresponding PONOP pincer complex was not observed even upon prolonged thermolysis.

To facilitate the formation of the PONOP pincer complex, reactions were also undertaken between the PONOP ligand **11** and $[PtCl_2(NCMe)_2]$ in acetonitrile- d_3 , as well as between **11**, $[PtCl_2(SET_2)_2]$ and $NaSbF_6$ in acetone- d_6 . Similar reaction conditions have been successfully employed in the synthesis of *tert*-butyl-substituted PONOP pincer complexes of platinum and palladium.¹⁵³ However, with the electron-poor ligand **11**, neither of these reaction mixtures showed any signs of the desired pincer complex $[(PONOP)PtCl]^+$. Analysis of both reaction mixtures by NMR spectroscopy revealed quantities of the oligomeric bridged species **48**. The observation of **48** having formed from starting materials with differing ancillary ligands helped to confirm its formulation as $[(PONOP)PtCl_2]_x$, as it ruled out **48** possessing any neutral ligands other than the PONOP ligand **11** (such as diethyl sulfide).

Reactions under more harsh conditions were not attempted, as the reason for the investigation of PNP pincer ligands was that they generally allowed for pincer complex formation under more mild conditions than for analogous PCPH pincer ligands. The coordination chemistry of ligands **10** and **11** with platinum dichloride starting

*For example, where the phosphine donor is $CH_2P^tBu_2$, the ^{31}P NMR data for the PCNCP pincer complex is $\delta_P = 53.7$ ppm, $^1J_{Pt-P} = 2403$ Hz;¹⁵² for the PCCCP pincer complex it is $\delta_P = 64.9$, $^1J_{Pt-P} = 2881$ Hz.⁸⁴

materials had clearly demonstrated that pincer complex formation was significantly more facile for the more electron-rich PNNNP ligand **10** than for the electron-poor PONOP ligand **11**. This low reactivity of ligand **11** was likely to be due to its inability to displace a chloride ligand from the metal centre. As the synthesis of PNP pincer complexes requires halide displacement from the metal by the nitrogen donor of the pyridyl backbone, the decreased electron density on metal centres with electron-poor ligands should lead to an increased electrostatic interaction between the metal and halide ligand, decreasing the ease of halide displacement. It may also be anticipated that cation formation for complexes of the more electron-poor PONOP ligand **11** would be less favourable than for complexes of the PNNNP ligand **10**, as there would be less electron density available for the PONOP ligand to stabilise the positive charge developed on the metal centre.

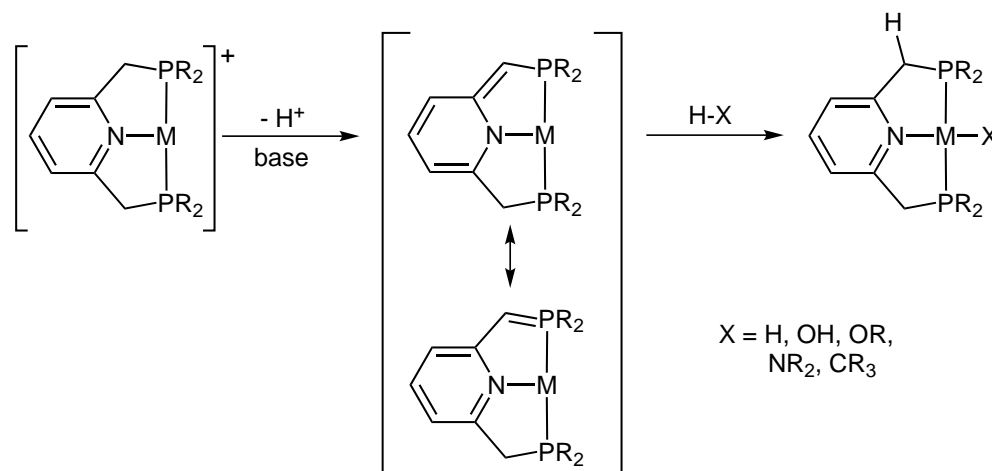
5.2 Synthesis of Rhodium PNP Species

While reactions of the electron-poor PNP ligands **10** and **11** with platinum dichloride starting materials provided an effective comparison of the ease of pincer complex formation between PCPH and PNP ligands, the reactivity of PNP pincer complexes was investigated using rhodium(I) chloride compounds, as they were neutral and isoelectronic with the Group 10 [(PCP)MCl] complexes reported in the Chapter 4. The preparation of iridium PNP pincer complexes may have offered more direct comparisons with the chemistry of the platinum PCP pincer compounds that are the predominant focus of this work, but it is the analogous rhodium compounds that have displayed the more interesting chemistry. Recent examples of methane σ -complexation²⁵ and amine N–H activation¹⁵⁴ facilitated by rhodium PNP pincer complexes serve to highlight the utility of and interest in these rhodium species. An added advantage of rhodium is that it is NMR active (¹⁰³Rh has a spin of $\frac{1}{2}$ and a natural abundance of 100%), and therefore is able to provide additional spectroscopic data on the coordination environment of the rhodium centre.

Initial reactions between PNNNP and PONOP ligands **10** and **11** with the rhodium and iridium precursors [RhCl(COD)]₂ and [IrCl(COE)₂]₂ indicated that the respective [(PNP)MCl] pincer complexes were readily formed in solution.[†] The PNNNP complexes offered an interesting point of difference from those of the PONOP ligand, as the presence of N–H groups linking the phosphorus donors to the aromatic backbone provided a site for deprotonation on the ligand, which may lead

[†]This work was carried out in conjunction with an undergraduate research project performed by Emma Aitken.

to “non-innocent” behaviour. Complexes of the analogous PCNCP ligands, possessing CH_2 rather than NH linker groups, have demonstrated a wide range of reactions based upon reversible deprotonation and reprotonation of the benzylic positions (Scheme 5.3).¹⁵⁵ Such behaviour exists predominantly due to the ability of the pyridyl backbone to undergo dearomatisation, with the nitrogen donor atom becoming formally anionic and bonding in a covalent (rather than dative) fashion to the metal centre.



Scheme 5.3 Non-innocent behaviour of PCNCP pincer complexes. Figure adapted from Gunanathan *et al.*,¹⁵⁵ ancillary ligands on the metal centre omitted for clarity.

Non-innocent ligand behaviour offers advantages in catalytic transformations; by possessing a remote proton acceptor site it aids H-X bond activation by allowing the cleavage to occur without a change in metal oxidation state, while the physical separation between the H and X groups can minimise the reverse H-X elimination reaction. This has enabled rhodium PNP and PNN complexes to display high activities for a variety of N-H , C-H , and H-H bond activations.^{154,156} Analogous reports of non-innocent behaviour of PNNNP ligands are substantially rarer; the reversible deprotonation of a N-H linker group of a PNNNP pincer ligand has only been reported on one occasion.¹⁵⁷

The rhodium PNNNP complex $[(\text{PNNNP})\text{RhCl}]$ (**49**) was synthesised according to a reported method for the synthesis of $[(\text{NNN})\text{RhCl}]$ pincer complexes.¹⁵⁸ The PNNNP ligand **10** and the rhodium starting material $[\text{RhCl}(\text{COD})]_2$ were dissolved in hot toluene, and within minutes the desired product began to crystallise out of the reaction mixture as the toluene solvate, $[(\text{PNNNP})\text{RhCl}] \cdot \text{C}_7\text{H}_8$. The toluene of crystallisation was removed by washing with dichloromethane, giving **49** in good yields. The formulation of **49** as $[(\text{PNNNP})\text{RhCl}]$ was confirmed by mass spectrometry, with the observation of the $[\text{M-Cl}]^+$ ion at $m/z = 940$ amu, and absence of

any ion corresponding to a dimer confirming that the chloride bridges of the starting material had been cleaved during the synthesis of **49**. While analysis of **49** by NMR spectroscopy in acetone- d_6 gave data consistent with $[(\text{PNNNP})\text{RhCl}]$, it revealed that the N–H groups readily underwent H/D exchange with the acetone- d_6 solvent. This was most evident in the ^{31}P NMR spectrum: the phosphorus signal appeared as three overlapping doublets, due to the isotopomers **49**, **49- d_1** , and **49- d_2** (Figure 5.1). Complete deuteration of the N–H groups could be achieved by the addition of one drop of D_2O to acetone- d_6 solutions of **49**.

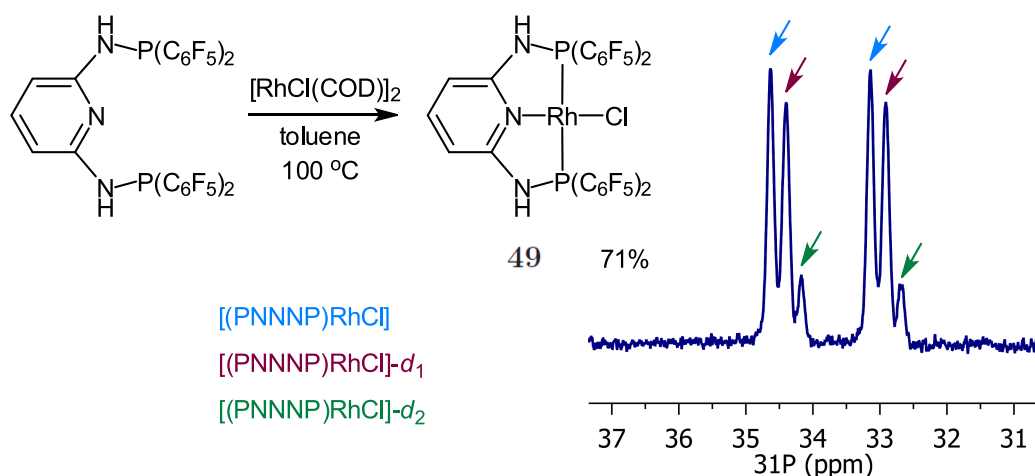


Figure 5.1 Synthesis of the PNNNP rhodium complex **49**, and ^{31}P NMR spectrum of **49** in acetone- d_6 showing isotopomers resulting from facile H/D exchange of N–H protons.

The methylation of the PNNNP pincer chloride complex **49** was subsequently investigated. Methylation of the $[(\text{PCP})\text{PtCl}]$ complexes had indicated that dimethylzinc possessed a sufficiently low nucleophilicity and high activity to be an appropriate choice of methylating agent for these bis(pentafluorophenyl)phosphine-substituted complexes (as described in Chapter 4). Dimethylzinc has also been used to good effect in the literature for methylation of $[(\text{PCNCP})\text{RhCl}]$ species, as the more basic methyllithium has been observed to result in benzylic deprotonation of the ligand backbone rather than methylation.^{159,160}

Reactions between complex **49** and dimethylzinc solutions in toluene were first investigated on an NMR scale in benzene- d_6 and toluene- d_8 (as toluene allowed for reaction mixtures to be cooled below 4 °C). The low solubility of the rhodium chloride starting material **49** in benzene and toluene allowed the appearance of new, soluble intermediates and products in the reaction mixture to be easily studied by NMR spectroscopy. Analysis of reaction mixtures by NMR spectroscopy revealed

that the reaction proceeded rapidly, forming a new product within 30 minutes at room temperature. This new product possessed NMR spectroscopic data consistent with it being the desired rhodium(I) methyl complex, [(PNNNP)RhMe] (**50**); the resonance for the rhodium methyl group was observed in the ^1H NMR spectrum as a broad triplet (at $\delta_{\text{H}} = 1.09$ ppm), and the increase in the magnitude of the rhodium-phosphorus coupling constant (from 180 to 218 Hz) was consistent with moving from a [(PNP)RhCl] to a [(PNP)RhMe] complex. The observation of three sharp, discrete resonances for the *ortho*, *meta*, and *para* aromatic fluorine resonances in the ^{19}F NMR spectrum was also consistent with **50** being a rhodium(I) compound, as the increased steric congestion at rhodium(III) centres in complexes of ligand **10** resulted in restricted rotation of the pentafluorophenyl substituents and inequivalence of fluorine environments in ^{19}F NMR spectra.

Unfortunately, the desired rhodium methyl complex **50** proved unstable in the reaction mixture at room temperature; the orange solution gave way to a dark solution with a brown precipitate within two hours at room temperature, accompanied by a decrease in signal-to-noise in the NMR spectra consistent with degradation or precipitation of PNP rhodium species out of solution. Prior to precipitate formation, the appearance of a new compound (**51**) in solution was observed. This species appeared to be a degradation product from the reaction between the rhodium methyl complex **50** and dimethylzinc: **51** was only detected in solution *following* the formation of **50**, and was present in greater amounts in reaction mixtures when greater amounts of dimethylzinc were used.

Spectroscopic data revealed that the degradation product **51** was an asymmetric species. The ^1H NMR spectrum showed that the symmetry of the ligand backbone had been destroyed; the signals for protons *meta* to the pyridyl nitrogen (H-4 and H-6, following the numbering scheme used for the PCP pincers) appeared as separate doublet resonances. The signal for H-5 was obscured by resonances from the toluene in the dimethylzinc solution, but COSY NMR experiments revealed that both H-4 and H-6 coupled to a resonance at approximately 7.1 ppm, proton H-5. Only one of the N–H protons was observed, shifted slightly upfield from the N–H protons of the rhodium(I) chloride and methyl complexes. The second N–H proton could not be detected by COSY or ^1H – ^{31}P NMBC experiments, therefore it was likely that the deprotonation of an N–H group by dimethylzinc had given rise to the asymmetry of **51**. This was also supported by the observation of methane in the ^1H NMR spectrum (at $\delta_{\text{H}} = 0.17$ ppm), and was consistent with the observation that the presence of more dimethylzinc led to an increased the amount of **51** in solution.

This N–H deprotonation was also supported by ^{31}P NMR spectroscopy. The ^{31}P

NMR data of **51** showed the presence of two different phosphorus environments, which appeared as doublets of doublets at $\delta_{\text{P}} = 74.4$ and 44.7 ppm, with each phosphorus donor coupling to the other strongly ($^2J_{\text{P-P}} = 522$ Hz). This spectroscopic data were consistent with that observed for the benzylic deprotonation of PCNCP ligands.¹⁵⁶ However, unlike for PCNCP complexes, deprotonation at the “arms” of the ligand did not appear to induce dearomatisation of the ligand backbone. Whereas dearomatisation of the pyridyl backbone has been observed to shift ^1H NMR resonances of the pyridyl protons upfield (as they are less aromatic and more alkene-like),^{152,161} in compound **51** each of the proton environments on the ligand backbone are similar in chemical shift to those of the PNNNP rhodium methyl complex **50** (Figure 5.2). This N–H deprotonation without backbone dearomatisation has previously been observed on an PNNNP iron complex.⁷⁸

The asymmetric compound **51** also possessed two distinctive, high-field resonances in the ^1H NMR spectrum. A Rh–Me group was observed at $\delta_{\text{H}} = 1.21$ ppm, similar in chemical shift and lineshape to the methyl group of the rhodium(I) methyl complex ($\delta_{\text{H}} = 1.16$ ppm). In both cases the resonances were too broad to discern any rhodium-proton coupling. Interestingly, a further high-field resonance was observed in the ^1H NMR spectrum at -0.17 ppm, and was much sharper than any of the rhodium-methyl signals. This indicated that the proton environment did not experience significant rhodium or phosphorus coupling, and so was suggestive of a zinc-methyl group rather than a second rhodium-methyl group.[‡] This high-field signal also integrated for three protons against the other proton environments of **51** in *all* the reaction mixtures studied, which confirmed that the Zn–Me moiety was associated with the rhodium complex.

The formation of a methylzinc adduct of a rhodium PNP pincer complex has been reported in a similar reaction with dimethylzinc,¹⁵⁹ but was not structurally characterised. As such, the structure the rhodium-methylzinc adduct **51** cannot be ascertained with the data on hand. Organozinc fragments have been reported to bind to rhodium centres in both bridging¹⁶² and terminal¹⁶³ coordination modes, and may also form outer-sphere adducts through interactions with the ligand.¹⁶⁴ Fluorine-19 NMR data for **52** revealed restricted rotation of the pentafluorophenyl substituents of the ligand, which was observed in spectra of the six-coordinate rhodium complexes [(PNNNP)RhClMeI] and [(PNNNP)RhI₃] (*vide infra*) but not in spectra of four-coordinate [(PNNNP)RhX] species. This suggests the presence of a degree

[‡]Analysis of full width at half maximum values for the Rh–Me and Zn–Me groups helped to confirm their assignment as such. Averaging data for seven ^1H spectra over four different methylation reactions, the Rh–Me resonance ($\delta_{\text{H}} = 1.21$ ppm) possessed an average FWHM of 24.5 Hz, while the Zn–Me resonance ($\delta_{\text{H}} = -0.17$) possessed an average FWHM of 6.3 Hz. This demonstrated that the signal at -0.17 ppm did not display the requisite coupling to rhodium and phosphorus to correspond to a second Rh–Me group.

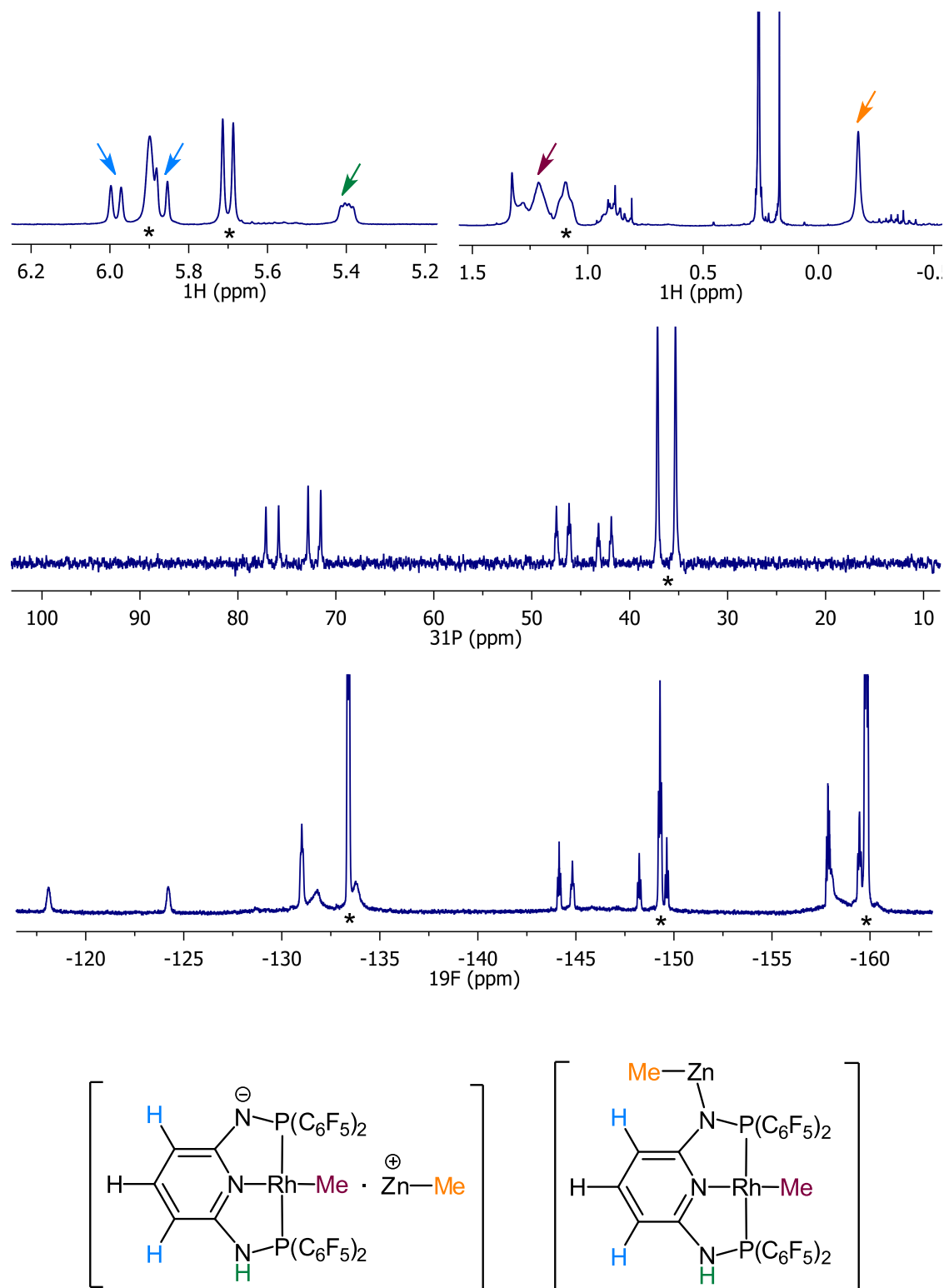


Figure 5.2 Multinuclear NMR spectra for the rhodium-methylzinc adduct **51** in toluene- d_8 . Structure comprising the functional groups suggested by the data at bottom left, with a possible structural configuration for **51** at bottom right. Asterisks denote resonances arising from the rhodium(I) methyl complex **50**.

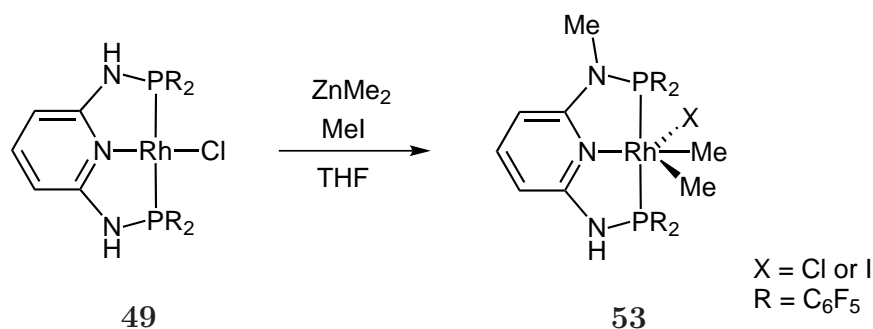
of steric crowding about the rhodium centre of **51**, but it is not possible to conclude what moiety is responsible for this hindrance. Thus, while the NMR data (Figure 5.2) is consistent with the formulation of **51** as a deprotonated methylzinc adduct $[(\text{PN}^*\text{NNP})\text{RhMe} \cdot \text{ZnMe}]$, it is difficult to speculate further on its nature.

In an attempt to isolate the rhodium methyl complex **50** without the formation of **51** and subsequent degradation, the PNNNP rhodium chloride complex **49** was treated with substoichiometric amounts of dimethylzinc in toluene- d_8 at -15°C . As the starting PNNNP rhodium chloride complex **49** was only sparingly soluble in toluene, it was hoped that decantation of the supernatant from the reaction mixture would allow the isolation of **50**, without excess dimethylzinc leading to degradation. However, in all reactions involving the treatment of **49** with dimethylzinc, small but significant amounts (*c.a.* 10%) of the methylzinc adduct **51** were detected. Methylation reactions were also attempted in THF, where the Lewis acid-base interactions between the solvent and the zinc were seen to reduce the Brønsted basicity of the dimethylzinc, and produce significantly smaller quantities of the methylzinc adduct **51**. However, reactions in THF demonstrated a lower selectivity than those in toluene, producing significant quantities of unidentified byproducts.

Attempts at the methylation of a rhodium PNP pincer complex with dimethylzinc have previously been reported to result in dark brown solutions of a rhodium zinc adduct, $[(\text{PNP})\text{Rh}(\text{CH}_3)\text{Zn}(\text{CH}_3)\text{X}]$, from which the zinc could be abstracted with bipy to yield the rhodium(I) methyl complex.¹⁵⁹ It appeared that in reactions of **49** with dimethylzinc that the initially formed rhodium methyl complex, **50**, further reacted with dimethylzinc to form a soluble methylzinc adduct, **51**, which decomposed to form an insoluble residue, from which the zinc might be removed to yield a rhodium pincer complex. However, attempts at zinc abstraction by treatment of these residues with bipy were unsuccessful, as they did not yield any soluble species with identifiable resonances in the ^{31}P or ^{19}F NMR spectra. Ultimately, the dark suspensions formed by the decomposition (or further reaction) of the rhodium methyl complex **50** proved to be intractable.

In attempting to synthesise the rhodium methyl complex **50** using solutions of dimethylzinc in diethyl ether that contained methyl iodide (as described in Chapter 4), further evidence that dimethylzinc facilitates N–H deprotonation in PNNNP rhodium complexes was obtained. Reactions with dimethylzinc in ether proceeded with a low selectivity, and formed a number of products with broad doublets between 2.8–2.2 ppm in the ^1H NMR spectra. Extraction of these reaction mixtures with pentane/diethyl ether yielded small amounts of material sufficiently pure to allow tentative characterisation of one of the major components of the reaction

mixture (**53**) by NMR spectroscopy. The ^{31}P NMR spectrum of **53** was similar to that of the asymmetric methylzinc adduct **51**, with two inequivalent phosphorus environments appearing as doublets of doublets at $\delta_{\text{P}} = 85.9$ and 50.9 ppm, with rhodium-phosphorus coupling constants ($^1J_{\text{Rh-P}} = 150$ and 135 Hz respectively) suggestive of a rhodium(III) complex. The ^1H NMR spectrum of **53** was also similar to that of the methylzinc adduct **51**, with three separate aromatic protons and one N–H proton observed from 7.0 – 5.5 ppm, as well as two distinctive broad triplet resonances of rhodium-methyl groups, which appeared at 1.43 and 0.14 ppm respectively. Where the new compound **53** differed significantly from that of the methylzinc adduct was that the sharp resonance of the Zn–Me group at -0.17 ppm was absent, while a broad doublet appeared at 2.62 ppm ($^3J_{\text{P-H}} = 9.0$ Hz) and integrated for three protons. This ^1H NMR data were consistent with the presence of an N-methyl group on the ligand backbone,¹⁶⁵ indicating that the presence of methyl iodide in the dimethylzinc solutions had resulted in methylation at the N–H position (Scheme 5.4). Therefore, this electrophilic N-methylation required to form **53** in reaction mixtures was seen as further evidence of N–H deprotonation by the dimethylzinc.



Scheme 5.4 Electrophilic methylation at an N–H position of the PNNNP ligand by methyl iodide in the presence of dimethylzinc.

To ensure that H/Me exchange between methyl iodide and **49** was not occurring in a manner similar to H/D exchange, **49** was treated with a large excess of methyl iodide in acetone- d_6 . Analysis of the reaction mixture by NMR spectroscopy revealed the immediate and quantitative formation of a new species **54** that possessed only one phosphine environment, and which ^1H NMR spectroscopy indicated had a Rh–Me group (which appeared as a broad triplet of doublets at $\delta_{\text{H}} = 1.13$ ppm), but not an N-methyl group. As for the previously discussed reaction intermediates, the small magnitude of the rhodium-phosphorus coupling constant ($^1J_{\text{Rh-P}} = 133$ Hz) and the observation of restricted rotation in the ^{19}F NMR spectrum indicated that **54** was a rhodium(III) complex, likely to be $[(\text{PNNNP})\text{RhClMeI}]$, produced by the oxidative addition of methyl iodide to the starting material **49**. Such oxidative additions have been reported as being facile for other other PNP rhodium(I) pincer

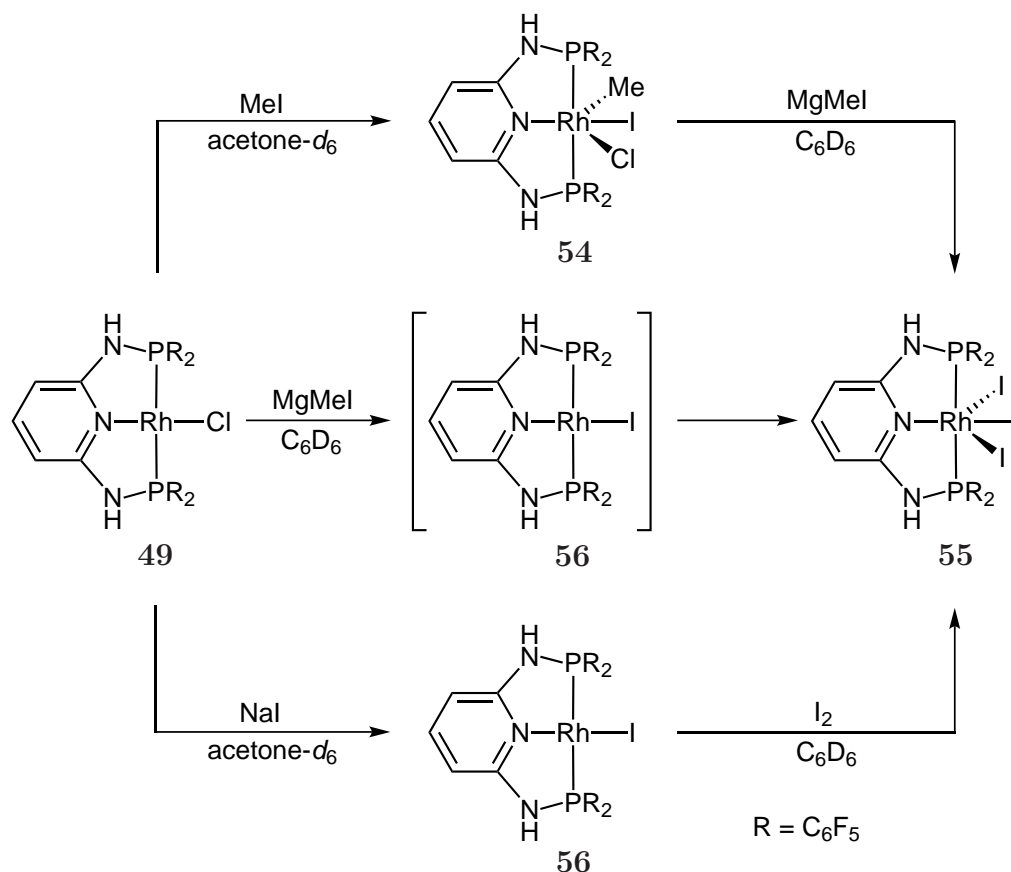
complexes.^{156,166,167} The reaction was repeated on a large scale in THF, providing **54** as a red-orange solid in 83% yield. Analysis of **54** by mass spectrometry confirmed its formulation as the methyl iodide oxidative addition product [(PNNNP)RhClMeI], with the [M+Na]⁺ ion detected at $m/z = 1140$ amu. Compound **54** was observed to be stable in acetone-*d*₆ in the presence of methyl iodide over the course of 12 hours, with no sign of reaction at the N–H groups. This confirmed that to achieve N-methylation, dimethylzinc was required to deprotonate an N–H group, which was then able to be methylated in the presence of the electrophilic methyl group of methyl iodide.

As the methylation reactions with dimethylzinc had been shown to promote ligand deprotonation, methylation with methylmagnesium iodide was pursued. Whereas methylmagnesium iodide was seen to be unsuccessful for the methylation of the [(PCP)PtCl] compounds, it was envisaged that the increased steric bulk of the rhodium(III) starting material [(PNNNP)RhClMeI], **54**, would promote nucleophilic attack by the smaller methyl group rather than by the larger iodide. Similar PNP rhodium(III) iodide complexes have been reported as possessing cationic, five-coordinate structures with iodide counterions,¹⁶⁶ which indicated that iodide dissociation from **54** may be facile, which would increase its susceptibility to nucleophilic attack by a methyl group. Treatment of the new rhodium(III) chloromethyl iodide complex **54** with methylmagnesium iodide in THF was observed to produce a new product **55** with a ³¹P NMR resonance at 36.6 ppm and a rhodium-phosphorus coupling of 115 Hz. This species did not contain an observable Rh–Me group, and so was postulated to be a rhodium trihalide complex [(PNNNP)RhX₃].

Similarly, treatment of the rhodium(I) chloride starting material **49** with methylmagnesium iodide resulted in the formation of the same rhodium(III) complex, **55**. *In situ* monitoring of this reaction by NMR spectroscopy indicated that it proceeded *via* a rhodium(I) intermediate **56**, with a ³¹P NMR signal at $\delta_P = 40.5$ ppm (¹*J*_{Rh-P} = 170 Hz). The lack of any discernible Rh–Me resonance in the ¹H NMR spectrum, together with a rhodium-phosphorus coupling constant similar to that of the rhodium(I) chloride complex **49** (180 Hz), indicated that this intermediate is likely to be the product of halide exchange with the methylmagnesium iodide, [(PNNNP)RhI]. The ready oxidation of the PNNNP rhodium chloride complex **49** to the rhodium(III) complex **55** in the presence methylmagnesium iodide has parallels to chemistry reported by the Albrecht research group.¹⁶⁸ In that work, the formation of a rhodium(III) N-heterocyclic carbene complex from a rhodium(I) chloride starting material was facilitated by potassium iodide — the unexpected oxidation was attributed to the presence of iodine, which was generated from the aerobic oxidation of the iodide anion. The formation of iodine in solutions of organomagne-

sium iodides has been reported by Wehmschulte and associates, who also attribute its formation to aerobic oxidation of iodide ions in solution by ambient air.¹⁶⁹

In order to verify the nature of the product **55** and intermediate **56**, the rhodium(I) iodide and rhodium(III) triiodide PNNNP pincer compounds were independently synthesised. A solution of the rhodium(I) chloride **49** in acetone-*d*₆ was treated with an excess of sodium iodide in a Finkelstein-type reaction, with NMR spectroscopy revealing quantitative formation of [(PNNNP)RhI] after ten minutes at room temperature. The rhodium(I) iodide species was isolated, dissolved in benzene-*d*₆ and treated with iodine, immediately forming [(PNNNP)RhI₃]. The formulae of these compounds were confirmed by HRMS, while NMR spectroscopy confirmed the rhodium(I) iodide complex to be identical to the reaction intermediate **56**, while the rhodium(III) iodide complex was found to be the same as the product of reactions involving methylmagnesium iodide. These reactions are summarised in Scheme 5.5.



Scheme 5.5 Attempts at producing rhodium(I) and rhodium(III) methyl complexes *via* methylation of **49** with methylmagnesium iodide. The synthesis of compounds **56** and **55** by treatment of **49** with sodium iodide then iodine was used to verify the nature of these compounds.

It therefore appeared that, much like the platinum chloride PCP pincer complexes, these isoelectronic rhodium PNP species do not undergo methylation with methyl-

magnesium iodide, rather they undergo halide exchange. However, unlike the platinum compounds, they are very susceptible to oxidation (to rhodium(III) species), and in all cases treatment of these PNP rhodium pincer complexes with methylmagnesium iodide eventually led to the formation of the PNNNP rhodium(III) triiodide complex **55**.

5.3 Concluding Remarks

The synthesis of complexes of the electron-poor PNP pincer ligands **10** and **11** was investigated. As the pyridyl ligand backbone can coordinate to metal centres without the C–H activation required for complexes of PCPH pincer ligands it was hoped that pincer formation would be more facile for electron-poor PNP ligands than for the analogous PCP ligands.

Reaction of the PNNNP and PONOP pincer ligands **10** and **11** with platinum dichloride starting materials was carried out. The reaction of the PNNNP ligand occurred slowly compared to those of more electron-rich ligands reported in the literature, forming the desired platinum PNNNP pincer complex $[(\text{PNNNP})\text{PtCl}]^+$, **47**, upon prolonged reaction at room temperature. However, reactions of the more electron-poor PONOP ligand did not yield a pincer complex, despite the use of polar solvents and application of heat to reaction mixtures. Instead, these reactions yielded the PONOP-bridged *cis*-oligomer **48**; a reactivity which bore similarities to the bridging coordination modes favoured by the POCOPH ligand **1**. It was proposed that the pronounced difference in reactivity between ligands **10** and **11** was due to an increased energy barrier for halide displacement and cation formation with decreasing electron density on the metal centre.

The synthesis of the rhodium PNP pincer complexes was subsequently investigated, as PNP complexes of Group 9 metals in the +1 oxidation state are isoelectronic with PCP pincer complexes of Group 10 metals in the +2 oxidation state. The rhodium(I) PNNNP pincer complex $[(\text{PNNNP})\text{RhCl}]$, **49**, was obtained in good yield from $[\text{RhCl}(\text{COD})]_2$. The methylation of **49** with dimethylzinc solutions was investigated, and while it appeared that the rhodium(I) methyl complex $[(\text{PNNNP})\text{RhMe}]$, **50**, was formed in solution, it was not able to be isolated. Careful *in situ* analysis of reactions between **49** and dimethylzinc revealed the presence of an asymmetric species as a minor product, which was deemed to be the methylzinc adduct **51**, having arisen from N–H deprotonation of the ligand by an organozinc species in

solution. Further evidence of N–H deprotonation was indicated by the formation of an asymmetric, N-methylated product **53** when methyl iodide was present in the dimethylzinc solution.

The reaction of methyl iodide with the PNNNP rhodium(I) chloride **49** in the absence of dimethylzinc resulted in facile oxidative addition to produce the rhodium(III) complex [(PNNNP)RhClMeI], **54**. Attempts at the methylation of both rhodium(I) and rhodium(III) complexes **49** and **54** with the milder methylating agent methylmagnesium iodide resulted in formation of the rhodium(III) triiodide complex, [(PNNNP)RhI₃], **55**, in both instances. This was confirmed by independent synthesis of the rhodium(I) and rhodium(III) iodide complexes. The facile formation of rhodium iodide complexes revealed the inability of methylmagnesium iodide to methylate these electron-poor rhodium PNNNP pincer complexes, as well as reinforcing the prevalence of oxidative addition reactions in the chemistry of these rhodium(I) species.

Chapter 6

Catalytic Activity of Palladium Pincer Complexes

6.1 Palladium Pincer Complexes in Catalysis

Since their inception, pincer complexes of palladium have demonstrated high activities and selectivities in a number of synthetically useful catalytic reactions.^{16,17} Their use in catalysis was first reported in 1993 by Seligson and Trogler, who employed a PCP palladium complex with an alkyl backbone to facilitate hydroamination of activated alkenes.¹⁷⁰ It was found that the rigid, tridentate coordination of the pincer ligand helped reduce catalyst decomposition, and placed the strongly *trans*-directing alkyl group *trans* to the active site. This resulted in a higher reaction rate, and a greater catalyst stability and selectivity when compared to *bis*-monodentate and bidentate chelate phosphine analogues.

Pincer complexes began to garner considerable interest in the field of homogeneous catalysis, and were first employed in palladium-catalysed cross-coupling reactions by the Milstein research group in 1997.⁵⁵ Their use of PCP palladium complexes in the Heck reaction revealed these species to be amongst the most active catalysts known at the time. This was attributed to the remarkable stability of these species, with no catalyst degradation observed even after 300 hours at the 140 °C employed in the reactions.

The analogous investigation of palladium pincer complexes in the Suzuki cross-coupling reaction was not reported until three years later. It was demonstrated by Bedford and co-workers that POCOP palladium triflates were very active for

the coupling of electronically deactivated and sterically hindered aryl bromides with phenylboronic acid.¹⁷¹ These pincer complexes were inexpensive, easily synthesised, and could carry out reactions at loadings as low as 0.0001 mol %, giving turnover numbers (TONs) amongst the highest then reported for the substrates examined.

As well as being highly active in palladium-mediated cross-coupling reactions, ECE pincer complexes have proven to be extremely effective catalysts for the allylation of electrophiles. The Szabó research group have demonstrated that SeCSe palladium pincer complexes are particularly effective in the synthesis of allylboranes and allylbenzene derivatives.^{172,173} These catalysts are tolerant to a variety of functional groups, with reactions proceeding under very mild conditions, generating products with a greater selectivity than the more commonly employed $[\text{Pd}_2(\text{dba})_3]$ and $[\text{Pd}(\text{PPh}_3)_4]$ species. The efficacy of pincer complexes in these reactions is attributed to the chelate effect reducing the possibility of ligand exchange, whilst the tridentate ligand leaves only one vacant coordination site on the metal, minimising unintended side reactions.

Since these initial reports, catalysis performed by pincer complexes of palladium has generated a good deal of excitement and controversy. The well defined, robust nature of pincer complexes, combined with their demonstration of considerable catalytic activity has made them attractive targets for research into the Heck and Suzuki reactions. It was hoped that their high thermal stability and ability to incorporate donor groups of different electronic and steric character would allow for the generation of highly active and selective catalysts that would resist leaching of palladium into the products synthesised.

6.2 Mechanistic Implications of Catalysis with PCP Pincer Complexes

The fixed, tridentate nature of ECE pincer ligands has raised questions over the reaction mechanisms pincer complexes employ during catalysis. It has long been known that the Heck reaction operates through a catalytic cycle dependent on a $\text{Pd}(0)$ active catalyst (Figure 6.1).¹⁷⁴ The $\text{Pd}(0)$ active species undergoes oxidative addition of the aryl halide to yield a $\text{Pd}(\text{II})$ -aryl halide complex, which is then capable of inserting the alkene substrate into the Pd -aryl bond. The subsequent alkyl-palladium species generated undergoes β -hydride elimination, giving the coupled styrene derivative and a palladium-hydrido species, which is reduced back to

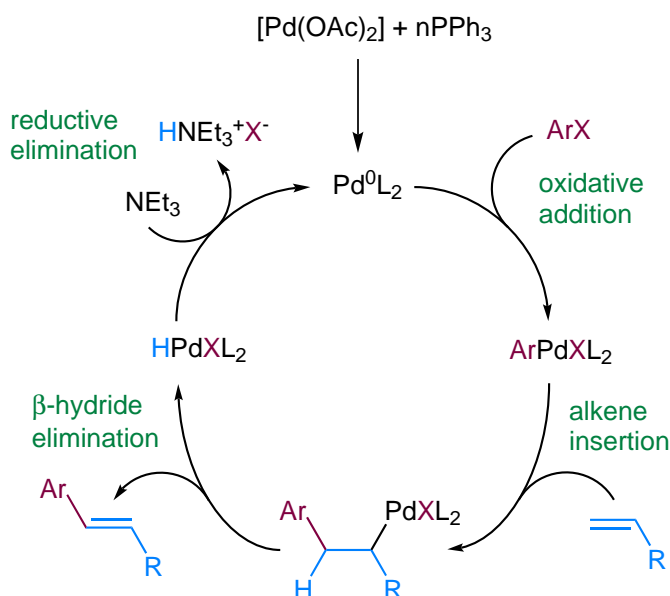


Figure 6.1 Outline of the classic “textbook” Heck catalytic cycle.

the active catalyst species through the action of the base. Conceptually the Suzuki reaction is very similar, except that the intermediate $\text{Pd}(\text{II})$ -aryl species undergoes transmetalation with an arylboronic acid, rather than undergoing alkene insertion.

Recent investigations have shown that this classic “textbook” catalytic cycle for the Heck reaction may not be an entirely accurate representation of the course of the reaction. Research by Amatore and Jutand has demonstrated that anionic, five-coordinate $\text{Pd}(\text{II})$ species play a role as vital intermediates in the catalytic cycle.¹⁷⁵ However, the essence of the mechanism remains the same; the $\text{Pd}(0)/\text{Pd}(\text{II})$ oxidative addition and reductive elimination cycle forms the foundation of these cross-coupling reactions.

This creates a conundrum when considering catalysis by ECE palladium pincer complexes. How can the $\text{Pd}(0)/\text{Pd}(\text{II})$ catalytic cycle be in operation when the catalyst is effectively “locked” in a $\text{Pd}(\text{II})$ resting state by the strong Pd-C bond? This has been a matter of much conjecture in the literature,¹⁷⁶ and there are two main schools of thought as to how this catalysis is carried out. It was originally proposed that the cyclometallated P-C chelates of the type **57** (Figure 6.2) formed in reaction mixtures of $\text{Pd}(\text{OAc})_2$ and $\text{P}(o\text{-tolyl})_3$ served as active Heck and Suzuki catalysts, operating through a $\text{Pd}(\text{II})/\text{Pd}(\text{IV})$ mechanism.^{177,178} A mechanism for this transformation was developed by Bernard Shaw,¹⁷⁹ and upon the discovery of PCP palladium Heck catalysts, their reaction mechanism was deemed to proceed *via* this $\text{Pd}(\text{II})/\text{Pd}(\text{IV})$ pathway.^{55,180}

The idea that cyclometallated palladium compounds accessed the $\text{Pd}(\text{IV})$ oxidation state during catalysis was met with less than unanimous agreement. It had

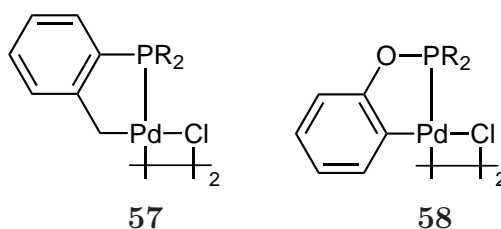
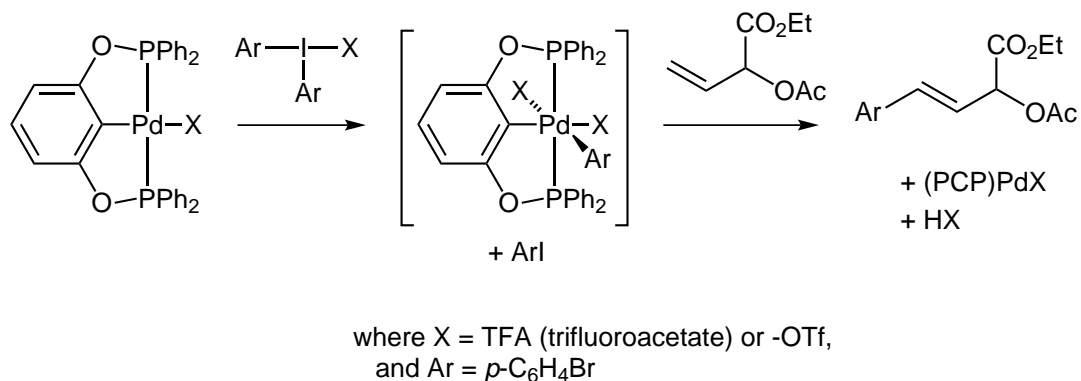


Figure 6.2 Representative examples of cyclometallated P–C chelates.

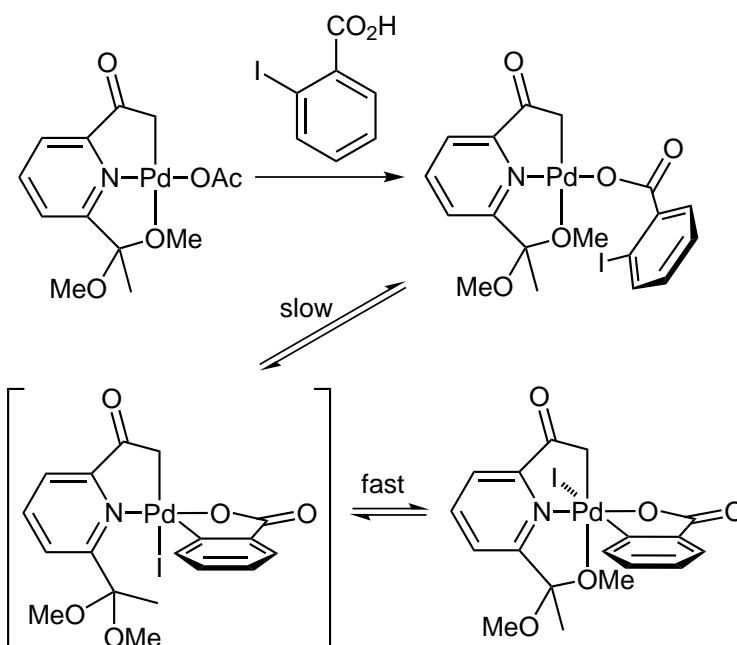
been demonstrated by Louie and Hartwig in 1996 that P–C chelates of the type **57** could be reduced under catalytic conditions, forming phosphine-stabilised Pd(0) complexes, which served as the active catalyst species.¹⁸¹ A breakthrough in the field came in 2000, when it was discovered that under catalytic conditions, Pd(II) species could be reduced to palladium nanoparticles, which efficiently catalysed cross-coupling reactions *via* a conventional Pd(0)/Pd(II) cycle.¹⁸² It was subsequently found that PCP¹⁸³ and SCS¹⁸⁴ palladium pincer complexes were likely to serve as depot forms of Pd(0) nanoparticles rather than serving as the active catalyst species themselves. In an assessment of the mechanism of the Heck reaction in 2006, de Vries stated “the conclusion seems justified that all palladacycles and pincers decompose during the Heck reaction at high temperatures to form palladium colloids.”¹⁸⁵

However, recent developments in the field of Pd(IV) chemistry have again encouraged debate as to whether high oxidation state pathways exist for these cross-coupling reactions. It has been demonstrated that in the presence of strong oxidants (such as trivalent iodine(III) salts, IXR_2), Pd(IV) species play an important role in catalytic cycles.^{186,187} It has also been shown that when these iodonium salts are used in place of aryl halides in pincer-catalysed Heck reactions, the reaction is likely to proceed through a Pd(II)/Pd(IV) cycle (Scheme 6.1).¹⁸⁸



Scheme 6.1 Pd(IV) intermediates in the Heck reaction promoted by strong oxidants.

In the absence of such strong oxidants, it has been proposed on the basis of computational calculations that Pd(IV) species are thermally accessible intermediates in the Heck and Negishi reactions between PCP pincer complexes and aryl halides in polar solvents at elevated temperatures.^{189,190} Supporting these calculations, the first example of Ar–X oxidative addition to form a Pd(IV) species has recently been published in the scientific literature.¹⁹¹ In this example, chelate-assisted oxidative addition of an aryl iodide species to an ONC palladium pincer complex yielded the stable, crystallographically characterised Pd(IV) product at room temperature (Scheme 6.2). This emphasises that despite many ECE palladium pincer complexes acting as sources of a Pd(0) active catalyst, Pd(II)/Pd(IV) cycles should continue to be assessed for their viability in cross-coupling reactions.



Scheme 6.2 Chelate-assisted oxidative addition to form a Pd(IV) complex.

6.3 Performance of [(PCP)PdCl] Species in the Heck Reaction

Owing to the high activity of PCP pincer-based catalysts, the electron-poor pincer complexes [(POCOP)PdCl] (**28**), [(PCCCP)PdCl] (**29**), and [(POCCP)PdCl] (**30**) had their performance in the Heck reaction evaluated. The basic Heck cross-coupling between bromobenzene and styrene was used to evaluate each catalyst. A survey of the literature revealed that N-methylpyrrolidone (NMP) and dimethylformamide (DMF) were commonly employed solvents, with most reactions also using

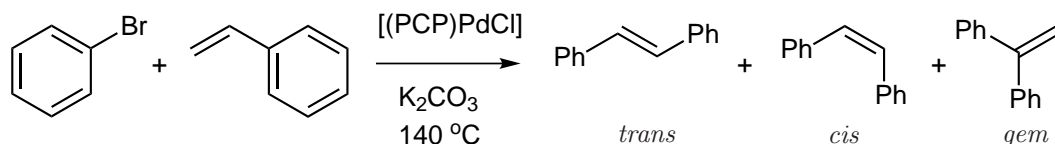
an inorganic base (such as a phosphate or carbonate), typically at temperatures of 140 °C.

Initial reactions focused on briefly optimising the base and solvent systems, and determining average TONs for each catalyst species. Methodology for a typical Heck reaction is outlined in the experimental section. Analysis of all Heck reactions was performed by gas chromatography mass spectrometry (GCMS). To avoid any bias arising from solvent evaporation between sampling and analysis, samples were stored in the dark at $-15\text{ }^{\circ}\text{C}$ and spiked with 2-methylnaphthalene as an internal standard. Storing the samples in the dark also served to minimise *cis/trans* isomerisation of stilbene, as samples that had been left in direct sunlight before being subjected to re-analysis showed substantially increased levels of *cis*-stilbene. All reactions were performed in duplicate at the least, with quoted values reflecting the averages of each reaction performed.

6.3.1 Results of Heck Reactions

Data obtained from the Heck reactions (Table 6.1) showed that the optimal reaction conditions were achieved in DMF with potassium carbonate as a base. Whilst using potassium phosphate monohydrate resulted in slightly higher yields than potassium carbonate, more consistent results were obtained with the carbonate. Utilising DMF as a solvent for these reactions gave much higher conversions than reactions performed with NMP — POCOP and POCCP catalysts **28** and **30**, which exhibited modest TONs in DMF, were found to be completely inactive in NMP. Moreover, in all reactions performed in NMP with **29**, a small amount of biphenyl (arising from the homocoupling of bromobenzene) was detected. No biphenyl was detected in any of the reactions performed in DMF. The reaction in DMF was also repeated without the addition of a catalyst, and no cross-coupling products were observed. This confirmed that the palladium pincer complexes were responsible for the activity, either as the catalyst or precatalyst; the reaction was not occurring under metal-free conditions or being promoted by persistent palladium residues adsorbed onto the surface of the reaction vessel.

Of the three complexes tested in these Heck reactions, activity was of the order $[(\text{PCCCP})\text{PdCl}]$ (**29**) $>$ $[(\text{POCOP})\text{PdCl}]$ (**28**) \gg $[(\text{POCCP})\text{PdCl}]$ (**30**). At a catalyst loading of 0.002 mole % all three compounds gave similar conversions of about 20–25% in 16 hours. However, on increasing the catalyst loading to 0.004 mole % and extending the reaction time to 22 hours it became clear that compounds **28** and

Table 6.1 Results of the Heck reaction with **28**, **29**, and **30**.

Ligand	Time (h)	Solvent	[Pd] (mol %)	Yield ^a (%)	TON	<i>gem/cis/trans</i>
POCOP	4	DMF	0.002	13	6,400	1/1/41
	16	DMF	0.002	18	8,900	1/5/14
	16	DMF	0.005	45	9,100	1/0/16
	22	DMF	0.004	68	17,000	1/2/27
	16	NMP	0.002	0	0	0/0/0
PCCCP	4	DMF	0.002	4	2,200	0/0/1
	16	DMF	0.002	24	12,000	1/4/15
	16 ^b	DMF	0.002	36	18,000	1/2/17
	16	DMF	0.005	54	11,000	1/0/16
	22	DMF	0.004	89	22,000	1/2/21
	16	NMP	0.002	24	12,000	1/2/17 ^c
POCCP	4	DMF	0.002	0	0	0/0/0
	16	DMF	0.002	25	13,000	1/4/15
	16	DMF	0.005	24	5,000	1/0/20
	22	DMF	0.004	16	4,000	1/14/16
	16	NMP	0.002	0	0	0/0/0

^a Determined by GCMS and based on bromobenzene and product.

^b Reaction performed with $\text{K}_3\text{PO}_4 \cdot \text{H}_2\text{O}$ instead of K_2CO_3 .

^c 3 equivalents of biphenyl also detected.

29 were more active than **30**. Under these conditions **29** gave the greatest average TON of 21,000. Complex **28** showed a similar activity giving an average TON of 18,000, while **30** displayed TONs of only 4,000.

In the literature, many PCP pincer catalysts have attained TONs of around 100,000 for the Heck reaction, with the greatest reported TON to date being 8,900,000.¹⁸⁰ Albeit many of these results are obtained using the more reactive aryl iodide substrates; lower activities can be expected (and in most cases are observed) for reactions involving aryl chlorides or bromides. More recently, an aminophosphine PNCNP pincer complex was found to give TONs of 5,000,000 in the cross-coupling of styrene and bromobenzene.¹³⁵ The pincer complexes **28**, **29** and **30** therefore display very modest activities in the Heck reaction; however, this is the first account of Heck catalysis using a complex containing a cyclometallated $\text{CH}_2\text{P}(\text{C}_6\text{F}_5)_2$ or $\text{OP}(\text{C}_6\text{F}_5)_2$ moiety. The pentafluorophenyl-substituted PCCCP complex **29** also displays a much higher activity than its perfluoroalkyl-substituted analogues, which recently demonstrated TONs on the order of hundreds — rather than tens of thousands — of cycles.¹⁹² Whilst complexes **28**, **29**, and **30** appear to be less active than their non-fluorinated phosphine and phosphinite PCP counterparts, they generally display a higher activity than NCN or SCS ligated complexes.^{193,194}

The reactions of the two most active palladium complexes, **28** and **29**, were monitored at regular intervals by GCMS. The plots of conversion against time for these reactions (Figure 6.3, top) confirmed that **29** was slightly more active than **28**, and also demonstrated that both reactions still proceeded up to 22 hours at 140 °C. Extrapolation to the point of 50% conversion gave turnover frequencies (TOFs) of 900 for **28** and 2,300 for **29**. These values pale in comparison to the TOF of 140,000 reported for the identical coupling of bromobenzene and styrene catalysed by a PNCNP pincer complex,¹³⁵ and are towards the low end of the TOFs generally observed for PCP pincer complexes (of the order of 1,000–10,000).¹⁶

Importantly, these plots suggested that the reactions involving **29** may display sigmoidal (S-shaped) kinetics (Figure 6.3, bottom graph). Such reactions display an induction period, during which time only a slight amount of product is formed while the catalyst precursor decomposes or reacts to form the active catalyst species. For pincer catalysed cross-coupling reactions the observation of an induction period is extremely indicative of decomposition to a nanoparticulate active catalyst.¹⁸³ An induction period was not detected in reactions performed with **28**, but may be present during the initial stages of the reaction for which data were not collected. To confirm that the active catalyst in these Heck reactions was a Pd(0) species (rather than the intact Pd(II) pincer complex), the mercury poisoning test was employed. This entailed the addition of a large excess of elemental mercury to the reaction mixture, to amalgamate any heterogeneous Pd(0) deposited during the reaction and hence negate any catalytic activity from Pd(0) species.^{195,196} Whilst elemental mercury has been shown to degrade molecular Pd(0) and Pt(0) alkene complexes,^{197,198} it does not react with Pd(II) pincer complexes, and hence is diagnostic for whether the pincer complex is acting as a catalyst or a source of active Pd(0) in a particular reaction.¹⁷⁶

Mercury poisoning tests were carried out by repeating the Heck reactions catalysed by **28** and **29** with the addition of approximately 50 mg (about 6,000 equivalents) of elemental mercury to each reaction mixture. Solutions were thoroughly stirred for two minutes prior to the addition of the catalyst to divide and distribute the mercury evenly throughout. Results are shown on the graphs in Figure 6.3; no trace of product was detected in any of the reaction mixtures in which mercury was present. This confirmed that pincer complexes themselves were not active catalysts for the Heck reaction, and instead acted as sources of catalytically active Pd(0), as is seen in the literature for almost all cyclometallated palladium compounds.¹⁸⁵

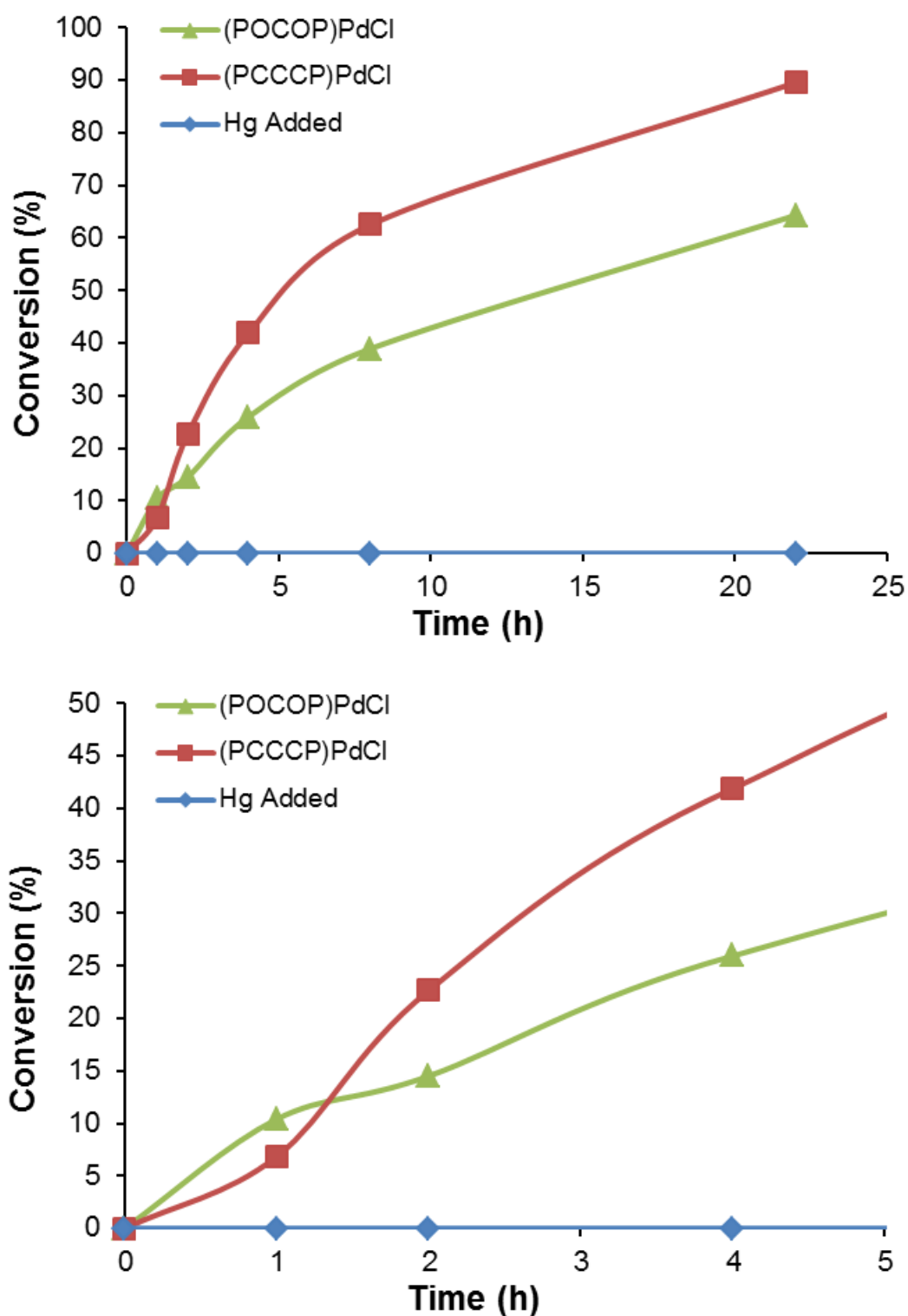
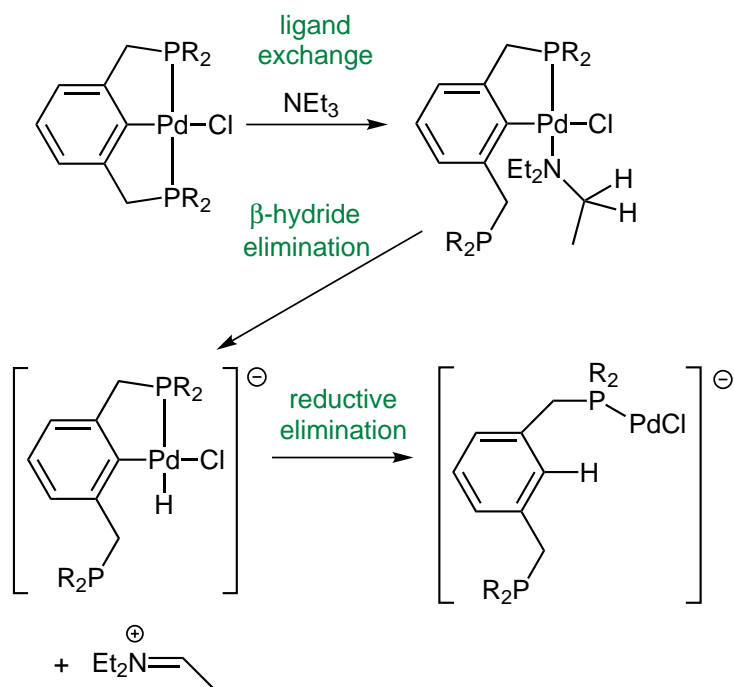


Figure 6.3 Conversion vs time: PhBr/styrene/K₂CO₃ at 140 °C with 4 mmol % of complexes **28** and **29**. Full duration of the reaction (top), and first four hours (bottom), showing the presence of an induction period.

6.3.2 Active Species Generation and Reaction Mechanism

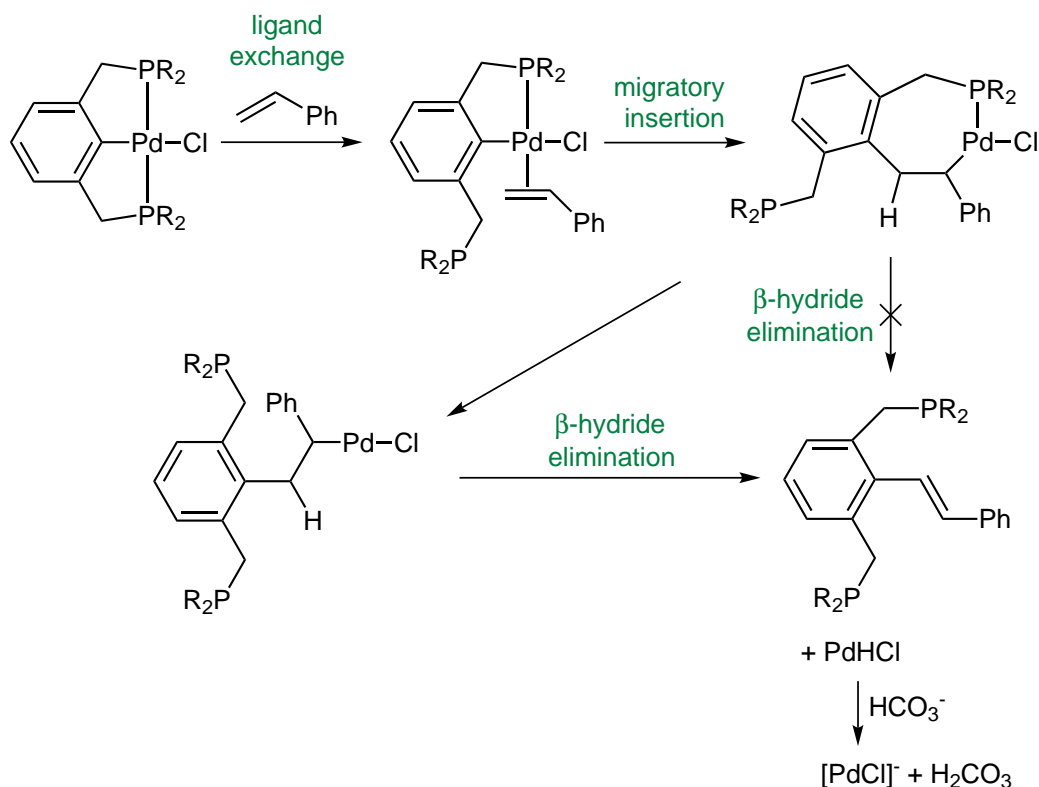
As these Heck reactions have been established to proceed through a heterogeneous Pd(0) active species, two pathways have been proposed in the literature for the reduction of the Pd(II) precatalyst. In the first, proposed originally by Louie and Hartwig¹⁸¹ then revised by Sommer and colleagues (Scheme 6.3),¹⁹⁹ a phosphorus-donor group of the pincer ligand is displaced by the amine base used, giving a cyclometallated palladium-amine intermediate. This is able to undergo β -hydride elimination from an alkyl group of the coordinated amine, to form a palladium hydride complex. As the cyclometallated carbon and hydride occupy coordination sites that are mutually *cis*-coordinated, reductive elimination of the aryl backbone of the pincer should be facile, yielding a Pd(0) species.



Scheme 6.3 Decomposition pathway for PCP pincer complexes in the presence of an amine base.

A second route to the Pd(0) species was proposed by Beletskaya²⁰⁰ for cyclometallated N-C chelates, but may also be applicable for the decomposition of PCP pincer complexes (Scheme 6.4). In this pathway a phosphorus donor group dissociates from the palladium and is replaced with the π -coordinated alkene. This is able to undergo insertion into the palladium-carbon bond of the pincer ligand, much like in the classical Heck mechanism (Figure 6.1). However, in this configuration β -hydride elimination is unable to occur, as the seven-membered ring formed in the insertion step prevents the β -hydrogen from interacting with the palladium. Dissociation of the second phosphorus donor allows free rotation that brings the hydrogen into the proximity of the palladium, rendering the insertion product susceptible to β -hydride

elimination and giving a styryl-substituted pincer ligand. The palladium-hydrido species generated is subsequently reduced to Pd(0) through hydride abstraction by the inorganic base, just as in the final step of the classical Heck reaction mechanism.



Scheme 6.4 Alternate decomposition pathway for PCP pincer complexes in the Heck reaction.

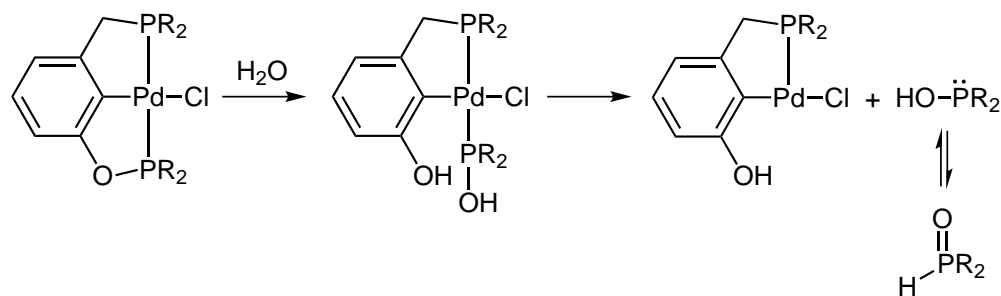
As these decomposition pathways are able to yield molecular Pd(0) species, and it has already been mentioned that mercury *may* poison some molecular Pd(0) species, further evidence was needed to unambiguously state that the active catalyst is a colloidal (rather than molecular) Pd(0) species. An observation in agreement with a nanoparticulate active catalyst is the behaviour of **30** at different catalyst loadings. This complex achieved a 25% conversion after 16 hours at a 0.002 mole % loading, but counterintuitively, the conversion *decreased* to 16% after 22 hours at double the catalyst loading (0.004 mole %). If a catalytic cycle involving a molecular catalyst species was operating, a greater yield of product would be expected at a greater catalyst loading. However, when nanoparticles are the active catalyst, the activity is extremely concentration dependent. Low concentrations of catalyst precursor often demonstrate a disproportionately high activity due to the formation of smaller colloidal particles of palladium, which have a greater ratio of palladium at the surface (active) sites than larger particles, and hence are more active.¹⁸⁵ Moreover, constant reaction of the aryl bromide with the surface of the nanoparticles prevents aggregation and Ostwald ripening; at a low palladium concentration more aryl bromide will be present per palladium atom, so this effect will be more pronounced.¹⁸⁵ The rate

of decomposition to form the active Pd(0) catalyst will depend on the coordination environment of the metal and therefore be specific to each complex,²⁰¹ explaining why **30** was the only complex used that displayed a decrease in conversion moving from 0.002 to 0.005 mole % loading.

Since the three complexes evaluated all showed similar product ratios (roughly 1:2:20 *gem:cis:trans*) the same active catalyst is expected in all reactions. It is worth noting that while **30** displayed an almost 1:1 *cis:trans* ratio after 22 hours, this is not seen as indicative of a molecular active catalyst. Increasing the steric bulk of the active catalyst is seen to increase the yield of the *gem* rather than *cis* product.²⁰² In this case, the predominance of the *cis* isomer was not seen in shorter reactions with **30**, and so the increased amount present in the longest reactions is likely to be due to *cis/trans* isomerisation in solution pending analysis.

From the decomposition pathways previously outlined (Scheme 6.3 and Scheme 6.4), a key step in the formation of the active catalyst species is the dissociation of one of the phosphorus donor atoms from the palladium. This allows for the formation of a complex with the correct *cis*-geometry for the reductive elimination or alkene insertion to occur. Dissociation of the remaining phosphorus donor group is then required for the formation of colloidal palladium. This requirement for Pd–P dissociation can help explain the different rates of reactivity seen between compounds **28**, **29**, and **30** in the Heck reaction. P–O bonds are notorious for undergoing facile hydrolysis;^{203,204} at millimole percent catalyst loadings it can be assumed that the amount of adventitious water present is sufficient to facilitate this cleavage. Moreover, under these basic reaction conditions (DMF solvent, excess potassium carbonate) this reaction will be more facile, as hydroxide is a better nucleophile than water. Once a P–O bond is broken, the chelate effect can no longer provide additional stabilisation to the phosphine hydroxide ligand, allowing it to more readily dissociate from the complex. Once the dissociation has occurred, phosphinous acid/phosphine oxide tautomerism will reduce the availability of the phosphorus lone pair of electrons for ligand-metal bonding, making the coordination site *cis* to the P–C bond more readily available, facilitating precatalyst decomposition (Scheme 6.5). Similar P–O cleavage was observed in reactions between methyllithium the POCOP platinum complex **25** (Chapter 4), where PMe(C₆F₅)₂ was observed as a minor product.

The ability for P–O bond hydrolysis to hasten complex degradation was demonstrated in the relative rates of active catalyst formation between **28** and **29**; data suggested that the PCCCP-ligated precatalyst displayed a longer induction period than the POCOP-ligated species (Figure 6.3, bottom). However, because **29** underwent a less facile decomposition it proved to be the better catalyst precursor. A



Scheme 6.5 P–O bond hydrolysis in a PCP pincer complex and subsequent tautomerism between phosphinous acid and phosphine oxide forms.

gradual deposition of colloidal palladium over time helps to prevent Ostwald ripening and palladium black formation, ensuring a steady stream of active palladium nanoparticles are entering the reaction mixture. This ‘slow release’ of active palladium has been repeatedly invoked to explain why the tridentate pincer compounds are better precatalysts in the harsh conditions of the Heck reaction than analogous bidentate cyclometallated compounds.²⁰⁵

This effect was also observed when comparing compound **28** to its non-fluorinated analogues. While **28** achieved a TON of 18,000 for the cross-coupling of styrene with bromobenzene, replacing the electron-withdrawing pentafluorophenyl substituents on the phosphorus donor with electron-donating isopropyl groups gave a reported TON of 140,000 for the identical reaction. This dramatic difference in activities can be attributed to the electronic effects these substituents have on the phosphorus centres. Because they are more nucleophilic and better able to stabilise a negative charge, phosphine ligands with electron-withdrawing substituents have been shown to be much more susceptible to hydrolysis under basic conditions than their more electron-rich counterparts.^{206,207} This propensity for hydrolysis and subsequent degradation shown by pentafluorophenyl-substituted PCP pincer complexes renders them less efficient at depositing catalytically active palladium nanoparticles than their non-fluorinated counterparts, making them poorer catalysts for the Heck reaction.

Counterintuitive to the notion that more stable precatalysts result in higher TONs was the observation that the complex with both phosphine and phosphinite functionalities, **30**, was a poorer precatalyst for the Heck reaction than the phosphinite complex **28**. The electronic effect that the ligands impart on the metal centre is responsible for this. As has been previously mentioned, *tert*-butyl phosphines are exceedingly good σ -donors, while pentafluorophenyl phosphines and phosphinites are very poor σ -donors.^{37,38} This results in increased electron density on the palladium in **30** compared to **28**; in the carbonyl analogues the C–O stretch is seen to decrease

from 2170 cm^{-1} in $[(\text{POCOP})\text{Pd}(\text{CO})]^+$ (**34**) to 2140 cm^{-1} in $[(\text{POCCP})\text{Pd}(\text{CO})]^+$ (**36**). Increasing the electron density on a metal centre has been shown to increase the energy barriers for alkene insertion and also reductive elimination.^{208,209} The effect of replacing a poorly donating pentafluorophenyl group with a strongly donating *tert*-butyl group therefore should increase the energy requirement for the decomposition pathways shown in Scheme 6.3 and Scheme 6.4, making formation of the initial Pd(0) species less facile. Furthermore, the strong Pd–P^{*t*}Bu₂ bond may hinder colloidal palladium formation, as the Pd(0) centres will not be able to aggregate and effectively form nanoparticles until the phosphine has dissociated. A similar phenomenon has previously been reported in the literature, whereby the presence of *tert*-butyl phosphine donors improve the stability of catalyst precursors, but at the cost of a lower activity.¹⁸³

There is clearly a fine balance in the relationship between ligand electronic effects and precatalyst activity. Complexes containing either very strongly donating or very weakly donating ligands display surprisingly modest activities as Heck precatalysts; a feature that is exacerbated rather than moderated when both donor types are combined in the same ligand.

Evidently these are complicated reaction mixtures. A number of potential Pd(II) to Pd(0) decomposition pathways are available, and there are surely a number of different factors at work influencing palladium nanoparticle formation. Whilst this section has sought to explain the observed reactivities of compounds **28**, **29** and **30**, the factors determining the activity of PCP pincer complexes may not play a part in reactions catalysed by other ECE pincer species. Van Koten notes that for SCS pincer-porphyrin complexes, the more electron-rich the porphyrin, the faster the active catalyst formation and the higher the conversions obtained.²⁰¹ Conversely, the work reported herein, along with that of Eberhard¹⁸³ suggests that for PCP pincer complexes the presence of an electron-rich P^{*t*}Bu₂ groups slows down the formation of Pd(0) species and results in poor catalyst activity. Therefore, the factors that influence palladium nanoparticle formation for one group of pincer complexes may not pertain to pincer complexes as a whole, and ligand electronic effects in each case must be balanced such that the desired ‘slow-release’ of the nanoparticulate active catalyst into solution is obtained.

6.4 Performance of [(PCP)PdCl] Species in the Suzuki Reaction

Pincer complexes **28-30** were also assessed for their activity in the Suzuki reaction. While the Suzuki reaction is conceptually similar to the Heck reaction — it is a palladium-catalysed C–C bond-forming reaction involving an aryl halide — the use of a boronic acid- or boronic ester-substituted aryl or vinyl group means that these reactions can generally be carried out under milder conditions than Heck reactions. It was hoped that under these conditions there would be less propensity for complex decomposition and palladium nanoparticle formation. The Suzuki reaction was therefore viewed as a greater hope for the observation of a Pd(II)/Pd(IV) catalytic cycle involving an intact palladium pincer complex.

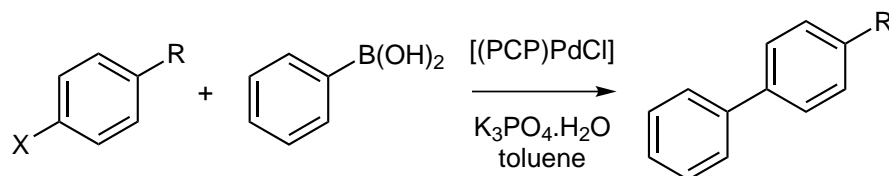
Initial reactions were performed with phenylboronic acid and 4-bromoanisole in toluene at 100 °C (see Experimental Chapter for details). Reactions in toluene at 100 °C are common for pincer species in the literature, thereby offering a good degree of comparability with established work. 4-Bromoanisole was chosen as the aryl halide for these reactions — being an electronically-deactivated aryl bromide it should prove sufficiently difficult to couple, therefore providing a clear difference in turnovers between good and bad catalysts. Reactions with aryl iodides generally give high TONs even with poor catalysts, while reactions with aryl chlorides do not proceed readily, so are unsuitable for initial reactivity studies. As in the Heck reactions, both potassium carbonate and potassium phosphate were trialled as external bases. Preliminary investigations to determine optimal catalyst loadings were carried out in toluene-*d*₈ and analysed by NMR (as this had a higher throughput than GCMS). NMR proved to be a valid analytical tool, giving similar results to GCMS. However, due to the higher cost of solvents, NMR reactions were necessarily performed on a smaller scale, giving rise to mass transfer problems and a noticeably lower reproducibility than reactions carried out for GCMS analysis. Control reactions were also performed after these initial studies using the same glassware, to ensure that there was no activity due to persistent palladium residues that had survived the cleaning process. As in the Heck analysis, all reactions were performed in at least duplicate; quoted values for conversions reflect the averages of all identical analyses.

6.4.1 Results of Suzuki Reactions

Results of the Suzuki reactions (Table 6.2) show that the activity of the complexes is of the order [(POCOP)PdCl] (**28**) > [(POCCP)PdCl] (**30**) > [(PCCCP)PdCl] (**29**). The most active catalyst, **28**, was tested under a range of reaction conditions, and was found to be slightly air sensitive, with greater yields obtained in reactions performed under inert atmospheres than those performed under ambient conditions. The addition of water to these reactions somewhat surprisingly increased the turnovers — it was expected that in the presence of water P–O bond hydrolysis in **28** would be more facile and the TON would be reduced. The increased activity can be attributed in part to an increased solubility of the inorganic base in the presence of water, but primarily due to the increased concentration of hydroxide ions in the reaction mixture. Whereas in the Heck reaction the base is used to regenerate the active catalyst after β -hydride elimination, in the Suzuki reaction the base aids in transmetallation of the boron to the palladium. It is not clear whether this transmetallation proceeds *via* base coordination to the metal²¹⁰ or to the boron,²¹¹ but in either case the high nucleophilicity of the OH[−] renders it much more effective at facilitating transmetallation than the inorganic bases alone. This also served to explain why the potassium phosphate was a better base for these reactions than potassium carbonate — the phosphate is used in its monohydrate form, meaning that as well as being a slightly stronger base, the water of crystallisation will provide the reaction mixture with additional hydroxide ions. Hydroxide bases themselves were not considered for this reaction as their increased basicity could potentially lead to more rapid catalyst degradation.

Reactions performed with potassium phosphate in the presence of a small amount of water produced the best results for the coupling of phenylboronic acid and 4-bromoanisole catalysed by compound **28**, giving 88 % conversion and an average TON of 176,000. These results indicate that **28** is amongst the most active pincer complexes for Suzuki reactions with aryl bromides. The most active pincer complexes have been reported by Bolliger and associates,⁵² whose PNCNP and POCOP complexes perform the coupling extremely rapidly, generating TONs of around 95,000 (with a 95% conversion) in just 5 minutes for the coupling of 4-bromoanisole with phenylboronic acid. Bedford²¹² and Garagorri⁷⁸ have also reported highly active POCOP and PNCNP complexes, attaining TONs of 190,000 and 180,000 respectively for this cross-coupling. However, these numbers represent conversions of just 19% and 18%; increasing the catalyst loading to obtain conversions in excess of 70% gives TONs of 7,200 and 77,000 respectively. Additionally, Bedford and Garagorri’s reactions were carried out above 100 °C for at least 16 hours, demonstrating that the achievement of 176,000 turnovers after two hours at

Table 6.2 Results of the Suzuki reaction with **28**, **29**, and **30**.



Ligand	Time (h)	Temp (°C)	ArX	[Pd] (mol %)	Yield ^a (%)	TON
POCOP	14 ^b	100	4-bromoanisole	0.001	39	39,000
	20	100	4-bromoanisole	0.001	89	89,000
	2	100	4-bromoanisole	0.001	74	74,000
	1 ^c	100	4-bromoanisole	0.001	64	64,000
	2	80	4-bromoanisole	0.001	55	55,000
	2 ^c	80	4-bromoanisole	0.001	44	44,000
	2	60	4-bromoanisole	0.001	13	13,000
	2	100	4-bromoanisole	0.0005	77	144,000
	2 ^d	100	4-bromoanisole	0.0005	35	70,000
	2 ^e	100	4-bromoanisole	0.0005	88	176,000
	2	100	4-chloroanisole	0.0005	0	0
	20	100	4-chlorobenzaldehyde	0.05	10	200
PCCCP	20	100	4-bromoanisole	0.001	56	56,000
	2	100	4-bromoanisole	0.001	25	25,000
	1 ^c	100	4-bromoanisole	0.001	2	2,000
POCCP	14 ^b	100	4-bromoanisole	0.001	17	17,000
	20	100	4-bromoanisole	0.001	66	66,000
	2	100	4-bromoanisole	0.001	53	53,000
	1 ^c	100	4-bromoanisole	0.001	6	6,000
	2	80	4-bromoanisole	0.001	14	14,000
	2	60	4-bromoanisole	0.001	0	0
	2	100	4-chloroanisole	0.0005	0	0
	20	100	4-chlorobenzaldehyde	0.05	60	1,200
DPPF ^f	2	100	4-bromoanisole	0.001	77	77,000

^a Determined by GCMS and based on aryl halide and biphenyl.

^b Reaction performed with K₂CO₃ instead of K₃PO₄ · H₂O.

^c Reaction performed with the addition of ~ 30,000 equivalents Hg.

^d Reaction performed in air.

^e Reaction performed with the addition of 0.1 mL water.

^f The formula of the complex used was [(DPPF)PdCl₂].

100 °C by **28** is very impressive for this class of complex.

While compound **28** displays a very high activity for a pincer complex in the Suzuki reaction, this activity is substantially lower than is displayed by other palladium species for this reaction. Cyclometallated P–C chelates such as **58** (Figure 6.2) have been observed to give TONs approaching 9,000,000 for reactions with electronically-deactivated aryl bromides.²¹² One of the most effective systems for the Suzuki reaction — Buchwald’s 2-dicyclohexylphosphinobiphenyl ligands with [Pd(OAc)₂] — catalyses reactions with electronically-deactivated aryl chlorides at room temperature.²¹³ In comparison, Suzuki reactions using aryl chlorides do not proceed well with these pincer complexes. Reactions with the electronically-activated 4-chlorobenzaldehyde only proceeded with very moderate turnovers of 1,200 (complex **30**) and 200 (complex **28**) after 18 hours at 100 °C. Interestingly, the reactivity displayed here was the reverse of that shown in reactions involving electron-poor aryl bromides — the POCCP complex **30** was more active than the POCOP complex **28**.

To assess the activity of these pincer complexes in the Suzuki reaction, they were compared to a commercially available catalyst, [(DPPF)PdCl₂]. This species was chosen as it is a highly active catalyst for cross-coupling reactions and is commonly used in organic synthesis. Reactions with **28**, **29**, **30** and [(DPPF)PdCl₂] were monitored by GCMS to observe the speed at which the reactions proceeded, and also to probe the nature of induction periods and catalyst lifetime. Results from these reactions (Figure 6.4, top) show that as well as giving the greatest conversions, complex **28** also promotes a very rapid reaction. Extrapolating from the point of 50% conversion gives TOFs of 330,000 for complex **28**, 88,000 for [(DPPF)PdCl₂] and 29,000 for complex **30**. A TOF value for **29** could not be established as the reaction had not reached 50% conversion during the time allotted. These data show that over the first hour, the POCOP complex **28** outperforms the commercially available [(DPPF)PdCl₂], reaching the 50% conversion mark in almost one quarter of the time for the DPPF complex. However, it appears catalyst stability is an issue under these conditions, with both **28** and **30** displaying a much reduced activity after 30 minutes, so much so that around the 90 minute mark [(DPPF)PdCl₂] surpasses the turnovers achieved by **28**.

This poor catalyst lifetime was also demonstrated by testing the supernatant for catalytic activity. The coupling of 4-bromoanisole with phenylboronic acid in the presence of 1 mmol % **28** was performed; after 30 minutes the supernatant containing the catalyst was reused with fresh starting materials, then after an additional 30 minutes the supernatant was used in a third subsequent reaction. Reactions were

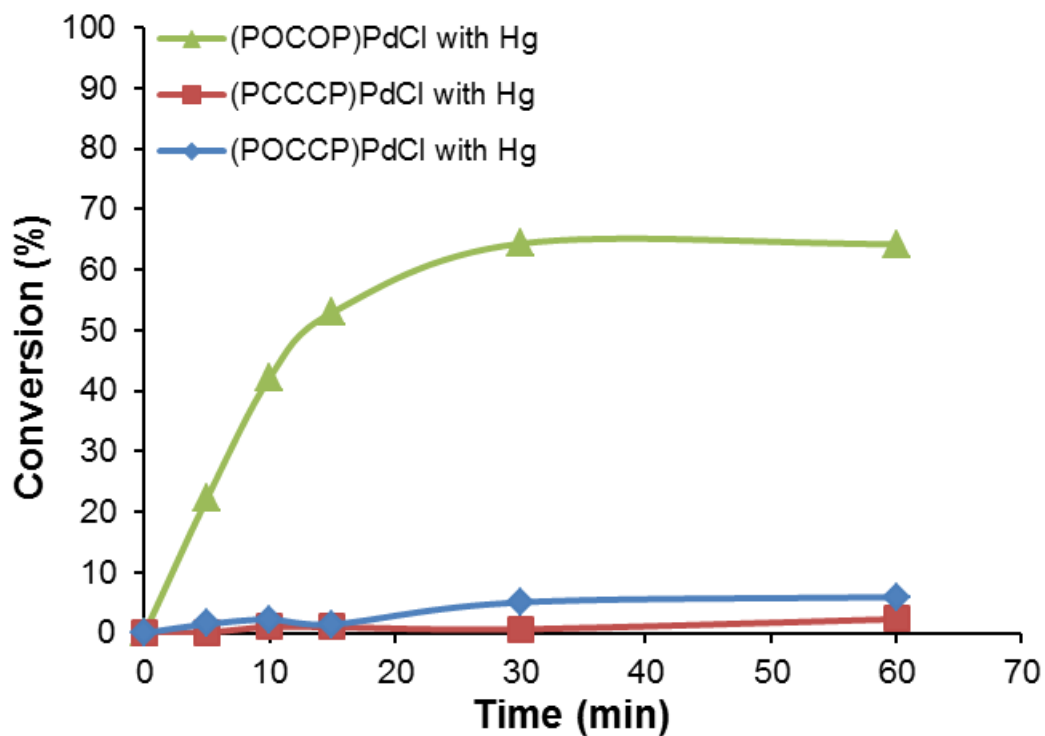
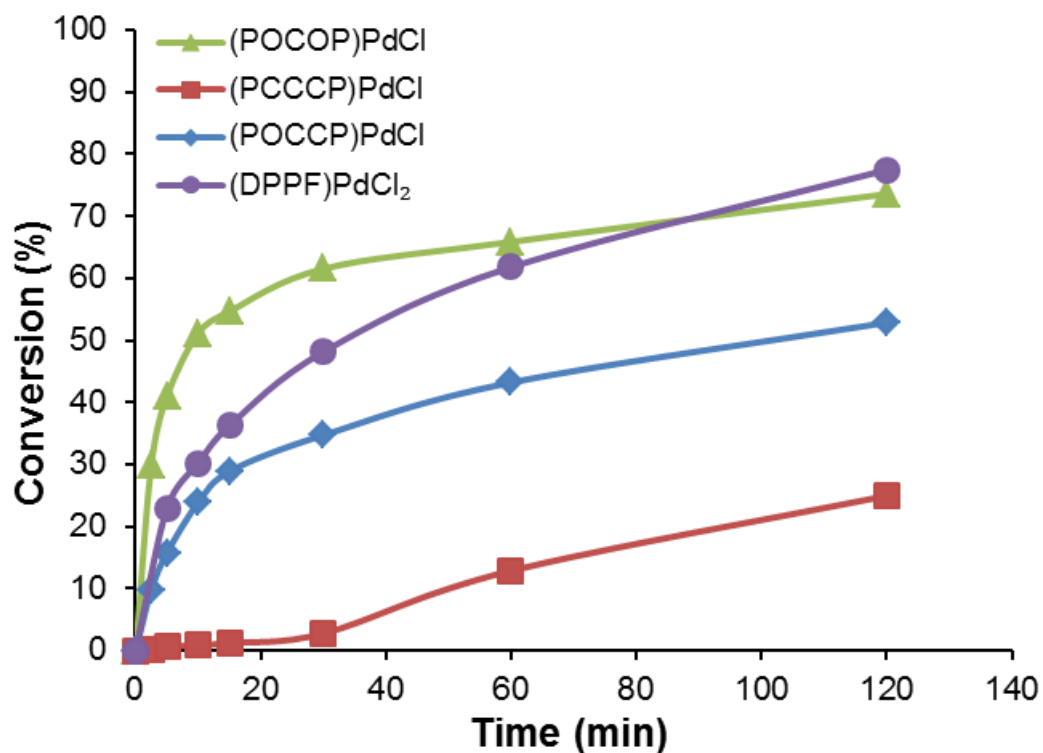


Figure 6.4 Conversion vs time: 4-bromoanisole/phenylboronic acid/ $\text{K}_3\text{PO}_4 \cdot \text{H}_2\text{O}$ at 100 °C with 1 mmol % of complexes **28**, **29**, **30** and $[(\text{DPPF})\text{PdCl}_2]$. Standard reaction conditions (top), reactions with the addition of approximately 30,000 equivalents mercury (bottom).

performed in duplicate, with the activity of **28** seen to decrease upon each subsequent reuse. Initially, a 73% conversion into the biphenyl product was observed, dropping to 50% then 21% on the second and third reuses respectively. The dramatic loss of activity between runs confirmed the decomposition of the active species, and indicated that severe difficulties may be encountered with catalyst recovery and reuse in this system.

As well as illustrating the rapidity at which the POCOP complex **28** carried out these Suzuki reactions, the plots of conversion against time (Figure 6.4) also demonstrate why the PCCCP complex **29** performed so poorly. The reaction catalysed by **29** clearly displays an induction period of approximately 30 minutes, during which time only traces of product are formed. As in the Heck reactions, the induction period and subsequent sigmoidal kinetics are characteristic of a colloidal Pd(0) active catalyst. To probe the nature of the active species in these Suzuki reactions, mercury poisoning experiments were again undertaken. The addition of one drop of mercury (about 30,000 equivalents per palladium) to the reaction mixtures was seen to dramatically reduce the activity of compounds **29** and **30** (Figure 6.4, bottom). After one hour in the presence of mercury, the TON of **30** dropped from 43,000 to 6,000, while the TON of **29** dropped from 13,000 to 2,000. However, somewhat surprisingly, the POCOP compound **28** was seen to give essentially the same conversions regardless of whether mercury was present or not (TON of 66,000 without mercury and 64,000 with mercury, after one hour). Since the mercury poisoning experiments had been seen to give no traces of product in Heck reactions with **28**, this served to establish that under the milder Suzuki reaction conditions the catalytic activity was due to a homogeneous palladium species in solution, rather than heterogeneous palladium nanoparticles.

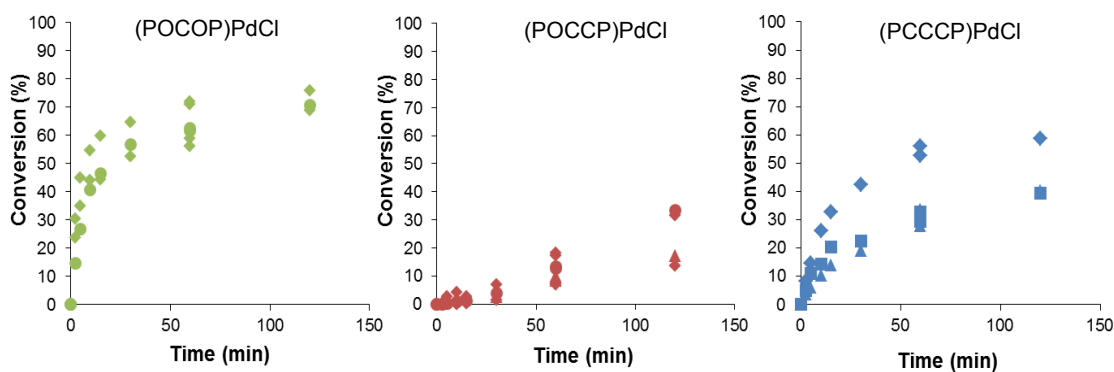


Figure 6.5 Raw data for Suzuki reactions at 100 °C catalysed by (from left to right) pincer complex **28**, **29**, and **30**.

It has been reported that kinetic irreproducibility is also an indicator of complex degradation to produce a heterogeneous active catalyst, as the nanoparticle formation is highly sensitive to reaction conditions.²¹⁴ Examination of the raw data from these Suzuki reactions (Figure 6.5) revealed that reactions performed with compound **28** were more reproducible than those performed with **29** and **30**. The percentage of starting material converted to product in reactions catalysed by **28** was spread over a 6% range (69–76% conversion) after 2 hours at 100 °C, compared to 20% and 19% (13–33% and 39–58% conversion) for **29** and **30** respectively. This provided a further indication that Suzuki reactions catalysed by the POCOP complex **28** proceed through a homogeneous active species, while the PCCCP complex **29** and the POCCP complex **30** degraded under Suzuki conditions to produce heterogeneous active catalysts.

To probe for the presence of an induction period in reactions involving **30**, and to further investigate the nature of the active species in these Suzuki reactions, reactions with complexes **28** and **30** were monitored at the lower temperatures of 80 °C and 60 °C, with the results shown in Figure 6.6. Performing kinetic studies at lower temperatures has been shown to dramatically reduce the rate of palladium nanoparticle formation, revealing sigmoidal kinetic behaviour in reactions that displayed none at higher temperatures.²¹⁵ The most striking feature of these plots is that even at 80 °C, compound **28** maintained a high activity, producing 55,000 turnovers at a TOF of 50,000. Conversely, the activity of **30** was reduced dramatically, giving only 14,000 turnovers after the two hour reaction had concluded. Further reduction of the temperature to 60 °C rendered **28** much less effective (TON of 13,000), while no traces of product were detected in the reaction of **30** at this temperature.

Looking at an expanded view of the reactions (Figure 6.6, bottom) the presence of an induction period is clearly visible for the reaction of the POCCP complex **30** at 80 °C, with only traces of product detected up until the 20 minute mark, at which point the reaction commenced. For the reaction of the POCOP complex **28** at 60 °C, the results are not quite as clear-cut, as a slight bump appears in the curve after 10 minutes. However, the 4-methoxybiphenyl product was detected in the first sample withdrawn after 2.5 minutes and appeared in ever-increasing amounts in every sample taken forthwith, rather than being present in trace amounts for the induction period, then appearing in increasing amounts. Thus the data were not conclusive as to whether sigmoidal kinetics are likely to be in effect for Suzuki reactions involving **28**. However if degradation of the pincer complex to an active species does occur, it must necessarily be very rapid to consistently produce detectable amounts of product after two minutes at 60 °C.

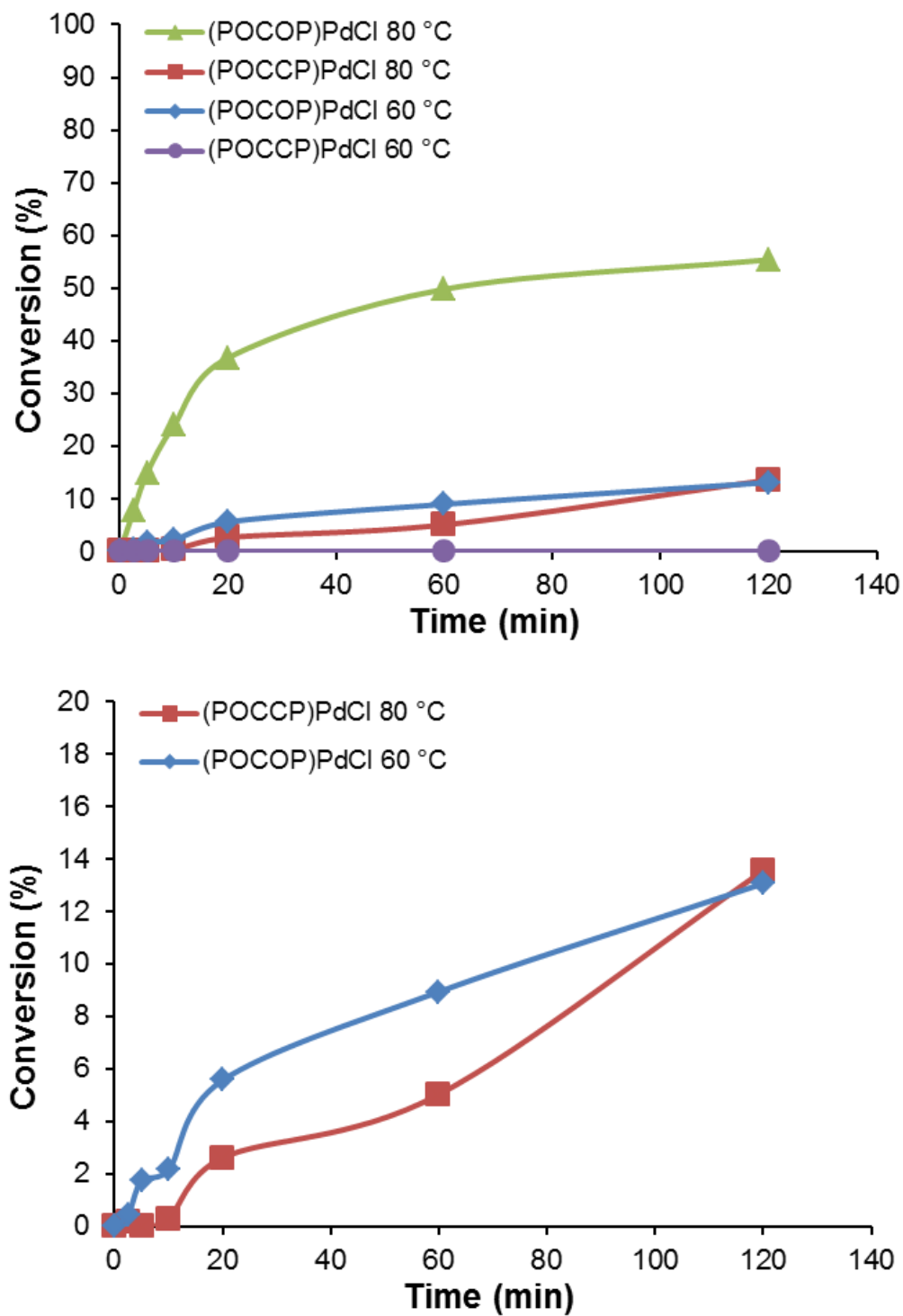


Figure 6.6 Conversion vs time: 4-bromoanisole/phenylboronic acid/K₃PO₄ · H₂O at 80 °C and 60 °C with 1 mmol % of complexes **28** and **30**. All data (top), expanded view of selected reactions (bottom).

Mercury poisoning reactions were also repeated for the reaction with compound **28** at 80 °C. This was done to ensure that the negative result in the mercury drop test performed at 100 °C was not due to the formation of Pd(0) being so rapid that the cross-coupling was completed before the mercury could amalgamate the palladium, as has been proposed for some rapid Suzuki reactions in the literature.²¹⁶ Upon reducing the reaction temperature from 100 °C to 80 °C, the observed TOF for **28** dropped from 330,000 to approximately 50,000 in the absence of mercury; a value close to that of the POCCP species **30** at 100 °C (TOF of 29,000). As **30** returned a positive mercury drop test at 100 °C (a drastic reduction in activity was observed), it can be concluded that at 80 °C nanoparticle formation from **28** would not be so rapid as to give a spurious result in the mercury drop test.

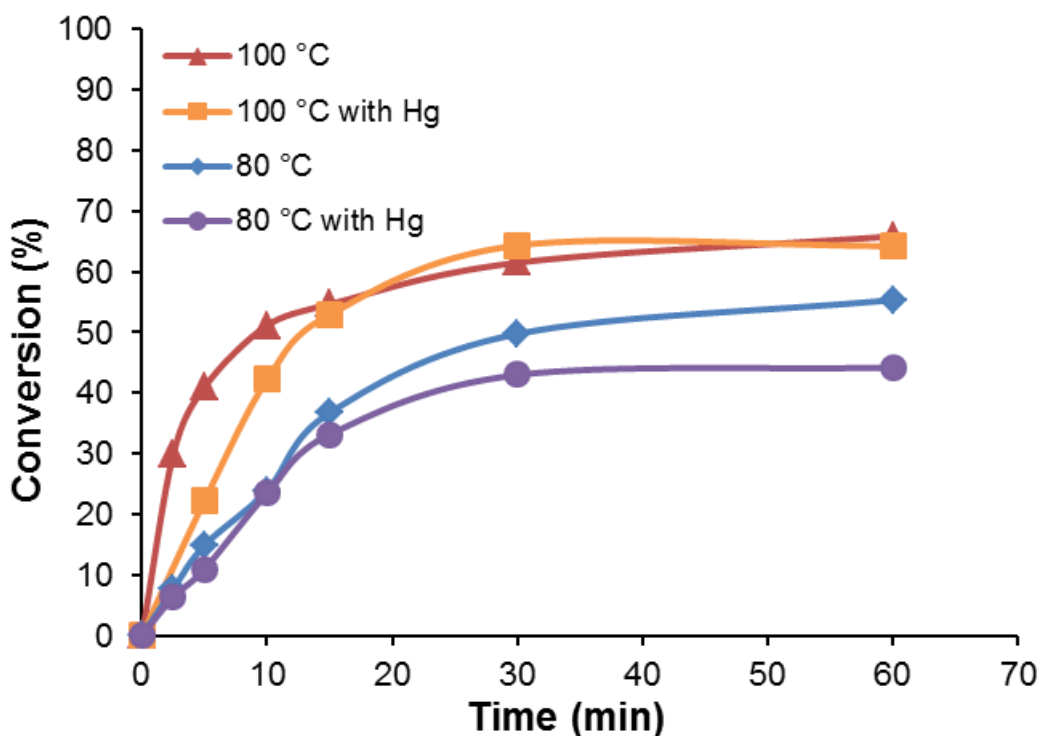


Figure 6.7 Conversion vs time: 4-bromoanisole/phenylboronic acid/ $\text{K}_3\text{PO}_4 \cdot \text{H}_2\text{O}$ at 100 °C and 80 °C with 1 mmol % of complex **28** in the presence and absence of 30,000 equivalents of mercury.

Again, the mercury drop test with **28** was negative; reactions at 80 °C gave essentially the same conversions whether mercury was present or not, just as they had at 100 °C. Looking at a plot of the reaction progress for these mercury poisoning experiments (Figure 6.7), it is evident that in both instances when mercury is present the activity is halted after about 30 minutes, while in the absence of mercury the reaction continues to progress after 60 minutes (albeit slowly). This is indicative that there are contributions to activity from both homogeneous and heterogeneous active species occurring concurrently in these reaction mixtures. In reactions involving **29** and **30** the activity was severely diminished by mercury poisoning, but not

eliminated altogether. This was in contrast to the Heck reaction, where no traces of product were observed in reactions where mercury was added, and indicated that a small amount of activity in these Suzuki reactions was probably due to homogeneous catalysis by palladium complexes in solution. For **28** the contribution from homogeneous catalysis was much greater, to the point where mercury addition was seen only to reduce activity after about 30 minutes, by which time colloidal degradation products of the homogeneous active catalyst must be responsible for the activity.

The effectiveness of compound **28** in catalysing the Suzuki reaction on a large scale was also investigated. The reaction between 4-bromoanisole and phenylboronic acid was performed in a round bottom flask at 20 times the scale of the previous reactions, with a catalyst loading of 1 mmol %. After 12 hours at 100 °C the reaction was stopped and the product isolated by extraction with ethyl acetate, followed by column chromatography on alumina to remove the excess phenylboronic acid. The 4-methoxybiphenyl was isolated in a 98% yield, giving a turnover number for **28** of 98,000 and indicating that this catalyst continues to perform well upon upscaling of the Suzuki reaction.

6.4.2 Active Species Generation and Reaction Mechanism

The observation that Suzuki reactions catalysed by compound **28** proceeded *via* a homogeneous active species meant the nature of the reaction mechanism needed to be addressed. Like the Heck reaction, the Suzuki reaction is typically catalysed out by a low-coordinate Pd(0) active species, with oxidative addition of the aryl halide to form a Pd(II) intermediate a key step in the mechanism (Figure 6.8). As this is conceptually similar to the Heck reaction, the Pd(II)/(IV) catalytic cycle proposed for pincer complexes participating in the Heck reaction has also been invoked to explain their reactivity in the Suzuki reaction.^{52,217}

In this work, it is highly unlikely that reactions catalysed by **28** proceed through a Pd(II)/(IV) catalytic cycle involving the intact pincer complex. The primary reason for this is electronic; **28** contains a very electron-poor metal centre. Palladium(IV) species are regarded as being significantly less stable than the corresponding platinum(IV) complexes,²¹⁸ hence for the oxidative addition step to be facile, the Pd(IV) product must be stabilised through electron donation to the metal from the surrounding ligands. As discussed in Chapter 4, the C–O stretching frequencies of the carbonyl derivatives $[(\text{POCOP})\text{Pd}(\text{CO})]^+$, $[(\text{PCCCP})\text{Pd}(\text{CO})]^+$, and

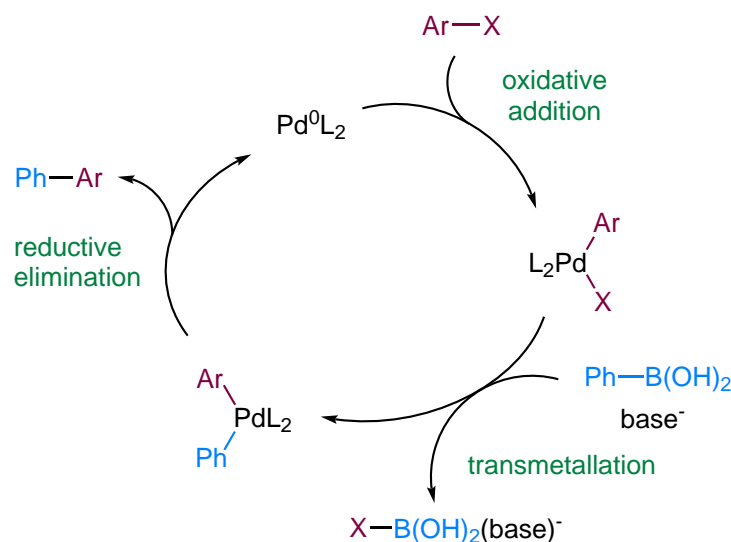


Figure 6.8 Outline of the classic “textbook” Suzuki catalytic cycle.

$[(\text{POCCP})\text{Pd}(\text{CO})]^+$ (compounds **34**, **35**, and **36** respectively) provided an indication of the electron density present on each metal centre. With a carbonyl C–O stretching frequency of 2170 cm^{-1} , complex **34** displayed the most electron-poor palladium centre of any pincer compound reported to date, and was significantly more electron-poor than the corresponding PCCCP and POCCP palladium complexes **35** and **36** (carbonyl C–O stretches of 2148 and 2140 cm^{-1} respectively). As any Pd(IV) intermediates generated from **28** will undergo minimal electronic stabilisation, they will be high in energy and consequently be poor candidates for intermediates in a reaction that was observed to be facile at temperatures as low as $60\text{ }^{\circ}\text{C}$. This rationale that an electron-poor metal centre will not readily undergo oxidative addition has been bolstered through the use of computational chemistry. Density Functional Theory (DFT) calculations on similar palladium pincer complexes have demonstrated that for this oxidative addition, “the higher the electron density on the metal centre, the lower the ground state energy and energetic barrier.”¹⁸⁹ To confirm this and correlate electron density on the metal centre with ease of oxidation, cyclic voltammetry (CV) was performed on complexes **28**, **29**, and **30**. However, meaningful results were unable to be obtained. Fortunately, a 2011 paper by Polukeev and colleagues²¹⁹ confirmed that the carbonyl C–O stretch of a pincer carbonyl adduct directly corresponds to the ease of oxidation of its metal centre. From these carbonyl stretching frequencies, this indicates the ease of oxidation of these complexes would be **30** > **29** > **28**. Since the compound that should be the most difficult to oxidise is the species that reacts *via* homogeneous catalysis, from an electronics point of view a Pd(II)/(IV) mechanism for this catalysis is highly unlikely.

Furthermore, there is a steric barrier to Pd(II)/(IV) catalysis. To achieve reductive elimination of the biphenyl product from a Pd(IV) species, the aryl groups need to

occupy mutually *cis* coordination sites, and be oriented in a “face-on” conformation to facilitate effective orbital overlap. However, it has been demonstrated that in *tert*-butyl-substituted PCP pincer complexes, the steric demands of the bulky *tert*-butyl groups above and below the coordination plane of the aryl groups force them to sit in a flat, “side-on” manner, significantly increasing the energy barrier for C–C reductive elimination (Figure 6.9).²²⁰ Bis(pentafluorophenyl)phosphine groups have a similar steric demand to di-*tert*-butyl phosphine groups,³⁷ therefore the coordinated aryl groups would be expected adopt a “side-on” conformation, providing another restriction to biphenyl formation. Hence because of the electron-poor, sterically crowded nature of the POCOP complex **28**, a mechanism involving Pd(IV) intermediates is highly unfavourable and can be disregarded as a plausible reaction pathway in this instance.

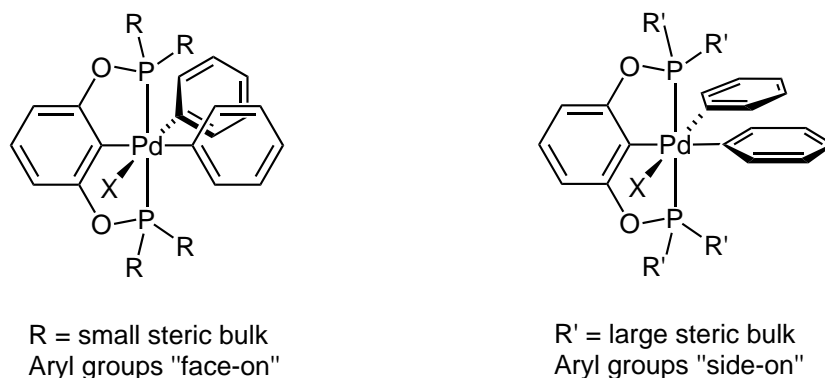


Figure 6.9 Steric effect of phosphorus substituents on aryl coordination. Reductive elimination of aryl groups is favoured by a “face-on” conformation.

Another consideration for the mechanism of the Suzuki reaction catalysed by **28** is a concerted, redox-free pathway (Figure 6.10). Such a pathway was proposed in 2009 by Olsson and Wendt,²²¹ and has been subsequently invoked to explain the reactivity of pincer catalysts in both the Suzuki and Negishi cross-coupling reactions.^{190,222} The key to this mechanism is that the first step — the transmetallation of the phenyl group from the boron to the palladium — can occur *via* a four-membered transition state, without any change in the oxidation state of the metal.²¹¹ The palladium-phenyl species generated by transmetallation then reacts with the aryl halide in a metathesis-type reaction. This is almost identical to the transmetallation step, proceeding through a similar four-membered transition state in a concerted fashion, with Pd–Br bond formation occurring concurrently with Pd–C bond cleavage. This produces the biphenyl product and also regenerates the (PCP)PdX active catalyst, leaving the pincer framework intact.

While this redox-free mechanism is a viable possibility for the Suzuki reaction, an

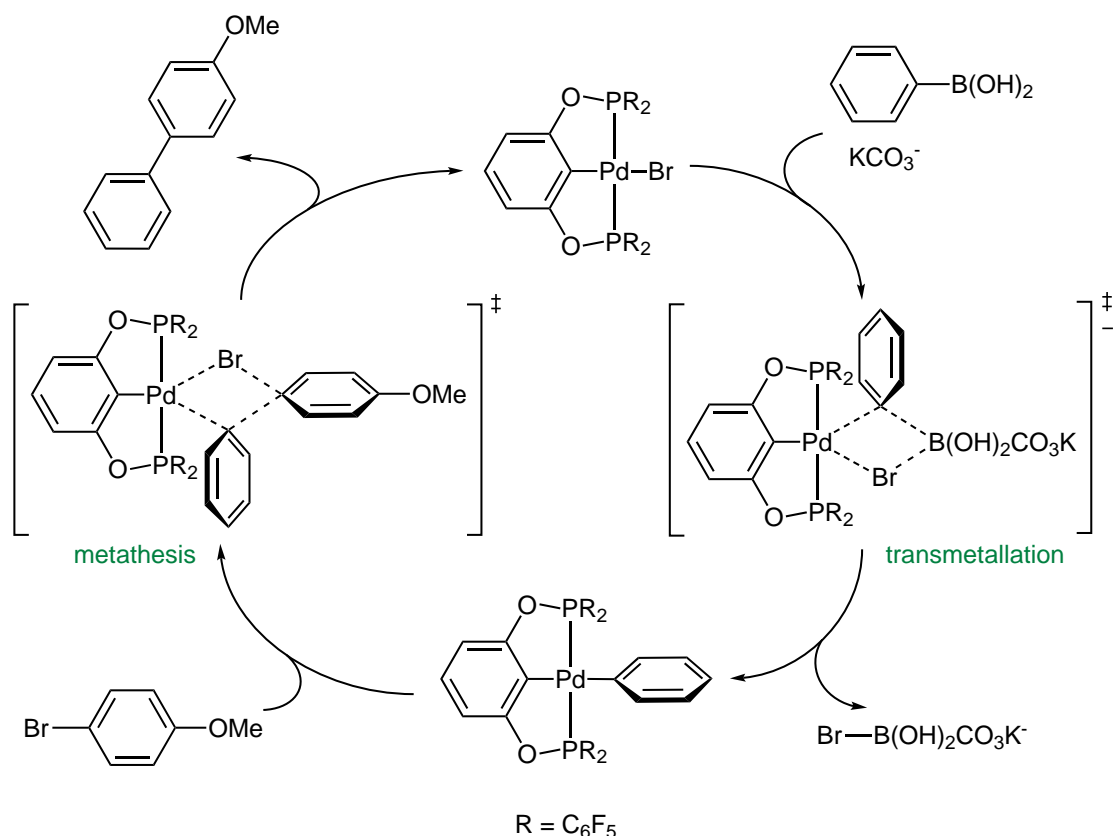


Figure 6.10 Proposed redox-free mechanism for compound **28** in the Suzuki reaction.

analogous mechanism is not possible for the Heck reaction. The Heck reaction requires alkene insertion into a palladium-aryl bond, meaning that oxidative addition of the aryl halide to the palladium has to be the first mechanistic step. In the Suzuki reaction there is no insertion step, meaning either the aryl halide oxidative addition *or* transmetalation of the arylboronic acid may occur first. As the transmetalation step occurs through a redox-free pathway, when the reaction is initiated by transmetalation it allows for the possibility of a redox-free mechanism, so long as the product-forming metathesis step is facile. Such metathesis steps are not well known for palladium, they are more prevalent in the chemistry of the harder, early transition metals.²²³ However, reports have indicated that these concerted, four-membered transition states are favoured for some palladium pincer complexes as a lower energy alternative to an oxidative addition/reductive elimination pathway.^{224,225} Moreover, in the well-established cross-coupling of vinyl epoxides with organoboronic acids, the nucleophilic attack step is conceptually similar to the metathesis.^{172,226,227} In this reaction, an aryl or vinyl group is transmetalated from a boronic acid to a palladium pincer species, as in the first step of Figure 6.10. The palladium-aryl species then undergoes nucleophilic attack on a vinyl epoxide, which can be seen as analogous to the metallated carbon of the phenyl group attacking the *ipso*-carbon of the aryl bromide in the second step of Figure 6.10.²²⁶ The fact that this reaction is catalysed

by palladium pincer complexes under mild conditions *via* a redox-free mechanism is a good indication that a similar redox-free mechanism may be in operation in the Suzuki reaction.

This proposed mechanism is consistent with the reactivity differences between compounds **28**, **29**, and **30**. For proton transfer reactions on late transition metals that can proceed *via* oxidative addition or σ -bond metathesis pathways, it has been observed that the four-centred metathesis transition state was favoured for less electron-rich metal centres.²²³ Similarly, in the aforementioned vinyl epoxide cross-coupling, it was noted that complexes with electron-poor metal centres catalysed the reaction significantly faster than their electron-rich counterparts. This trend of a higher reactivity for more electron-poor metal centres can explain the results obtained in these Suzuki reactions. For the most electron-poor complex **28**, the C–Br bond metathesis step is facile and the reaction is catalysed by a palladium pincer complex in solution. For the comparatively more electron-rich complexes **29** and **30** the metathesis step will be less favourable, meaning that the colloidal palladium decomposition products catalyse the reaction faster than the parent pincer complex can, and the reactions proceed predominantly through a heterogeneous active species. As this mechanism is not possible for the Heck reaction, this also explains why small amounts (*c.a.* 2–5%) of product appear in mercury-poisoned Suzuki reactions catalysed by **29** and **30**, but no traces of product are detected in analogous Heck reactions: the catalyst precursors display a limited activity proceeding *via* this redox-free mechanism, and can therefore undergo a small number of turnovers before the heterogeneous Pd(0) is liberated and amalgamated.

Comparing the TONs displayed by compound **28** with literature values also supports the notion of the Suzuki reaction proceeding through this redox-free mechanism. Both pincer species in the literature that are deemed to catalyse the reaction in this manner are considerably more electron-rich than the POCOP complex **28**, consisting of aliphatic (rather than aromatic) backbones, and cyclohexyl²²² or *tert*-butyl²²¹ substituted phosphine donor groups. These species displayed TONs of 9,100 and 1,100 respectively, with a greater activity shown by the PCy₂-substituted complex than by the more strongly electron-donating P^{*t*}Bu₂-substituted complex. As expected, under similar conditions the more electron-poor POCOP complex **28** significantly outperformed its more electron-rich analogues, with a TON of 74,000. This is consistent with all three complexes catalysing the Suzuki reaction through a redox-free pathway, with the exceptional stability conferred to the literature compounds by their aliphatic backbones and strong P-donor ligands preventing Pd(0) deposition, and allowing the contributions to catalysis by the intact pincer species to be observed.

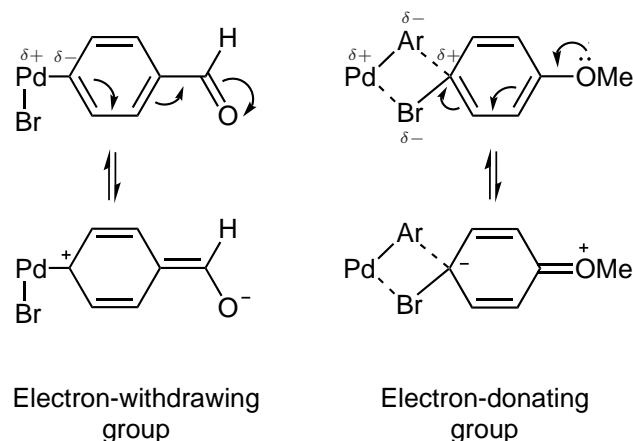
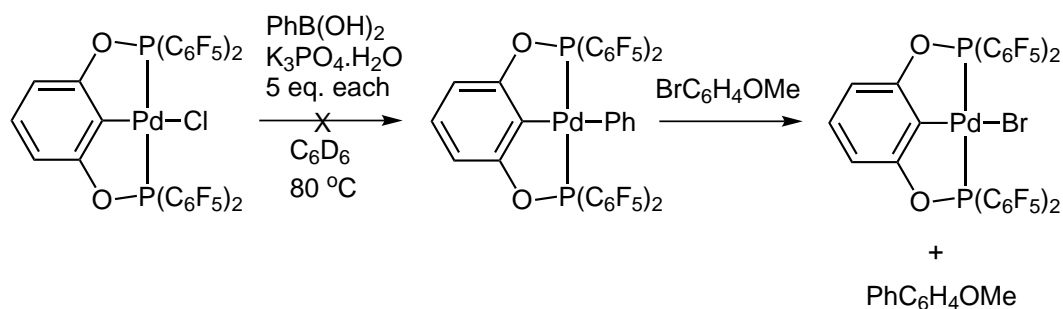


Figure 6.11 Comparison of resonance stabilisation in oxidative addition/reductive elimination mechanism (left) and redox-free mechanism (right). Ancillary ligands omitted for clarity.

Furthermore, this redox-free mechanism provides an explanation as to why the more electron-rich POCCP complex **30** outperformed the POCOP complex **28** in the cross-coupling of 4-chlorobenzaldehyde (TONs of 1,200 vs 200 respectively). Due to the differences in the electronic character of oxidative addition compared to C–X bond metathesis, what constitutes an ‘activated’ or ‘deactivated’ aryl halide will differ between the oxidative addition/reductive elimination mechanism and the redox-free mechanism. When the aryl halide undergoes oxidative addition to the metal centre, a partial negative charge ($\delta-$) is developed on the metallated carbon atom. Aryl groups with *para*-substituted electron-withdrawing groups can stabilise this species through resonance effects, drawing some of the negative charge away and making the oxidative addition reaction more facile (Figure 6.11, left). Conversely, during C–X bond metathesis, a partial positive charge ($\delta+$) is developed on this same carbon of the aryl halide (as it is bound to the electronegative halogen rather than the electropositive metal centre). This charge can be stabilised in a similar fashion through resonance effects from *para*-positioned electron-donating groups (Figure 6.11, right). Hence, for an oxidative addition/reductive elimination pathway aryl halides possessing *para* electron-withdrawing groups will be ‘activated’, whereas for the redox-free pathway aryl halides with *para* electron-donating groups will be ‘activated’. This decreased activity when moving from traditionally ‘deactivated’ (electron-donating) to ‘activated’ (electron-withdrawing) aryl halides has been previously observed where a redox-free mechanism was proposed;²²¹ however, it was marked as a “surprising” result and not attributed to the innate nature of the redox-free mechanism itself. In this work, the observation that **28** outperforms **30** with the electron-donating 4-bromoanisole, while **30** outperforms **28** with the electron-withdrawing 4-chlorobenzaldehyde is consistent with **28** proceeding through

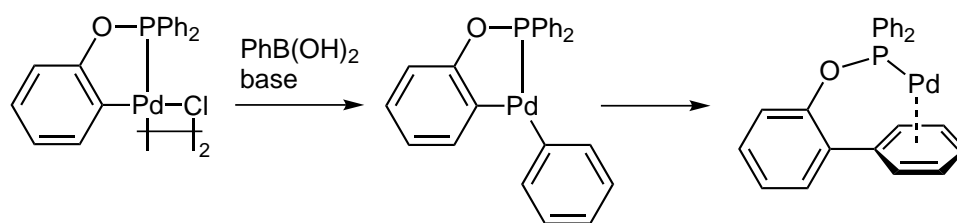


Scheme 6.6 NMR-scale Suzuki reaction attempted with **28**.

a redox-free mechanism, while **30** proceeds *via* a (heterogeneous) oxidative addition/reductive elimination cycle.

Whilst all the experimental evidence was in good agreement with the Suzuki reaction of **28** proceeding through a redox-free pathway, confirmation of this was attempted with NMR experiments. The reaction between **28** and excess phenylboronic acid in the presence of potassium phosphate (Scheme 6.6) was attempted on an NMR scale in order to observe the palladium-phenyl intermediate $[(\text{POCOP})\text{PdPh}]$, which could then be reacted directly with the 4-bromoanisole to confirm that the Suzuki reaction did proceed through the intact pincer complex. While the previous results had indicated that **28** was stable for a number of hours when heated in the presence of base, in the presence of a large excess of phenylboronic acid and base at elevated temperatures solutions of **28** discoloured within two minutes, turning first a bright orange and then a dark yellow/brown colour, indicative of complex degradation. This was confirmed by NMR spectroscopy; after five minutes at 80 °C only trace amounts of **28** remained in solution.

This introduced the possibility that Suzuki reactions involving **28** under these conditions were proceeding *via* a homogeneous Pd(0)/Pd(II) mechanism, catalysed by a molecular Pd(0) degradation product. Such a scenario has not been observed or even postulated for palladium PCP pincer complexes, but the notion of a molecular degradation product serving as the active catalyst species was posited for cyclometallated P–C chelate complexes by Bedford and colleagues in 2003.²¹² In that work, the active catalyst was identified as a biphenyl species arising from the coupling of the phenyl group from the boronic acid with the ligand backbone (Scheme 6.7). These degradation products bear a close resemblance to complexes of the extremely effective Buchwald-type ligands such as SPhos and XPhos: they consist of a singular phosphorus donor atom attached to a bulky biphenyl group.²¹³ As such, these cyclometallated P–C chelates demonstrated remarkable activity in the Suzuki reaction, catalysing the cross-coupling of 4-bromoanisole and phenylboronic acid with TONs in excess of 4,000,000.²¹²



Scheme 6.7 Pathway for Pd(0) active catalyst formation in P–C chelates.²¹²

However, for pincer complexes the formation of a similar monodentate, biphenyl-substituted phosphine complex should be substantially less facile. Whereas in P–C chelate complexes the coordination site *cis* to the metallated aryl ring is occupied by a relatively easy to displace bridging halide, in pincer complexes the displacement of a more strongly binding phosphorus donor group is required to achieve phenylation of the aryl backbone of the pincer complex. There is the possibility that P–O bond hydrolysis and subsequent phosphinous acid dissociation (as in Scheme 6.5) creates this vacant coordination site *cis* to the metallated aryl backbone. This hydrolysis and biphenyl active catalyst formation needs to be extremely facile, as no induction periods were definitively observed for Suzuki reactions with **28**, even at 60 °C. While such a fast hydrolysis is possible, if this reaction was rapid, it would be expected that a second hydrolysis event would also be rapid, leading to equally fast catalyst degradation and 2,6-dihydroxybiphenyl formation. Moreover, the POCCP complex **30** would not be susceptible to a second hydrolysis, so would be expected to form a more stable biphenylphosphine active catalyst. As Suzuki reactions with **30** proceeded through a heterogeneous rather than homogeneous active catalyst, this pathway for active catalyst formation is unlikely to occur in these reactions.

To determine if the pincer complex decomposition was yielding homogeneous Pd(0) species capable of catalysing the Suzuki reaction, these degradation products were analysed by GCMS in tandem with NMR spectroscopy. As in the first step of Scheme 6.6, palladium complexes **28**, **29** and **30** were reacted with excess phenylboronic acid and potassium phosphate in benzene-*d*₆ at 80 °C. Hexafluorobenzene was used as an internal standard so that ¹⁹F NMR spectroscopy could be used quantitatively to determine the degree of decomposition, as well as the proportions of different degradation products present. Control experiments were also undertaken with **28** and phenylboronic acid, as well as **28** and potassium carbonate, to assess the effect of each of the starting materials individually on the pincer complex.

Monitoring the reactions by NMR spectroscopy, it was clear that phenylation of the pincer complex **28** by the base-activated phenylboronic acid facilitates pincer complex degradation. In the presence of both phenylboronic acid and potassium carbonate, less than 1% of **28** remained in solution and was detectable by ¹⁹F NMR

spectroscopy after 5 minutes at 80 °C. Conversely, in the presence of the base alone the rate of decomposition was decidedly slower (greater than 40% of **28** remained after three hours at 80 °C), and **28** was seen to be extremely stable in the presence of phenylboronic acid alone (only trace amounts of decomposition products were observed after 24 hours at 80 °C).

Compounds **29** and **30** displayed markedly different reactivities to compound **28** in reactions with phenylboronic acid and potassium carbonate. The POCOP complex **28** decomposed to give complicated mixtures of phosphorus and fluorine-containing products that were not readily identifiable by ^{31}P NMR spectroscopy. Conversely, the PCCCP and POCCP complexes both reacted to form typically three or four different stable molecular species. However, due to the number of compounds present in these reaction mixtures the decomposition products were not able to be unambiguously characterised. Data from ^{31}P NMR spectra of these reactions suggests that these species were asymmetric Pd(II) complexes; they typically possessed one phosphorus environment at a similar chemical shift to the starting material and one phosphorus environment shifted 20–40 ppm downfield of the starting material, with P–P coupling values of approximately 400–500 Hz, typical for a *trans* two-bond phosphorus-phosphorus coupling. The concentration of these species decreased slowly over time, indicating that these compounds were potential precatalysts for the Suzuki reaction; being formed rapidly then undergoing a gradual decomposition to deposit Pd(0) nanoparticles into solution.

After monitoring by NMR spectroscopy for seven hours at 80 °C, these reaction mixtures were analysed by GCMS. Samples from each reaction were hydrolysed prior to GCMS analysis, in order to cleave P–O bonds and therefore create more volatile species in solution. Results were compared to samples that had not been subjected to hydrolysis, to assist with the identification of species that had arisen from the P–O cleavage. Somewhat surprisingly in all reaction mixtures with phenylboronic acid and potassium carbonate, the major volatile products were decafluorobiphenyl, 2,3,4,5,6-pentafluorobiphenyl, and biphenyl. The ^{19}F NMR spectra of these decomposition reactions indicated that initially pentafluorobiphenyl was formed, then as the decomposition reactions proceeded pentafluorobiphenyl formation ceased and the concentration of decafluorobiphenyl slowly increased (Figure 6.12). The gradual formation of decafluorobiphenyl was also observed in the decomposition of **28** in the presence of base alone. Biaryl formation in *cis*-bidentate P–P chelate complexes has been reported as occurring through the insertion of palladium-aryl centres into phosphorus-aryl bonds.²²⁸ Thus, a similar decomposition pathway may be present for these complexes, with the requisite palladium-phenyl species being generated by the boronic acid (as in the first step of Figure 6.10). Alternately, the phenylboronic

acid could directly phenylate one of the phosphorus donors *via* nucleophilic attack, in a manner analogous to the previously proposed P–O hydrolysis, a reaction that would necessarily be more facile at the $\text{OP}(\text{C}_6\text{F}_5)_2$ groups compared to the more electron-rich and less Lewis acidic $\text{CH}_2\text{P}(\text{C}_6\text{F}_5)_2$ and $\text{CH}_2\text{P}^t\text{Bu}_2$ groups. Either of these pathways would account for the initial appearance of pentafluorobiphenyl, and the observation that the decomposition was much more facile in the presence of both phenylboronic acid and base.

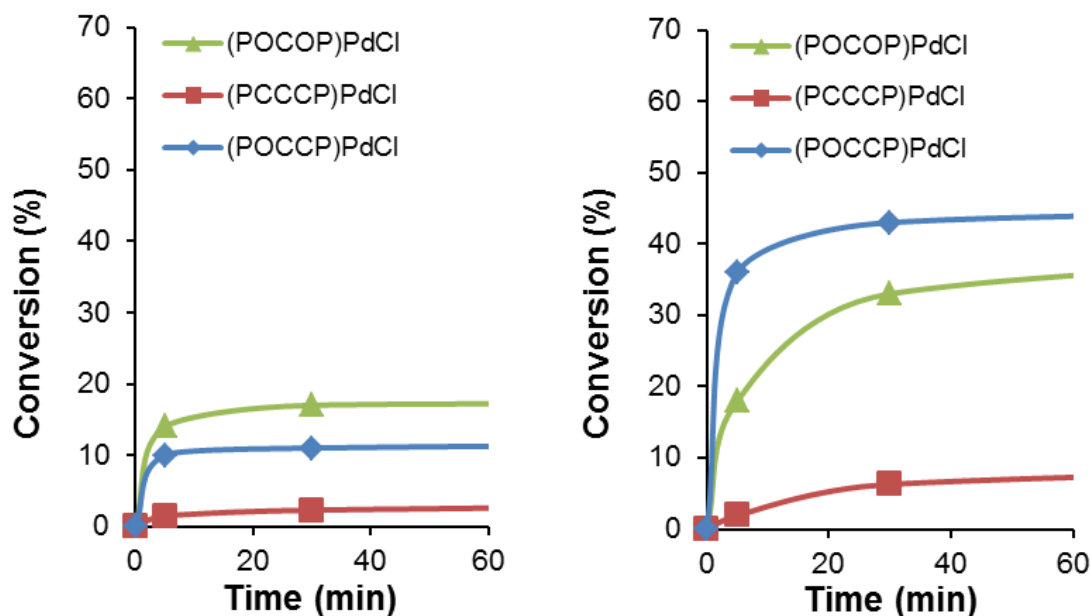


Figure 6.12 Plot of the appearance of pentafluorobiphenyl (left) and decafluorobiphenyl (right) in NMR-scale catalyst degradation experiments. Conversions represent the moles of pentafluorophenyl generated per mole of pentafluorophenyl present in the starting material. Data obtained at $t = 180$ min was plotted but is not displayed.

During this decomposition, it is interesting to note the difference in rates of biphenyl formation between the complexes (Figure 6.12), particularly with respect to the catalytic activity of each species. Biphenyl formation plateaued after 30 minutes at 80°C for the POCOP complex **28**, and after 10 minutes for the POCCP complex **30**, with the formation of the major biphenyl component (decafluorobiphenyl) being much more rapid in the case of **30**. This correlated well with the heterogeneous catalytic activity of each complex; there was an approximately 10 minute induction period at 80°C for **30**, after which time heterogeneous catalysis commenced. For **28**, mercury poisoning experiments have shown that homogeneous catalysis concluded after about 30 minutes, after which time there was still a contribution to catalysis from a heterogeneous active species. For the PCCCP complex **29**, only small amounts of biphenyl product were detected, while minimal catalytic activity was observed in the first hour even at 100°C . Hence the formation of these fluorinated biphenyls can be seen as a precursor to the formation of colloidal palladium

and heterogeneous catalysis, and potentially offers an explanation as to the fate of the homogeneous active species in the case of **28**.

Further analysis of reaction mixtures by GCMS did not reveal any traces of 2,6-substituted biphenyls, confirming that a biphenylphosphine- or phosphinite-ligated active species (as in Scheme 6.7) is not formed with **28**, or indeed any of the palladium complexes. However, in reactions involving the POCOP complex **28**, there were small amounts of the phosphines $\text{P}(\text{C}_6\text{F}_5)_3$ and $\text{PPh}(\text{C}_6\text{F}_5)_2$, as well as the phosphinite $\text{P}(\text{OPh})(\text{C}_6\text{F}_5)_2$ present. Amongst the decomposition products from **30**, minor traces of PPh^tBu_2 were observed, but no other phosphorus-containing species were identified from the decomposition of complexes **29** and **30**. This may indicate that in the Suzuki reaction, compound **28** is reduced to a low coordinate $\text{Pd}(0)$ complex, stabilised by the presence of phosphorus-donor ligands in solution. Such a species has previously been proposed as the active catalyst in C–S cross-coupling reactions catalysed by a $[(\text{POCOP})\text{NiCl}]$ species.²²⁹

The possibility of the active species in Suzuki reactions involving **28** being a $\text{Pd}(0)$ complex bound to monodentate phosphine ligands formed from the degradation of the pincer complex certainly bears consideration. This is able to explain how the reaction proceeds when the parent complex is not stable for more than a few minutes under catalytic conditions, and also follows the established $\text{Pd}(0)/(\text{II})$ reaction mechanism. On the contrary, it does not explain the reactivity difference between **28** and **30** in coupling “activated” aryl chlorides. Nor does it account for lack of an observed induction period, even at low temperatures — both the cyclometallated P–C chelates and $[(\text{POCOP})\text{NiCl}]$ complexes display distinct induction periods during the active catalyst formation.^{212,229} Due to the fact that this reaction proceeds so rapidly and may be catalysed by such small amounts of palladium, it is extremely difficult to conclude whether Suzuki reactions involving **28** proceed through a redox-free mechanism catalysed by the pincer complex, or whether the pincer complex acts as a precatalyst for a homogeneous, phosphine-ligated $\text{Pd}(0)$ catalyst. One thing is clear though, unlike the complexes **29** and **30**, the POCOP complex **28** catalyses the Suzuki reaction through a homogeneous active species, and is one of the most active pincer catalysts for this reaction reported to date.

6.5 Concluding remarks

The palladium pincer compounds [(POCOP)PdCl] (**28**), [(PCCCP)PdCl] (**29**), and [(POCCP)PdCl] (**30**) were assessed for their activity as catalysts in the Heck and Suzuki cross-coupling reactions. While catalysts containing fluoroaryl phosphines traditionally have not demonstrated high activities,⁸⁰ it was hoped that the electronic and structural variations provided by this series of compounds would provide insight into factors that assist efficient catalyst design.

In the Heck reaction, it was observed that compounds **28**, **29**, and **30** displayed modest activities, giving TONs of 4,000–22,000 after 22 hours. By undertaking mercury poisoning experiments, it was shown that all the palladium pincer complexes functioned as precatalysts, decomposing under catalytic conditions to give catalytically active palladium nanoparticles. The PCCCP complex **29** was the most active precatalyst; unlike the POCOP complex **28** it contains no readily-hydrolysed P–O bonds and therefore underwent a longer induction period, but proved to be more efficient at providing the reaction mixture with a steady stream of active palladium. Incorporation of an electron-donating di-*tert*-butyl phosphine group into the pincer framework (**30**) did not stabilise the precatalyst and assist with the desired ‘slow-release’ of active palladium into solution. Instead this precatalyst displayed the worst features of the two functionalities; it was still prone to P–O hydrolysis while undergoing a less facile decomposition to Pd(0), making for poor performance in the Heck reaction.

These electron-poor PCP pincer complexes proved to be substantially more active in the Suzuki reaction. Compound **28** in particular was highly active, giving an average TON of 176,000 in just two hours, making it one of the most active pincer complexes reported for the Suzuki reaction to date. This corresponds to just 5 ppm of palladium required for a conversion of 88%. Comparison to [(DPPF)PdCl₂] showed that while **28** gave similar turnovers to the commercially available catalyst after two hours, **28** performed the reaction at a substantially faster rate, reaching the 50% conversion mark almost four times faster than [(DPPF)PdCl₂]. This activity was somewhat unexpected, especially as **28** outperformed the activity reported for its proteo analogue,¹⁷¹ a feat not often reported for palladium-catalysed cross coupling reactions.

Performing low temperature kinetic tests as well as mercury poisoning experiments on these Suzuki reactions indicated that reactions involving **29** and **30** proceeded *via* a heterogeneous active catalyst — as in the Heck reactions — whereas reactions with **28** were catalysed by a homogeneous species. In considering the nature

of this homogeneous active species, the sterically-crowded, electron-poor nature of **28** renders catalysis through a Pd(II)/(IV) cycle highly unlikely. However, due to aryl halide oxidative addition not being an explicit requirement for the Suzuki reaction, catalysis through an alternate, redox-free mechanistic pathway is plausible. This mechanism offers parallels with established Pd(II) chemistry, and can explain the observed reactivity differences between **28** and similar pincer complexes in the literature, as well as relatively poor performance of **28** in coupling “activated” aryl chlorides. However, assessment of the stability of these pincer complexes under pseudo-catalytic conditions revealed that **28** has a dramatically shorter lifetime than compounds **29** and **30**, yielding degradation products that suggested the active species may be a Pd(0) centre stabilised by tertiary phosphine ligands such as $\text{P}(\text{C}_6\text{F}_5)_3$ present in solution. As these reactions proceeded rapidly in the presence of very little palladium, it was very difficult to unambiguously identify the active species present in reactions involving **28**.

From these investigations, it could be concluded that the performance of pincer species in palladium-catalysed cross-coupling reactions does not have a simple correlation with the electronic nature of the metal centre. It appears instead that both the stability and the electronic character of the phosphorus donor groups needs to be considered, in conjunction with the nature of active catalyst formation under catalytic conditions. In the Heck reaction, $[(\text{PCCCP})\text{PdCl}]$ (**29**) considerably outperforms $[(\text{POCCP})\text{PdCl}]$ (**30**) as a precatalyst, while in the Suzuki reactions the reverse is true, despite all of these reactions proceeding *via* a heterogeneous active species. The reason for this becomes evident when considering the reaction conditions — the Heck reaction is performed at high temperature in the absence of a good nucleophile, while the Suzuki reaction is performed at considerably lower temperatures in the presence of base-activated phenylboronic acid, which acts as a phenylating agent.

In the Heck reaction, displacement of a phosphorus donor group from the palladium is an essential step in colloidal palladium formation (Scheme 6.3, Scheme 6.4), therefore the replacement of a poorly donating $\text{P}(\text{C}_6\text{F}_5)_2$ group with a strongly donating P^tBu_2 group hinders ligand dissociation, and subsequently leads to a lower catalyst activity. Moreover, as the active catalyst formation is slow (half lives of the order of 5-10 hours are common, Figure 6.3), thermal stability of the precatalyst is of benefit, with the more robust PCCCP species **29** demonstrating a higher activity than the complexes comprising the more labile P–O bonds, **28** and **30**. Conversely, in the Suzuki reaction nucleophilic attack on the phosphorus centre appears to play a major part in the active catalyst formation, as evidenced by the observation of fluorinated biphenyls in GCMS and NMR analysis of reaction mixtures. With the

similarity of this nucleophilic attack to P–O hydrolysis (Scheme 6.5) and the correlation of low activities with low amounts of biphenyl formation in the case of the PCCCP complex **29**, this indicates that in the presence of a nucleophile, incorporation of the less robust and more Lewis acidic phosphinite functionality into the precatalyst aids heterogeneous active catalyst formation. These results emphasise that whilst the Heck and Suzuki reactions are conceptually similar, they have individual, specific, and even conflicting factors than need to be taken into account when considering efficient precatalyst design.

Drawing further conclusions on how the structural and electronic nature of PCP pincer complexes affect their activities in these reactions is complicated by the observation that the POCOP complex **28** catalyses the Suzuki reaction *via* a homogeneous active species. While the exact nature of the catalyst species is uncertain, this does highlight that conceptually small structural modifications may have a large effect on the nature of the catalysis. A further point of emphasis is that pincer complexes may not be as robust *under catalytic conditions* as many have anticipated, and further, due to the high activity of colloidal and low-ligated homogeneous palladium species, confirmation of the active catalyst species in solution is extremely difficult. This is put best by Phan and colleagues, “indeed, if ppt levels of palladium are capable of easily catalyzing some reactions, probing the nature of the true catalyst by most spectroscopic or other techniques may currently be impossible”.¹⁷⁶

Chapter 7

Conclusions

Transition metal complexes stabilised by phosphorus-containing pincer ligands have been at the forefront of chemical research in recent years. They have facilitated the selective bond cleavage of some of the most difficult-to-activate substrates, and have shown considerable promise in two catalytic technologies that may help alleviate a potential energy crisis in the years to come: alkane metathesis and water splitting. The rigid, well-defined coordination geometry of pincer complexes generally minimises decomposition reactions, providing pincer complexes with a stability that helps to ensure they remain intact and catalytically active even under demanding reaction conditions.

While much of the research undertaken with pincer complexes involves the use of electron-rich ligands, this study entailed the synthesis of PCP and PNP pincer ligands bearing bulky electron-poor bis(pentafluorophenyl)phosphine substituents. It was envisaged that the incorporation of these electron-poor groups into the pincer coordination motif would provide an insight into the factors that influence the synthesis and reactivity of these PCP and PNP pincer complexes.

The synthesis of the PCP and PNP pincer ligands was performed by attaching the electron-poor phosphines to phenyl or pyridyl backbones with CH₂, NH, or O linkages. Installation of the phosphines *via* condensation reactions between bis(pentafluorophenyl)phosphine bromide and aromatic alcohol or amine functionalities was observed to give the desired pincer ligands in moderate to good yields, with the added advantage of being carried out under milder conditions than have been reported for the synthesis of more electron-rich analogues. This synthetic methodology was also tolerant of other functionalities present on the ligand, enabling the synthesis of the mixed phosphine-phosphinite POCCPH ligand **3**. The previously

reported diphosphine PCCCPH ligand **2** was also synthesised; by using magnesium-anthracene methods to produce the required Grignard reagent, ligand **2** was obtained in a greater yield than previously reported.

The coordination chemistry of the most electron-poor POCOPH pincer ligand **1** was investigated with a range of platinum and palladium starting materials. Reaction of **1** with $[\text{Pt}(\text{nb})_3]$ yielded the *cis*-bridged dimer $[(\text{POCOPH})\text{Pt}(\text{nb})]_2$ (**14**), which was characterised by single crystal X-ray diffraction, and was shown to be stabilised by favourable π - π interactions between the aromatic ligand backbones. A similar preference for the formation of κ^2 -PP bridged structures was indicated in reactions between ligand **1** and $[\text{PtMe}_2(\text{hex})]$. None of the species arising from norbornene- or methyl-substituted starting materials could be induced to undergo metallation to form platinum PCP pincer complexes.

Reactions of ligand **1** with platinum and palladium dichloride or chloromethyl starting materials led to the formation of rare examples of *cis,trans*-dimers **19**, **21**, and **23** as precursors to the metallated PCP pincer complexes. The formation of these *cis,trans*-dimers is likely to be the result of having to balance steric and electronic effects — bulky bridging ligands are seen to favour *trans*-coordination modes due to steric constraints, while π -acceptor donor groups favour *cis*-coordination in order to minimise unfavourable electronic interactions. The extensive coordination chemistry demonstrated by ligand **1** was in part attributed to its electron-poor nature increasing the barrier to C–H activation and ligand metallation, favouring the formation of bridged coordination complexes over mononuclear pincer species.

As ligand **1** proved difficult to metallate, the influence of both ligand and starting material on pincer complex formation was assessed. It was revealed that the ease of ligand metallation increases with increasing electron-donating ability of the ligand. Substitution of a bis(pentafluorophenyl)phosphinite group on the ligand for a di-*tert*-butyl phosphine group — moving from ligand **1** to ligand **3** — resulted in the formation of roughly double the amount of metallated product in half the time. It was also determined that the nature of the ancillary ligand on the platinum starting material had a significant influence on the ease of pincer complex formation. Somewhat counterintuitively, strongly binding ancillary ligands promoted faster ligand metallation, as their less facile dissociation from the metal centre disfavoured the formation of thermodynamically stable dimers and oligomers as metallation intermediates.

The electronic character of ligands **1**, **2**, and **3** were assessed *via* the synthesis of the appropriate platinum or palladium carbonyl species, $[(\text{PCP})\text{M}(\text{CO})]^+$. Infrared

spectroscopy of these carbonyl complexes confirmed the expected trend, from most electron-poor to most electron-rich, $\text{POCOP} > \text{PCCCP} > \text{POCCP}$. The palladium POCOP carbonyl **34** possessed the largest value reported to date for the C–O stretching frequency of a pincer carbonyl complex in the IR spectrum, while the platinum POCOP complex **31** and the palladium PCCCP complex **35** also displayed C–O stretching frequencies greater than that of free carbon monoxide. All three of the palladium carbonyl complexes demonstrated the reversible binding of carbon monoxide, with the displacement of the CO ligand increasing in ease with increasing magnitude of the C–O stretching frequency in the infrared spectrum. This observation was attributed to the more electron-poor metal centres being less able to bind the carbon monoxide *via* π -backbonding.

The synthesis of platinum methyl pincer complexes $[(\text{PCP})\text{PtMe}]$ from the parent platinum chlorides was investigated. Reactions with methylmagnesium iodide were found to result in halide exchange to produce the corresponding platinum iodide species, while the greater nucleophilicity of methyllithium resulted in nucleophilic attack at the electron-deficient $\text{P}(\text{C}_6\text{F}_5)_2$ centres. In the case of $[(\text{POCCP})\text{PtCl}]$ (**27**), this nucleophilic attack at phosphorus was observed to result in pentafluorophenyl migration to the platinum, producing a platinum pentafluorophenyl complex (**46**), amongst other byproducts. Successful methylation was achieved with the less nucleophilic dimethylzinc; however, the more electron-rich pincer complex **27** underwent methylation at a significantly slower rate than its more electron-poor counterparts **25** and **26** did.

Reaction of the PNP ligands **10** and **11** with platinum chloride starting materials revealed a large electronic influence on pincer complex formation. Whereas PNP pincer complex formation proceeded under mild conditions for the more electron-rich PNNNP ligand **10**, reactions with the more electron-poor PONOP ligand **11** did not yield any traces of the pincer species. This was likely due to the chloride dissociation required for PNP pincer formation becoming less facile for more electron-poor metal centres. The chemistry of $[(\text{PNNNP})\text{RhCl}]$ (**49**) was also investigated, as it was isoelectronic with the Group 10 PCP pincer complexes studied. Despite possessing a relatively electron-withdrawing ligand, the chemistry of **49** was dominated by facile oxidation to rhodium(III) species. Furthermore, reactions with dimethylzinc resulted in the deprotonation of an N–H group on the ligand, to form a methylzinc adduct (**51**), which was observed to be stabilised by Lewis acid-base interactions with ethers.

The catalytic activity of the electron-poor $[(\text{PCP})\text{PdCl}]$ complexes **28**, **29**, and **30** were assessed in Heck and Suzuki cross-coupling reactions. All three complexes were

found to possess only modest activity in the Heck reaction, in all cases functioning as precatalysts, which decomposed to give catalytically-active Pd(0) colloids. Under the milder reaction conditions required for the Suzuki reactions, the most electron-poor complex, [(POCOP)PdCl], **28**, was able to couple electronically-deactivated aryl bromides with a high activity *via* a homogeneous active species. This reactivity is consistent with that expected for an intact pincer species operating through a redox-free mechanism. However, the susceptibility of these electron-poor pincer species to nucleophilic attack and decomposition means that catalysis by unidentified homogeneous degradation products cannot be ruled out.

While electron-withdrawing PCP and PNP pincer ligands possessing phosphinite or phosphinamide linkers can be more readily synthesised than their more electron-donating analogues, there are significant difficulties associated with the metallation of these electron-deficient ligands. The resultant electron-poor pincer complexes are also rendered increasingly susceptible to nucleophilic attack at the phosphorus and degradation, counteracting the stability conferred to complexes by the pincer coordination motif. However, the increased barrier to ligand metallation makes such species ideally suited to investigating the coordination chemistry and metallation of pincer ligands. Furthermore, it appears that highly electron-deficient POCOP palladium complexes display reversible uptake of carbon monoxide, and enhanced activity in the Suzuki reaction over their more electron-rich counterparts.

An area of this work that may be explored in future investigations is the isolation and characterisation of the deprotonated form of the rhodium PNNNP pincer complex [(PNNNP)RhCl], **49**. Research into the behaviour of this deprotonated species in stoichiometric and catalytic reactions may reveal whether **49** is capable of the non-innocent behaviour that is prevalent in the chemistry of related PCNCP complexes. Further work into conclusively determining the nature of the active species arising from [(POCOP)PdCl], **28**, in the Suzuki reaction would also be beneficial. One way in which this may be achieved is through the comparison of the activity of **28** with that of independently synthesised potential degradation products, to determine if a degradation product is responsible for the high homogeneous catalytic activity of **28**. Moreover, characterisation of any of the *cis,trans* dimers by X-ray diffraction would be highly desirable.

Chapter 8

Experimental

8.1 General Procedures

All reactions and manipulations of products and reagents were carried out under an inert nitrogen atmosphere using standard Schlenk techniques unless otherwise stated. Dichloromethane, diethyl ether, and tetrahydrofuran were dried by heating to reflux over the appropriate drying agent (calcium hydride for dichloromethane, sodium/benzophenone ketyl for ethers) and distilled prior to use. Other solvents were degassed and purged with nitrogen before use, with most stored over the appropriate size molecular sieve.²³⁰ Methyl iodide, dibutyl ether, bromobenzene, and styrene were purified by passage through a short neutral alumina column prior to use. The compounds 3-hydroxybenzyl alcohol,⁷⁰ 3-hydroxybenzyl bromide,⁷¹ (3-hydroxybenzyl)di-*tert*-butyl phosphine,¹³ and bis(pentafluorophenyl)bromophosphine,²³¹ were synthesised using literature procedures. The transition metal precursors $[\text{PdCl}_2(\text{NCMe})_2]$,²³² $[\text{PtCl}(\text{COD})\text{N}(\text{SiMe}_3)_2]$,¹²⁴ $[\text{PtCl}_2(\text{hex})]$,²³³ $[\text{PtCl}_2(\text{SEt}_2)_2]$,¹¹⁷ $[\text{PtMe}_2(\text{hex})]$,²³⁴ and $[\text{RhCl}(\text{COD})]_2$,²³⁵ were prepared by literature methods. The platinum compounds $[\text{PtCl}_2(\text{COD})]$ ²³⁶ and $[\text{Pt}(\text{nb})_3]$ ²³⁴ were obtained from colleagues at Victoria University of Wellington, having been prepared by literature procedures.

NMR spectra were obtained using a Varian Unity Inova 300 (300 MHz for ^1H , 121 MHz for ^{31}P , and 282 MHz for ^{19}F), a Varian Unity Inova 500 (500 MHz for ^1H and 125 MHz for ^{13}C), or a Varian DirectDrive 600 (600 MHz for ^1H and 150 MHz for ^{13}C). The 600 MHz instrument was equipped with a Varian inverse-detected triple-resonance HCN cold probe operating at 25 K. All ^1H and ^{13}C resonances were referenced to the residual solvent peak. All ^{31}P and ^{19}F resonances were referenced

to H_3PO_4 and CFCl_3 respectively. NMR samples were prepared under an inert atmosphere unless otherwise stated. Infrared spectra were obtained with a PerkinElmer Spectrum One FT-IR spectrophotometer using pressed KBr discs. GCMS analysis was performed on a Shimadzu GC-2010 GCMS with a RTX-5sil stationary phase. Microanalyses were performed by the Campbell Microanalytical Laboratory at the University of Otago. Single-crystal X-ray diffraction data were obtained by the X-ray Crystallography Laboratory at the University of Canterbury. Electrospray ionisation mass spectra were performed by the GlycoSyn QC Laboratory at Industrial Research Limited using a Waters Q-TOF Premier Tandem mass spectrometer, or in-house using an Agilent 6530 Series Q-TOF mass spectrometer.

Crystallography

Diffraction data* (see appropriate tables for details) were collected using Bruker CCD diffractometers with $\text{Mo K}\alpha$ radiation (0.71073 \AA) from fine focus sealed tubes with graphite monochromators, using phi and omega scans. Multi-scan absorption corrections were applied. The structures were solved using Patterson methods, and refined using a full-matrix least squares method,[†] with anisotropic thermal motion parameters for all non-hydrogen atoms.²³⁷ Hydrogen atoms were placed in calculated positions and allowed to refine freely using a riding model. OLEX2 (Version 1.1.5)²³⁸ was used as a front-end for the SHELX executables during structure solution and refinement. All relevant bond distances and angles were calculated using MERCURY (Version 2.4.5), and molecular drawings were generated using ORTEP3 (Version 1.0.3).

8.2 Transition Metal Precursors

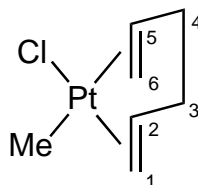
[PtClMe(hex)]

Dichloroplatinum-1,5-hexadiene (1.01 g, 2.9 mmol) was suspended in diethyl ether (20 mL). To this was added a solution of 1 mol dm^{-3} dimethylzinc in diethyl ether (3.5 mL, 3.5 mmol) portionwise with stirring over 20 min. The dark brown solution was stirred for a further 45 min, then washed with a saturated ammonium

*Bruker SMART (Version 5.054), SADABS (Version 2.03), and SAINT (Version 6.02A), Bruker AXS Inc., Madison, Wisconsin, USA, 1997.

[†]G. M. Sheldrick, SHELX-97. Programmes for the Solution and Refinement of Crystal Structures, 1997.

chloride solution (15 mL). The organic layer was decanted, and the aqueous layer was further extracted with diethyl ether (5×15 mL). The combined organic extracts were dried over magnesium sulfate, then volatiles were removed *in vacuo* carefully (as the product may sublime), giving a yellow oil that crystallised into an off-white solid ([PtMe₂(hex)]) at −15 °C. The solid was then dissolved in a 2:3 methanol/dichloromethane mixture (15 mL), and acetyl chloride (160 μL, 2.3 mmol) was added dropwise over 1 minute. The solution was stirred for a further 10 min, and the solvent was reduced to about 2 mL *in vacuo*. The product was isolated as a cream-coloured solid by crystallisation from the reaction mixture at −15 °C and washing with pentane (435 mg, 46%). The product could also be isolated as a minor impurity (typically *c.a.* 1% yield) in the synthesis of [PtMe₂(hex)] during purification by sublimation.



¹H-NMR: (500 MHz, CDCl₃) δ_H 5.52 (dd, ²J_{Pt-H} = 28.9 Hz, ³J_{H-H} = 8.4 Hz, ³J_{H-H} = 1.8 Hz, 1H, C=CH₂ H-1), 5.38 (m, 1H, C=CH H-2), 4.64 (m, ²J_{Pt-H} = 65.2 Hz, 1H, C=CH H-5), 4.37 (d, ²J_{Pt-H} = 29.4 Hz, ³J_{H-H} = 14.4 Hz, 1H, C=CH₂ H-1), 3.46 (d, ²J_{Pt-H} = 72.3 Hz, ³J_{H-H} = 7.8 Hz, 1H, C=CH₂ H-6), 3.31 (d, ²J_{Pt-H} = 71.8 Hz, ³J_{H-H} = 13.4 Hz, 1H, C=CH₂ H-6), 2.65 (m, 1H, C-CH₂ H-4), 2.54 (m, 1H, C-CH₂ H-4), 2.33 (m, 1H, C-CH₂ H-3), 1.84 (m, 1H, C-CH₂ H-3), 0.99 (s, ²J_{Pt-H} = 73.8 Hz, 3H, CH₃). ¹³C-NMR: (125 MHz, CDCl₃) δ_C 118.9 (s, 1C, C-2), 103.3 (s, 1C, C-1), 86.4 (s, ¹J_{Pt-C} = 210 Hz, 1C, C-5), 58.5 (s, ¹J_{Pt-C} = 224 Hz, 1C, C-6), 33.9 (s, ²J_{Pt-C} = 31.2 Hz, 1C, C-4), 26.7 (s, 1C, C-3), 6.4 (s, ¹J_{Pt-C} = 618 Hz, 1C, CH₃).

ZnMe₂

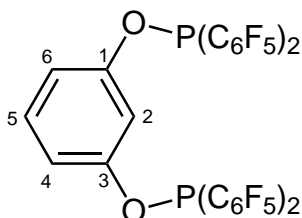
Zinc powder (13.8 g, 0.21 mol) and magnesium powder (5.4 g, 0.22 mol) were dry stirred under nitrogen for 3 hours, then suspended in dibutyl ether (90 mL). Methyl iodide (26.1 mL, 0.42 mol) was added to the stirred suspension at a rate that kept the reaction mixture around 60 °C. The suspension was then heated to 70 °C for 18 hours, after which time the product was isolated by fractional distillation from the reaction mixture, taking care as the product is extremely pyrophoric (13.9 g, 70%). Solutions of dimethylzinc in diethyl ether employed were prepared using

diethyl ether in place of dibutyl ether, distilling the dimethylzinc across with the ether. Concentrations of diethyl etheric solutions of dimethylzinc were determined by back-titration with standard 1 mol dm⁻³ hydrochloric acid. ¹H-NMR: (300 MHz, C₆D₆) δ_{H} -0.68 (br s, 6H, CH₃).

8.3 Ligands

1,3-[(C₆F₅)₂PO]₂C₆H₄ (POCOPH) (1)

Resorcinol (1.00 g, 9.1 mmol) was suspended in a solution of triethylamine (2.6 mL, 18.6 mmol) in diethyl ether (80 mL). The reaction mixture was cooled on ice and a solution of BrP(C₆F₅)₂ (4.1 mL, 18.2 mmol) in diethyl ether (10 mL) was added dropwise. Stirring was continued for 1 hour on ice, then for 18 hours at room temperature. The reaction mixture was filtered thorough celite, washing with diethyl ether (3×14 mL). The diethyl ether was removed *in vacuo*, and **1** was isolated by recrystallisation from 1:1 toluene/hexane (25 mL) at -15 °C, washing the white needles obtained with hexane (6.61 g, 87%).



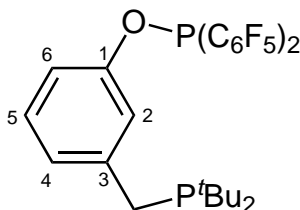
¹H-NMR: (500 MHz, CD₂Cl₂) δ_{H} 7.24 (t, ³*J*_{H-H} = 7.8 Hz, 1H, H-5), 6.86 (dd, ³*J*_{H-H} = 7.5 Hz, ⁴*J*_{H-H} = 1.6 Hz, 2H, H-4,6), 6.85 (s, 1H, H-2). ³¹P-NMR: (121 MHz, CD₂Cl₂) δ_{P} 87.1 (quint, ³*J*_{P-F} = 35.0 Hz). ¹⁹F-NMR: (282 MHz, CD₂Cl₂) δ_{F} -133.1 (m, 2F, *o*-C₆F₅), -148.6 (t, ³*J*_{F-F} = 19.7 Hz, 1F, *p*-C₆F₅), -160.6 (m, 2F, *m*-C₆F₅). ¹³C-NMR: (125 MHz, CD₂Cl₂) δ_{C} 156.5 (d, ²*J*_{P-C} = 16.3 Hz, 2C, C-1,3) 146.7 (d, ¹*J*_{F-C} = 256 Hz, 8C, *o*-C₆F₅), 143.2 (d, ¹*J*_{F-C} = nr, 4C, *p*-C₆F₅), 137.7 (d, ¹*J*_{F-C} = 255 Hz, 8C, *m*-C₆F₅), 130.8 (s, 1C, C-5), 113.6 (d, ³*J*_{P-C} = 13.4 Hz, 2C, C-4,6), 111.1 (m, 4C, *i*-C₆F₅), 109.1 (t, ³*J*_{P-C} = 10.9 Hz, 1C, C-2). Anal. Calcd for C₃₀H₄O₂F₂₀P₂: C, 42.98; H, 0.48. Found C, 42.86; H, 0.63. HRMS calcd for (C₃₀H₈NO₄F₂₀P₂) [M+2O+NH₄]⁺: *m/z* = 887.9609, found = 887.9618.

1,3-[(C₆F₅)₂PCH₂]₂C₆H₄ (PCCCPH) (**2**)

Method A: As per the method of Chase *et al.*,⁵⁷ half-scale (1.00 g, 39%). Method B: Magnesium powder (0.10 g, 4.1 mmol) in THF (24 mL) was activated by the addition of 1,2-dibromoethane (0.1 mL) followed by heating with a heat gun until rapid bubbling was observed. After bubbling had ceased, anthracene (1.4 g, 9.0 mmol) was added, and the reaction mixture was stirred at room temperature for 4 days. The supernatant was decanted and the orange solid isolated was washed with THF (4×10 mL) and dried briefly *in vacuo*. The solid [Mg(anth)(THF)₃] was resuspended in THF and a solution of dichloro-*m*-xylene (350 mg, 2.0 mmol) in THF (6 mL) was added dropwise and stirred overnight. The supernatant was isolated by decantation and cooled to -78 °C. To this cooled solution was added BrP(C₆F₅)₂ (0.84 mL, 3.68 mmol) dropwise. The reaction mixture was allowed to warm to room temperature overnight, then the volatiles were removed *in vacuo* and the remaining solid extracted with hexane (4×50 mL) and filtered through celite. Volatiles were again removed under vacuum, and chromatography on silica in air (petroleum ether eluent, R_f = 0.1) afforded **2** as a white solid (1.03 g, 67%). Spectroscopic data matched that previously reported for **2**.⁵⁷ ¹H-NMR: (300 MHz, C₆D₆) δ_H 6.93 (s, 1H, H-2), 6.67 (t, ³J_{H-H} = 7.7 Hz, 1H, H-5), 6.54 (dd, ³J_{H-H} = 8.0 Hz, ⁴J_{H-H} = 1.5 Hz, 2H, H-4,6), 3.47 (d, ²J_{P-H} = 4.0 Hz, 4H, CH₂). ³¹P-NMR: (121 MHz, C₆D₆) δ_P -46.3 (quint, ³J_{P-F} = 25.0 Hz). ¹⁹F-NMR: (282 MHz, C₆D₆) δ_F -130.5 (m, 8F, *o*-C₆F₅), -149.3 (t, ³J_{F-F} = 21.2 Hz, 4F, *p*-C₆F₅), -160.4 (m, 8F, *m*-C₆F₅).

1-[(C₆F₅)₂PO]-3-(^{*t*}Bu₂PCH₂)C₆H₄ (POCCPH) (**3**)

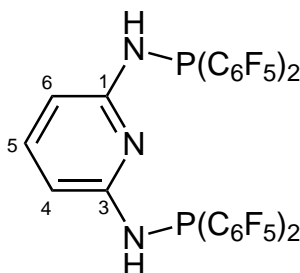
A solution of (3-hydroxybenzyl)di-*tert*-butyl phosphine (1.15 g, 4.56 mmol) and triethylamine (1.4 mL, 10 mmol) in THF (50 mL) was cooled on ice, and a solution of BrP(C₆F₅)₂ (1.04 mL, 4.56 mmol) in THF (15 mL) was added over 10 min. The solution was stirred on ice for a further 10 min, then at room temperature overnight. The reaction mixture was filtered through celite, and the filter cake washed with THF (5×15 mL). The crude material was dried *in vacuo*, and purified by extraction with hexane (3×12 mL) at -78 °C, followed by filtration through celite. Removal of hexane *in vacuo* gave **3** as a viscous, pale yellow oil (2.42 g, 86%).



^1H -NMR: (500 MHz, C_6D_6) δ_{H} 7.47 (s, 1H, H-2), 7.02 (m, 3H, H-4,5,6), 2.65 (d, $^2J_{\text{P-H}} = 2.6$ Hz, 2H, CH_2), 0.99 (d, $^3J_{\text{P-H}} = 10.8$ Hz, 18H, $\text{C}(\text{CH}_3)_3$). ^{31}P -NMR: (121 MHz, C_6D_6) δ_{P} 82.9 (quint, $^3J_{\text{P-F}} = 35.5$ Hz, 1P, $\text{P}(\text{C}_6\text{F}_5)_2$), 34.3 (s, 1P, P^tBu_2). ^{19}F -NMR: (282 MHz, C_6D_6) δ_{F} -133.2 (m, 4F, *o*- C_6F_5), -148.5 (t, $^3J_{\text{F-F}} = 21.3$ Hz, 2F, *p*- C_6F_5), -160.3 (tm, $^3J_{\text{F-F}} = 21.5$ Hz, 4F, *m*- C_6F_5). ^{13}C -NMR: (125 MHz, C_6D_6) δ_{C} 155.5 (d, $^2J_{\text{P-C}} = 15.3$ Hz, 1C, C-1), 146.6 (dm, $^1J_{\text{F-C}} = 256$ Hz, 4C, *o*- C_6F_5), 144.8 (d, $^2J_{\text{P-C}} = 13.4$ Hz, 1C, C-3), 142.8 (dm, $^1J_{\text{F-C}} = 257$ Hz, 2F, *p*- C_6F_5), 137.4 (dm, $^2J_{\text{F-C}} = 254$ Hz, 4F, *m*- C_6F_5), 129.5 (s, 1C, C-5), 125.5 (d, $^3J_{\text{P-C}} = 8.1$ Hz, 1C, C-4), 119.4 (vt, $^3J_{\text{P-C}} = 11.5$ Hz, 1C, C-2), 114.9 (d, $^3J_{\text{P-C}} = 12.5$ Hz, 1C, C-6), 110.9 (dt, $^1J_{\text{P-C}} = 44.2$ Hz, $^2J_{\text{F-C}} = 22.1$ Hz, 2C, *i*- C_6F_5), 31.3 (d, $^1J_{\text{P-C}} = 24.0$ Hz, 2C, $\text{C}(\text{CH}_3)_3$), 29.3 (d, $^2J_{\text{P-C}} = 13.4$ Hz, 6C, $\text{C}(\text{CH}_3)_3$), 28.5 (d, $^1J_{\text{P-C}} = 25.9$ Hz, 1C, CH_2). HRMS calcd for $(\text{C}_{27}\text{H}_{24}\text{OF}_{10}\text{P}_2)$ $[\text{M}+\text{H}]^+$: $m/z = 617.1215$, found = 617.1220. HRMS calcd for $(\text{C}_{15}\text{H}_{25}\text{OP})$ $[\text{M}-\text{P}(\text{C}_6\text{F}_5)_2+2\text{H}]^+$: $m/z = 253.1716$, found = 253.1756.

1,3-[(C_6F_5) $_2\text{PNH}$] $_2\text{C}_6\text{H}_3\text{N}$ (PNNNP) (**10**)

A solution of 2,6-diaminopyridine (187 mg, 1.71 mmol) and triethylamine (0.96 mL, 6.9 mmol) in THF (15 mL) was cooled on ice, and then a solution of $\text{BrP}(\text{C}_6\text{F}_5)_2$ (0.77 mL, 3.39 mmol) in THF (8 mL) was added dropwise. The reaction mixture was stirred on ice for 1 hour, then at room temperature for a further 14 hours. The reaction mixture was filtered through celite, and the filter cake washed with toluene (3×5 mL). Volatiles were removed *in vacuo*, and recrystallisation from 1:1 hexane/toluene (7 mL) at -15 °C and subsequent washing with hexane gave **10** as an off-white, microcrystalline solid (948 mg, 66%).



^1H -NMR: (500 MHz, C_6D_6) δ_{H} 7.03 (t, $^3J_{\text{H-H}} = 8.1$ Hz, 1H, H-5), 6.21 (d, $^3J_{\text{H-H}} = 8.0$ Hz, 2H, H-4,6), 5.80 (d, $^2J_{\text{P-H}} = 8.5$ Hz, 2H, NH). ^{31}P -NMR: (121 MHz, C_6D_6) δ_{P} -10.8 (quint, $^3J_{\text{P-F}} = 38.2$ Hz). ^{19}F -NMR: (282 MHz, C_6D_6) δ_{F} -134.6 (m, 8F, *o*- C_6F_5), -149.4 (t, $^3J_{\text{F-F}} = 21.2$ Hz, 4F, *p*- C_6F_5), -160.0 (tm, $^3J_{\text{F-F}} = 22.8$ Hz, 8F, *m*- C_6F_5). ^{13}C -NMR: (125 MHz, C_6D_6) δ_{C} 155.4 (d, $^2J_{\text{P-C}} = 25.5$ Hz, 2C, C-1,3),

146.8 (d, $^1J_{\text{F-C}} = 244$ Hz, 8C, *o*-C₆F₅), 142.4 (dm, $^1J_{\text{F-C}} = 257$ Hz, 4C, *p*-C₆F₅), 140.3 (s, 1C, C-5), 137.3 (dm, $^1J_{\text{F-C}} = 255$ Hz, 8C, *m*-C₆F₅), 110.3 (m, 4C, *i*-C₆F₅), 101.6 (d, $^3J_{\text{P-C}} = 11.5$ Hz, 2C, C-4,6). HRMS calcd for (C₂₉H₆N₃F₂₀P₂) [M+H]⁺: $m/z = 837.9718$, found = 837.9738.

1,3-[(C₆F₅)₂PO]₂C₆H₃N (PONOP) (11)

A solution of 2,6-dihydroxypyridine hydrochloride (250 mg, 1.69 mmol) and triethylamine (0.96 mL, 6.9 mmol) in THF (15 mL) was cooled on ice, and then a solution of BrP(C₆F₅)₂ (0.77 mL, 3.39 mmol) in THF (8 mL) was added dropwise. The reaction mixture was stirred on ice for 1 hour, then at room temperature for a further 15 hours. The reaction mixture was filtered through celite, and the filter cake washed with THF (3×5 mL). Volatiles were removed *in vacuo*, and recrystallisation from 1:1 hexane/dichloromethane (15 mL) at −15 °C and subsequent washing with hexane gave **11** as white, crystalline solid (871 mg, 61%). ¹H-NMR: (300 MHz, C₆D₆) δ_H 6.87 (t, $^3J_{\text{H-H}} = 7.9$ Hz, 1H, H-5), 6.31 (d, $^3J_{\text{H-H}} = 8.2$ Hz, 2H, H-4,6). ³¹P-NMR: (121 MHz, C₆D₆) δ_P 70.2 (quint, $^3J_{\text{P-F}} = 42.8$ Hz). ¹⁹F-NMR: (282 MHz, C₆D₆) δ_F −134.0 (m, 8F, *o*-C₆F₅), −147.8 (t, $^3J_{\text{F-F}} = 21.0$ Hz, 4F, *p*-C₆F₅), −160.0 (m, 8F, *m*-C₆F₅). ¹³C-NMR: (125 MHz, C₆D₆) δ_C 159.2 (d, $^2J_{\text{P-C}} = 9.1$ Hz, 2C, C-1,3), 146.8 (dm, $^1J_{\text{F-C}} = 247$ Hz, 8C, *o*-C₆F₅), 143.2 (s, 1C, C-5), 143.1 (dm, $^1J_{\text{F-C}} = 259$ Hz, 4C, *p*-C₆F₅), 137.5 (dm, $^1J_{\text{F-C}} = 255$ Hz, 8C, *m*-C₆F₅), 110.2 (m, 4C, *i*-C₆F₅), 105.8 (s, 2C, C-4,6). HRMS calcd for (C₂₉H₃NO₄F₂₀P₂Na) [M+2O+Na]⁺: $m/z = 893.9116$, found = 893.9142.

8.4 Platinum Complexes

[(POCOPH)Pt(nb)]₂ (14)

A solution of Pt(nb)₃ (117 mg, 0.25 mmol) and **1** (204 mg, 0.24 mmol) in dichloromethane (7 mL) was heated at 40 °C for 36 hours, at which point all volatiles were removed *in vacuo*. The oily solid was washed with ice-cold pentane, then redissolved in toluene (5 mL) and heated at 50 °C for 12 hours. The volume was reduced *in vacuo* to approximately 2 mL, with the addition of hexane to the toluene solution causing the precipitation of **14** as a white solid, which was isolated by decantation of the supernatant and washing with pentane (107 mg, 39%). Crystals suitable for single crystal X-ray diffraction were obtained by solvent diffusion at room temperature,

with methanol layered above a dichloromethane solution of **14**. ^1H -NMR: (500 MHz, CD_2Cl_2) δ_{H} 6.85 (t, $^3J_{\text{H-H}} = 8.1$ Hz, 1H, H-5), 6.69 (d, $^3J_{\text{H-H}} = 8.1$ Hz, 2H, H-4,6), 6.12 (s, 1H, H-2), 2.75 (d, $^2J_{\text{Pt-H}} = 70.8$ Hz, $^3J_{\text{H-H}} = 10.7$ Hz, 2H, nb C=CH), 2.20 (d, $^2J_{\text{H-H}} = 10.0$ Hz, 2H, nb C-CH), 1.44 (d, $^2J_{\text{H-H}} = 7.3$ Hz, 2H, nb $\text{H}_2\text{C-CH}_2$), 0.96 (d, $^2J_{\text{H-H}} = 7.6$ Hz, 2H, nb $\text{H}_2\text{C-CH}_2$), 0.42 (m, 1H, nb HC-CH₂-CH), 0.15 (d, $^2J_{\text{H-H}} = 8.5$ Hz, 1H, nb HC-CH₂-CH). ^{31}P -NMR: (121 MHz, CD_2Cl_2) δ_{P} 100.5 (s, $^1J_{\text{Pt-P}} = 4623$ Hz). ^{19}F -NMR: (282 MHz, CD_2Cl_2) δ_{F} -131.5 (m, 8F, *o*-C₆F₅), -149.3 (m, 4F, *p*-C₆F₅), -160.8 (m, 8F, *m*-C₆F₅). ^{13}C -NMR: (125 MHz, CD_2Cl_2) δ_{C} 152.5 (s, 2C, C-1,3), 145.0 (d, $^3J_{\text{F-C}} = 244$ Hz, 8C, *o*-C₆F₅), $\approx 142^\ddagger$ (d, $^3J_{\text{F-C}} = \text{nr}$, 4C, *p*-C₆F₅), 136.9 (d, $^3J_{\text{F-C}} = 249$ Hz, 8C, *m*-C₆F₅), 128.5 (s, 1C, C-5), 113.4 (s, 2C, C-4,6), 112.1 (m, 4C, *i*-C₆F₅), 111.7 (s, 1C, C-2), 65.7 (m, $^1J_{\text{Pt-C}} = 259$ Hz, 2C, nb C=CH), 42.0 (s, 2C, nb C-CH), 39.8 (s, 1C, nb HC-CH₂-CH), 27.7 (s, $^3J_{\text{Pt-C}} = 53.2$ Hz, 2C, $\text{H}_2\text{C-CH}_2$). Anal. Calcd for $\text{C}_{74}\text{H}_{28}\text{O}_4\text{F}_{40}\text{P}_4\text{Pt}_2 \cdot \text{CH}_2\text{Cl}_2$: C, 38.50; H, 1.29. Found C, 38.80; H, 1.40. HRMS calcd for $(\text{C}_{60}\text{H}_8\text{O}_4\text{F}_{40}\text{NaP}_4\text{Pt}_2) [\text{M}-2\text{nb}+\text{Na}]^+$: $m/z = 2086.7886$, found = 2086.7883.

[(POCOPH)PtMe₂]₂ (15)

A solution of ligand **1** (200 mg, 0.24 mmol) and $[\text{PtMe}_2(\text{hex})]$ (73.3 mg, 0.24 mmol) in toluene (15 mL) was stirred at room temperature for 72 hours. The solution was concentrated *in vacuo* to about 3 mL, and the oligomeric byproduct **16** precipitated out by the addition of 3 mL hexane to the solution. Decantation and isolation of the supernatant, followed by removal of the solvent *in vacuo* and washing with hexane afforded **15** as a yellow, microcrystalline solid (199 mg, 78%). ^1H -NMR: (300 MHz, CD_2Cl_2) δ_{H} 7.05 (t, $^3J_{\text{H-H}} = 8.3$ Hz, 2H, H-5), 6.82 (d, $^3J_{\text{H-H}} = \text{H-4,6 Hz}$, 4H, H-4,6), 6.42 (s, 2H, H-2), 0.21 (vt, $^2J_{\text{Pt-H}} = 71.0$ Hz, $^3J_{\text{P-H}} = \text{nr}$, 12H, CH₃). ^{31}P -NMR: (121 MHz, CDCl_3) δ_{P} 89.9 (s, $^1J_{\text{Pt-P}} = 2202$ Hz). ^{19}F -NMR: (282 MHz, CDCl_3) δ_{F} -129.4 (br s, 16F, *o*-C₆F₅), -145.7 (br s, 8F, *p*-C₆F₅), -159.1 (br s, 18F, *m*-C₆F₅). ^{13}C -NMR: (125 MHz, CD_2Cl_2) δ_{C} 153.4 (s, 4C, C-1,3), 146.4 (dm, $^1J_{\text{P-F}} = 259$ Hz, 16C, *o*-C₆F₅), 143.7 (dm, $^1J_{\text{P-F}} = 262$ Hz, 8C, *p*-C₆F₅), 137.6 (dm, $^1J_{\text{P-F}} = 259$ Hz, 16C, *m*-C₆F₅), 129.3 (s, 2C, C-5), 116.5 (s, 4C, C-4,6), 112.4 (s, 2C, C-2), 108.8 (m, 8C, *i*-C₆F₅), 1.7 (dd, $^2J_{\text{P-C}} = 116$ Hz, 4C, CH₃). HRMS calcd for $(\text{C}_{64}\text{H}_{20}\text{O}_4\text{F}_{40}\text{NaP}_4\text{Pt}_2) [\text{M}+\text{Na}]^+$: $m/z = 2146.8825$, found = 2146.8855.

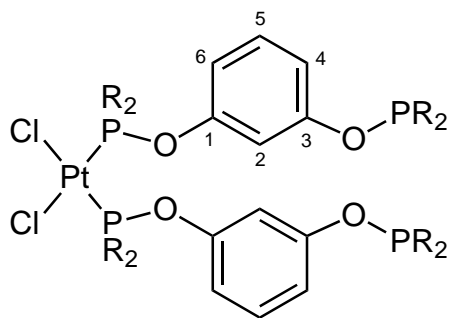
[‡]The chemical shift δ_{C} and coupling constants for the *p*-C₆F₅ carbon environment could not be determined due to peak overlap with the adjacent *o*-C₆F₅ environment.

[(POCOPH)PtMe₂]_x (16)

The oligomeric species **16** could be isolated as a byproduct during the synthesis of the dimer **15** as above, with shorter reaction times in dichloromethane were observed to increase the yield of **16**. A solution of ligand **1** (50 mg, 60 μ mol) and [PtMe₂(hex)] (18.5 mg, 60 μ mol) in dichloromethane (5 mL) was stirred at room temperature for 24 hours. The solvent was reduced to about 0.5 mL *in vacuo*, and precipitation of the product with hexane followed by decantation of the supernatant and washing of the precipitate *in situ* with pentane afforded **16** as a white solid (48 mg, 76%). Samples of **16** were found to be contaminated with small quantities of the dimer **15**. ¹H-NMR: (300 MHz, CD₂Cl₂) δ_{H} 7.14 (t, ³J_{H-H} = 8.2 Hz, 1H, H-5), 6.94 (s, 1H, H-2), 6.77 (d, ³J_{H-H} = H-4,6 Hz, 2H, H-4,6), 0.42 (dd, ²J_{Pt-H} = 70.6 Hz, ³J_{P-H} = 3.0 Hz, nr, 6H, CH₃). ³¹P-NMR: (121 MHz, CD₂Cl₂) δ_{P} 90.9 (s, ¹J_{Pt-P} = 2150 Hz). ¹⁹F-NMR: (282 MHz, CD₂Cl₂) δ_{F} -129.0 (dm, ³J_{P-F} = 16.4 Hz, 8F, *o*-C₆F₅), -146.5 (tm, ³J_{F-F} = 20.8 Hz, 4F, *m*-C₆F₅), -159.7 (m, 8F, *p*-C₆F₅). ¹³C-NMR: (125 MHz, CD₂Cl₂) δ_{C} 153.4 (s, 4C, C-1,3), 146.4 (dm, ¹J_{P-F} = 259 Hz, 8C, *o*-C₆F₅), 143.7 (dm, ¹J_{P-F} = 262 Hz, 4C, *p*-C₆F₅), 137.6 (dm, ¹J_{P-F} = 259 Hz, 8C, *m*-C₆F₅), 129.9 (s, 1C, C-5), 115.8 (s, 2C, C-4,6), 112.3 (s, 1C, C-2), 108.8 (m, 4C, *i*-C₆F₅), 4.0 (dd, ²J_{P-C} = 115 Hz, 2C, CH₃).

Observation of *cis*-(κ^1 -POCOPH)₂PtCl₂] (18)

Ligand **1** (30 mg, 36 μ mol) and [PtCl₂(hex)] (12.5 mg, 36 μ mol) were dissolved in benzene-*d*₆ in an NMR tube, and the course of the reaction monitored by NMR spectroscopy. After two hours at room temperature, NMR spectroscopy revealed the formation of **18** along with the presence of unreacted starting material. Heating of the reaction mixture to 60 °C for two minutes to encourage dissolution of the [PtCl₂(hex)] resulted instead in the formation of significant quantities of the dimer **19**. As such, compound **18** was not isolated for further analysis.

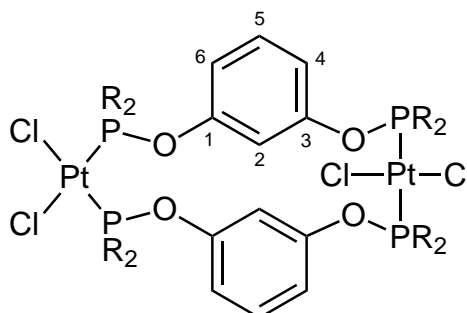


where R = C₆F₅

^1H -NMR: (300 MHz, C_6D_6) δ_{H} 6.91 (s, 2H, H-2), 6.79 (d, $^3J_{\text{H-H}} = 7.9$ Hz, 2H, H-6), 6.73 (vt, $^3J_{\text{H-H}} = 8.2$ Hz, 2H, H-5), 6.57 (d, $^3J_{\text{H-H}} = 7.7$ Hz, 2H, H-4). ^{31}P -NMR: (121 MHz, C_6D_6) δ_{P} 85.4 (quint, $^3J_{\text{P-F}} = 36.8$ Hz, 2P, $\text{P}(\text{C}_6\text{F}_5)_2$), 51.4 (s, $^1J_{\text{Pt-P}} = 4531$ Hz, 2P, P-*trans*-Cl). ^{19}F -NMR: (282 MHz, C_6D_6) δ_{F} -127.5—-130.7 (br m, 16F, *o*- C_6F_5), -151.4—-153.3 (br m, 8F, *p*- C_6F_5), -158.9—-160.0 (br m, 16F, *m*- C_6F_5).

***cis,trans*-[(POCOPH)PtCl₂]₂ (**19**)**

A solution of ligand **1** (30 mg, 36 μmol) and $[\text{PtCl}_2(\text{hex})]$ (12.5 mg, 36 μmol) in benzene- d_6 was heated to 90 °C for three minutes (to ensure dissolution of starting material), then left standing at room temperature for 12 hours. The reaction mixture was heated for a further 80 minutes at 90 °C, at which point NMR spectroscopy revealed almost quantitative formation of **19**. Removal of the volatiles *in vacuo* and repeated washing with hexane afforded the product **19** as a cream-coloured solid (8 mg, 20%).

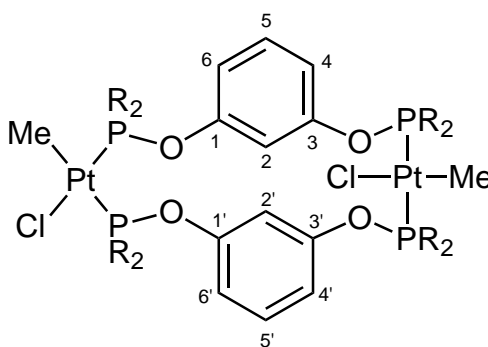


where $\text{R} = \text{C}_6\text{F}_5$

^1H -NMR: (300 MHz, C_6D_6) δ_{H} 7.38 (s, 2H, H-2), 6.68 (d, 2H, H-6), 6.61 (t, 2H, H-5), 6.53 (d, 2H, H-4). ^{31}P -NMR: (121 MHz, C_6D_6) δ_{P} 80.6 (s, $^1J_{\text{Pt-P}} = 3357$ Hz, 2P, P-*trans*-P), 55.5 (s, $^1J_{\text{Pt-P}} = 4582$ Hz, 2P, P-*trans*-Cl). ^{19}F -NMR: (282 MHz, C_6D_6) δ_{F} -126.9—-130.5 (br m, 16F, *o*- C_6F_5), -141.0—-142.3 (br m, 8F, *p*- C_6F_5), -158.2—-158.6 (br m, 16F, *m*- C_6F_5). HRMS calcd for $(\text{C}_{60}\text{H}_8\text{O}_4\text{F}_{40}\text{NaCl}_4\text{P}_4\text{Pt}_2)$ $[\text{M}+\text{Na}]^+$: $m/z = 2230.6665$, found = 2230.6653. Samples of **19** were contaminated with small amounts of **18**, preventing satisfactory elemental analysis data from being obtained.

cis,trans-[(POCOPH)PtClMe]₂ (**21**)

A solution of [PtClMe(hex)] (101 mg, 0.30 mmol) and ligand **1** (249 mg, 0.31 mmol) in toluene (5 mL) was heated at 40 °C for 24 hours, then stirred at room temperature for a further 8 hours. The solution was filtered through a short column of alumina in air, washing the column with toluene (3×2 mL). Volatiles were removed *in vacuo*, and the white solid redissolved in a 1:1 toluene/hexane solution, purifying the product by precipitation of byproducts from solution at −15 °C. The supernatant was decanted and collected, and removal of the volatiles *in vacuo* followed by washing with pentane gave **21** as a white, microcrystalline solid (65 mg, 20%).



where R = C₆F₅

¹H-NMR: (600 MHz, C₆D₆) δ_H 7.54 (s, 1H, H-2), 7.34 (s, 1H, H-2'), 6.68 (d, ³J_{H-H} = 7.9 Hz, 1H, H-6), 6.62 (m, 3H, H-5,5',6'), 6.55 (d, ³J_{H-H} = 8.2 Hz, 1H, H-4), 6.53 (d, ³J_{H-H} = 7.0 Hz, 1H, H-4'), 1.27 (br m, 3H, CH₃-*trans*-P), 0.26 (br t, ³J_{P-H} = 6.6 Hz, 3H, CH₃-*trans*-Cl). ³¹P-NMR: (121 MHz, C₆D₆) δ_P 94.4 (d, ²J_{P-P} 15.4, ¹J_{Pt-P} = 2066 Hz, 1P, P-*trans*-CH₃), 90.3 (s, ¹J_{Pt-P} = 4028 Hz, 2P, P-*trans*-P), 62.1 (d, ²J_{P-P} 15.4, ¹J_{Pt-P} = 5494 Hz, 1P, P-*trans*-Cl). ¹⁹F-NMR: (282 MHz, C₆D₆) δ_F −127.6—−129.5 (m, 16F, *o*-C₆F₅), −142.7—−144.0 (m, 8F, *p*-C₆F₅), −158.2—−159.6 (m, 16F, *m*-C₆F₅). ¹³C-NMR: (150 MHz, C₆D₆) δ_C 153.9 (d, ²J_{P-C} = nr, 1C, C-1'), 153.8 (d, ²J_{P-C} = 13.8 Hz, 2C, C-3,3'), 153.1 (d, ²J_{P-C} = 17.9 Hz, 1C, C-1), 148.2–144.3 (br m, 24C, *o,p*-C₆F₅), 138.4 (br d, ¹J_{F-C} = 255 Hz, 16C, *m*-C₆F₅), 130.4 (s, 1C, C-5'), 130.3 (s, 1C, C-5), 118.5 (s, 1C, C-4), 118.3 (s, 1C, C-4'), 116.5 (s, 1C, C-6'), 116.2 (s, 1C, C-6), 114.5 (s, 1C, C-2), 114.3 (s, 1C, C-2'), 108.2–105.8 (br m, 8C, *i*-C₆F₅), 5.9 (br d, ²J_{P-C} = 116 Hz, 1C, CH₃-*trans*-P), −18.3 (br s, 1C, CH₃-*trans*-Cl). HRMS calcd for (C₆₄H₁₇NO₄F₄₀P₄ClPt₂) [M−Cl+NcMe]⁺: *m/z* = 2170.8430, found = 2170.8496. Accurate elemental analysis data was not able to be obtained for **21**.

[(POCOP)PtCl] (**25**)

A solution of [PtClMe(hex)] (79 mg, 0.24 mmol) and **1** (203 mg, 0.24 mmol) in toluene (6 mL) was heated at reflux for 48 hours. All volatiles were then removed *in vacuo* and the oily yellow residue was triturated with hexane to give the crude material as a pale yellow solid. Precipitation of [(POCOPH)PtClMe]_x species from a solution of 2:1 hexane/toluene at $-15\text{ }^{\circ}\text{C}$, followed by removal of volatiles *in vacuo* and washing with pentane at $-78\text{ }^{\circ}\text{C}$ gave **25** as a pale yellow solid (121 mg, 47%). ¹H-NMR: (300 MHz, C₆D₆) δ_{H} 6.87 (t, ³*J*_{H-H} = 8.0 Hz, 1H, H-5), 6.79 (d, ³*J*_{H-H} = 7.8 Hz, 2H, H-4,6). ³¹P-NMR: (121 MHz, C₆D₆) δ_{P} 107.8 (s, ¹*J*_{Pt-P} = 3663 Hz). ¹⁹F-NMR: (282 MHz, C₆D₆) δ_{F} -128.4 (dm, ³*J*_{P-F} = 22.2 Hz, 8F, *o*-C₆F₅), -141.8 (tt, ³*J*_{F-F} = 20.0 Hz, ⁵*J*_{F-F} = 6.8 Hz, 4F, *p*-C₆F₅), -157.6 (m, 8F, *m*-C₆F₅). ¹³C-NMR: (125 MHz, C₆D₆) δ_{C} 161.2 (s, 2C, C-1,3), 146.6 (dm, ¹*J*_{F-C} = 256 Hz, 8C, *o*-C₆F₅), 144.6 (dm, ¹*J*_{F-C} = 264 Hz, 4C, *p*-C₆F₅), 137.7 (dm, ¹*J*_{F-C} = 257 Hz, 8C, *m*-C₆F₅), 129.5 (s, 1C, C-5), 123.7 (s, 1C, C-2), 108.2 (t, ³*J*_{PC} = 7.5 Hz, 2C, C-4,6), 102.5 (m, 4C, *i*-C₆F₅). Anal. Calcd for C₃₀H₃O₂F₂₀P₂ClPt · CH₂Cl₂: C, 32.30; H, 0.44. Found C, 32.45; H, 0.55. HRMS calcd for (C₃₀H₃O₂F₂₀NaP₂ClPt) [M+Na]⁺: *m/z* = 1088.8502, found = 1088.8513.

[(PCCCP)PtCl] (**26**)

A solution of [PtClMe(hex)] (82 mg, 0.25 mmol) and **2** (206 mg, 0.25 mmol) in toluene (5 mL) was heated at 100 $^{\circ}\text{C}$ for 18 hours. All volatiles were then removed *in vacuo* and the oily yellow residue was triturated with hexane to give a cream-coloured solid, which was washed with pentane to afford **26** as an off-white solid (252 mg, 96%). ¹H-NMR: (500 MHz, CDCl₃) δ_{H} 7.11 (m, 3H, H-4,5,6), 4.26 (vt, ³*J*_{Pt-H} = 29.8 Hz, ²*J*_{P-H} = 4.5 Hz, 4H, CH₂). ³¹P-NMR: (121 MHz, CDCl₃) δ_{P} 11.5 (s, ¹*J*_{Pt-P} = 3379 Hz). ¹⁹F-NMR: (282 MHz, CDCl₃) δ_{F} -126.7 (m, 8F, *o*-C₆F₅), -144.6 (t, ³*J*_{F-F} = 20.7 Hz, 4F, *p*-C₆F₅), -157.9 (m, 8F, *m*-C₆F₅). ¹³C-NMR: (125 MHz, CDCl₃) δ_{C} 147.2 (dm, ¹*J*_{F-C} = 255 Hz, 8C, *o*-C₆F₅), 144.1 (dm, ¹*J*_{F-C} = 262 Hz, 4C, *p*-C₆F₅), 144.0 (s, ¹*J*_{Pt-C} = 875 Hz, 1C, C-2), 143.6 (t, ²*J*_{P-C} = 9.4 Hz, 2C, C-1,3), 138.0 (dm, ¹*J*_{F-C} = 258 Hz, 8C, *m*-C₆F₅), 126.6 (s, 1C, C-5), 123.8 (t, ³*J*_{P-C} = 11.0 Hz, 2C, C-4,6), 103.0 (m, 4C, *i*-C₆F₅), 43.4 (t, ¹*J*_{P-C} = 17.8 Hz, 2C, CH₂). Anal. Calcd for C₃₂H₇F₂₀P₂ClPt: C, 36.13; H, 0.66. Found C, 36.13; H, 0.88. HRMS calcd for (C₃₄H₁₀NF₂₀P₂Pt) [M-Cl+CH₃CN]⁺: *m/z* = 1063.9568, found = 1063.9564.

[(POCCP)PtCl] (27)

A solution of $[\text{PtCl}_2(\text{SEt}_2)_2]$ (191 mg, 0.43 mmol) and **3** (265 mg, 0.24 mmol) in toluene (15 mL) was heated at reflux for 64 hours. Removal of volatiles *in vacuo* gave a oily yellow residue, which was purified by recrystallisation from 3:1 hexane/dichloromethane at $-15\text{ }^\circ\text{C}$ followed by washing with hexane, yielding **27** as a yellow microcrystalline solid (181 mg, 50%). $^1\text{H-NMR}$: (500 MHz, CDCl_3) δ_{H} 7.04 (vt, $^3J_{\text{H-H}} = 7.6\text{ Hz}$, 1H, H-5), 6.95 (d, $^3J_{\text{H-H}} = 7.3\text{ Hz}$, 1H, H-4), 6.76 (d, $^4J_{\text{Pt-H}} = 16.7\text{ Hz}$, $^3J_{\text{H-H}} = 7.9\text{ Hz}$, 1H, H-6), 3.42 (d, $^3J_{\text{Pt-H}} = 22.8\text{ Hz}$, $^2J_{\text{P-H}} = 10.3\text{ Hz}$, 2H, CH_2), 1.45 (d, $^3J_{\text{P-H}} = 14.3\text{ Hz}$, 18H, $\text{C}(\text{CH}_3)_3$). $^{31}\text{P-NMR}$: (121 MHz, CDCl_3) δ_{P} 107.8 (d, $^1J_{\text{Pt-P}} = 3294\text{ Hz}$, $^2J_{\text{P-P}} = 469\text{ Hz}$, 1P, $\text{P}(\text{C}_6\text{F}_5)_2$), 72.1 (d, $^1J_{\text{Pt-P}} = 3088\text{ Hz}$, $^2J_{\text{P-P}} = 468\text{ Hz}$, 1P, P^tBu_2). $^{19}\text{F-NMR}$: (282 MHz, CDCl_3) δ_{F} -128.1 (m, 4F, *o*- C_6F_5), -144.6 (tm, $^3J_{\text{F-F}} = 20.7\text{ Hz}$, 2F, *p*- C_6F_5), -158.4 (m, 4F, *m*- C_6F_5). $^{13}\text{C-NMR}$: (125 MHz, CDCl_3) δ_{C} 161.5 (dd, $^2J_{\text{P-C}} = 15.4\text{ Hz}$, $^3J_{\text{P-C}} = 3.9\text{ Hz}$, 1C, C-1), 149.1 (dd, $^2J_{\text{Pt-C}} = 77.8\text{ Hz}$, $^2J_{\text{P-C}} = 10.4\text{ Hz}$, $^3J_{\text{P-C}} = 5.1\text{ Hz}$, 1C, C-3), 146.7 (dm, $^1J_{\text{F-C}} = 257\text{ Hz}$, 4C, *o*- C_6F_5), 144.4 (dm, $^1J_{\text{F-C}} = 262\text{ Hz}$, 2C, *p*- C_6F_5), 137.9 (dm, $^1J_{\text{F-C}} = 252\text{ Hz}$, 4C, *m*- C_6F_5), 133.8 (s, $^1J_{\text{Pt-C}} = 453\text{ Hz}$, 1C, C-2), 126.6 (s, 1C, C-5), 119.6 (d, $^3J_{\text{Pt-C}} = 39.4\text{ Hz}$, $^3J_{\text{P-C}} = 16.3\text{ Hz}$, 1C, C-4), 110.4 (d, $^3J_{\text{P-C}} = 16.8\text{ Hz}$, $^3J_{\text{Pt-C}} = 15.4\text{ Hz}$, 1C, C-6), 107.8 (m, 2C, *i*- C_6F_5), 36.3 (dd, $^2J_{\text{Pt-C}} = 24.0\text{ Hz}$, $^1J_{\text{P-C}} = 20.0\text{ Hz}$, $^3J_{\text{P-C}} = 5.1\text{ Hz}$, 2C, $\text{C}(\text{CH}_3)_3$), 34.8 (dd, $^2J_{\text{Pt-C}} = 102\text{ Hz}$, $^1J_{\text{P-C}} = 29.8\text{ Hz}$, $^3J_{\text{P-C}} = 2.4\text{ Hz}$, 1C, CH_2), 29.1 (s, 6C, $\text{C}(\text{CH}_3)_3$). HRMS calcd for $(\text{C}_{27}\text{H}_{27}\text{NOF}_{10}\text{P}_2\text{ClPt}) [\text{M}+\text{NH}_4]^+$: $m/z = 864.0737$, found = 864.0720. HRMS calcd for $(\text{C}_{23}\text{H}_{27}\text{NO}_2\text{F}_5\text{P}_2\text{Pt}) [\text{M}-\text{Cl}-\text{C}_6\text{F}_5+\text{OH}+\text{NCMe}]^+$: $m/z = 701.1036$, found = 701.1031.

[(POCOP)PtMe] (43)

A solution of **25** (79 mg, 74 μmol) in toluene (5 mL) was cooled to $-78\text{ }^\circ\text{C}$ and treated with a 1.5 mol dm^{-3} dimethylzinc solution in toluene (60 μL , 90 μmol). The reaction mixture was then stirred at room temperature for five hours, at which point all volatiles were removed *in vacuo*. The resultant yellow oil was repeatedly extracted with a 1:1 mixture of hexane and toluene, with the extracts filtered through celite and collected. Removal of all volatiles *in vacuo* and washing with hexane at $-15\text{ }^\circ\text{C}$ afforded compound **43** as a white solid (58.6 mg, 76%). $^1\text{H-NMR}$: (600 MHz, C_6D_6) δ_{H} 7.05 (m, 3H, H-4,5,6). 1.34 (br vt, $^2J_{\text{Pt-H}} = 57.4\text{ Hz}$, $^2J_{\text{P-H}} = \text{nr}$, 3H, CH_3). $^{31}\text{P-NMR}$: (121 MHz, C_6D_6) δ_{P} 108.5 (s, $^1J_{\text{Pt-P}} = 3752\text{ Hz}$). $^{19}\text{F-NMR}$: (282 MHz, C_6D_6) δ_{F} -130.3 (m, 8F, *o*- C_6F_5), -144.0 (tt, $^3J_{\text{P-F}} = 21.6\text{ Hz}$, $^5J_{\text{P-F}} = \text{nr}$, 4F, *p*- C_6F_5), -158.3 (m, 8F, *m*- C_6F_5). $^{13}\text{C-NMR}$: (125 MHz, C_6D_6) δ_{C} 160.4 (vt, $^2J_{\text{P-C}} = 8.2\text{ Hz}$, 2C, C-1,3), 146.6 (d, $^1J_{\text{F-C}} = 253\text{ Hz}$, 8C, *o*- C_6F_5), 144.2 (d, $^1J_{\text{F-C}} =$

262 Hz, 4C, *p*-C₆F₅), 138.1 (d, ¹*J*_{F-C} = 256 Hz, 8C, *m*-C₆F₅), 129.5 (s, 1C, C-5), 107.7 (vt, ³*J*_{P-C} = 7.5 Hz, 2C, C-4,6), 107.4 (m, 4C, *i*-C₆F₅), -15.1 (s, ¹*J*_{Pt-C} = 522 Hz, 1C, CH₃). The signal for C-2 could not be conclusively assigned due to overlap with other resonances, but appears to be at 141.9 ppm. HRMS calcd for (C₃₄H₁₀NF₂₀P₂Pt) [M-CH₃+CH₃CN]⁺: *m/z* = 1072.9154, found = 1072.9200.

[(PCCCP)PtMe] (44)

A solution of **26** (102 mg, 96 μmol) in toluene (5 mL) was cooled to -78 °C and treated with a 1.5 mol dm⁻³ dimethylzinc solution in toluene (80 μL, 120 μmol). The reaction mixture was then stirred at room temperature for two hours, at which point all volatiles were removed *in vacuo*. The resultant pale yellow residue was repeatedly extracted with a 1:1 mixture of hexane and toluene, with the extracts filtered through celite and collected. Removal of all volatiles *in vacuo* gave a pale yellow oil that was triturated with hexane to give compound **44** as a white solid, which was subsequently washed with hexane (87.3 mg, 87%). ¹H-NMR: (500 MHz, C₆D₆) δ_H 7.26 (br s, 3H, H-4,5,6), 4.20 (vt, ³*J*_{Pt-H} = 28.5 Hz, ²*J*_{P-H} = 4.5 Hz, 4H, CH₂), 1.02 (br vt, ²*J*_{Pt-H} = 55.8 Hz, ²*J*_{P-H} = nr, 3H, CH₃). ³¹P-NMR: (121 MHz, C₆D₆) δ_P 9.6 (s, ¹*J*_{Pt-P} = 3496 Hz). ¹⁹F-NMR: (282 MHz, C₆D₆) δ_F -129.2 (m, 8F, *o*-C₆F₅), -146.2 (t, ³*J*_{F-F} = 21.8 Hz, 4F, *p*-C₆F₅), -158.9 (m, 8F, *m*-C₆F₅). ¹³C-NMR: (150 MHz, C₆D₆) δ_C 172.0 (s, ¹*J*_{Pt-C} = 510 Hz, 1C, C-2), 146.6 (dm, ¹*J*_{F-C} = 252 Hz, 8C, *o*-C₆F₅), 144.8 (t, ²*J*_{Pt-C} = 64 Hz, ²*J*_{P-C} = 9.5 Hz, 2C, C-1,3), 142.9 (dm, ¹*J*_{F-C} = 260 Hz, 4C, *p*-C₆F₅), 137.6 (dm, ¹*J*_{F-C} = 255 Hz, 8C, *m*-C₆F₅), 125.8 (s, 1C, C-5), 122.1 (t, ³*J*_{P-C} = 10.7 Hz, 2C, C-4,6), 104.5 (m, 4C, *i*-C₆F₅), 48.8 (t, ¹*J*_{P-C} = 20.0 Hz, 2C, CH₂), -12.3 (s, ¹*J*_{Pt-C} = 470 Hz, 1C, CH₃). Anal. Calcd for C₃₃H₁₀F₂₀P₂Pt: C, 37.99; H, 0.97. Found C, 38.06; H, 1.02. HRMS calcd for (C₃₄H₁₀NF₂₀P₂Pt) [M-CH₃+CH₃CN]⁺: *m/z* = 1068.9615, found = 1068.9629.

[(POCCP)PtMe] (45)

A solution of complex **45** (82.0 mg, 97 μmol) in toluene (4 mL) was cooled to -78 °C, and 1.6 mol dm⁻³ dimethylzinc solution in toluene (440 μL, 0.71 mmol) was added, with the reaction mixture left stirring in the cold bath to gradually warm to room temperature over the course of 10 hours. The reaction was stirred at room temperature for a further 44 hours, at which point all volatiles were removed *in vacuo*. The residue was extracted with 1:1 hexane/toluene (4 × 2 mL), with the extracts combined, filtered through celite and taken to dryness under vacuum. The yellow oil was triturated then washed with pentane at -20 °C, giving compound **45**

as a white solid (50.4 mg, 63%). $^1\text{H-NMR}$: (600 MHz, C_6D_6) δ_{H} 7.04 (vt, $^3J_{\text{H-H}} = 7.5$ Hz, 1H, H-5), 7.01 (d, $^3J_{\text{H-H}} = 7.7$ Hz, 1H, H-4), 6.81 (d, $^3J_{\text{H-H}} = 7.6$ Hz, 1H, H-6), 3.65 (d, $^3J_{\text{Pt-H}} = 20.0$ Hz, $^2J_{\text{P-H}} = 9.7$ Hz, 2H, CH_2), 1.33 (d, $^3J_{\text{P-H}} = 13.8$ Hz, 18H, $\text{C}(\text{CH}_3)_3$), 0.53 (d, $^2J_{\text{Pt-H}} = 57.1$ Hz, $^3J_{\text{P-H}} = 7.6$ Hz, 3H, Pt-CH_3). $^{31}\text{P-NMR}$: (121 MHz, C_6D_6) δ_{P} 108.7 (d, $^1J_{\text{Pt-P}} = 3464$ Hz, $^2J_{\text{P-P}} = 489$ Hz, 1P, $\text{P}(\text{C}_6\text{F}_5)_2$), 70.2 (d, $^1J_{\text{Pt-P}} = 3102$ Hz, $^2J_{\text{P-P}} = 489$ Hz, 1P, P^tBu_2). $^{19}\text{F-NMR}$: (282 MHz, C_6D_6) δ_{F} -130.9 (m, 4F, *o*- C_6F_5), -146.7 (tm, $^3J_{\text{F-F}} = 20.7$ Hz, 2F, *p*- C_6F_5), -159.6 (m, 4F, *m*- C_6F_5). $^{13}\text{C-NMR}$: (150 MHz, C_6D_6) δ_{C} 160.6 (dd, $^2J_{\text{P-C}} = 14.3$ Hz, $^3J_{\text{P-C}} = 4.8$ Hz, 1C, C-1), 158.3 (s, $^1J_{\text{Pt-C}} = 509$ Hz, 1C, C-2), 149.8 (dd, $^2J_{\text{Pt-C}} = 40.3$ Hz, $^2J_{\text{P-C}} = 9.5$ Hz, $^3J_{\text{P-C}} = 5.1$ Hz, 1C, C-3), 146.6 (dm, $^1J_{\text{F-C}} = 253$ Hz, 4C, *o*- C_6F_5), 143.9 (dm, $^1J_{\text{F-C}} = 259$ Hz, 2C, *p*- C_6F_5), 138.2 (dm, $^1J_{\text{F-C}} = 248$ Hz, 4C, *m*- C_6F_5), 125.9 (s, 1C, C-5), 120.0 (d, $^3J_{\text{Pt-C}} = 17.6$ Hz, $^3J_{\text{P-C}} = 16.1$ Hz, 1C, C-4), 109.8 (m, 2C, *i*- C_6F_5), 108.9 (d, $^3J_{\text{P-C}} = 16.9$ Hz, 1C, C-6), 40.5 (dd, $^2J_{\text{Pt-C}} = 41.0$ Hz, $^1J_{\text{P-C}} = 19.9$ Hz, $^3J_{\text{P-C}} = 5.2$ Hz, 1C, CH_2), 36.2 (d, $^2J_{\text{Pt-C}} = 47.6$ Hz, $^1J_{\text{P-C}} = 33.1$ Hz, 2C, $\text{C}(\text{CH}_3)_3$), 29.3 (s, 6C, $\text{C}(\text{CH}_3)_3$), -16.5 (s, $^1J_{\text{Pt-C}} = 492$ Hz, 1C, Pt-CH_3). HRMS calcd for $(\text{C}_{29}\text{H}_{26}\text{NOF}_{10}\text{P}_2\text{Pt}) [\text{M-Me+MeCN}]^+$: $m/z = 850.0957$, found = 850.0993. HRMS calcd for $(\text{C}_{24}\text{H}_{29}\text{NOF}_5\text{P}_2\text{Pt}) [\text{M-C}_6\text{F}_5+\text{MeCN}]^+$: $m/z = 698.1271$, found = 698.1274.

Reaction of **25** with MeMgI: Formation of [(POCOP)PtI] (**41**)

To a solution of **25** (95.0 mg, 94 μmol) in diethyl ether (5 mL) was added a 0.5 mol dm^{-3} solution of MeMgI in diethyl ether (0.2 mL, 100 μmol). The solution was stirred at room temperature for 4 hours, at which point all volatiles were removed *in vacuo*. The solid was extracted with 1:1 toluene/hexane, with the extracts filtered through celite under ambient conditions. Removal of the solvent under reduced pressure gave a yellow oil, which was dissolved in dichloromethane and purified by passage through a short alumina column. The dichloromethane was subsequently removed *in vacuo*, with recrystallisation of the residue from an acetone/hexane mixture yielded **41** as a yellow solid (43.2 mg, 42%). $^1\text{H-NMR}$: (500 MHz, C_6D_6) δ_{H} 6.96 (t, $^3J_{\text{H-H}} = 8.0$ Hz, 1H, H-5), 6.85 (d, $^3J_{\text{H-H}} = 8.1$ Hz, 2H, H-4,6). $^{31}\text{P-NMR}$: (121 MHz, C_6D_6) δ_{P} 109.2 (s, $^1J_{\text{Pt-P}} = 3541$ Hz). $^{19}\text{F-NMR}$: (282 MHz, C_6D_6) δ_{F} -125.9 (m, 8F, *o*- C_6F_5), -142.1 (tm, $^3J_{\text{F-F}} = 20.9$ Hz, 4F, *p*- C_6F_5), -157.1 (m, 4F, *m*- C_6F_5). $^{13}\text{C-NMR}$: (125 MHz, C_6D_6) δ_{C} 160.6 (vt, $^2J_{\text{P-C}} =$ Hz, 2C, C-1,3), 146.4 (dm, $^1J_{\text{F-C}} = 259$ Hz, 8C, *o*- C_6F_5), ~ 144 (d, $^3J_{\text{F-C}} \approx 260$ Hz, 4C, *p*- C_6F_5), 137.7 (dm, $^1J_{\text{F-C}} = 257$ Hz, 8C, *m*- C_6F_5), 130.4 (s, 1C, C-2), 129.5 (s, 1C, C-5), 108.0 (t, $^3J_{\text{PC}} = 7.6$ Hz, 2C, C-4,6), 105.1 (m, 4C, *i*- C_6F_5). Exact chemical shift and coupling constants for the *p*- C_6F_5 environment could not be determined due to peak overlap with the adjacent *o*- C_6F_5 environment. Analysis

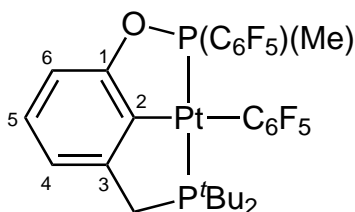
of **41** by HRMS was not able to confirm the presence of a Pt–I moiety.

Reaction of **27** with MeMgI: Formation of [(POCCP)PtI] (**42**)

To a solution of **27** (15.6 mg, 18 μ mol) in diethyl ether (0.5 mL) was added a 0.5 mol dm^{−3} solution of MeMgI in diethyl ether (50 μ L, 25 μ mol). After 14 hours at room temperature all volatiles were removed *in vacuo*, and the product was repeatedly extracted into toluene. Removal of the toluene under vacuum and followed by washing of the residue with hexane at −15 °C gave **42** as a red-brown solid (9.2 mg, 53%). ¹H-NMR: (500 MHz, C₆D₆) δ_{H} 7.04 (m, 2H, H-4,5), 6.85 (d, ³*J*_{H-H} = 6.8 Hz, 1H, H-6), 3.07 (d, ³*J*_{Pt-H} = 23.7 Hz, ²*J*_{P-H} = 9.7 Hz, 2H, CH₂), 1.22 (d, ³*J*_{P-H} = 14.1 Hz, 18H, C(CH₃)₃). ³¹P-NMR: (121 MHz, C₆D₆) δ_{P} 108.6 (d, ¹*J*_{Pt-P} = 3184 Hz, ²*J*_{P-P} = 468 Hz, 1P, P(C₆F₅)₂), 72.9 (d, ¹*J*_{Pt-P} = 3023 Hz, ²*J*_{P-P} = 468 Hz, 1P, P^{*t*}Bu₂). ¹⁹F-NMR: (282 MHz, C₆D₆) δ_{F} −127.5 (m, 4F, *o*-C₆F₅), −144.4 (tm, ³*J*_{F-F} = 20.7 Hz, 2F, *p*-C₆F₅), −159.0 (m, 4F, *m*-C₆F₅). HRMS calcd for (C₂₇H₂₃OF₁₀NaP₂IPt) [M+Na]⁺: *m/z* = 958.9647, found = 958.9634.

Reaction of **27** with MeLi: Observation of [(P^{Me}OCCP)Pt(C₆F₅)] (**46**)

A solution of complex **45** (79.9 mg, 94 μ mol) in toluene (4 mL) was cooled to −78 °C, and 1.3 mol dm^{−3} methyllithium solution in diethyl ether (80 μ L, 104 μ mol) was added, with the reaction mixture stirred cold for 5 minutes, then at room temperature for a further 90 minutes. All volatiles were then removed *in vacuo* and the residue extracted with 1:1 toluene/hexane (3×2 mL), with the extracts combined, filtered through celite and taken to dryness under vacuum. This off-white solid was further extracted with hot hexane (3×2 mL), with the extracts dried and analysed by NMR spectroscopy. NMR data showed a mixture of **46** and starting material **27**, as well as small quantities of unidentified products.



¹H-NMR: (300 MHz, C₆D₆) δ_{H} 6.97 (m, 3H, H-4,5,6), 3.21 (m, 2H, CH₂), 1.68 (d, ³*J*_{Pt-H} = 26.6 Hz, ²*J*_{P-H} = 9.5 Hz, 3H, P–CH₃), 0.97 (d, ³*J*_{P-H} = 13.3 Hz, 9H, C(CH₃)₃), 0.92 (d, ³*J*_{P-H} = 13.1 Hz, 9H, C(CH₃)₃). ³¹P-NMR: (121 MHz, C₆D₆) δ_{P}

132.0 (d, $^1J_{\text{Pt-P}} = 3157$ Hz, $^2J_{\text{P-P}} = 421$ Hz, 1P, $\text{P}(\text{C}_6\text{F}_5)(\text{CH}_3)$), 73.8 (d, $^1J_{\text{Pt-P}} = 3157$ Hz, $^2J_{\text{P-P}} = 421$ Hz, 1P, P^tBu_2). ^{19}F -NMR: (282 MHz, C_6D_6) δ_{F} -114.3 (dm, $^3J_{\text{Pt-F}} = 267$ Hz, $^5J_{\text{F-F}} = 32.7$ Hz, 1F, $\text{Pt-C}_6\text{F}_5$ *o*-F), -115.5 (dm, $^3J_{\text{Pt-F}} = 230$ Hz, $^5J_{\text{F-F}} = 32.0$ Hz, 1F, $\text{Pt-C}_6\text{F}_5$ *o*-F), -132.4 (dm, $^3J_{\text{F-F}} = 17.4$ Hz, 2F, $\text{P-C}_6\text{F}_5$ *o*-F), -147.8 (tm, $^3J_{\text{F-F}} = 20.9$ Hz, 1F, $\text{P-C}_6\text{F}_5$ *p*-F), -160.1 (m, 2F, $\text{P-C}_6\text{F}_5$ *o*-F), -161.1 (vtm, $^3J_{\text{F-F}} = 19.9$ Hz, 2F, $\text{Pt-C}_6\text{F}_5$ *p*-F), -163.1 (m, 2F, $\text{Pt-C}_6\text{F}_5$ *m*-F), -163.8 (m, 2F, $\text{Pt-C}_6\text{F}_5$ *m*-F).

[(POCOP)Pt(CO)][SbF₆] (31)

A foil-wrapped flask containing **25** (50 mg, 0.047 mmol) and AgSbF_6 (18 mg, 0.052 mmol) was cooled to -78°C and dichloromethane (10 mL) was added. Carbon monoxide was then bubbled through solution as the reaction mixture was allowed to warm to room temperature. After 30 minutes the carbon monoxide addition was stopped and the foil removed from the flask. After stirring for a further 20 hours the reaction mixture was subsequently filtered through celite and all volatiles removed *in vacuo*. The oily pale yellow residue was washed with diethyl ether, and **31** was isolated as colourless rod-like crystals by slow evaporation of a dichloromethane solution (17.9 mg, 30%). ^1H -NMR: (300 MHz, CD_2Cl_2) δ_{H} 7.51 (t, $^3J_{\text{H-H}} = 8.2$ Hz, 1H, H-5), 7.10 (m, 2H, H-4,6). ^{31}P -NMR: (121 MHz, CD_2Cl_2) δ_{P} 104.4 (s, $^1J_{\text{Pt-P}} = 3345$ Hz). ^{19}F -NMR: (282 MHz, CD_2Cl_2) δ_{F} -129.1 (m, 8F, *o*- C_6F_5), -139.3 (m, 4F, *p*- C_6F_5), -156.6 (m, 8F, *m*- C_6F_5). ^{13}C -NMR: (125 MHz, CD_2Cl_2) δ_{C} 177.5 (s, $^1J_{\text{Pt-C}} = \text{nr}$, 1C, CO), 162.2 (s, 2C, C-1,3), 146.9 (dm, $^1J_{\text{F-C}} = 257$ Hz, 8C, *o*- C_6F_5), 146.5 (dm, $^1J_{\text{F-C}} = 264$ Hz, 4C, *p*- C_6F_5), 138.7 (dm, $^1J_{\text{F-C}} = 256$ Hz, 8C, *m*- C_6F_5), 135.0 (s, 1C, C-5), 131.0 (s, $^1J_{\text{PtC}} = \text{nr}$, 1C, C-2), 109.4 (s, 2C, C-4,6), 103.2 (m, 4C, *i*- C_6F_5). IR (KBr): $\nu_{\text{max}}(\text{CO}) = 2145\text{ cm}^{-1}$. Anal. Calcd for $\text{C}_{31}\text{H}_3\text{O}_3\text{F}_{26}\text{P}_2\text{SbPt}$: C, 28.67; H, 0.38. Found C, 28.73; H, 0.23. HRMS calcd for $(\text{C}_{32}\text{H}_8\text{NO}_3\text{F}_{20}\text{P}_2\text{Pt})[\text{M-CO}+\text{CH}_3\text{CN}+\text{H}_2\text{O}]^+$: $m/z = 1090.9305$, found = 1090.9317.

[(PCCCP)Pt(CO)][SbF₆] (32)

A foil-wrapped flask containing **26** (50 mg, 0.047 mmol) and AgSbF_6 (17 mg, 0.049 mmol) was cooled to -78°C and dichloromethane (10 mL) was added. Carbon monoxide was then bubbled through solution as the reaction mixture was allowed to warm to room temperature. After 30 minutes the carbon monoxide addition was stopped and the foil removed from the flask. After stirring for a further 17 hours the reaction mixture was subsequently filtered through celite and all volatiles removed *in vacuo*. The oily residue was washed with diethyl ether, then twice recrystallised

from dichloromethane/diethyl ether mixtures to give **32** as an off-white, microcrystalline solid (20.0 mg, 33%). $^1\text{H-NMR}$: (300 MHz, acetone- d_6) δ_{H} 7.59 (m, 2H, H-4,6), 7.44 (m, 1H, H-5), 5.06 (t, $^3J_{\text{Pt-H}} = 36.6$ Hz, $^2J_{\text{P-H}} = 5.3$ Hz, 4H, CH_2). $^{31}\text{P-NMR}$: (121 MHz, acetone- d_6) δ_{P} 6.2 (s, $^1J_{\text{Pt-P}} = 3056$ Hz). $^{19}\text{F-NMR}$: (282 MHz, acetone- d_6) δ_{F} -123.7 (m, 8F, $o\text{-C}_6\text{F}_5$), -140.0 (tt, $^3J_{\text{F-F}} = 20.6$ Hz, $^4J_{\text{F-F}} = 6.7$ Hz, 4F, $p\text{-C}_6\text{F}_5$), -154.5 (m, 8F, $m\text{-C}_6\text{F}_5$). $^{13}\text{C-NMR}$: (150 MHz, acetone- d_6) δ_{C} 180.6 (s, $^1J_{\text{Pt-C}} = 1068$ Hz, 1C, CO), 153.6 (s, $^1J_{\text{Pt-C}} = 723$ Hz, 1C, C-2), 148.2 (dm, $^1J_{\text{F-C}} = 256$ Hz, 8C, $o\text{-C}_6\text{F}_5$), 147.2 (t, $^2J_{\text{Pt-C}} = 70.2$ Hz, $^2J_{\text{P-C}} = 9.0$ Hz, 2C, C-1,3), 145.8 (dm, $^1J_{\text{F-C}} = 261$ Hz, 4C, $p\text{-C}_6\text{F}_5$), 139.1 (dm, $^1J_{\text{F-C}} = 255$ Hz, 8C, $m\text{-C}_6\text{F}_5$), 131.6 (s, 1C, 5-C), 125.3 (m, 2C, C-4,6), 102.2 (m, 4C, $i\text{-C}_6\text{F}_5$), 43.3 (t, $^2J_{\text{Pt-C}} = 71.8$ Hz, $^1J_{\text{P-C}} = 18.2$ Hz, 2C, CH_2). IR (KBr): $\nu_{\text{max}}(\text{CO}) = 2127$ cm^{-1} . HRMS calcd for $(\text{C}_{33}\text{H}_7\text{OF}_{20}\text{P}_2\text{Pt})$ $[\text{M}]^+$: $m/z = 1055.9298$, found = 1055.9038.

$[(\text{POCCP})\text{Pt}(\text{CO})][\text{SbF}_6]$ (33**)**

A foil-wrapped flask containing **27** (50 mg, 0.059 mmol) and AgSbF_6 (22 mg, 0.064 mmol) was cooled to -78 $^{\circ}\text{C}$ and dichloromethane (10 mL) was added. Carbon monoxide was then bubbled through solution as the reaction mixture was allowed to warm to room temperature. After 30 minutes the carbon monoxide addition was stopped and the foil removed from the flask. After stirring for a further 19 hours the reaction mixture was filtered through celite and reduced to approximately 2 mL *in vacuo*. Addition of diethyl ether to the dichloromethane solution afforded **33** as a pale yellow solid, which was washed with diethyl ether and dried *in vacuo* (36.1 mg, 57%). $^1\text{H-NMR}$: (300 MHz, CD_2Cl_2) δ_{H} 7.38 (vt, $^3J_{\text{H-H}} = 7.9$ Hz, 1H, H-5), 7.29 (d, $^3J_{\text{H-H}} = 7.5$ Hz, 1H, H-4), 7.13 (d, $^4J_{\text{Pt-H}} = 11.6$ Hz, $^3J_{\text{H-H}} = 7.8$ Hz, 1H, H-6), 3.96 (d, $^3J_{\text{Pt-H}} = 24.0$ Hz, $^2J_{\text{P-H}} = 10.1$ Hz, 2H, CH_2), 1.47 (d, $^3J_{\text{P-H}} = 15.4$ Hz, 18H, $\text{C}(\text{CH}_3)_3$). $^{31}\text{P-NMR}$: (121 MHz, CD_2Cl_2) δ_{P} 108.3 (d, $^1J_{\text{Pt-P}} = 2800$ Hz, $^2J_{\text{P-P}} = 326$ Hz, 1P, $\text{P}(\text{C}_6\text{F}_5)_2$), 91.4 (d, $^1J_{\text{Pt-P}} = 2616$ Hz, $^2J_{\text{P-P}} = 324$ Hz, 1P, P^tBu_2). $^{19}\text{F-NMR}$: (282 MHz, CD_2Cl_2) δ_{F} -129.7 (m, 4F, $o\text{-C}_6\text{F}_5$), -140.2 (ttd, $^3J_{\text{F-F}} = 20.7$ Hz, $^3J_{\text{F-F}} = 7.7$ Hz, $^5J_{\text{P-F}} = 1.9$ Hz, 2F, $p\text{-C}_6\text{F}_5$), -156.7 (tm, $^3J_{\text{F-F}} = 20.1$ Hz, 4F, $m\text{-C}_6\text{F}_5$). $^{13}\text{C-NMR}$: (150 MHz, CD_2Cl_2) δ_{C} 180.1 (s, $^1J_{\text{Pt-C}} = 1064$ Hz, 1C, CO), 162.8 (dd, $^2J_{\text{Pt-C}} = 39$ Hz, $^2J_{\text{P-C}} = 14$ Hz, $^3J_{\text{P-C}} = 3.9$ Hz, 1C, C-1), 152.0 (dd, $^2J_{\text{Pt-C}} = 87$ Hz, $^2J_{\text{P-C}} = 8.5$ Hz, $^3J_{\text{P-C}} = 5.9$ Hz, 1C, C-3), 146.1 (dm, $^1J_{\text{F-C}} = 253$ Hz, 4F, $o\text{-C}_6\text{F}_5$), 145.3 (dm, $^1J_{\text{F-C}} = 265$ Hz, 2F, $p\text{-C}_6\text{F}_5$), 144.1 (d, $^1J_{\text{Pt-C}} = 746$ Hz, $^2J_{\text{P-C}} = 6.5$ Hz, 1C, C-2), 137.9 (dm, $^1J_{\text{F-C}} = 258$ Hz, 4C, $m\text{-C}_6\text{F}_5$), 131.8 (s, 1C, C-5), 120.4 (d, $^3J_{\text{Pt-C}} = 30.2$ Hz, $^3J_{\text{P-C}} = 18.3$ Hz, 1C, C-4), 110.8 (d, $^3J_{\text{P-C}} = 18.2$ Hz, $^3J_{\text{Pt-C}} = 11.2$ Hz, 1C, C-6), 103.7 (dt, $^1J_{\text{P-C}} = 62.8$ Hz, $^2J_{\text{F-C}} = 17.6$ Hz, 2C, $i\text{-C}_6\text{F}_5$), 36.9 (dd, $^2J_{\text{Pt-C}} = 25.2$ Hz, $^1J_{\text{P-C}} = 21.5$ Hz, $^3J_{\text{P-C}} = 3.0$ Hz, 2C, $\text{C}(\text{CH}_3)_3$), 35.0 (d, $^2J_{\text{Pt-C}} = 80.7$ Hz, $^1J_{\text{P-C}} = 35.1$ Hz, 1C, CH_2), 28.1 (s, 6C,

$\text{C}(\text{CH}_3)_3$). IR (KBr): $\nu_{\text{max}}(\text{CO}) = 2111 \text{ cm}^{-1}$.

[(PNNNP)PtCl][Cl] (47)

A solution of **10** (200 mg, 0.24 mmol) and $[\text{PtCl}_2(\text{COD})]$ (89 mg, 0.24 mmol) in dichloromethane (10 mL) was stirred at room temperature for 48 hours. Volatiles were removed *in vacuo* and the residue washed with diethyl ether ($3 \times 10 \text{ mL}$). Purification of the ether-washed solid by recrystallation from 1:1 dichloromethane/diethyl ether afforded **59** as a white, microcrystalline solid (97 mg, 37%). ^1H -NMR: (300 MHz, acetone- d_6) δ_{H} 12.48 (br s, 2H, N-H), 7.90 (tt, $^3J_{\text{H-H}} = 8.1 \text{ Hz}$, $^5J_{\text{P-H}} = 2.0 \text{ Hz}$, 1H, H-5), 7.22 (d, $^3J_{\text{H-H}} = 8.2 \text{ Hz}$, 2H, H-4,6). ^{31}P -NMR: (121 MHz, acetone- d_6) δ_{P} 30.6 (s, $^1J_{\text{Pt-P}} = 3153 \text{ Hz}$). ^{19}F -NMR: (282 MHz, acetone- d_6) δ_{F} -128.3 (d, $^3J_{\text{F-F}} = 20.1 \text{ Hz}$, 8F, *o*- C_6F_5), -144.4 (br s, 4F, *p*- C_6F_5), -160.0 (m, 8F, *m*- C_6F_5). Anal. Calcd for $\text{C}_{29}\text{H}_5\text{N}_3\text{F}_{20}\text{P}_2\text{Cl}_2\text{Pt} \cdot \frac{1}{2}\text{CH}_2\text{Cl}_2$: C, 28.67; H, 0.38. Found C, 28.73; H, 0.23. HRMS calcd for $(\text{C}_{29}\text{H}_5\text{N}_3\text{F}_{20}\text{P}_2\text{ClPt}) [\text{M}]^+$: $m/z = 1065.8955$, found = 1065.8970.

Observation of [(PONOP)PtCl₂]_x (48)

A solution of ligand **11** (20 mg, 24 μmol) and $[\text{PtCl}_2(\text{SEt}_2)_2]$ (8.5 mg, 24 μmol) in acetone- d_6 was monitored *in situ* by NMR spectroscopy. After 15 hours at room temperature almost quantitative formation of **48** in solution was indicated. No significant changes were observed in the reaction mixture after an additional 48 hours at 60 °C. HRMS analysis of this reaction mixture did not reveal any further information about the nature of **48**. ^1H -NMR: (300 MHz, acetone- d_6) δ_{H} 8.23 (t, $^3J_{\text{H-H}} = 8.4 \text{ Hz}$, 1H, H-5), 6.83 (d, $^3J_{\text{H-H}} = 8.5 \text{ Hz}$, 2H, H-4,6). ^{31}P -NMR: (121 MHz, acetone- d_6) δ_{P} 29.0 (s, $^1J_{\text{Pt-P}} = 4148 \text{ Hz}$). ^{19}F -NMR: (282 MHz, acetone- d_6) δ_{F} -130.1 (m, 8F, *o*- C_6F_5), -151.5 (t, $^3J_{\text{F-F}} = 20.4 \text{ Hz}$, 4F, *p*- C_6F_5), -163.8 (m, 8F, *m*- C_6F_5).

8.5 Palladium Complexes

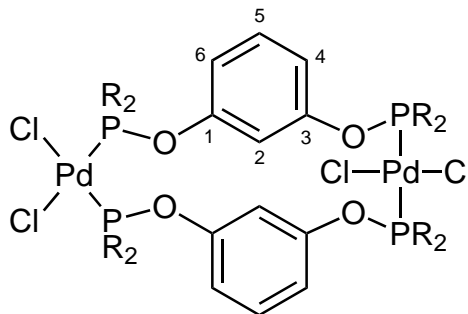
Observation of *trans*-[(POCOPH)PdCl₂]₂ (22)

Ligand **1** (30 mg, 36 μmol) and $[\text{PdCl}_2(\text{NCMe})_2]$ (9.6 mg, 37 μmol) were dissolved

in dichloromethane- d_2 in an NMR tube, and analysed immediately by NMR spectroscopy, which revealed the quantitative formation of **60**. However, isomerisation to compound **23** occurred readily at room temperature, and further characterisation of **60** was not able to be performed. ^1H -NMR: (300 MHz, CD_2Cl_2) δ_{H} 7.42 (t, $^3J_{\text{H-H}} = 8.5$ Hz, 2H, H-5), 7.24 (d, $^3J_{\text{H-H}} = 8.5$ Hz, 4H, H-4,6), 7.02 (s, 2H, H-2). ^{31}P -NMR: (121 MHz, CD_2Cl_2) δ_{P} 87.7 (s). ^{19}F -NMR: (282 MHz, CD_2Cl_2) δ_{F} -127.0 (br s, 16F, *o*- C_6F_5), -144.5 (m, 8F, *p*- C_6F_5), -159.7 (br s, 16F, *m*- C_6F_5).

cis,trans-[(POCOPH)PdCl₂]₂ (**23**)

A solution of ligand **1** (101 mg, 0.12 mmol) and $[\text{PdCl}_2(\text{NCMe})_2]$ (32 mg, 0.12 mmol) in dichloromethane (15 mL) was heated in an oil bath at 45 °C for 12 hours, at which point the volume of the solution was reduced to approximately 2 mL *in vacuo*, and the supernatant decanted and retained. Addition of hexane to the supernatant gave a pale yellow precipitate, which was isolated and washed thoroughly with pentane, affording **23** as a pale yellow solid (101 mg, 83%). Samples of **23** were observed to undergo a degree of rearrangement to higher oligomers on standing in polar solvents such as chloroform or acetone.



where R = C_6F_5

^1H -NMR: (500 MHz, CD_2Cl_2) δ_{H} 7.17 (s, 2H, H-2), 7.16 (vt, $^3J_{\text{H-H}} = 8.3$ Hz, 2H, H-5), 6.85 (dd, $^3J_{\text{H-H}} = 8.3$ Hz, $^4J_{\text{H-H}} = 2.0$ Hz, 2H, H-4), 6.55 (d, $^3J_{\text{H-H}} = 8.1$ Hz, 2H, H-6). ^{31}P -NMR: (121 MHz, CD_2Cl_2) δ_{P} 88.7 (s, 2P, *P-trans*-P), 78.5 (s, 2P, *P-trans*-Cl). ^{19}F -NMR: (282 MHz, CD_2Cl_2) δ_{F} -126.4 (s, 8F, *o*- C_6F_5), -126.8 (s, 8F, *o*- C_6F_5), -141.7 (s, 4F, *p*- C_6F_5), -143.1 (s, 4F, *p*- C_6F_5), -158.5 (t, $^3J_{\text{F-F}} = 19.3$ Hz, 8F, *m*- C_6F_5), -158.9 (td, $^3J_{\text{F-F}} = 21.7$, 6.9 Hz, 8F, *m*- C_6F_5). ^{13}C -NMR: (125 MHz, CD_2Cl_2) δ_{C} 153.2 (s, 2C, C-3), 152.1 (s, 2C, C-1), 146.8 (dd, $^1J_{\text{F-C}} = 246$ Hz, $^2J_{\text{C-F}} = 40.8$ Hz, 16C, *o*- C_6F_5), 145.3 (dm, $^1J_{\text{F-C}} = 255$ Hz, 8C, *p*- C_6F_5), 138.0 (dm, $^1J_{\text{F-C}} = 254$ Hz, 16C, *m*- C_6F_5), 130.9 (s, 2C, C-5), 119.5 (s, 2C, C-6), 116.0 (s, 2C, C-4), 112.8 (s, 2C, C-2). The resonance of the *i*- C_6F_5 environment was

unable to be identified. Anal. Calcd for $C_{60}H_8O_4F_{40}P_4Cl_4Pd_2$: C, 35.48; H, 0.40. Found C, 35.64; H, 0.38. HRMS calcd for $(C_{60}H_8O_4F_{40}P_4Cl_3Pd_2) [M-Cl]^+$: $m/z = 1994.5881$, found = 1994.5869.

[(POCOP)PdCl] (28)

A solution of $[PdCl_2(NCMe)_2]$ (96.5 mg, 0.37 mmol) and **1** (316 mg, 0.38 mmol) in toluene (15 mL) was heated at reflux for 80 hours. All volatiles were then removed *in vacuo* and the viscous yellow oil was triturated with hexane to give a pale yellow solid. Repeated washing with hexane at $-78\text{ }^\circ\text{C}$ gave **28** as a pale yellow solid (291 mg, 80%). $^1\text{H-NMR}$: (300 MHz, $CDCl_3$) δ_H 7.20 (t, $^3J_{H-H} = 8.3$ Hz, 1H, H-5), 6.78 (d, $^3J_{H-H} = 7.9$ Hz, 2H, H-4,6). $^{31}\text{P-NMR}$: (121 MHz, $CDCl_3$) δ_P 114.4 (s). $^{19}\text{F-NMR}$: (282 MHz, $CDCl_3$) δ_F -127.0 (m, 8F, *o*- C_6F_5), -141.9 (tt, $^3J_{F-F} = 20.9$ Hz, $^4J_{F-F} = 6.4$ Hz, 4F, *p*- C_6F_5), -157.0 (m, 8F, *m*- C_6F_5). $^{13}\text{C-NMR}$: (150 MHz, C_6D_6) δ_C 162.3 (t, $^2J_{P-C} = 9.0$ Hz 2C, C-1,3), 145.9 (dm, $^1J_{F-C} = 258$ Hz, 8C, *o*- C_6F_5), ~ 144 (dm, $^1J_{F-C} \approx 260$ Hz, 4C, *p*- C_6F_5), 137.1 (dm, $^1J_{F-C} = 257$ Hz, 8C, *m*- C_6F_5), 132.1 (s, 1C, C-2), 130.1 (s, 1C, C-5), 108.1 (t, $^3J_{P-C} = 9.3$ Hz, 2C, C-4,6), 104.1 (m, 4C, *i*- C_6F_5). Exact chemical shift and coupling constants for the *p*- C_6F_5 environment could not be determined due to peak overlap with the adjacent *o*- C_6F_5 environment. HRMS calcd for $(C_{30}H_4O_2F_{20}P_2ClPt) [M+H]^+$: $m/z = 976.8501$, found = 976.8498.

[(PCCCP)PdCl] (29)

A solution of $PdCl_2(NCMe)_2$ (59 mg, 0.23 mmol) and **2** (189 mg, 0.23 mmol) in toluene (6 mL) was heated at reflux for 48 hours. All volatiles were then removed *in vacuo* and the orange expanded oil obtained triturated with hexane. Precipitation of $[(PCCCPH)PdCl_2]_x$ species from a solution of 1:1 hexane:toluene at $-15\text{ }^\circ\text{C}$, followed by recrystallisation from 3:1 hexane/toluene at $-15\text{ }^\circ\text{C}$ gave **26** as a yellow, microcrystalline solid (142 mg, 64%). $^1\text{H-NMR}$: (300 MHz, $CDCl_3$) δ_H 7.08 (m, 3H, H-4,5,6). $^{31}\text{P-NMR}$: (121 MHz, $CDCl_3$) δ_P 5.9 (s). $^{19}\text{F-NMR}$: (282 MHz, $CDCl_3$) δ_F -126.7 (d, $^3J_{P-F} = 20.3$ Hz, 8F, *o*- C_6F_5), -144.2 (t, $^3J_{F-F} = 20.6$ Hz, 4F, *p*- C_6F_5), -157.6 (m, 8F, *m*- C_6F_5). $^{13}\text{C-NMR}$: (150 MHz, $CDCl_3$) δ_C 154.9 (s, 1C, C-2), 147.3 (dm, $^1J_{F-C} = 253$ Hz, 8C, *o*- C_6F_5), 144.8 (t, $^2J_{P-C} = 11.0$ Hz, 2C, C-1,3), 144.3 (dm, $^1J_{F-C} = 262$ Hz, 4C, *p*- C_6F_5), 138.2 (dm, $^1J_{F-C} = 257$ Hz, 8C, *m*- C_6F_5), 127.7 (s, 1C, C-5), 124.7 (t, $^3J_{P-C} = 12.8$ Hz, 2C, C-4,6), 103.4 (m, 4C, *i*- C_6F_5), 42.7 (br t, $^1J_{P-C} = \text{nr}$, 2C, CH_2). Anal. Calcd for $C_{32}H_7F_{20}P_2ClPt \cdot \frac{1}{2}C_7H_8$: C, 41.65; H, 1.07. Found C, 41.50; H, 1.18. HRMS calcd for $(C_{34}H_{10}NF_{20}P_2Pt) [M-Cl+CH_3CN]^+$:

$m/z = 975.9025$, found = 975.9022.

[(POCCP)PdCl] (**30**)

A solution of [PdCl₂(NCMe)₂] (71.9 mg, 0.28 mmol) and **3** (172 mg, 0.28 mmol) in toluene (6 mL) was heated at 100 °C for 20 hours, at which point all volatiles were removed *in vacuo*. The resultant oil was triturated with hexane and washed with pentane, affording **30** as a bright yellow solid (115 mg, 55%). ¹H-NMR: (500 MHz, CDCl₃) δ_H 7.04 (vt, ³J_{H-H} = 7.7 Hz, 1H, H-5), 6.95 (d, ³J_{H-H} = 7.6 Hz, 1H, H-4), 6.76 (d, ³J_{H-H} = 7.8 Hz, 1H, H-6), 3.47 (d, ²J_{P-H} = 9.5 Hz, 2H, CH₂), 1.45 (d, ³J_{P-H} = 14.4 Hz, 18H, C(CH₃)₃). ³¹P-NMR: (121 MHz, CDCl₃) δ_P 111.5 (d, ²J_{P-P} = 460 Hz, 1P, P(C₆F₅)₂), 83.5 (d, ²J_{P-P} = 460 Hz, 1P, P^tBu₂). ¹⁹F-NMR: (282 MHz, CDCl₃) δ_F -127.8 (dm, ³J_{P-F} = 21.3 Hz, 4F, *o*-C₆F₅), -144.4 (t, ³J_{F-F} = 20.6 Hz, 2F, *p*-C₆F₅), -158.3 (m, 4F, *m*-C₆F₅). ¹³C-NMR: (125 MHz, CDCl₃) δ_C 162.8 (dd, ²J_{P-C} = 21.1 Hz, ⁴J_{P-C} = nr, 1C, C-1), 151.4 (dd, ²J_{P-C} = 15.4 Hz, ⁴J_{P-C} = 1.9 Hz, 1C, C-3), 146.7 (dm, ¹J_{F-C} = 256 Hz, 4C, *o*-C₆F₅), 144.5 (dm, ¹J_{F-C} = 267 Hz, 2C, *p*-C₆F₅), 144.0 (s, 1C, C-2), 137.8 (dm, ¹J_{F-C} = 252 Hz, 4C, *m*-C₆F₅), 127.6 (s, 1C, C-5), 119.9 (d, ³J_{P-C} = 20.1 Hz, 1C, C-4), 111.1 (d, ³J_{P-C} = 19.2 Hz, 1C, C-6), 106.8 (m, 2C, *i*-C₆F₅), 35.8 (dd, ¹J_{P-C} = 13.3 Hz, ³J_{P-C} = 5.1 Hz, 2C, C(CH₃)₃), 35.0 (dd, ¹J_{P-C} = 26.4 Hz, ³J_{P-C} = 3.4 Hz, 1C, CH₂), 29.1 (dd, ²J_{P-C} = 4.3 Hz, ⁴J_{P-C} = 2.4 Hz, 6C, C(CH₃)₃). Anal. Calcd for C₂₇H₂₃OF₁₀P₂ClPd · $\frac{1}{2}$ CH₂Cl₂: C, 41.38; H, 3.03. Found C, 41.28; H, 3.08. HRMS calcd for (C₂₉H₂₆NOF₁₀P₂Pt) [M-Cl+CH₃CN]⁺: $m/z = 758.0386$, found = 758.0357. HRMS calcd for (C₂₃H₂₇NO₂F₅P₂Pt) [M-Cl-C₆F₅+OH+NCMe]⁺: $m/z = 612.0493$, found = 612.0456.

[(POCOP)Pd(CO)][SbF₆] (**34**)

A foil-wrapped flask containing **28** (64.1 mg, 66 μmol) and AgSbF₆ (23.0 mg, 67 μmol) was cooled to -78 °C and dichloromethane (9 mL) was added. The solution was stirred at -78 °C for 10 minutes, then carbon monoxide was bubbled through solution as the reaction mixture was allowed to warm to room temperature. After 60 minutes the reaction mixture was filtered through celite, and the filter cake washed with dichloromethane. The filtrate was subsequently reduced in volume to approximately 1 mL *in vacuo*, and the crude product was precipitated out by the addition of 6 mL hexane to the dichloromethane solution saturated with carbon monoxide. Decantation of the supernatant and washing the precipitate with hexane gave **34** as an off-white solid (61.5 mg, 78%). ¹H-NMR: (300 MHz, CD₂Cl₂) δ_H

7.46 (t, $^3J_{\text{H-H}} = 8.1$ Hz, 1H, H-5), 7.03 (d, $^3J_{\text{H-H}} = 8.3$ Hz, 1H, H-4,6). ^{31}P -NMR: (121 MHz, CD_2Cl_2) δ_{P} 119.4 (s). ^{19}F -NMR: (282 MHz, CD_2Cl_2) δ_{F} -129.5 (m, 8F, *o*- C_6F_5), -140.0 (tt, $^3J_{\text{F-F}} = 20.6$ Hz, $^5J_{\text{F-F}} = 7.8$ Hz, 4F, *p*- C_6F_5), -156.9 (m, 8F, *p*- C_6F_5). ^{13}C -NMR: (150 MHz, CD_2Cl_2) δ_{C} 176.0 (s, 1C, CO), 163.1 (t, $^2J_{\text{P-C}} = 8.1$ Hz, 2C, C-1,3), 147.1 (dm, $^1J_{\text{F-C}} = 255$ Hz, 8C, *o*- C_6F_5), 146.7 (dm, $^1J_{\text{F-C}} = 268$ Hz, 4C, *p*- C_6F_5), 139.0 (dm, $^1J_{\text{F-C}} = 258$ Hz, 8C, *m*- C_6F_5), 134.3 (s, 1C, C-5), 132.0 (br s, 1C, C-2), 110.4 (t, $^3J_{\text{P-C}} = 9.9$ Hz, 2C, C-4,6), 103.7 (m, 4C, *i*- C_6F_5). IR (KBr): $\nu_{\text{max}}(\text{CO}) = 2170\text{ cm}^{-1}$.

[(PCCCP)Pd(CO)][SbF₆] (**35**)

A foil-wrapped flask containing **29** (75 mg, 77 μmol) and AgSbF_6 (28 mg, 81 μmol) was cooled to $-78\text{ }^\circ\text{C}$ and dichloromethane (10 mL) was added. The solution was stirred at $-78\text{ }^\circ\text{C}$ for 5 minutes, then carbon monoxide was bubbled through solution as it was allowed to warm to room temperature over the course of 15 minutes. The reaction mixture was stirred under a carbon monoxide atmosphere for a further 12 hours, then filtered through celite, washing the filter cake with dichloromethane. The filtrate was subsequently reduced in volume to approximately 2 mL *in vacuo*, and the crude product was precipitated out by the addition of 20 mL hexane into the dichloromethane solution saturated with carbon monoxide. Decantation of the supernatant and washing the precipitate with hexane gave **34** as a white microcrystalline solid (35 mg, 38%).

An alternate synthesis of **35** containing the tetrafluoroborate anion was performed as follows, filtering the reaction mixture after halide abstraction but prior to carbonylation, owing to the lower than expected solubility of **35** in dichloromethane: A foil-wrapped flask containing **29** (89.8 mg, 0.092 mmol) and AgBF_4 (23.9 mg, 0.123 mol) was cooled to $-78\text{ }^\circ\text{C}$ and dichloromethane (9 mL) was added. After stirring for 30 minutes at $-78\text{ }^\circ\text{C}$ and 5 hours at room temperature, the reaction mixture was filtered through celite and then carbon monoxide was bubbled through solution for 15 minutes. Slow evaporation of a dichloromethane solution of **35** saturated with carbon monoxide yielded $[(\text{PCCCP})\text{Pd}(\text{CO})][\text{BF}_4]$ as colourless crystals (61.7 mg, 64%). ^1H -NMR: (300 MHz, CD_2Cl_2) δ_{H} 7.34 (m, 3H, H-4,5,6), 4.63 (t, $^2J_{\text{P-H}} = 5.6$ Hz, 4H, CH_2). ^{31}P -NMR: (121 MHz, CD_2Cl_2) δ_{P} 7.1 (s). ^{19}F -NMR: (282 MHz, CD_2Cl_2) δ_{F} -128.7 (m, 8F, *o*- C_6F_5), -142.5 (tt, $^3J_{\text{F-F}} = 20.9$ Hz, $^5J_{\text{F-F}} = 6.3$ Hz, 4F, *p*- C_6F_5), -157.1 (m, 8F, *m*- C_6F_5). ^{13}C -NMR: (150 MHz, CD_2Cl_2) δ_{C} 177.9 (br s, 1C, CO), 157.2 (s, 1C, C-2), 146.5 (dm, $^1J_{\text{F-C}} = 253$ Hz, 8C, *o*- C_6F_5), 144.5 (t, $^2J_{\text{P-C}} = \text{nr}$, 2C, C-1,3), 144.1 (dm, $^1J_{\text{F-C}} = 261$ Hz, 4C, *p*- C_6F_5), 137.6 (dm, $^1J_{\text{F-C}} = 255$ Hz, 8C, *m*- C_6F_5), 129.3 (s, 1C, 5-C), 124.3 (t, $^3J_{\text{P-C}} = 14.2$ Hz, 2C,

C-4,6), 101.5 (m, 4C, *i*-C₆F₅), 41.6 (t, ¹J_{P-C} = nr, 2C, CH₂). IR (KBr): $\nu_{\max}(\text{CO}) = 2148 \text{ cm}^{-1}$.

[(POCCP)Pd(CO)][SbF₆] (**36**)

A foil-wrapped flask containing **30** (51.2 mg, 67 μmol) and AgSbF₆ (24.1 mg, 70 μmol) was cooled to -78°C and dichloromethane (6 mL) was added. Carbon monoxide was then bubbled through solution as the reaction mixture was allowed to warm to room temperature. After 20 minutes the carbon monoxide addition was stopped, the reaction mixture left to stir for a further hour, then subsequently filtered through celite, and the filter cake washed with dichloromethane. The solvent was reduced *in vacuo* and the resultant residue triturated and washed with hexane to give **36** as a yellow solid (41.0 mg, 62%). ¹H-NMR: (300 MHz, CD₂Cl₂) δ_{H} 7.33 (t, ³J_{H-H} = 7.7 Hz, 1H, H-5), 7.19 (d, ³J_{H-H} = 7.6 Hz, 1H, H-4), 7.06 (d, ³J_{H-H} = 7.9 Hz, 1H, H-6), 3.85 (d, ²J_{P-H} = 10.0 Hz, 2H, CH₂), 1.47 (d, ³J_{P-H} = 15.3 Hz, 18H, C(CH₃)₃). ³¹P-NMR: (121 MHz, CD₂Cl₂) δ_{P} 117.0 (br dq, ²J_{P-P} = 320 Hz, ³J_{P-F} = 16.7 Hz, 1P, P(C₆F₅)₂), 109.1 (d, ²J_{P-P} = 320 Hz, 1P, P^{*t*}Bu₂). ¹⁹F-NMR: (282 MHz, CD₂Cl₂) δ_{F} -130.0 (m, 4F, *o*-C₆F₅), -141.0 (tt, ³J_{F-F} = 20.6 Hz, ⁵J_{F-F} = 7.5 Hz, 2F, *p*-C₆F₅), -156.7 (m, 4F, *m*-C₆F₅). ¹³C-NMR: (150 MHz, CD₂Cl₂) δ_{C} 179.7 (br s, 1C, CO), 163.2 (d, ²J_{P-C} = 19.7 Hz, 1C, C-1), 152.7 (d, ²J_{P-C} = 12.8 Hz, 1C, C-3), 147.8 (s, 1C, C-2), 146.7 (dm, ¹J_{F-C} = 252 Hz, 4C, *o*-C₆F₅), 145.8 (dm, ¹J_{F-C} = 264 Hz, 2C, *p*-C₆F₅), 138.5 (dm, ¹J_{F-C} = 256 Hz, 4C, *m*-C₆F₅), 131.5 (s, 1C, C-5), 121.4 (d, ³J_{P-C} = 22.0 Hz, 1C, C-4), 112.4 (d, ³J_{P-C} = 20.3 Hz, 1C, C-6), 104.5 (dm, ¹J_{P-C} = 43.9 Hz, 2C, *i*-C₆F₅), 37.1 (dd, ¹J_{P-C} = 15.0 Hz, ³J_{P-C} = 3.5 Hz, 2C, C(CH₃)₃), 35.8 (d, ¹J_{P-C} = 29.5 Hz, 1C, CH₂), 28.9 (s, 6C, C(CH₃)₃). IR (ATR film from CH₂Cl₂): $\nu_{\max}(\text{CO}) = 2140 \text{ cm}^{-1}$.

Observation of [(PCP)Pd(CO)][SbF₆] decarbonylation products [(PCP)Pd][SbF₆] (**38**, **39**, and **40**)

Compounds **38**, **39**, and **40** were observed in solution arising from the decarbonylation of the parent palladium carbonyl compounds **34**, **35**, and **36** respectively, either by passage of inert gas through dichloromethane solutions, or upon prolonged standing under ambient conditions.

[(POCOP)Pd][SbF₆] (**38**): ¹H-NMR: (300 MHz, CD₂Cl₂) δ_{H} 7.30 (t, ³J_{H-H} = 7.8 Hz, 1H, H-5), 8.85 (d, ³J_{H-H} = 8.0 Hz, 2H, H-4,6). ³¹P-NMR: (121 MHz, CD₂Cl₂) δ_{P} 112.6 (s). ¹⁹F-NMR: (282 MHz, CD₂Cl₂) δ_{F} -129.9 (br s, 8F, *o*-C₆F₅), -141.0

(tm, $^3J_{\text{F-F}} = 20.5$ Hz, 4F, *p*-C₆F₅), -157.5 (tm, $^3J_{\text{F-F}} = 18.9$ Hz, 8F, *m*-C₆F₅).

[(PCCCP)Pd][SbF₆] (**39**): $^1\text{H-NMR}$: (300 MHz, CD₂Cl₂) δ_{H} 7.15 (br s, 3H, H-4,5,6), 4.38 (t, $^2J_{\text{P-H}} = 4.7$ Hz, 4H, CH₂). $^{31}\text{P-NMR}$: (121 MHz, CD₂Cl₂) δ_{P} 1.7 (s). $^{19}\text{F-NMR}$: (282 MHz, CD₂Cl₂) δ_{F} -129.7 (m, 8F, *o*-C₆F₅), -143.6 (tm, $^3J_{\text{F-F}} = 20.4$ Hz, 4F, *p*-C₆F₅), -157.8 (tm, $^3J_{\text{F-F}} = 20.2$ Hz, 8F, *m*-C₆F₅). $^{13}\text{C-NMR}$: (150 MHz, CD₂Cl₂) δ_{C} 147.3 (dm, $^1J_{\text{F-C}} = 247$ Hz, 8C, *o*-C₆F₅), 144.9 (m, 3C, C-1,2,3), 144.7 (dm, $^1J_{\text{F-C}} = 264$ Hz, 4C, *p*-C₆F₅), 138.3 (dm, $^1J_{\text{F-C}} = 257$ Hz, 8C, *m*-C₆F₅), 128.7 (s, 1C, 5-C), 125.7 (t, $^3J_{\text{P-H}} = 13.0$ Hz, 2C, C-4,6), 102.0 (m, 4C, *i*-C₆F₅), 39.5 (br s, 2C, CH₂).

[(POCCP)Pd][SbF₆] (**40**): $^1\text{H-NMR}$: (300 MHz, CD₂Cl₂) δ_{H} 7.13 (t, $^3J_{\text{H-H}} = 7.6$ Hz, 1H, H-5), 7.03 (d, $^3J_{\text{H-H}} = 7.3$ Hz, 1H, H-4), 6.81 (d, $^3J_{\text{H-H}} = 8.0$ Hz, 1H, H-6), 3.47 (d, $^2J_{\text{P-H}} = 9.9$ Hz, 2H, CH₂), 1.44 (d, $^3J_{\text{P-H}} = 14.5$ Hz, 18H, C(CH₃)₃). $^{31}\text{P-NMR}$: (121 MHz, CD₂Cl₂) δ_{P} 107.9 (br dq, $^2J_{\text{P-P}} = 392$ Hz, $^3J_{\text{P-F}} = 16.5$ Hz, 1P, P(C₆F₅)₂), 87.7 (d, $^2J_{\text{P-P}} = 392$ Hz, 1P, P^{*t*}Bu₂). $^{19}\text{F-NMR}$: (282 MHz, CD₂Cl₂) δ_{F} -130.5 (m, 4F, *o*-C₆F₅), -142.8 (t, $^3J_{\text{F-F}} = 20.2$ Hz, 2F, *p*-C₆F₅), -158.3 (t, $^3J_{\text{F-F}} = 18.9$ Hz, 4F, *m*-C₆F₅).

8.6 Rhodium Complexes

[(PNNNP)RhCl] (**49**)

A solution of ligand **10** (343 mg, 0.41 mmol) and [Rh(COD)Cl]₂ (93 mg, 0.19 mmol) in toluene (6 mL) was heated gently with a heat gun to dissolve the starting material, then heated at 100 °C for 4 hours and 75 °C for 10 hours, without stirring. The formation of bright red crystals of the toluene solvate [(PNNNP)RhCl] · xC₇H₈ on the walls of the reaction vessel was observed, with crystallisation completed by cooling the solution to -15 °C. Decantation of the supernatant and washing of the crystalline solid with ice-cold dichloromethane destroyed the crystals, and afforded **49** as an orange powder (297.6 mg, 71%). $^1\text{H-NMR}$: (300 MHz, acetone-*d*₆) δ_{H} 8.72 (br s, 2H, NH), 7.56 (t, $^3J_{\text{H-H}} = 8.1$ Hz, 1H, H-5), 6.70 (d, $^3J_{\text{H-H}} = 8.2$ Hz, 2H, H-4,6). $^{31}\text{P-NMR}$: (121 MHz, acetone-*d*₆) δ_{P} 34.0 (d, $^1J_{\text{Rh-P}} = 180$ Hz). $^{19}\text{F-NMR}$: (282 MHz, acetone-*d*₆) δ_{F} -131.1 (d, $^3J_{\text{P-F}} = 20.9$ Hz, 8F, *o*-C₆F₅), -150.6 (t, $^3J_{\text{F-F}} = 20.3$ Hz, 4F, *p*-C₆F₅), -162.2 (m, 8F, *m*-C₆F₅). $^{13}\text{C-NMR}$: (125 MHz, acetone-*d*₆) δ_{C} 158.9 (s, 2C, C-1,3), 146.8 (dm, $^1J_{\text{F-C}} = 256$ Hz, 8C, *o*-C₆F₅), 143.8 (dm, $^1J_{\text{F-C}} = 258$ Hz, 4C, *p*-C₆F₅), 137.2 (s, 1C, C-5), 137.7 (dm, $^1J_{\text{F-C}} = 254$ Hz, 8C, *m*-C₆F₅),

105.3 (m, 4C, *i*-C₆F₅), 100.8 (s, 2C, C-4,6). Anal. Calcd for C₂₉H₅N₃F₂₀P₂ClRh: C, 35.70; H, 0.52; N, 4.31. Found C, 35.56; H, 0.71; N, 4.25. HRMS calcd for (C₂₉H₅N₃F₂₀P₂Rh) [M–Cl]⁺: *m/z* = 939.8694, found = 939.8701.

Methylation of **49** with dimethylzinc in toluene-*d*₈

Typical procedure was as follows: To a solution of **49** (15.0 mg, 15 μmol) in toluene-*d*₈ (0.4 mL), was added a 1.5 mol dm^{−3} dimethylzinc solution in toluene (20 μL, 30 μmol). The reaction mixture was agitated, and the progress of the reaction to form **50** was monitored *in situ* by NMR spectroscopy. The temperature of the dimethylzinc addition was also varied (at either room temperature, 0 °C, or −78 °C) in order to determine whether the formation of the degradation product **51** was favoured at lower reaction temperatures.

Spectroscopic data for product **50**, [(PNNNP)RhMe]: ¹H-NMR: (300 MHz, toluene-*d*₈) δ_H 5.89 (s, 2H, N–H), 5.69 (d, ³*J*_{H–H} = 7.9 Hz, 2H, H-4,6), 1.09 (br t, ³*J*_{P–H} = 6.3 Hz, 3H, Rh–Me). ³¹P-NMR: (121 MHz, toluene-*d*₈) δ_P 36.3 (d, ¹*J*_{Rh–P} = 222 Hz). ¹⁹F-NMR: (282 MHz, toluene-*d*₈) δ_F −133.4 (d, ³*J*_{P–F} = 22.3 Hz, 8F, *o*-C₆F₅), −149.3 (t, ³*J*_{F–F} = 20.5 Hz, 4F, *p*-C₆F₅), −159.8 (m, 8F, *m*-C₆F₅). The resonance of the H-5 environment was obscured by the presence of toluene. Approximate chemical shift (δ_H ≈ 7.0 ppm) was confirmed by COSY experiment.

Spectroscopic data for degradation product **51**, [(PN^{*}NNP)RhMe · ZnMe]: ¹H-NMR: (300 MHz, toluene-*d*₈) δ_H 5.98 (d, ³*J*_{H–H} = 7.7 Hz, 1H, H-4 or H-6), 5.86 (d, ³*J*_{H–H} = 8.2 Hz, 1H, H-4 or H-6), 5.39 (br s, 1H, N–H), 1.21 (br s, 3H, Rh–Me), −0.18 (s, 3H, Zn–Me). ³¹P-NMR: (121 MHz, toluene-*d*₈) δ_P 74.4 (dd, ²*J*_{P–P} = 522 Hz, ¹*J*_{Rh–P} = 156 Hz, 1P, N–P(C₆F₅)₂) 44.7 (dd, ²*J*_{P–P} = 522 Hz, ¹*J*_{Rh–P} = 158 Hz, 1P, N–P(C₆F₅)₂). ¹⁹F-NMR: (282 MHz, toluene-*d*₈) δ_F −118.1 (br s, 1F, *o*-C₆F₅), −124.2 (br s, 1F, *o*-C₆F₅), −131.0 (br m, 2F, *o*-C₆F₅), −131.8 (br m, 2F, *o*-C₆F₅), −133.7 (br m, 2F, *o*-C₆F₅), −144.1 (vt, ³*J*_{F–F} = 21.7 Hz, 1F, *p*-C₆F₅), −144.8 (vt, ³*J*_{F–F} = 20.0 Hz, 1F, *p*-C₆F₅), −148.2 (vt, ³*J*_{F–F} = 21.5 Hz, 1F, *p*-C₆F₅), −149.6 (vt, ³*J*_{F–F} = 21.0 Hz, 1F, *p*-C₆F₅), −157.8 (m, 2F, *m*-C₆F₅), −158.0 (br m, 2F, *m*-C₆F₅), −159.4 (m, 2F, *m*-C₆F₅), −160.3 (br m, 2F, *m*-C₆F₅). The resonance of the H-5 environment was obscured by the presence of toluene. Approximate chemical shift (δ_H ≈ 7.1 ppm) was confirmed by COSY experiment.

When traces of methyl iodide were present in the dimethylzinc solution used, reactions were observed to produce quantities of the N-methylated complex **53**.

Spectroscopic data for product **53**, [(PN^{Me}NNP)RhMe₂Cl]: ¹H-NMR: (300 MHz, toluene-*d*₈) δ_{H} 6.84 (vt, $^3J_{\text{H-H}} = 7.8$ Hz, 1H, H-5), 6.21 (d, $^3J_{\text{H-H}} = 8.2$ Hz, 1H, H-4/6), 6.09 (br s, 1H, N-H), 5.65 (d, $^3J_{\text{H-H}} = 7.9$ Hz, 1H, H-4/6), 2.68 (br d, $^3J_{\text{P-H}} = 9.7$ Hz, 3H, N-Me), 0.14 (br vt, $^3J_{\text{P-H}} = 6.5$ Hz, 3H, Rh-Me). ³¹P-NMR: (121 MHz, toluene-*d*₈) δ_{P} 85.9 (dd, $^2J_{\text{P-P}} = 615$ Hz, $^1J_{\text{Rh-P}} = 150$ Hz, 1P), 50.9 (dd, $^2J_{\text{P-P}} = 615$ Hz, $^1J_{\text{Rh-P}} = 135$ Hz, 1P). The sample of **53** was not sufficiently pure to allow unambiguous assignment of the ¹⁹F NMR spectrum.

[(PNNNP)RhClMeI] (**54**)

To a solution of **49** (100 mg, 0.10 mmol) in THF (3 mL) was added methyl iodide in excess (50 μL , 0.80 mmol). After 10 minutes at room temperature the solution was reduced to about 1 mL *in vacuo* and 4 mL hexane added. The supernatant was isolated and dried *in vacuo* to give a pale orange precipitate. This crude product was purified by recrystallisation from a warm mixture of 1:2:2 acetone/hexane/diethyl ether followed by washing with diethyl ether, giving **54** as pale orange, microcrystalline blocks (95 mg, 83%). ¹H-NMR: (300 MHz, acetone-*d*₆) δ_{H} 8.52 (br s, 2H, NH), 7.69 (tt, $^3J_{\text{H-H}} = 8.1$ Hz, $^5J_{\text{P-H}} = 1.8$ Hz, 1H, H-5), 7.05 (dm, $^3J_{\text{H-H}} = 8.2$ Hz, 2H, H-4,6), 1.13 (br td, $^3J_{\text{P-H}} = 6.8$ Hz, $^2J_{\text{Rh-H}} = 1.7$ Hz, 3H, Rh-CH₃). ³¹P-NMR: (121 MHz, acetone-*d*₆) δ_{P} 54.7 (d, $^1J_{\text{Rh-P}} = 133$ Hz). ¹⁹F-NMR: (282 MHz, acetone-*d*₆) δ_{F} -117.2 (v br s, 2F, *o*-C₆F₅), -127.6 (br s, 4F, *o*-C₆F₅), -132.3 (v br s, 2F, *o*-C₆F₅), -148.0 (tt, $^3J_{\text{P-P}} = 20.4$ Hz, $^5J_{\text{P-P}} = 5.4$ Hz, 2F, *p*-C₆F₅), -150.0 (tt, $^3J_{\text{P-P}} = 20.9$ Hz, $^5J_{\text{P-P}} = \text{nr}$ Hz, 2F, *p*-C₆F₅), -161.5 (m, 4F, *m*-C₆F₅), -163.0 (br s, 4F, *m*-C₆F₅). ¹³C-NMR: (125 MHz, acetone-*d*₆) δ_{C} 157.1 (vt, $^3J_{\text{P-C}} = 8.1$ Hz, 2C, C-1,3), 146.8 (dm, $^1J_{\text{F-C}} = 256$ Hz, 8C, *o*-C₆F₅), 143.8 (dm, $^1J_{\text{F-C}} = 258$ Hz, 4C, *p*-C₆F₅), 141.1 (s, 1C, C-5), 137.7 (dm, $^1J_{\text{F-C}} = 254$ Hz, 8C, *m*-C₆F₅), 105.3 (m, 4C, *i*-C₆F₅), 103.3 (s, 2C, C-4,6), 8.1 (d, $^1J_{\text{Rh-C}} = 19.0$ Hz, 1C, Rh-CH₃). Anal. Calcd for C₃₀H₈N₃F₂₀P₂ClIRh: C, 32.24; H, 0.72; N, 3.76. Found C, 32.49; H, 0.91; N, 3.81. HRMS calcd for (C₃₀H₈N₃F₂₀NaP₂ClIRh) [M+Na]⁺: $m/z = 1139.7555$, found = 1139.7582.

Observation of [(PNNNP)RhI] (**56**)

To a solution of **49** (17.3 mg, 18 μmol) in benzene-*d*₆, was added an excess of sodium iodide (21.0 mg, 140 μmol). Analysis of the solution after 10 minutes by NMR spectroscopy revealed the formation of **56**. ¹H-NMR: (300 MHz, acetone-*d*₆) δ_{H} 9.20 (br s, 2H, NH), 7.60 (t, $^3J_{\text{H-H}} = 8.1$ Hz, 1H, H-5), 6.93 (m, 2H, H-4,6). ³¹P-NMR: (121 MHz, acetone-*d*₆) δ_{P} 40.5 d, $^1J_{\text{Rh-P}} = 170$ Hz. ¹⁹F-NMR: (282 MHz,

acetone- d_6) δ_F -128.8 (m, 8F, o -C₆F₅), -151.1 (s, 4F, p -C₆F₅), -162.3 (m, 8F, m -C₆F₅). HRMS calcd for (C₃₁H₈N₄F₂₀P₂I₂Rh) [M+I+NCMe]⁺: m/z = 1234.7044, found = 1234.7053.

Observation of [(PNNNP)RhI₃] (**55**)

To the solution of **56** above was added toluene (0.5 mL), and the solution filtered through celite, washing with toluene (3×0.5 mL). The filtrate had all volatiles removed *in vacuo*, and the residue was redissolved in benzene- d_6 . To this was added one crystal of iodine. Analysis of the reaction mixture by NMR spectroscopy revealed immediate and quantitative formation of **55**. ¹H-NMR: (300 MHz, C₆D₆) δ_H 6.46 (t, ³ J_{H-H} = 8.2 Hz, 1H, H-5), 6.27 (br s, 2H, H-4,6), 5.37 (d, ² J_{P-H} = 8.0 Hz, 2-H, NH). ³¹P-NMR: (121 MHz, C₆D₆) δ_P 36.6 (d, ¹ J_{Rh-P} = 115 Hz). ¹⁹F-NMR: (282 MHz, C₆D₆) δ_F -112.0 (br s, 4F, o -C₆F₅), -134.2 (br s, 4F, o -C₆F₅), -143.7 (m, 4F, p -C₆F₅), -156.7 (br s, 4F, m -C₆F₅), -159.7 (br s, 4F, m -C₆F₅), ¹³C-NMR: (150 MHz, acetone- d_6) δ_C 157.4 (dt, ² J_{Rh-C} = 11.0 Hz, ³ J_{P-C} = 7.5 Hz, 2C, C-1,3), 147.5 (br d, ¹ J_{F-C} = 252 Hz, 8C, o -C₆F₅), 144.9 (dm, ¹ J_{F-C} = 258 Hz, 4C, p -C₆F₅), 142.9 (s, 1C, C-5), 138.4 (br d, ¹ J_{F-C} = 254 Hz, 8C, m -C₆F₅), 111.4 (m, 4C, i -C₆F₅), 104.5 (s, 2C, C-4,6), HRMS calcd for (C₂₉H₉N₄F₂₀P₂I₃Rh) [M+NH₄]⁺: m/z = 1338.6167, found = 1338.6207.

8.7 Catalytic Testing

Standard solutions of 1 mmol dm⁻³ [(POCOP)PdCl] (**28**), [(PCCCP)PdCl] (**29**), and [(POCCP)PdCl] (**30**) were prepared by dissolving 9.8 mg of **28**, 9.8 mg of **29**, or 7.6 mg of **30** in 10 mL toluene in a volumetric flask. Each reaction was carried out in a 10 mL Young's tube, heating to the desired temperature with stirring for 2 minutes to ensure adequate mixing. The appropriate amount of 1 mmol dm⁻³ catalyst solution was added by microsyringe and the reaction commenced. At the appropriate time interval, 0.1 mL aliquots of the reaction mixture were withdrawn by syringe, then stored in stoppered glass vials at -15 °C. Mercury poisoning reactions were carried out under standard catalytic conditions, with the addition of one drop (roughly 60 mg) of mercury prior to the mixing of reactants.

Samples withdrawn from reaction mixtures were diluted by taking 10 μ L and making up to 10 mL with dichloromethane. Each sample was spiked with 10 μ L of a

7.0 mmol dm⁻³ solution of 2-methylnaphthalene, used as an internal standard, and analysed by GCMS. Standard solutions of 4-methoxybiphenyl and 4-bromoanisole were analysed over the desired concentration range to confirm a linear response of the detector to the analytes. Reaction progress was determined from peak integrations, looking at the disappearance of the starting material (bromobenzene in Heck reactions, 4-bromoanisole in Suzuki reactions) as well as the appearance of products.

Typical Heck Reaction

Performed with bromobenzene (105 μ L, 1.0 mmol), styrene (128 μ L, 1.1 mmol), and K₂CO₃ (152 mg, 1.1 mmol) in 2.5 mL DMF under a nitrogen atmosphere. To this, 20 μ L of catalyst solution (0.002 mol %) was added, with the reaction carried out at 140 °C for 16 hours.

Typical Suzuki Reaction

Performed with phenylboronic acid (146 mg, 1.2 mmol), 4-bromoanisole (100 μ L, 0.80 mmol), and K₃PO₄ · H₂O (368 mg, 1.6 mmol) in 4 mL toluene under a nitrogen atmosphere. To this, 8 μ L of catalyst solution (0.001 mol %) was added, with the reaction carried out at 100 °C for 2 hours.

Large-Scale Suzuki Reaction

Phenylboronic acid (2.92 g, 24 mmol), 4-bromoanisole (2.00 mL, 16 mmol), and K₃PO₄ · H₂O (7.36 g, 32 mmol) were combined in toluene (80 mL) under a nitrogen atmosphere. The reaction vessel was pre-heated to 100 °C with stirring, and a 1 mmol dm⁻³ solution of catalyst **28** was added (160 μ L, 0.001 mol %). Heating was stopped after 11 hours. The reaction was quenched with 2 mol dm⁻³ HCl (150 mL) and extracted with ethyl acetate (3×50 mL). The combined extracts were washed with saturated sodium bicarbonate solution (3×50 mL) and water (2×50 mL), and dried over magnesium sulfate. Volatiles were removed *in vacuo*, and the crude product purified by column chromatography on neutral alumina, eluting with toluene. Recrystallisation from a mixture of dichloromethane and hexane yielded 4-methoxybiphenyl as a white solid (2.90 g, 98%). NMR characterisation data matches that known for 4-methoxybiphenyl.

Catalyst Stability Tests

Palladium complexes **28** (15 mg, 0.015 mmol), **29** (15 mg, 0.015 mmol), or **30** (12 mg, 0.016 mmol) were combined with phenylboronic acid (9.3 mg, 0.077 mmol) and $\text{K}_3\text{PO}_4 \cdot \text{H}_2\text{O}$ (18 mg, 0.077 mmol) in benzene- d_6 . Hexafluorobenzene (10 μL) was added as an internal standard. Control experiments with **28** and phenylboronic acid, and **28** and $\text{K}_3\text{PO}_4 \cdot \text{H}_2\text{O}$ were also undertaken. Reaction mixtures were heated at 80 °C for 3 hours, monitoring reaction progress by NMR spectroscopy at 0, 5, 30 and 180 minutes. The relative amounts of decafluorobiphenyl and 2,3,4,5,6-pentafluorobiphenyl present were determined by integration of the *ortho* and *para* ^{19}F NMR resonances against those of the starting material prior to degradation, normalised against the hexafluorobenzene internal standard. At the conclusion of heating, each reaction mixture had 2×0.1 mL aliquots withdrawn and diluted with 1 mL dichloromethane. One of the aliquots was hydrolysed by stirring with 1 mL water for 10 min, after which time the organic fraction was decanted and both the hydrolysed and non-hydrolysed aliquots were subjected to GCMS analysis.

Cyclic Voltammetry

Standard solutions of **28** (2.4 mg, 2.5 μmol), **29** (2.4 mg, 2.5 μmol), and **30** (1.9 mg, 2.5 μmol) were prepared with tetrabutylammonium hexafluorophosphate (190 mg, 0.5 μmol) in acetonitrile (5 mL). Solutions were analysed by cyclic voltammetry using a platinum working electrode and a Ag/AgCl reference electrode, scanning from −0.5–1.8 V at a rate of 100 mV s $^{-1}$. No meaningful oxidation events were observed for any of the solutions analysed.

References

1. Kostova, I. *Recent Patents on Anti-Cancer Drug Discovery* **2006**, *1*, 1–22.
2. Breslow, R.; Belvedere, S.; Gershell, L.; Leung, D. *Pure Appl. Chem.* **2000**, *72*, 333–342.
3. Jeffrey, J. C.; Rauchfuss, T. B. *Inorg. Chem.* **1979**, *18*, 2658–2666.
4. Tan, X.; Li, L.; Zhang, J.; Han, X.; Jiang, L.; Li, F.; Su, C.-Y. *Chem. Mater.* **2012**, *24*, 480–485.
5. Allendorf, M. D.; Bauer, C. A.; Bhakta, R. K.; Houk, R. J. T. *Chem. Soc. Rev.* **2009**, *38*, 1330–1352.
6. Nishiyama, H. *Chem. Soc. Rev.* **2007**, *36*, 1133–1141.
7. Fan, L.; Foxman, B. M.; Ozerov, O. V. *Organometallics* **2004**, *23*, 326–328.
8. Hill, A. F.; Lee, S. B.; Park, J.; Shang, R.; Willis, A. C. *Organometallics* **2010**, *29*, 5661–5669.
9. Haenel, M. W.; Oevers, S.; Angermund, K.; Kaska, W. C.; Fan, H.-J.; Hall, M. B. *Angew. Chem., Int. Ed.* **2001**, *40*, 3596–3600.
10. Pugh, D.; Danopoulos, A. A. *Coord. Chem. Rev.* **2007**, *251*, 610–641.
11. Koridze, A. A.; Kuklin, S. A.; Sheloumov, A. M.; Dolgushin, F. M.; Lagunova, V. Y.; Petukhova, I. I.; Ezernitskaya, M. G.; Peregudov, A. S.; Petrovskii, P. V.; Vorontsov, E. V.; Baya, M.; Poli, R. *Organometallics* **2004**, *23*, 4585–4593.
12. Albrecht, M.; van Koten, G. *Angew. Chem., Int. Ed.* **2001**, *40*, 3750–3781.
13. Eberhard, M. R.; Matsukawa, S.; Yamamoto, Y.; Jensen, C. M. *J. Organomet. Chem.* **2003**, *687*, 185–189.
14. Gunanathan, C.; Ben-David, Y.; Milstein, D. *Science* **2007**, *317*, 790–792.
15. Choi, J.; MacArthur, A. H. R.; Brookhart, M.; Goldman, A. S. *Chem. Rev.* **2011**, *111*, 1761–1779.
16. Selander, N.; Szabó, K. J. *Chem. Rev.* **2011**, *111*, 2048–2076.
17. Serrano-Becerra, J. M.; Morales-Morales, D. *Curr. Org. Synth.* **2009**, *6*, 169–192.

18. Morales-Morales, D. *Mini-Rev. Org. Chem.* **2008**, *5*, 141–152.
19. Singleton, J. T. *Tetrahedron* **2003**, *59*, 1837–1857.
20. van der Boom, M. E.; Milstein, D. *Chem. Rev.* **2003**, *103*, 1759–1792.
21. Gupta, M.; Hagen, C.; Flesher, R. J.; Kaska, W. C.; Jensen, C. M. *Chem. Commun.* **1996**, 2083–2084.
22. Haibach, M. C.; Kundu, S.; Brookhart, M.; Goldman, A. S. *Acc. Chem. Res.* **2012**, *45*, 947–958.
23. Goldman, A. S.; Roy, A. H.; Huang, Z.; Ahuja, R.; Schinski, W.; Brookhart, M. *Science* **2006**, *312*, 257–261.
24. Arndtsen, B. A.; Bergman, R. G.; Mobley, T. A.; Peterson, T. H. *Acc. Chem. Res.* **1995**, *28*, 154–162.
25. Bernskoetter, W. H.; Schauer, C. K.; Goldberg, K. I.; Brookhart, M. *Science* **2009**, *326*, 553–556.
26. Perutz, R. N.; Turner, J. J. *J. Am. Chem. Soc.* **1975**, *97*, 4791–4800.
27. Piers, W. E. *Organometallics* **2011**, *30*, 13–16.
28. Poverenov, E.; Efremenko, I.; Frenkel, A. I.; Ben-David, Y.; Shimon, L. J. W.; Leitens, G.; Konstantinovski, L.; Martin, J. M. L.; Milstein, D. *Nature* **2008**, *455*, 1093–1096.
29. Kohl, S. W.; Weiner, L.; Schwartsburd, L.; Konstantinovski, L.; Shimon, L. J. W.; Ben-David, Y.; Iron, M. A.; Milstein, D. *Science* **2009**, *324*, 74–77.
30. Mann, G.; Hartwig, J. F. *Tetrahedron Lett.* **1997**, *38*, 8005–8008.
31. Liu, S.; Saidi, O.; Berry, N.; Ruan, J.; Pettman, A.; Thomson, N.; Xiao, J. *Lett. Org. Chem.* **2009**, *6*, 60–64.
32. Banet Osuna, A. M.; Chen, W.; Hope, E. G.; Kemmitt, R. D. W.; Paige, D. R.; Stuart, A. M.; Xiao, J.; Xu, L. *J. Chem. Soc., Dalton Trans.* **2000**, 4052–4055.
33. Ess, D. H.; Goddard, W. A.; Periana, R. A. *Organometallics* **2010**, *29*, 6459–6472.
34. Sakaki, S.; Biswas, B.; Sugimoto, M. *Organometallics* **1998**, *17*, 1278–1289.
35. Moloy, K. G.; Petersen, J. L. *J. Am. Chem. Soc.* **1995**, *117*, 7696–7710.
36. Dias, P. B.; de Piedade, M. E.; Simes, J. A. *Coord. Chem. Rev.* **1994**, *135–136*, 737–807.
37. Tolman, C. A. *Chem. Rev.* **1977**, *77*, 313–348.
38. Fernandez, A. L.; Wilson, M. R.; Prock, A.; Giering, W. P. *Organometallics* **2001**, *20*, 3429–3435.
39. Pollock, C. L.; Saunders, G. C.; Smyth, E. S.; Sorokin, V. I. *J. Fluorine Chem.* **2008**, *129*, 142–166.

40. Göttker-Schnetmann, I.; White, P.; Brookhart, M. *J. Am. Chem. Soc.* **2004**, *126*, 1804–1811.
41. Orpen, A. G.; Connelly, N. G. *Organometallics* **1990**, *9*, 1206–1210.
42. Göttker-Schnetmann, I.; Brookhart, M. *J. Am. Chem. Soc.* **2004**, *126*, 9330–9338.
43. Adams, J. J.; Arulsamy, N.; Roddick, D. M. *Organometallics* **2011**, *30*, 697–711.
44. Kossoy, E.; Rybtchinski, B.; Diskin-Posner, Y.; Shimon, L. J. W.; Leitun, G.; Milstein, D. *Organometallics* **2009**, *28*, 523–533.
45. Kossoy, E.; Iron, M. A.; Rybtchinski, B.; Ben-David, Y.; Shimon, L. J. W.; Konstantinovski, L.; Martin, J. M. L.; Milstein, D. *Chem. Eur. J.* **2005**, *11*, 2319–2326.
46. Huang, Z.; White, P. S.; Brookhart, M. *Nature* **2010**, *465*, 598–601.
47. Dani, P.; Richter, B.; van Klink, G. P.; van Koten, G. *Eur. J. Inorg. Chem.* **2001**, *2001*, 125–131.
48. Aydin, J.; Kumar, K. S.; Eriksson, L.; Szabó, K. J. *Adv. Synth. Catal.* **2007**, *349*, 2585–2594.
49. Aydin, J.; Kumar, K. S.; Sayah, M. J.; Wallner, O. A.; Szabó, K. J. *J. Org. Chem.* **2007**, *72*, 4689–4697.
50. Schuster, E. M.; Botoshansky, M.; Gandelman, M. *Angew. Chem.* **2008**, *120*, 4631–4634.
51. Kimura, T.; Uozumi, Y. *Organometallics* **2006**, *25*, 4883–4887.
52. Bolliger, J. L.; Blacque, O.; Frech, C. M. *Angew. Chem., Int. Ed.* **2007**, *46*, 6514–6517.
53. Heck, R. F.; Nolley, J. P. *J. Org. Chem.* **1972**, *37*, 2320–2322.
54. Miyaura, N.; Yamada, K.; Suzuki, A. *Tetrahedron Lett.* **1979**, *20*, 3437–3440.
55. Ohff, M.; Ohff, A.; van der Boom, M. E.; Milstein, D. *J. Am. Chem. Soc.* **1997**, *119*, 11687–11688.
56. Gagliardo, M.; Chase, P. A.; Lutz, M.; Spek, A. L.; Hartl, F.; Havenith, R. W. A.; van Klink, G. P. M.; van Koten, G. *Organometallics* **2005**, *24*, 4553–4557.
57. Chase, P. A.; Gagliardo, M.; Lutz, M.; Spek, A. L.; van Klink, G. P. M.; van Koten, G. *Organometallics* **2005**, *24*, 2016–2019.
58. Adams, J. J.; Lau, A.; Arulsamy, N.; Roddick, D. M. *Inorg. Chem.* **2007**, *46*, 11328–11334.
59. Brinkmann, Y.; Madhushaw, R. J.; Jazzar, R.; Bernardinelli, G.; Kündig, E. P. *Tetrahedron* **2007**, *63*, 8413–8419.

60. Alezra, V.; Bernardinelli, G.; Corminboeuf, C.; Frey, U.; Kündig, E. P.; Merbach, A. E.; Saudan, C. M.; Viton, F.; Weber, J. *J. Am. Chem. Soc.* **2004**, *126*, 4843–4853.
61. Morales-Morales, D.; Grause, C.; Kasaoka, K.; Redón, R.; Cramer, R. E.; Jensen, C. M. *Inorg. Chim. Acta* **2000**, *300–302*, 958–963.
62. Motoyama, Y.; Shimozone, K.; Nishiyama, H. *Inorg. Chim. Acta* **2006**, *359*, 1725–1730.
63. Kündig, E. P.; Saudan, C. M.; Bernardinelli, G. *Angew. Chem., Int. Ed.* **1999**, *38*, 1219–1223.
64. RajanBabu, T. V.; Radetich, B.; You, K. K.; Ayers, T. A.; Casalnuovo, A. L.; Calabrese, J. C. *J. Org. Chem.* **1999**, *64*, 3429–3447.
65. Harvey, S.; Junk, P. C.; Raston, C. L.; Salem, G. *J. Org. Chem.* **1988**, *53*, 3134–3140.
66. Hoge, B.; Thösen, C.; Herrmann, T.; Pantenburg, I. *Inorg. Chem.* **2002**, *41*, 2260–2265.
67. Cooke, M.; Green, M.; Kirkpatrick, D. *J. Chem. Soc. A* **1968**, 1507–1510.
68. Klein, J.; Medlik, A.; Meyer, A. *Tetrahedron* **1976**, *32*, 51–56.
69. Ahuja, R.; Punji, B.; Findlater, M.; Supplee, C.; Schinski, W.; Brookhart, M.; Goldman, A. S. *Nat. Chem.* **2011**, *3*, 167–171.
70. Guiso, M.; Betrow, A.; Marra, C. *Eur. J. Org. Chem.* **2008**, *2008*, 1967–1976.
71. Chand, S.; Banwell, M. G. *Aust. J. Chem.* **2007**, *60*, 243–250.
72. Yandulov, D. V.; Tran, N. T. *J. Am. Chem. Soc.* **2007**, *129*, 1342–1358.
73. Park, S.; Pontier-Johnson, M.; Roundhill, D. M. *Inorg. Chem.* **1990**, *29*, 2689–2697.
74. Mohr, W.; Stark, G.; Jiao, H.; Gladysz, J. *Eur. J. Inorg. Chem.* **2001**, *2001*, 925–933.
75. McGibbon, A.; Nieuwenhuyzen, M.; Saunders, G. C. *J. Fluorine Chem.* **2011**, *132*, 495–500.
76. Nycz, J. E. *Phosphorus, Sulfur Silicon Relat. Elem.* **2009**, *184*, 2605–2612.
77. Bernskoetter, W. H.; Hanson, S. K.; Buzak, S. K.; Davis, Z.; White, P. S.; Swartz, R.; Goldberg, K. I.; Brookhart, M. *J. Am. Chem. Soc.* **2009**, *131*, 8603–8613.
78. Benito-Garagorri, D.; Bocokić, V.; Mereiter, K.; Kirchner, K. *Organometallics* **2006**, *25*, 3817–3823.
79. Schirmer, W.; Flörke, U.; Haupt, H.-J. *Z. Anorg. Allg. Chem.* **1987**, *545*, 83–97.

80. Clarke, M. L.; Ellis, D.; Mason, K. L.; Orpen, A. G.; Pringle, P. G.; Wingad, R. L.; Zaher, D. A.; Baker, R. T. *Dalton Trans.* **2005**, 1294–1300.
81. Casalnuovo, A. L.; RajanBabu, T. V.; Ayers, T. A.; Warren, T. H. *J. Am. Chem. Soc.* **1994**, *116*, 9869–9882.
82. Darcel, C.; Moulin, D.; Henry, J.-C.; Lagrelette, M.; Richard, P.; Harvey, P. D.; Jugé, S. *Eur. J. Org. Chem.* **2007**, *2007*, 2078–2090.
83. Wolfe, B.; Livinghouse, T. *J. Am. Chem. Soc.* **1998**, *120*, 5116–5117.
84. Moulton, C. J.; Shaw, B. L. *J. Chem. Soc., Dalton Trans.* **1976**, 1020–1024.
85. Al-Salem, N. A.; Empsall, H. D.; Markham, R.; Shaw, B. L.; Weeks, B. *J. Chem. Soc., Dalton Trans.* **1979**, 1972–1982.
86. Rimml, H.; Venanzi, L. M. *J. Organomet. Chem.* **1983**, *259*, C6–C7.
87. Paganelli, S.; Matteoli, U.; Scrivanti, A.; Botteghi, C. *J. Organomet. Chem.* **1990**, *397*, 375–381.
88. Petzold, H.; Görls, H.; Weigand, W. *J. Organomet. Chem.* **2007**, *692*, 2736–2742.
89. Carr, N.; Dunne, B. J.; Mole, L.; Orpen, A. G.; Spencer, J. L. *J. Chem. Soc., Dalton Trans.* **1991**, 863–871.
90. Baker, M. J.; Harrison, K. N.; Orpen, A. G.; Pringle, P. G.; Shaw, G. *J. Chem. Soc., Dalton Trans.* **1992**, 2607–2614.
91. van der Boom, M. E.; Gozin, M.; Ben-David, Y.; Shimon, L. J. W.; Frolow, F.; Kraatz, H.-B.; Milstein, D. *Inorg. Chem.* **1996**, *35*, 7068–7073.
92. Baber, R. A.; Bedford, R. B.; Betham, M.; Blake, M. E.; Coles, S. J.; Haddow, M. F.; Hursthouse, M. B.; Orpen, A. G.; Pilarski, L. T.; Pringle, P. G.; Wingad, R. L. *Chem. Commun.* **2006**, 3880–3882.
93. Sinnokrot, M. O.; Valeev, E. F.; Sherrill, C. D. *J. Am. Chem. Soc.* **2002**, *124*, 10887–10893.
94. Pandarus, V.; Zargarian, D. *Organometallics* **2007**, *26*, 4321–4334.
95. Sjövall, S.; Andersson, C.; Wendt, O. F. *Inorg. Chim. Acta* **2001**, *325*, 182–186.
96. Sjövall, S.; Johansson, M.; Andersson, C. *Eur. J. Inorg. Chem.* **2001**, *2001*, 2907–2912.
97. Olsson, D.; Arunachalampillai, A.; Wendt, O. F. *Dalton Trans.* **2007**, 5427–5433.
98. Nandy, R.; Subramoni, M.; Varghese, B.; Sankararaman, S. *J. Org. Chem.* **2007**, *72*, 938–944.
99. Fanjul, T.; Eastham, G.; Fey, N.; Hamilton, A.; Orpen, A. G.; Pringle, P. G.; Waugh, M. *Organometallics* **2010**, *29*, 2292–2305.

100. Bennett, M. A.; Jin, H.; Willis, A. C. *J. Organomet. Chem.* **1993**, *451*, 249–256.
101. Hill, W. E.; Minahan, D. M. A.; Taylor, J. G.; McAuliffe, C. A. *J. Am. Chem. Soc.* **1982**, *104*, 6001–6005.
102. Pearson, R. G. *Inorg. Chem.* **1973**, *12*, 712–713.
103. Harvey, J. N.; Heslop, K. M.; Orpen, A. G.; Pringle, P. G. *Chem. Commun.* **2003**, 278–279.
104. Nifant'ev, E. E.; Rasadkina, E. N.; Vasyanina, L. K.; Belsky, V. K.; Stash, A. I. *J. Organomet. Chem.* **1997**, *529*, 171–176.
105. Armstrong, S.; Cross, R.; Farrugia, L.; Nichols, D.; Perry, A. *Eur. J. Inorg. Chem.* **2002**, *2002*, 141–151.
106. Cooper, S. J.; Brown, M. P.; Puddephatt, R. J. *Inorg. Chem.* **1981**, *20*, 1374–1377.
107. Albrecht, M.; Dani, P.; Lutz, M.; Spek, A. L.; van Koten, G. *J. Am. Chem. Soc.* **2000**, *122*, 11822–11833.
108. Canty, A. J.; van Koten, G. *Acc. Chem. Res.* **1995**, *28*, 406–413.
109. Garrou, P. E. *Chem. Rev.* **1981**, *81*, 229–266.
110. Johnson, M. T.; Wendt, O. F. *Inorg. Chim. Acta* **2011**, *367*, 222–224.
111. Ozerov, O. V.; Guo, C.; Foxman, B. M. *J. Organomet. Chem.* **2006**, *691*, 4802–4806.
112. Clark, H.; Manzer, L. *J. Organomet. Chem.* **1973**, *59*, 411–428.
113. Even, T.; Genge, A. R. J.; Hill, A. M.; Holmes, N. J.; Levason, W.; Webster, M. *J. Chem. Soc., Dalton Trans.* **2000**, 655–662.
114. Babai, A.; Deacon, G. B.; Meyer, G. Z. *Anorg. Allg. Chem.* **2004**, *630*, 399–402.
115. Flapper, J.; Wormald, P.; Lutz, M.; Spek, A. L.; van Leeuwen, P. W. N. M.; Elsevier, C. J.; Kamer, P. C. J. *Eur. J. Inorg. Chem.* **2008**, *2008*, 4968–4976.
116. Drahos, B.; Rohlik, Z.; Kotek, J.; Cisarova, I.; Hermann, P. *Dalton Trans.* **2009**, 4942–4953.
117. Albrecht, M.; Gossage, R. A.; Lutz, M.; Spek, A. L.; van Koten, G. *Chem. Eur. J.* **2000**, *6*, 1431–1445.
118. Appleton, T. G.; Bennett, M. A. *Inorg. Chem.* **1978**, *17*, 738–747.
119. Abdullah, B. H.; Abdullah, M. A.; Al-Jibori, S. A.; Al-Allaf, T. A. K. *Asian J. Chem.* **2007**, *19*, 1334–1340.
120. Deacon, G.; Nelson-Reed, K. *J. Organomet. Chem.* **1987**, *322*, 257–268.
121. Espinet, P.; Martínez-Ilarduya, J. M.; Pérez-Briso, C.; Casado, A. L.; Alonso, M. *J. Organomet. Chem.* **1998**, *551*, 9–20.

122. Kemmitt, R. D. W.; Nichols, D. I.; Peacock, R. D. *J. Chem. Soc. A* **1968**, 2149–2152.
123. Cross, R.; Kennedy, A.; Muir, K. *J. Organomet. Chem.* **1995**, 487, 227–233.
124. Arunachalampillai, A.; Johnson, M. T.; Wendt, O. F. *Organometallics* **2008**, 27, 4541–4543.
125. Siegbahn, P. E. M.; Crabtree, R. H. *J. Am. Chem. Soc.* **1996**, 118, 4442–4450.
126. Bruce, M. I. *Angew. Chem., Int. Ed.* **1977**, 16, 73–86.
127. Omae, I. *J. Organomet. Chem.* **2011**, 696, 1128–1145.
128. Brookhart, M.; Green, M. L. H.; Parkin, G. *Proc. Natl. Acad. Sci. U.S.A.* **2007**, 104, 6908–6914.
129. Wang, Z.; Sugiarti, S.; Morales, C. M.; Jensen, C. M.; Morales-Morales, D. *Inorg. Chim. Acta* **2006**, 359, 1923–1928.
130. Ryabov, A. D.; Sakodinskaya, I. K.; Yatsimirsky, A. K. *J. Chem. Soc., Dalton Trans.* **1985**, 2629–2638.
131. Ryabov, A. D. *Chem. Rev.* **1990**, 90, 403–424.
132. Albrecht, M. *Chem. Rev.* **2010**, 110, 576–623, PMID: 20017477.
133. Davies, D. L.; Donald, S. M. A.; Macgregor, S. A. *J. Am. Chem. Soc.* **2005**, 127, 13754–13755.
134. Goldman, A. S.; Krogh-Jespersen, K. *J. Am. Chem. Soc.* **1996**, 118, 12159–12166.
135. Bolliger, J. L.; Blacque, O.; Frech, C. M. *Chem. Eur. J.* **2008**, 14, 7969–7977.
136. Gerber, R.; Fox, T.; Frech, C. M. *Chem. Eur. J.* **2010**, 16, 6771–6775.
137. Vuzman, D.; Poverenov, E.; Diskin-Posner, Y.; Leitun, G.; Shimon, L. J. W.; Milstein, D. *Dalton Trans.* **2007**, 5692–5700.
138. Horton, A. D.; de With, J.; van der Linden, A. J.; van de Weg, H. *Organometallics* **1996**, 15, 2672–2674.
139. Schwartsburd, L.; Poverenov, E.; Shimon, L. J. W.; Milstein, D. *Organometallics* **2007**, 26, 2931–2936.
140. Shelly, K.; Bartczak, T.; Scheidt, W. R.; Reed, C. A. *Inorg. Chem.* **1985**, 24, 4325–4330.
141. Salem, H.; Ben-David, Y.; Shimon, L. J. W.; Milstein, D. *Organometallics* **2006**, 25, 2292–2300.
142. Poverenov, E.; Leitun, G.; Shimon, L. J. W.; Milstein, D. *Organometallics* **2005**, 24, 5937–5944.
143. Tong, J.; Liu, S.; Zhang, S.; Li, S. Z. *Spectrochim. Acta, Part A* **2007**, 67, 837–846.

144. Wawrzyniak, P.; Fuller, A. L.; Slawin, A. M. Z.; Kilian, P. *Inorg. Chem.* **2009**, *48*, 2500–2506, PMID: 19216557.
145. Baber, R. A.; Haddow, M. F.; Middleton, A. J.; Orpen, A. G.; Pringle, P. G.; Haynes, A.; Williams, G. L.; Papp, R. *Organometallics* **2007**, *26*, 713–725.
146. Schwartsburd, L.; Cohen, R.; Konstantinovski, L.; Milstein, D. *Angew. Chem., Int. Ed.* **2008**, *47*, 3603–3606.
147. Nakajima, Y.; Ozawa, F. *Organometallics* **2012**, *31*, 2009–2015.
148. Sánchez-Cabrera, G.; Leyva, M. A.; Zuno-Cruz, F. J.; Hernández-Cruz, M. G.; Rosales-Hoz, M. J. *J. Organomet. Chem.* **2009**, *694*, 1949–1958.
149. Zhu, H.; Ziegler, T. *Organometallics* **2009**, *28*, 2773–2777.
150. Zhu, H.; Ziegler, T. *Organometallics* **2008**, *27*, 1743–1749.
151. Hughes, E. D.; Ingold, C. K. *J. Chem. Soc.* **1935**, 244–255.
152. Feller, M.; Ben-Ari, E.; Iron, M. A.; Diskin-Posner, Y.; Leituss, G.; Shimon, L. J. W.; Konstantinovski, L.; Milstein, D. *Inorg. Chem.* **2010**, *49*, 1615–1625.
153. Kundu, S.; Brennessel, W. W.; Jones, W. D. *Inorg. Chem.* **2011**, *50*, 9443–9453.
154. Feller, M.; Diskin-Posner, Y.; Shimon, L. J. W.; Ben-Ari, E.; Milstein, D. *Organometallics* **2012**, *31*, 4083–4101.
155. Gunanathan, C.; Milstein, D. *Acc. Chem. Res.* **2011**, *44*, 588–602.
156. Schwartsburd, L.; Iron, M. A.; Konstantinovski, L.; Ben-Ari, E.; Milstein, D. *Organometallics* **2011**, *30*, 2721–2729.
157. Benito-Garagorri, D.; Kirchner, K. *Acc. Chem. Res.* **2008**, *41*, 201–213.
158. Burkill, H. A.; Vilar, R.; White, A. J. *Inorg. Chim. Acta* **2006**, *359*, 3709–3722.
159. Hanson, S. K.; Heinekey, D. M.; Goldberg, K. I. *Organometallics* **2008**, *27*, 1454–1463.
160. Hahn, C.; Spiegler, M.; Herdtweck, E.; Taube, R. *Eur. J. Inorg. Chem.* **1998**, *1998*, 1425–1432.
161. Huff, C. A.; Kampf, J. W.; Sanford, M. S. *Organometallics* **2012**, *31*, 4643–4645.
162. Fryzuk, M. D.; McConville, D. H.; Rettig, S. J. *Organometallics* **1993**, *12*, 2152–2161.
163. Geerts, R. L.; Huffman, J. C.; Caulton, K. G. *Inorg. Chem.* **1986**, *25*, 590–591.
164. Moszner, M.; Ciunik, Z.; Ziolkowski, J. J. *Polyhedron* **2003**, *22*, 3195–3203.
165. Blank, B.; Glatz, G.; Kempe, R. *Chem. Asian J.* **2009**, *4*, 321–327.
166. Feller, M.; Iron, M. A.; Shimon, L. J. W.; Diskin-Posner, Y.; Leituss, G.; Milstein, D. *J. Am. Chem. Soc.* **2008**, *130*, 14374–14375.

167. Hahn, C.; Spiegler, M.; Herdtweck, E.; Taube, R. *Eur. J. Inorg. Chem.* **1999**, *1999*, 435–440.
168. Yang, L.; Kruger, A.; Neels, A.; Albrecht, M. *Organometallics* **2008**, *27*, 3161–3171.
169. Wehmschulte, R. J.; Twamley, B.; Khan, M. A. *Inorg. Chem.* **2001**, *40*, 6004–6008.
170. Seligson, A. L.; Trogler, W. C. *Organometallics* **1993**, *12*, 744–751.
171. Bedford, R. B.; Draper, S. M.; Noelle Scully, P.; Welch, S. L. *New J. Chem.* **2000**, *24*, 745–747.
172. Kjellgren, J.; Aydin, J.; Wallner, O. A.; Saltanova, I. V.; Szabó, K. J. *Chem. Eur. J.* **2005**, *11*, 5260–5268.
173. Sebelius, S.; Olsson, V. J.; Szabó, K. J. *J. Am. Chem. Soc.* **2005**, *127*, 10478–10479.
174. Crisp, G. T. *Chem. Soc. Rev.* **1998**, *27*, 427–436.
175. Amatore, C.; Jutand, A. *Acc. Chem. Res.* **2000**, *33*, 314–321.
176. Phan, N. T. S.; Van Der Sluys, M.; Jones, C. W. *Adv. Synth. Catal.* **2006**, *348*, 609–679.
177. Herrmann, W. A.; Brossmer, C.; Öfele, K.; Reisinger, C.-P.; Priermeier, T.; Beller, M.; Fischer, H. *Angew. Chem., Int. Ed.* **1995**, *34*, 1844–1848.
178. Beller, M.; Fischer, H.; Herrmann, W. A.; Öfele, K.; Brossmer, C. *Angew. Chem., Int. Ed.* **1995**, *34*, 1848–1849.
179. Shaw, B. L. *New J. Chem.* **1998**, *22*, 77–79.
180. Miyazaki, F.; Yamaguchi, K.; Shibasaki, M. *Tetrahedron Lett.* **1999**, *40*, 7379–7383.
181. Louie, J.; Hartwig, J. F. *Angew. Chem., Int. Ed.* **1996**, *35*, 2359–2361.
182. Reetz, M. T.; Westermann, E. *Angew. Chem., Int. Ed.* **2000**, *39*, 165–168.
183. Eberhard, M. R. *Org. Lett.* **2004**, *6*, 2125–2128.
184. Yu, K.; Sommer, W.; Richardson, J. M.; Weck, M.; Jones, C. W. *Adv. Synth. Catal.* **2005**, *347*, 161–171.
185. de Vries, J. G. *Dalton Trans.* **2006**, 421–429.
186. Xu, L.-M.; Li, B.-J.; Yang, Z.; Shi, Z.-J. *Chem. Soc. Rev.* **2010**, *39*, 712–733.
187. Sehnal, P.; Taylor, R. J. K.; Fairlamb, I. J. S. *Chem. Rev.* **2010**, *110*, 824–889.
188. Aydin, J.; Larsson, J. M.; Selander, N.; Szabó, K. J. *Org. Lett.* **2009**, *11*, 2852–2854.
189. Blacque, O.; Frech, C. M. *Chem. Eur. J.* **2010**, *16*, 1521–1531.

190. Gerber, R.; Blacque, O.; Frech, C. M. *Dalton Trans.* **2011**, *40*, 8996–9003.
191. Vicente, J.; Arcas, A.; Juliá-Hernández, F.; Bautista, D. *Angew. Chem., Int. Ed.* **2011**, *50*, 6896–6899.
192. Duncan, D.; Hope, E. G.; Singh, K.; Stuart, A. M. *Dalton Trans.* **2011**, *40*, 1998–2005.
193. Jung, I. G.; Son, S. U.; Park, K. H.; Chung, K.-C.; Lee, J. W.; Chung, Y. K. *Organometallics* **2003**, *22*, 4715–4720.
194. Gruber, A. S.; Zim, D.; Ebeling, G.; Monteiro, A. L.; Dupont, J. *Org. Lett.* **2000**, *2*, 1287–1290.
195. Whitesides, G. M.; Hackett, M.; Brainard, R. L.; Lavalleye, J. P. P. M.; Sowinski, A. F.; Izumi, A. N.; Moore, S. S.; Brown, D. W.; Staudt, E. M. *Organometallics* **1985**, *4*, 1819–1830.
196. Widegren, J. A.; Finke, R. G. *J. Mol. Catal. A: Chem.* **2003**, *198*, 317–341.
197. van Asselt, R.; Elsevier, C. J. *J. Mol. Catal.* **1991**, *65*, L13–L19.
198. Stein, J.; Lewis, L. N.; Gao, Y.; Scott, R. A. *J. Am. Chem. Soc.* **1999**, *121*, 3693–3703.
199. Sommer, W. J.; Yu, K.; Sears, J. S.; Ji, Y.; Zheng, X.; Davis, R. J.; Sherrill, C. D.; Jones, C. W.; Weck, M. *Organometallics* **2005**, *24*, 4351–4361.
200. Beletskaya, I. P.; Kashin, A. N.; Karlstedt, N. B.; Mitin, A. V.; Cheprakov, A. V.; Kazankov, G. M. *J. Organomet. Chem.* **2001**, *622*, 89–96.
201. Suijkerbuijk, B. M. J. M.; Herreras Martínez, S. D.; Koten, G. v.; Klein Gebbink, R. J. M. *Organometallics* **2008**, *27*, 534–542.
202. Beletskaya, I. P.; Cheprakov, A. V. *Chem. Rev.* **2000**, *100*, 3009–3066.
203. Salem, H.; Shimon, L. J. W.; Diskin-Posner, Y.; Leituss, G.; Ben-David, Y.; Milstein, D. *Organometallics* **2009**, *28*, 4791–4806.
204. Benito-Garagorri, D.; Mereiter, K.; Kirchner, K. *Eur. J. Inorg. Chem.* **2006**, *2006*, 4374–4379.
205. Beletskaya, I. P.; Cheprakov, A. V. *J. Organomet. Chem.* **2004**, *689*, 4055–4082.
206. Hoge, B.; Neufeind, S.; Hettel, S.; Wiebe, W.; Thösen, C. *J. Organomet. Chem.* **2005**, *690*, 2382–2387.
207. Ali, R.; Dillon, K. B. *J. Chem. Soc., Dalton Trans.* **1990**, 2593–2596.
208. von Schenck, H.; Åkermarck, B.; Svensson, M. *Organometallics* **2002**, *21*, 2248–2253.
209. Ariafard, A.; Yates, B. F. *J. Organomet. Chem.* **2009**, *694*, 2075–2084.
210. Amatore, C.; Jutand, A.; Le Duc, G. *Chem. Eur. J.* **2011**, *17*, 2492–2503.

211. Braga, A. A. C.; Morgon, N. H.; Ujaque, G.; Maseras, F. *J. Am. Chem. Soc.* **2005**, *127*, 9298–9307.
212. Bedford, R. B.; Hazelwood, S. L.; Horton, P. N.; Hursthouse, M. B. *Dalton Trans.* **2003**, 4164–4174.
213. Martin, R.; Buchwald, S. L. *Acc. Chem. Res.* **2008**, *41*, 1461–1473.
214. Crabtree, R. H. *Chem. Rev.* **2012**, *112*, 1536–1554.
215. Kozlov, V. A.; Aleksanyan, D. V.; Nelyubina, Y. V.; Lyssenko, K. A.; Petrovskii, P. V.; Vasil'ev, A. A.; Odinets, I. L. *Organometallics* **2011**, *30*, 2920–2932.
216. Bolliger, J. L.; Frech, C. M. *Chem. Eur. J.* **2010**, *16*, 4075–4081.
217. Takemoto, T.; Iwasa, S.; Hamada, H.; Shibatomi, K.; Kameyama, M.; Motoyama, Y.; Nishiyama, H. *Tetrahedron Lett.* **2007**, *48*, 3397–3401.
218. Zhang, H.; Lei, A. *Dalton Trans.* **2011**, *40*, 8745–8754.
219. Polukeev, A. V.; Kuklin, S. A.; Petrovskii, P. V.; Peregodova, S. M.; Smol'yakov, A. F.; Dolgushin, F. M.; Koridze, A. A. *Dalton Trans.* **2011**, *40*, 7201–7209.
220. Ghosh, R.; Emge, T. J.; Krogh-Jespersen, K.; Goldman, A. S. *J. Am. Chem. Soc.* **2008**, *130*, 11317–11327.
221. Olsson, D.; Wendt, O. F. *J. Organomet. Chem.* **2009**, *694*, 3112–3115.
222. Gerber, R.; Blacque, O.; Frech, C. M. *ChemCatChem* **2009**, *1*, 393–400.
223. Lin, Z. *Coord. Chem. Rev.* **2007**, *251*, 2280–2291.
224. Fulmer, G. R.; Muller, R. P.; Kemp, R. A.; Goldberg, K. I. *J. Am. Chem. Soc.* **2009**, *131*, 1346–1347.
225. Johansson, R.; Wendt, O. F. *Organometallics* **2007**, *26*, 2426–2430.
226. Bonnet, S.; van Lenthe, J. H.; Siegler, M. A.; Spek, A. L.; van Koten, G.; Gebbink, R. J. M. K. *Organometallics* **2009**, *28*, 2325–2333.
227. Bonnet, S.; Lutz, M.; Spek, A. L.; van Koten, G.; Klein Gebbink, R. J. M. *Organometallics* **2010**, *29*, 1157–1167.
228. Widenhoefer, R. A.; Zhong, H. A.; Buchwald, S. L. *J. Am. Chem. Soc.* **1997**, *119*, 6787–6795.
229. Zhang, J.; Medley, C. M.; Krause, J. A.; Guan, H. *Organometallics* **2010**, *29*, 6393–6401.
230. Armarego, L., Wilfred; Chai, L., Christina *Purification of Laboratory Chemicals (5th Edition)*; Elsevier, 2003.
231. Kündig, E. P.; Dupré, C.; Bourdin, B.; Cunningham, A.; Pons, D. *Helv. Chim. Acta* **1994**, *77*, 421–428.

232. Hartley, F. R.; Murray, S. G.; McAuliffe, C. A. *Inorg. Chem.* **1979**, *18*, 1394–1397.
233. Jensen, K. A. *Acta Chem. Scand.* **1953**, *7*, 868–70.
234. Vaughan, T. F.; Koedyk, D. J.; Spencer, J. L. *Organometallics* **2011**, *30*, 5170–5180.
235. Giordano, G.; Crabtree, R. H. *Inorg. Synth.* **1979**, *19*, 218–20.
236. Drew, D.; Doyle, J. R. *Inorg. Synth.* **1990**, *28*, 346–9.
237. Sheldrick, G. M. *Acta Crystallogr., Sect. A: Found. Crystallogr.* **2008**, *64*, 112–122.
238. Dolomanov, O. V.; Bourhis, L. J.; Gildea, R. J.; Howard, J. A. K.; Puschmann, H. *J. Appl. Crystallogr.* **2009**, *42*, 339–341.